Targeting Troubled Translation: Investigating Novel Therapeutic Targets in Mouse Models of Fragile X and 16p11.2 Deletion Syndrome

By

Laura J. Stoppel

B.A. Biology
Harvard University, 2008

SUBMITTED TO THE DEPARTMENT OF BRAIN AND COGNITIVE SCIENCES
IN PARTIAL FULFILLMENT OF THE REQUIREMENTS FOR THE DEGREE OF

DOCTOR OF PHILOSOPHY IN NEUROSCIENCE

AT THE
MASSACHUSETTS INSTITUTE OF TECHNOLOGY

SEPTEMBER 2016 [February 2017]

Signature of Author: Signature redacted
Laura J. Stoppel
Department of Brain and Cognitive Sciences
September 9, 2016

Certified by: Signature redacted
Mark F. Bear
Picower Professor of Neuroscience
Thesis Supervisor

Accepted by: Signature redacted
Matthew A. Wilson
Sherman Fairchild Professor of Neuroscience and Picower Scholar
Director of Graduate Education for Brain and Cognitive Sciences

Targeting Troubled Translation: Investigating Novel Therapeutic Targets in Mouse Models of Fragile X and 16p11.2 Deletion Syndrome

By

Laura J. Stoppel

Submitted to the Department of Brain and Cognitive Sciences on September 9, 2016 in Partial Fulfillment of the Requirements for the Degree of Doctor of Philosophy in Neuroscience

Abstract

1 in 68 children born in the United States meets the diagnostic criteria for Autism Spectrum Disorder (ASD), a psychiatric illness that shares a high comorbidity with intellectual disability (ID). Despite the high prevalence of ASD, there are currently no mechanism-based treatments available due to a lack of understanding of the pathophysiological processes in the brain that disrupt behavior in affected individuals. Identifying convergent molecular pathways involved in known genetic causes of ASD and ID may broaden our understanding of these disorders and help advance potential targeted treatments for ASD. Synaptic protein synthesis is essential for modification of the brain through experience and is altered in several genetically-defined disorders, notably fragile X (FX), a heritable cause of ASD and ID. Neural activity directs local protein synthesis via activation of metabotropic glutamate receptor 5 ($mGlu_5$), yet the mechanism by which $mGlu_5$ couples to the intracellular signaling pathways that regulate synaptic mRNA translation is poorly understood. In this dissertation, we show that manipulation of two novel targets, β-arrestin2 and glycogen synthase kinase 3α (GSK3α) are able to independently modulate translation downstream of $mGlu_5$. Avoiding dose-limiting consequences and unwanted side effects of globally targeting $mGlu_5$ signaling, pharmacological inhibition of these targets has the potential to provide significant advantages over first-generation $mGlu_5$ inhibitors for the treatment of FX. Finally, we show that a mouse model of 16p11.2 microdeletion disorder, a polygenic disorder known to confer risk for ASD and ID in humans, shares common features of synaptic dysfunction downstream of $mGlu_5$ with the *Fmr1* KO mouse. Chronic administration of pharmaceutical agents previously shown to restore synaptic function in the *Fmr1* KO mouse successfully corrected many biochemical, cognitive and behavioral impairments in 16p11.2 *df/+* mice supporting the hypothesis that troubled translation downstream of $mGlu_5$ may be a convergent point of dysfunction between these two genetically-defined disorders.

Thesis Supervisor: Mark F. Bear, Ph.D.
Title: Picower Professor of Neuroscience

Laura J. Stoppel

EDUCATION

Massachusetts Institute of Technology, Cambridge, MA
Ph.D., Neuroscience, Department of Brain and Cognitive Sciences, 2016

Harvard University, Cambridge, MA
B.A., Biology with a secondary in Psychology, 2008

RESEARCH EXPERIENCE

Massachusetts Institute of Technology, Cambridge, MA
Graduate Student with Dr. Mark Bear, 2011-2016

Ph.D. Thesis: *Targeting Troubled Translation: Investigating Novel Therapeutic Targets in mouse models of Fragile X and 16p11.2 Deletion Syndrome*

Harvard University, Cambridge, MA
Research Technician for Dr. Joshua R. Sanes, 2008-2011

Project: *Identifying central targets of mouse retinal ganglion cell subsets with a genetically encoded transneuronal tracer*

PUBLICATIONS

Stoppel LJ, Senter RK, Wagner, FF, Preza AR, Heynen AJ, Lewis, M, Coronado, A, Holson, E, Scolnick, E, Bear, MF. Selective Inhibition of GSK3α but not GSK3β corrects many phenotypes associated with a mouse model of Fragile X. (manuscript in preparation)

Stoppel LJ, Auerbach BD, Senter RK, Preza AR, Lefkowitz RJ, Bear MF. β-Arrestin2 couples metabotropic glutamate receptor 5 to synaptic protein synthesis in Fragile X. (in review, *Neuron*)

Stoppel LJ, Osterweil EK, Bear MF. "The mGluR theory of fragile X." *Fragile X Syndrome: From Genetics to Targeted Treatment*. Willemsen R, Kooy, F. Elsevier. (in press)

Tian D, **Stoppel LJ**, Heynen AJ, Lindemann L, Jaeschke G, Mills AA, Bear MF. Contribution of mGluR5 to pathophysiology in a mouse model of human chromosome 16p11.2 microdeletion. *Nature Neuroscience* 2015 Feb;18 (2):182-4

PRESENTATIONS

Stoppel LJ, Preza AR, Heynen AJ, Bear MF. Correction of cognitive and behavioral deficits in a 16p11.2 CNV mouse model by selective activation of GABA B receptors with R-baclofen. *Annual Meeting of the Society for Neuroscience. San Diego, CA.* November 12-16, 2016 (poster)

Stoppel LJ, Auerbach BD, Senter RK, Preza AR, Lefkowitz RJ, Bear MF. Beta Arrestin2 couples $mGlu_5$ to FMRP-regulated protein synthesis.

-Brain Lunch Seminar Series, Cambridge, MA, 2015 (lecture)
-Integrative Neuronal Systems Conference, Cambridge, MA, 2015 (poster)
-MCN Student Symposium, Cambridge, MA 2016 (lecture)
-Gordon Research Conference: Fragile X and Autism-related Disorders, Mt. Snow, VT, 2016 (poster)

Stoppel LJ, Heynen AJ, Tian D, Bear MF. Contribution of mGluR5 to hippocampal pathophysiology in a mouse model of human chromosome 16p11.2 microdeletion.

-Integrative Neuronal Systems Conference, Cambridge, MA, 2014 (poster)
-Simons Center Poster Session, Cambridge, MA, 2014 (poster)

Laura Stoppel, Xin Duan, Dawen Cai, Masahito Yamagata and Joshua Sanes. Identifying central targets of mouse retinal ganglion cell subsets with a genetically encoded transneuronal tracer. *Annual Meeting of the Society for Neuroscience. Washington DC.* November 12-16, 2011 (poster)

HONORS AND AWARDS

Graduate Women of Excellence Award Recipient, MIT (2015)
NIH Neural Learning and Memory Training Fellowship, MIT (2013-2015)
Walle Nauta Award for Continuing Dedication to Teaching, MIT (2014)
Angus MacDonald Award for Excellence in Undergraduate Teaching, MIT (2013, 2015)
NIH Integrative Neuronal Systems Training Fellowship, MIT (2011-2013)
Certificate of Distinction in Teaching from the Derek Bok Center, Harvard University (2010)
Herchel Smith Harvard Summer Undergraduate Research Fellowship (2007)
Museum of Comparative Zoology GUR Grant (2007)
Alex G. Booth '30 Fund Fellowship Recipient (2007)

TEACHING AND LEADERSHIP EXPERIENCE

MIT Graduate Resident Tutor (2012-2016)
MIT Kaufman Teaching Certificate Program (Summer 2015)
MIT Teaching Assistant for 9.01 Introduction to Neuroscience (Fall 2015)
MIT BCS Career Fair Co-Organizer (2014-2015)
MIT Teaching Assistant for 9.013 Molecular and Cellular Neuroscience II (Spring 2014)
MIT Teaching Assistant for 9.12 Neurobiology Lab (Fall 2012, Fall 2013)
MIT Teaching Lab Manager for 9.12 Neurobiology Lab (Spring 2015, Spring 2016)
MIT Fall Teuber Lecture Student Organizer and Host (Fall 2013)
MIT Brain Lunch Seminar Series Organizer (Fall, Spring 2012)
MIT NIH Integrative Neural Systems Conference Co-organizer (Summer 2012)
Harvard Head Teaching Assistant for Topics in Marine Biology Seminar (Spring 2011)
Harvard Teaching Assistant for The Foundations of Biological Diversity (Fall 2009)
Harvard Teaching Assistant for Marine Biology (Fall 2008)

Acknowledgements

First and foremost, I would like to thank my advisor, Mark Bear. His strive to not only understand fragile X but also to cure it and make a real difference in the lives of those affected is inspiring. He allowed me to take full ownership of my PhD, supported the many collaborations that I was involved with and allowed me to pursue a love of teaching while being a member of the lab. I also thank him for putting (unsubstantiated) confidence in my abilities as a budding biochemist, trusting me with the lab's radioactivity license, and tolerating my stubborn refusal to use Keynote.

I would like to thank the members of my thesis committee: Guoping Feng and Weifeng Xu for their mentorship and thoughtful advice over the years. I would especially like to thank Emily Osterweil for providing unmatched knowledge about fragile x and great mentorship as a member of my committee. I consider you a major role model and I appreciate all the time and effort you have devoted to teaching me.

I would like to thank my undergraduate mentors: Bob Woollacott for continuing mentorship and friendship, after all these years; the late Farish Jenkins for believing in me, inspiring me, and challenging me to explore my passions; and the late David Hubel for introducing me to the wonders of neuroscience and sharing his passion for music with me. I would also like to thank Josh Sanes who allowed me the opportunity to re-discover my curiosity about the brain, and Xin Duan, my post-doc mentor in the Sanes' lab, for three years of great collaboration and encouraging the pursuit of graduate school, in particular, MIT.

Much of this work was the result of a collaboration with the Broad Institute so I would like to acknowledge Ed Scolnick, Ed Holson, and Mike Lewis for compelling ideas and keen insight. In particular, I'd like to acknowledge Flo Wagner for her patience, optimism, genuine support and encouragement throughout our collaboration. I'd also like to thank our collaborators at UC Davis- Jacki Crawley and Tatiana Kazdoba-Leach for great advice regarding an impossibly challenging mutant mouse model.

Very importantly, I'd like to express my enormous appreciation for three undergrads that I had the pleasure of working with during my PhD: Anthony Preza, Jasmin Joseph-Chazan, and David Bowen. I was constantly blown away by their dedication, curiosity, independence and proficiency as young scientists.

I'd like to thank the support staff in the Bear Lab- in particular Amanda Coronado for her help with audiogenic seizures and her patience when I forgot to order things until I'd already run out. Suzanne Meagher and Nina Palisano have been incredibly helpful during my time in the Bear lab.

Many thanks to all the members of the Bear lab for amazing scientific advice and less amazing fantasy football advice. In particular, I'd like to acknowledge Becca Senter for saving the day (and our research) time and again; Rachel Schecter for keeping the grad office lively and offering constant reassurance; Ming Fai-Fong for inspiring me as a power woman in science; Aurore Thomazeau for her contagious smile and help with French; Sam Cooke for inspiring me to pay attention to semantics and double the "n"; [Slippery] Pete Finnie for so readily caving at 5PM on Thursdays and inspiring me to

embrace my inner Canadian; T-Kay Kim for being the most polite, supportive, and quiet office mate ever; Patrick McCamphill for keeping the Canadian presence strong and re-analyzing the data from Figure 3.12 after my laptop kicked the bucket, taking precious files that had not been backed up with it (lesson learned). Finally, I'd like to thank Rob Komorowski and Eitan Kaplan for keeping me simultaneously hydrated and sane and for supporting the Jets and the 49ers, respectively, both of which are equally as miserable as the Dolphins. A special thanks to Rob for hiking back up the mountain to find my ID.

I'd like to express my deepest gratitude and appreciation for Arnie Heynen who has been my fairy godfather throughout this PhD. If it weren't for Arnie, I might still be (metaphorically) stuck in the tissue culture room. Arnie has been a teacher, collaborator, mentor, editor, therapist, and most importantly, friend to me over the past 5 years. He has gone above and beyond his job description and I feel very grateful that he was in my corner throughout this PhD.

Last and anything but least, I'd like to thank my friends and family. I am so lucky to have the most amazing and supportive friends. If I were to name them all this thesis might double in size. I want to thank my Maseeh family- my fellow GRTs, the House Exec Team, Mickey and all the incredible students who have inspired me every day over the past 4 years- MIT will always feel like home.

I'd like to thank my parents, Doug and Maggie Stoppel, who have been my cheerleaders and unconditional supporters my entire life. Thank you for enthusiastically championing all my life ambitions- from rock collector to geologist, to dolphin trainer, to pediatric cardiologist, to neuroscientist, to marine biologist, to patent lawyer, back to neuroscientist, back to patent lawyer, to neuroscientist once again... don't worry- I may never figure out what I want to be when I grow up. It means a lot to me that no matter what decisions I make, you both will always have my back, 100%.

I'd like to thank my brother, David Stoppel for always being there for me. Whether I need life advice, science advice, relationship advice, technology advice, fantasy football advice- he the first one I call because I know I will receive the most meaningful guidance. Thank you for talking me off the PhD ledge time and again and thank you for being such an amazing role model.

Finally, I'd like to thank Matthew John Smith- my rock, my best friend, and my Adobe Illustrator Tutor. You're the best thing that came out of this PhD and I wouldn't have been able to make it here, to the end, without you (and your family). Thank you for always being by my side- to celebrate the highs and pull me out of the lows. You believed in me when I didn't believe in myself. Thank you for everything.

Table of Contents

Chapter 1

Aberrant protein synthesis at $mGlu_5$: a common theme in monogenic and polygenic causes of ASD

Chapter 2

β-Arrestin2 couples $mGlu_5$ to FMRP-regulated protein synthesis and is a novel target for the treatment of Fragile X

Chapter 3

Selective inhibition of GSK3α but not GSK3β corrects many phenotypes associated with a mouse model of Fragile X

Chapter 4

Selective activation of $GABA_B$ receptors with R-baclofen corrects several cognitive and behavioral deficits in a 16p11.2 CNV mouse model

Chapter 5

Implications and Future Directions

Figures

Chapter 1

Aberrant protein synthesis at $mGlu_5$:
a common theme in monogenic and polygenic causes of ASD

1.1: Introduction

Recent estimates suggest that 1 in 68 children meets the diagnostic criteria for Autism Spectrum Disorder (ASD) in the United States (Christensen, Baio et al. 2016). Characterized by (1) impairments in social communication, language, and related cognitive skills and behavioral and emotional regulation and (2) the presence of restricted, repetitive behaviors (Volkmar and Reichow 2013), ASD is a debilitating disorder for both patients and families alike. ASD is more common among males (1 in 42) than among females (1 in 189) (Christensen, Baio et al. 2016) and reported prevalence rates have been steadily rising over the past 50 years. Case in point, in 2000 it was reported that 1 in 150 children presented with ASD compared with 1 in 68 children in 2012 (Figure 1.1). It is not completely clear the extent to which this trend reflects a true increase in the prevalence of ASD rather than increased awareness and/or advances in diagnostic services. One study, which has gained further support from an analysis of sporatic autism exomes (O'Roak, Vives et al. 2012), suggests that the rising prevalence rate may be attributed to an increased *de novo* mutation rate that is positively correlated with paternal age (Hultman, Sandin et al. 2011). ASD also represents a significant economic burden to families of patients and healthcare providers alike, with the total costs per year for children with ASD in the United States in 2011 estimated to be between $11.5 - $60.9 billion dollars (Buescher, Cidav et al. 2014, Lavelle, Weinstein et al. 2014). Taken together, these alarming statistics highlight a pressing unmet need for targeted pharmacological interventions to manage the deficits associated with ASD.

1.2: Convergent pathways in autism.

Among neuropsychiatric disorders, ASDs and (highly co-morbid) intellectual disability (ID) have been identified to be some of the most heritable. Early studies of monozygotic and dizygotic twins revealed concordance rates of ~90% and 10%, respectively (Steffenburg, Gillberg et al. 1989, Bailey, Le Couteur et al. 1995). This evidence highlighted an obvious genetic component for ASD and ID, motivating research aimed at identifying genetic variants underlying risk, with the ultimate goal of

designing genetic diagnostic markers and identifying molecules for targeted drug development (Gokoolparsadh, Sutton et al. 2016). Over the past two decades, genetic association studies have identified hundreds of loci contributing to genetic risk, revealing that ASDs are highly genetically heterogeneous in nature. However, network analyses have revealed convergent pathways downstream of these heterogeneous genetic variants, some of which have gained supporting evidence from studies of animal models of known monogenic and polygenic causes of autism (Auerbach, Osterweil et al. 2011, Bhattacharya, Kaphzan et al. 2012, O'Roak, Vives et al. 2012, Barnes, Wijetunge et al. 2015, Tian, Stoppel et al. 2015, Zantomio, Chana et al. 2015, Gokoolparsadh, Sutton et al. 2016). In particular, altered function of Group 1 metabotropic glutamate receptors, specifically $mGlu_5$, and consequently, aberrant $mGlu_5$-mediated synaptic translation, has been implicated time and again, in multiple animal models of neurodevelopmental disorders associated with autism and intellectual disability (Dolen, Osterweil et al. 2007, Auerbach, Osterweil et al. 2011, Michalon, Sidorov et al. 2012, D'Antoni, Spatuzza et al. 2014, Pignatelli, Piccinin et al. 2014, Barnes, Wijetunge et al. 2015, Ebrahimi-Fakhari and Sahin 2015, Tian, Stoppel et al. 2015, Zantomio, Chana et al. 2015, Gogliotti, Senter et al. 2016). Most notably, studies using animal models of fragile X syndrome (FX), the most commonly inherited cause of intellectual disability and autism in humans (Wang, Berry-Kravis et al. 2010), have greatly enhanced our understanding of synaptic dysfunction caused by altered signaling through $mGlu_5$. Furthermore, because FX is a monogenic and highly penetrant cause of autism, it has been a useful model for investigating the pathophysiology that may apply more broadly to genetically heterogeneous ASDs.

1.3: Monogenetic causes of autism and intellectual disability: Fragile X Syndrome.

Fragile X syndrome (FX) is the most prevalent inherited monogenic cause of autism and intellectual disability, affecting 1:4000 males and 1:4000-6000 females (Turner, Webb et al. 1996, Song, Barton et al. 2003, Bailey, Raspa et al. 2008, Hagerman, Berry-Kravis et al. 2009, Budimirovic and Kaufmann 2011). Most often, FX

is caused by an expansion of GCC trinucleotide repeats in the 5'- untranslated region of the X-linked *FMR1* gene, which encodes the protein FMRP (fragile X mental retardation protein) (Pieretti, Zhang et al. 1991, Verkerk, Pieretti et al. 1991, Devys, 1993 #62, Devys, Lutz et al. 1993). Normal individuals have between 5 and 54 GCC repeats (with 29 or 30 being the most common); however, when the number of repeats exceeds 200, the *FMR1* gene is hypermethylated, leading to an epigenetic silencing of the gene, loss of FMRP, and FX (Fu, Kuhl et al. 1991, Pieretti, Zhang et al. 1991). When the number of repeats falls between 55 and 200, typically found in maternal carriers, it is referred to as fragile X premutation. In rare cases, point mutations or deletion of the *Fmr1* gene can also lead to loss of FMRP expression and FX (Coffee, Ikeda et al. 2008). Individuals with the full FX mutation have characteristic crainiofacial abnormalities that often result in a long thin face with prominent ears as well as enlargement of the testes (macroorchidism). They are also prone to seizure disorders, as well as behavioral phenotypes including hyperactivity, attention deficit disorders, mild to severe intellectual disability, learning disorders, hyperarousal to sensory stimuli, anxiety, and autism (Tsiouris and Brown 2004, Garber, Visootsak et al. 2008, Hagerman, Berry-Kravis et al. 2009). Significant progress has been made over the past 30 years in understanding the important role that FMRP plays in cellular processes as well as the functional and molecular consequences caused by the loss of FMRP in FX. Integral to this progress in our understanding of the synaptic pathophysiology of FX has been the use of animal models of FX, most notably, the *Fmr1* KO mouse model.

1.4: Animal models of Fragile X Syndrome.

The *Fmr1* KO mouse, developed by the Dutch-Belgian Fragile X Consortium in 1994, remains the most widely studied animal model of FX today and has greatly advanced our understanding of the pathophysiology of this complex disorder (Bakker, Verheij et al. 1994). Initial investigation of the *Fmr1* KO mouse was directed at identifying pathogenic phenotypes, in particular, common features that the mouse model shares with humans afflicted with FX. In the seminal paper characterizing the *FMR1* KO mouse, it was revealed that male mice exhibit enlarged testes similar to

human males with FX, as well as hyperactivity and impaired cognitive function (Bakker, Verheij et al. 1994). Further similarities have since been identified, including hyperarousal to sensory stimuli and network hyperexcitability (Gibson, Bartley et al. 2008, Olmos-Serrano, Paluszkiewicz et al. 2010, Zhang and Alger 2010); epileptiform activity and a resulting increased susceptibility to seizures (Musumeci, Hagerman et al. 1999, Musumeci, Bosco et al. 2000, Musumeci, Ferri et al. 2001, Osterweil, Chuang et al. 2013); deficits in social interaction (Liu and Smith 2009); as well as learning and memory impairments (Qin, Kang et al. 2002, Zhao, Toyoda et al. 2005, Brennan, Albeck et al. 2006, Dolen, Osterweil et al. 2007). *Fmr1* KO mice also exhibit increased dendritic spine density, with a shift towards predominantly thin, immature spines, characteristic of spine abnormalities that are a hallmark of FX in humans (Hinton, Brown et al. 1991, Comery, Harris et al. 1997, Irwin, Galvez et al. 2000, Irwin, Patel et al. 2001). Despite a plethora of common features shared (to some degree) between the *Fmr1* KO mouse and humans with FX, there are some phenotypes that seem to be opposing. Most notably, while patients with FX most often exhibit severe generalized anxiety, *Fmr1* KO mice exhibit decreased anxiety-like behavior in tests designed to assess general anxiety such as the elevated plus maze and open field exploration assay (Li, Zhang et al. 2001, Yuskaitis, Mines et al. 2010, Liu, Chuang et al. 2011, Chen, Sun et al. 2013). Interestingly, one compelling theory suggests that these behavioral paradigms, designed to be measures of anxiety in mice, may otherwise be measuring impulsivity or deficits in executive function (Liu and Smith 2014). In 2000, a *Drosophila* model of FX was generated upon the discovery of *dfmr1*, the invertebrate correlate of the *Fmr1* gene (Wan, Dockendorff et al. 2000). More recently, a zebrafish model lacking *Fmr1* was generated and characterized, as well as two distinct rat models of FX (den Broeder, van der Linde et al. 2009, Hamilton, Green et al. 2014, Till, Asiminas et al. 2015). It is likely that investigation of the *Fmr1* KO rat models will offer added insight into our understanding of FX that has not been possible with the mouse model, particularly in disease-relevant complex behaviors and network-level dysfunctions. Although animal models provide a means for direct manipulation and probing of gene function, there are obvious limitations to the conclusions we can

reasonably make about FX in humans, particularly regarding cognition, complex behavior, and social interaction. Nonetheless, these animal models have not only led to the identification of common phenotypes between mice and humans lacking *Fmr1*, they have also generated an overwhelming wealth of literature dissecting the role of FMRP and more generally, the synaptic pathophysiology of FX (to be discussed in this and later chapters).

1.5: FMRP negatively regulates translation.

Fragile X mental retardation protein (FMRP) is an RNA binding protein (RBP) that is highly expressed in the brain and the testes (Ashley, Wilkinson et al. 1993, Bachner, Steinbach et al. 1993, Devys, Lutz et al. 1993, Hinds, Ashley et al. 1993). In the post-natal brain, FMRP is found in neurons and mature astrocytes (Gholizadeh, Halder et al. 2015), and within neurons, it is found in the soma, spines, and dendrites (Weiler, Irwin et al. 1997, Na, Park et al. 2016). FMRP largely plays an inhibitory role in synaptic protein synthesis, most often repressing (although not always) translation of its target mRNAs, which represent ~4% of the mRNAs transcribed in the brain (Chen, Yun et al. 2003, Miyashiro, Beckel-Mitchener et al. 2003, Santoro, Bray et al. 2012). FMRP contains three RNA binding domains: two of the domains are hnRNP K-homology KH domains and the third is an RGG box. The variety of binding domains allows FMRP to selectively bind to a broad range of mRNA targets (Sethna, Moon et al. 2014). FMRP also contains a nuclear localization signal and nuclear export signal, which enable FMRP to transport nuclear-bound mRNAs to the cytoplasm (Eberhart, Malter et al. 1996). Protein interaction domains also allow FMRP to associate with polyribosomes, supporting the role of FMRP as a regulator of synaptic protein synthesis (Feng, Absher et al. 1997, Napoli, Mercaldo et al. 2008). Taken together, the structure and features of FMRP, including multiple binding domains for mRNAs, support its role as a regulator of translation, specifically at the synapse. However, the mechanism(s) by which FMRP achieves this translational regulation remain controversial.

1.6: Mechanisms of translational regulation by FMRP.

As mentioned previously, it is now appreciated that FMRP is an RNA binding protein that predominantly negatively regulates protein synthesis at the synapse (Chen, Yun et al. 2003, Miyashiro, Beckel-Mitchener et al. 2003, Santoro, Bray et al. 2012). Some activity-regulated translational control pathways, such as the ERK and mTOR pathways that regulate translation initiation or eEF2 activation involved in translation elongation, have been identified (Sutton, Taylor et al. 2007, Hoeffer and Klann 2010, Osterweil, Krueger et al. 2010). However, the precise mechanism by which FMRP achieves translational control is still under investigation. The majority of FMRP co-sediments with polyribosomes in proximal dendrites (Tamanini, Meijer et al. 1996, Feng, Gutekunst et al. 1997, Ceman, O'Donnell et al. 2003, Khandjian, Huot et al. 2004). Additionally, a missense mutation in the 1304N binding domain of FMRP prohibits association with polyribosomes, leading to FX in both humans and the *Fmr1* KO mouse model (De Boulle, Verkerk et al. 1993, Feng, Absher et al. 1997, Zang, Nosyreva et al. 2009). Taken together, these observations support a role for FMRP in the repression of the elongation step of translation. This hypothesis received strong support in 2011, when the Darnell group used high-throughput sequencing of RNAs isolated by crosslinking immunoprecipitation (HITS-CLIP) to identify FMRP interactions with polyribosomal mRNAs in the mouse brain. In addition to identifying 842 unique mRNA targets of FMRP, they demonstrated that FRMP is associated with transcripts on which ribosomes were stalled (Darnell, Van Driesche et al. 2011). According to their model, which remains widely accepted, FMRP reversibly represses translation in a complex that consists of target mRNAs and stalled ribosomes (Figure 1.2). Thus, the loss of a "translational brake" on the synthesis of synaptic proteins that are targets of FMRP is pathogenic in FX (Darnell, Van Driesche et al. 2011, Bhakar, Dolen et al. 2012). Another hypothesis suggests that FMRP represses the initiation step of translation by recruiting cytoplasmic FMRP-interacting protein (CYFIP1), which consequently blocks the formation of the eIF4F complex thus preventing cap-dependent initiation of translation (Napoli, Mercaldo et al. 2008). However, the *in vivo* relevance of this association has been questioned, due to the observation that vast majority of FMRP is associated with polyribosomes (Stefani, Fraser et al. 2004, Wang, Iacoangeli et al.

2005, Iacoangeli, Rozhdestvensky et al. 2008, Iacoangeli, Rozhdestvensky et al. 2008, Darnell, Van Driesche et al. 2011).

1.7: Dysregulation of synaptic protein synthesis in the *Fmr1* KO mouse has functional consequences on synaptic plasticity.

Given the role of FMRP as a suppressor of translation, one of the hallmark phenotypes of the *Fmr1* KO mouse that has been elucidated is elevated rates of basal protein synthesis. This was first shown in the mouse hippocampus *in vivo* using autoradiography (Qin, Kang et al. 2005) (Figure 1.3A). Interestingly, the same group observed decreased rates of cerebral protein synthesis (rCPS) in human patients with FX using PET imaging. However, it was believed that this was due to the use of propofol to sedate FX patients prior to imaging, as a similar decrease in rCPS was observed in *Fmr1 KO* mice treated with propofol (Qin, Schmidt et al. 2013). Nonetheless, elevated rates of translation in the *Fmr1* KO mouse hippocampus and cortex have been observed using a number of different labeling techniques, by multiple independent research groups (Dolen, Osterweil et al. 2007, Muddashetty, Kelic et al. 2007, Osterweil, Krueger et al. 2010, Bhattacharya, Kaphzan et al. 2012, Henderson, Wijetunge et al. 2012, Barnes, Wijetunge et al. 2015). Even prior to the observation that cerebral protein synthesis was elevated in the *Fmr1* KO mouse, the functional consequences of the loss of FMRP at the synapse were being investigated. Based on evidence that FMRP, *Fmr1* mRNA and polyribosomes were all found at the base of dendritic spines, it was theorized that FMRP may provide an integral substrate for the structural changes necessary for protein-synthesis-dependent forms of synaptic plasticity including long-term potentiation (LTP) and long-term depression (LTD), the functional correlates of learning and memory (Kang and Schuman 1996, Weiler and Greenough 1999, Huber, Kayser et al. 2000). Surprisingly, initial investigation of the *Fmr1* KO mouse revealed that late-phase LTP, which is protein-synthesis dependent, was normal in CA1 of the mouse hippocampus (Godfraind, Reyniers et al. 1996, Paradee, Melikian et al. 1999). Based on the observation that FMRP is synthesized upon activation of group 1 mGluRs with the agonist DHPG as well as the finding that

local *de novo* protein synthesis was required for stable expression of late-phase LTD induced by activation of group 1 mGluRs with DHPG, it was hypothesized that mice lacking FMRP may have impaired mGluR-LTD (Weiler and Greenough 1999, Huber, Kayser et al. 2000, Huber, Roder et al. 2001, Snyder, Philpot et al. 2001, Huber, Gallagher et al. 2002). Indeed, mGluR-LTD was found to be significantly altered in CA1 of the hippocampus of *Fmr1* KO mice. Surprisingly however, the magnitude of LTD was greatly enhanced rather than diminished (Figure 1.3B) (Huber, Gallagher et al. 2002). Furthermore, mGluR-LTD was not blocked by the protein synthesis inhibitor anisomycin in the *Fmr1* KO mouse, indicating that long-term changes in synaptic plasticity persist in the absence of FMRP, even without *de novo* protein synthesis (Nosyreva and Huber 2006). Of course, we can now appreciate that augmented mGluR-LTD would be expected and likely be independent of new protein synthesis in the *Fmr1* KO mouse, given the exaggerated rate of translation due to a loss of FMRP.

In order to make direct comparisons between observations of elevated rates of protein synthesis in the *Fmr1* KO mouse and the functional consequences of this aberrant translation, it is imperative to match the experimental conditions between metabolic labeling assays and electrophysiological recordings as closely as possible. Osterweil et. al (2010) developed a metabolic labeling protocol that models methods used in electrophysiology recordings, with age-matched animals and comparable slice recovery conditions. They confirmed, similar to prior reports, that a 4 hr post-slicing recovery period is optimal to achieve stability of the slice and maximize rates of synaptic protein synthesis (Figure 1.3C) (Whittingham, Lust et al. 1984, Kirov, Sorra et al. 1999, Huber, Roder et al. 2001, Ho, Delgado et al. 2004, Sajikumar, Navakkode et al. 2005, Osterweil, Krueger et al. 2010). Therefore, for all metabolic labeling and electrophysiology experiments described in Chapters 2-4, conditions were carefully designed and monitored to allow for reliable comparisons between biochemical readouts of protein synthesis and signaling pathway activation and electrophysiological readouts of changes in synaptic plasticity.

1.8: The mGluR theory of FX.

It had long been established that Group 1 mGluRs are potent regulators of protein synthesis (Weiler and Greenough 1993, Job and Eberwine 2001, Todd, Mack et al. 2003). This knowledge, along with the observation that mGluR-LTD in CA1 of the *Fmr1* KO mouse hippocampus is exaggerated and no longer dependent on *de novo* protein synthesis, led to the mGluR theory of FX (Bear, Huber et al. 2004). The fact that mGluR-LTD was maintained even in the absence of *de novo* protein synthesis suggested that "plasticity proteins" necessary for the induction and maintenance of LTD were already present in sufficient abundance in the *Fmr1* KO mouse. While the identity of such plasticity proteins are still being elucidated, candidate proteins including activity-regulated cytoskeletal protein (Arc) (Busquets-Garcia, Gomis-Gonzalez et al.), microtubule associated protein 1β (Map1β), and α calcium/calmodulin-dependent kinase II (αCAMKII) are reportedly upregulated in the *Fmr1* KO mouse (Zalfa, Giorgi et al. 2003). In particular, glutamate-induced Arc translation has been shown to co-localize with FMRP, indicating that when FMRP is absent, Arc translation is not in check (Na, Park et al. 2016). Furthermore, evidence suggests that Arc primes CA1 pyramidal neurons for the induction of mGluR-LTD, strongly implicating Arc as an important plasticity protein regulated by FMRP (Waung, Pfeiffer et al. 2008, Niere, Wilkerson et al. 2012, Jakkamsetti, Tsai et al. 2013). The mGluR theory of FX proposed that in WT mice, synthesis of FMRP in response to mGluR activation acts as a brake on mGluR-LTD, keeping protein synthesis in check, and allowing the synapse to respond appropriately to the next stimulus. In the *Fmr1* KO mouse, the brake is lifted resulting in aberrant signaling and augmented LTD (Bear, Huber et al. 2004). The mGluR theory hypothesized that inappropriate signaling through mGluRs might explain many deficits shared between the *Fmr1* KO mouse and humans with FX. Intriguingly, many of the shared impairments, including epilepsy or heightened sensitivity to seizures, cognitive impairments and abnormal spine morphology, are all protein synthesis-dependent (Merlin, Bergold et al. 1998, Huber, Kayser et al. 2000, Raymond, Thompson et al. 2000, Snyder, Philpot et al. 2001, Vanderklish and Edelman 2002, Zho, You et al. 2002, Stoop, Conquet et al. 2003). Furthermore, it suggested important implications for potential treatments for FX. In particular, it suggested that dampening signaling through

mGluRs, such as with the $mGlu_5$ antagonist MTEP, could be beneficial in treating many of the impairments that are protein synthesis-dependent in patients with FX (Bear, Huber et al. 2004).

1.9: Signaling pathways involved in the pathology of FX.

Signaling through $mGlu_5$, a G_q coupled receptor, activates phospholipase C (PLC), which activates protein kinase C (PKC) as well as other signal transduction pathways necessary for important cellular processes (Figure 1.4) (Nicoletti, Valerio et al. 1988, Dudek and Bear 1989, Houamed, Kuijper et al. 1991, Masu, Tanabe et al. 1991, Schoepp and Conn 1993). Interestingly, blocking PKC activation, inhibition of PLCβ, or depletion of intracellular Ca^{2+} stores does not prevent the induction of mGluR-LTD, implying that G_q signaling is not coupled to the synaptic translational machinery necessary for this protein synthesis-dependent form of plasticity (Schnabel, Kilpatrick et al. 1999, Fitzjohn, Palmer et al. 2001, Rush, Wu et al. 2002, Mockett, Guevremont et al. 2011). Rather, the induction of mGluR-LTD is blocked by inhibition of two other intracellular signaling pathways, which we now appreciate are coupled to cap-dependent translation by regulating translation initiation at the synapse: (1) the extracellular signal-regulated kinase (ERK) pathway and (2) the mammalian target of rapamycin (mTOR) pathway (Figure 1.5) (Gallagher, Daly et al. 2004, Hou and Klann 2004). Although many groups have probed the involvement of the ERK and mTOR pathways in the pathophysiology of FX, there have been conflicting observations in the literature. While some groups observe a basal increase in ERK activation in the *Fmr1* KO mouse (Hou, Antion et al. 2006, Price, Rashid et al. 2007, Michalon, Sidorov et al. 2012), others have seen no difference in basal activation of ERK between WT and *Fmr1* KO mice (Hu, Qin et al. 2008, Gross, Nakamoto et al. 2010, Osterweil, Krueger et al. 2010, Liu, Huang et al. 2012). Still another group observed that mGluR stimulation induced an aberrant dephosphorylation of ERK in *Fmr1* KO cortical synaptoneurosomes (Kim, Markham et al. 2008). Similarly, some have observed a basal increase in AKT-mTOR signaling in the *Fmr1* KO mouse that appears saturated, occluding further activation upon stimulation of mGluR (Gross, Nakamoto et al. 2010, Sharma, Hoeffer et

al. 2010), while others find basal AKT-mTOR signaling is indistinguishable from WT mice (Osterweil, Krueger et al. 2010, Michalon, Sidorov et al. 2012). One study (Osterweil, Krueger et al. 2010) set out to examine the role of ERK and mTOR under the same experimental conditions used to induce mGluR-LTD and found no evidence for altered signaling under basal or mGluR-stimulated conditions in either pathway. While application of the mGluR-agonist DHPG activated the ERK pathway in both WT and *Fmr1* KO hippocampal slices, it had no effect on activation of either AKT or mTOR. Furthermore, elevated protein synthesis in the *Fmr1* KO mouse could be restored to WT levels by inhibition of either $mGlu_5$ or ERK but was unaffected by inhibition of mTOR. Taken together, this suggests that exaggerated protein synthesis in the *Fmr1* KO mouse is not caused by increased activation of $mGlu_5$, but rather a hypersensitivity of the translational machinery to $mGlu_5$ and ERK signaling specifically.

1.10 Correction of phenotypes in the *Fmr1* KO mouse model.

Since the original publication of the mGluR theory of FX in 2004, countless observations have been made supporting the hypothesis that downregulation of signaling through $mGlu_5$ may be therapeutically beneficial in treating some of the aberrant phenotypes associated with the *Fmr1* KO mouse. A number of strategies have been investigated, including directly targeting the receptor itself (either genetically or pharmacologically), as well as manipulation of signaling pathways downstream of $mGlu_5$, known to be involved in translation.

1.10.1: Correcting FX: targeting $mGlu_5$.

The seminal study investigating a "correction" of FX phenotypes in mice directly tested the mGluR theory of FX in a proof of principle approach. *Fmr1*$^{+/-}$ females were mated to *Grm5*$^{+/-}$ males, which lack a copy of the *Grm5* gene, which encodes $mGlu_5$. The rationale was that in male offspring lacking both the *Fmr1* gene and one copy of *Grm5*, reduction of $mGlu_5$ expression would downregulate $mGlu_5$ signaling. If the mGluR theory of FX was correct, this genetic reduction strategy should ameliorate many of the pathogenic phenotypes seen in the *Fmr1* KO mouse. Indeed, this genetic cross strategy seemed beneficial in rescuing many synaptic functions known to be aberrant in

the *Fmr1* KO mouse, including excessive protein synthesis, exaggerated mGluR-LTD, susceptibility to audiogenic seizure, and cognitive deficits in a passive avoidance task, in addition to other deficits (Dolen, Osterweil et al. 2007). One significant caveat of this proof of principle approach was that $mGlu_5$ expression was reduced embryonically, persisting postnatally. In humans with FX, reduction of signaling through $mGlu_5$ would necessarily occur pharmacologically, even if diagnosed in infancy. Along those lines, the genetic reduction strategy did not allow an opportunity to evaluate whether post-natal downregulation of $mGlu_5$ signaling would show any therapeutic benefit. To evaluate these limitations, many studies have validated that acute administration of MPEP, an $mGlu_5$ antagonist is effective in treating many deficits and pathogenic phenotypes in the *Fmr1* KO mouse (see Table 1.1 for a complete list of preclinical studies investigating $mGlu_5$ modulation in the *Fmr1* KO mouse) (Aschrafi, Cunningham et al. 2005, Chuang, Zhao et al. 2005, Koekkoek, Yamaguchi et al. 2005, Yan, Rammal et al. 2005, Nakamoto, Nalavadi et al. 2007, de Vrij, Levenga et al. 2008, Min, Yuskaitis et al. 2009, Osterweil, Krueger et al. 2010, Suvrathan, Hoeffer et al. 2010, Hays, Huber et al. 2011, Levenga, Hayashi et al. 2011, Meredith, de Jong et al. 2011, Su, Fan et al. 2011, Thomas, Bui et al. 2012, Vinueza Veloz, Buijsen et al. 2012). Another study investigated chronic or acute administration of CTEP, a selective allosteric antagonist of $mGlu_5$ with a longer duration of action than MPEP, in post-adolescent mice. They found that acute CTEP treatment corrected elevated protein synthesis and deficits in mGluR-LTD, and reduced the incidence of audiogenic seizures. Chronic administration of CTEP rescued cognitive deficits, auditory hypersensitivity, aberrant spine density and overactive ERK and mTOR signaling, as well as partial correction of phenotypic macroorchidism (Michalon, Sidorov et al. 2012). Taken together these studies motivated the hypothesis that direct manipulation of $mGlu_5$, even in adulthood, could be a useful therapeutic target in humans with FX. Unfortunately, while pre-clinical studies have produced results which are quite promising, clinical trials have not been met with comparable success.

1.10.2: Correcting FX: targeting the Ras-ERK and mTOR pathways.

As discussed previously, there is convincing evidence that the ERK and mTOR pathways are coupled to the translation initiation machinery downstream of $mGlu_5$ and may contribute to the synaptic pathophysiology of FX. As such, it has been hypothesized that directly (or indirectly) targeting these pathways may hone in on a disease relevant target, offering potential therapeutic advantages over global modulation of $mGlu_5$. Direct inhibition of ERK1/2 with U0126 as well as inhibition of Ras farnesylation (upstream of ERK1/2) using FDA-approved Lovastatin, have been successful at rescuing many deficits in the *Fmr1* KO mouse, including aberrant protein synthesis and mGluR-LTD, prolonged epileptiform discharges and enhanced audiogenic seizures (see Table 1.2) (Osterweil, Krueger et al. 2010, Osterweil, Chuang et al. 2013). Other groups have looked at manipulation of the mTOR pathway as a potential target for treating FX. Interestingly, one group found that enhancing mTOR signaling via a genetic reduction of *Tsc2*, a negative regulator of mTOR, led to improvements in cognitive and synaptic dysfunction in the *Fmr1* KO mouse (Auerbach, Osterweil et al. 2011). Other groups have found that reducing mTOR signaling, which has been shown to be overactive in the *Fmr1* KO mouse in some preparations, by either pharmacological inhibition of mTOR or a genetic reduction (or pharmacological inhibition) of the downstream target p70 S61 Kinase, is also effective in correcting a number of FX phenotypes (see Table 1.2 for a full list) (Osterweil, Krueger et al. 2010, Bhattacharya, Kaphzan et al. 2012, Busquets-Garcia, Gomis-Gonzalez et al. 2013, Bhattacharya, Mamcarz et al. 2016). It is interesting to note that although pre-clinical reports have suggested that both ERK1/2 or mTOR may be viable targets for pharmacological intervention in FX, thus far only the inhibitor of Ras farnesylation, Lovastatin, has shown promise in clinical trials with FX patients (Caku, Pellerin et al. 2014, Pellerin, Caku et al. 2016).

1.10.3: Correcting FX: targeting GSK3α/β.

Lithium, a mood stabilizer that had been traditionally used to treat bipolar disorder, has shown promise as a therapeutic intervention for patients with FX in an open-label clinical trial (Berry-Kravis, Sumis et al. 2008). At the time, mechanistic benefit was misattributed to the effects of Lithium as an inhibitor of phospholipase C and

inositol signaling downstream of $mGlu_5$ activation. It has since been revealed that the disease-relevant target of lithium is glycogen synthase kinase-3 (GSK3), a serine/threonine kinase initially identified as an enzyme important for glycogen synthesis (Embi, Rylatt et al. 1980). It is now well established that GSK3 is involved in a number of important fundamental processes including gene expression, apoptosis and microtubule dynamics, and altered GSK3 signaling has been implicated in the pathogenesis of a number of neuropsychiatric conditions including mood disorders, schizophrenia, and Alzheimer's disease (Grimes and Jope 2001). GSK3 has two paralogs, GSK3α and GSK3β, which are negatively regulated by phosphorylation (GSK3α at Ser21, GSK3β at Ser9) (Woodgett 1990). Accumulating evidence suggests that GSK3 paralogs play a crucial role in the pathogenesis of FX phenotypes in the *Fmr1* KO mouse. GSK3β is a target of FMRP (Darnell, Van Driesche et al. 2011), and the inhibitory serines of both GSK3α and GSK3β are hypoactive in the *Fmr1* KO mouse, implying overactive GSK3α/β may be pathogenic in FX (Min, Yuskaitis et al. 2009, Yuskaitis, Mines et al. 2010, Liu, Chuang et al. 2011, Guo, Murthy et al. 2012). Indeed, inhibition of GSK3α/β with either lithium or non-specific GSK3 inhibitors corrects a multitude of synaptic and cognitive deficits (Table 1.3) in the *Fmr1* KO mouse, including excessive protein synthesis, indicating that GSK3α/β is either directly or indirectly coupled to translation (Min, Yuskaitis et al. 2009, Mines, Yuskaitis et al. 2010, Yuskaitis, Mines et al. 2010, Choi, Schoenfeld et al. 2011, Liu, Chuang et al. 2011, Guo, Murthy et al. 2012, Liu, Huang et al. 2012, Chen, Sun et al. 2013, King and Jope 2013, Chen, Lu et al. 2014, Franklin, King et al. 2014). Interestingly, acute MPEP treatment reduces aberrant GSK3 signaling in *Fmr1* KO mice and dual administration of MPEP with lithium did not show additive benefit implying that MPEP and GSK3 may be acting within the same signaling pathway (Yuskaitis, Mines et al. 2010).

1.10.4: Correcting FX: other targets.

A number of other rescue strategies have seen success in pre-clinical investigations as relevant targets for therapeutic intervention in FX. Targeting $mGlu_5$ has proven to be more efficacious than targeting other G-coupled receptors known to be dysregulated in FX (Volk, Pfeiffer et al. 2007), including another group 1 GPCR, $mGlu_1$,

or muscarinic receptors M1 and M4 (Thomas, Bui et al. 2011, Veeraragavan, Bui et al. 2011, Veeraragavan, Bui et al. 2011, Thomas, Bui et al. 2012, Veeraragavan, Graham et al. 2012). Another strategy which has seen success not only in the *Fmr1* KO mouse but in clinical trials as well, is increasing gamma-aminobutyric acid (GABA) signaling. Impaired $GABA_A$ expression and GABAergic signaling has been implicated in the pathophysiology of FX (El Idrissi, Ding et al. 2005, D'Hulst, De Geest et al. 2006, Selby, Zhang et al. 2007, Centonze, Rossi et al. 2008, Curia, Papouin et al. 2009, D'Hulst, Heulens et al. 2009, Pacey, Heximer et al. 2009, Adusei, Pacey et al. 2010, Olmos-Serrano, Paluszkiewicz et al. 2010, Pacey, Tharmalingam et al. 2011, Heulens, D'Hulst et al. 2012, He, Nomura et al. 2014, Martin, Corbin et al. 2014, Braat, D'Hulst et al. 2015, Wahlstrom-Helgren and Klyachko 2015, Zhao, Wang et al. 2015, Martin, Martinez-Botella et al. 2016). Supporting this observation, administration of R-baclofen, a $GABA_B$ agonist, has improved many phenotypic deficits in the *Fmr1* KO mouse (Table 1.4) (Henderson, Wijetunge et al. 2012, Qin, Huang et al. 2015). Other rescue strategies have targeted genetic deletion of scaffolding proteins downstream of either $mGlu_5$ (Homer1a) or GPCRs more generally (RGS4) (Pacey, Heximer et al. 2009, Ronesi, Collins et al. 2012, Guo, Molinaro et al. 2016) as well as modulation of select targets of FMRP including AβPP, Matrix Metalloproteinase 9 (MMP9), the big potassium channel BK_{CA}, PI3K enhancer (PIKE), and the PI3K catalytic subunit p110β (Gross, Nakamoto et al. 2010, Sharma, Hoeffer et al. 2010, Westmark, Westmark et al. 2011, Gkogkas, Khoutorsky et al. 2014, Sidhu, Dansie et al. 2014, Gross, Chang et al. 2015, Gross, Raj et al. 2015, Deng and Klyachko 2016).

1.11: From mice to men: clinical trials for FX.

The overwhelming success in correcting a wide range of phenotypic deficits in the *Fmr1* KO mouse in pre-clinical studies has motivated a number of early proof-of-concept clinical trials and subsequent larger, later phase trials investigating similar targeted interventions in patients with FX. Two open-label studies, one investigating the safety and efficacy of lithium, the other lovastatin in FX, were inspired by studies in *Fmr1* KO animal models (McBride, Choi et al. 2005, Berry-Kravis, Sumis et al. 2008,

Osterweil, Chuang et al. 2013, Caku, Pellerin et al. 2014, Pellerin, Caku et al. 2016). Chronic lithium treatment resulted in significant improvement in behavioral scales, verbal memory, and abnormal ERK activation rates, all secondary outcome measures, but failed to show more than mild improvement on the ABC-C Irritability Subscale, the study's primary endpoint (Berry-Kravis, Sumis et al. 2008). Chronic administration of Lovastatin has seen more promising outcomes. Significant improvement was demonstrated on pre-defined behavioral scales, including a recently-developed behavioral scale tailored to patients with FX, with the study meeting both primary and secondary endpoints (Caku, Pellerin et al. 2014). Additionally, elevated phosphorylated ERK1/2 levels in FX platelets were normalized upon treatment with Lovastatin (Pellerin, Caku et al. 2016). Despite promising preliminary outcomes and observations that the drug was well tolerated with minimal side effects, others have cautioned the use of this targeted treatment. Lovastatin is an FDA-approved statin, originally intended to manage high cholesterol. Lowering cholesterol in males with FX, a group observed to have pathologically low baseline cholesterol levels, could lead to unintended negative consequences (Berry-Kravis, Levin et al. 2015). A pilot randomized, double-blind, placebo-controlled crossover trial using minocycline, an antibiotic that inhibits overexpressed synaptic MMP9, a known target of FMRP, has also shown promise in the clinic. Chronic minocycline treatment demonstrated mild global clinical improvement as well as a significant reduction in MMP levels in the blood of responders (Dziembowska, Pretto et al. 2013, Leigh, Nguyen et al. 2013). Treatment with the $GABA_B$ agonist R-baclofen (STX209) in a phase II double-blind placebo-controlled crossover trial showed improvement over placebo in measures of social withdrawal and parent-identified "problem behaviors", prompting a larger phase III placebo-controlled trial in adults and adolescents with FX (Berry-Kravis, Hessl et al. 2012). Despite showing significant improvements on various behavioral scales and meeting secondary endpoints, the study fell short of meeting its primary outcome measure of social withdrawal (Gross, Hoffmann et al. 2015). Perhaps most disappointing, based on the optimism generated by the multitude of studies providing pre-clinical validation in the *Fmr1* KO mouse model, has been the failure of $mGlu_5$ inhibitors in clinical trials.

Multiple negative modulators of $mGlu_5$ have been developed and investigated in patients with FX. Treatment with fenobam, basimglurant (AFQ056; Roche), or mavoglurant (RO4917523; Novartis), all negative allosteric modulators of $mGlu_5$, have demonstrated no therapeutic benefit in patients with FX and have ultimately failed to achieve FDA approval (Scharf, Jaeschke et al. 2015).

1.12: Failure in the clinic and what we can learn.

Thus far, pre-clinical targets identified by investigation of animal models of FX have not successfully translated to therapeutically beneficial treatments for behavioral and cognitive impairments in patients with FX. This raises a number of possibilities that are important to evaluate prior to the development and evaluation of the next generation of drugs for FX. One obvious possibility is that current interventions are missing the disease relevant target(s) in FX. While the evidence implicating troubled translation downstream of $mGlu_5$ in the absence of FMRP is compelling, perhaps the mGluR theory of FX is overly simplistic and other receptors are equally relevant to the disease pathophysiology. Studies in the *Fmr1* KO mouse do not support this conclusion thus far (Thomas, Bui et al. 2011, Veeraragavan, Bui et al. 2011, Veeraragavan, Bui et al. 2011, Thomas, Bui et al. 2012, Veeraragavan, Graham et al. 2012). A more compelling possibility is that targeting global $mGlu_5$ signaling, either by direct modulation of the receptor (as with fenobam, basimglurant, and mavogurant) or by modulating glutamatergic signaling through $mGlu_5$ (as with R-baclofen) is too broad of a target. As discussed previously, activation of $mGlu_5$, a G_q coupled receptor, initiates a wide variety of signaling pathways, most of which are not relevant to the pathophysiology of FX. Global inhibition of $mGlu_5$ signaling certainly inhibits unintended targets, many of which are crucial for fundamental cellular processes unrelated to synaptic translation. For instance, $mGlu_5$ is known to be physically and indirectly coupled to NMDA receptors, which are vital for protein synthesis-independent synaptic function and plasticity (Collett and Collingridge 2004, Okubo, Kakizawa et al. 2004, Chen, Liao et al. 2011). The ideal target would be one that physically couples glutamatergic activation of $mGlu_5$ to the translational machinery, bypassing unintended canonical signaling pathways.

Furthermore, although initial suppression of the disease-relevant pathway may be effective in normalizing synaptic processes, it could consequently trigger inadvertent modulation of non-disease-relevant signaling pathways via a homeostatic mechanism, thus preserving pathological signaling. This possibility would be corroborated by observations that the $mGlu_5$ allosteric modulator CTEP exhibits tolerance in certain assays upon chronic administration (see Chapter 3).

Regardless, there are notable obstacles inherent in clinical trial design and regulatory guidelines which have impeded the ability of drugs for the treatment of FX to successfully gain FDA approval as well. Although FX (and more generally speaking, ASD) is largely a neurodevelopmental disorder, the FDA requires proof of efficacy in adults before studying children. Other potentially significant trial design issues in FX trials include limitations on dosing windows; regulations preventing evaluation over the length of treatment that may be necessary to exhibit efficacy; a need for better measures of cognitive or behavioral interventions that are specific to children who may exhibit severe intellectual disability and may be incapable of verbal communication; a need for more sensitive and more relevant biomarkers, including biomarkers that measure known disease-pertinent consequences; and a need for more relevant functional outcome measures (Berry-Kravis, Hessl et al. 2013, Gross, Hoffmann et al. 2015).

1.13: Beta arrestins: a scaffold for Ras-ERK and modulator of signaling.

Honing in on the disease-relevant targets in the pathology of FX could lead to better targeted-drug development and greater success in restoring social, behavioral and cognitive impairments in clinical trials. Indirect inhibition of the ERK signaling pathway has yielded promising results in pre-clinical and clinical studies (Osterweil, Chuang et al. 2013, Caku, Pellerin et al. 2014, Pellerin, Caku et al. 2016). However, there are significant concerns regarding global inhibition of Ras farnesylation in patients with FX (Berry-Kravis, Levin et al. 2015). The ideal target would be one that couples $mGlu_5$ activation to synaptic translation but leaves G-protein-dependent signaling unaltered. β-arrestins are adaptor proteins that are important for the regulation of G-

protein coupled receptors (GPCRs), and have been shown to be directly involved in G-protein-independent signaling pathways. Recently, many studies have shown a functional divergence of β-arrestin isoforms in GPCR function (Srivastava, Gupta et al. 2015). Specifically, at the Angiotensin II receptor, β-arrestin2 has been shown to recruit the ERK pathway in a manner that is both temporally and spatially distinct from G-protein dependent ERK activation (DeWire, Kim et al. 2008, Ahn, Kim et al. 2009). As discussed above, G-protein-independent ERK signaling (but not ERK activation downstream of GPCR activation) is required for mGluR-dependent protein synthesis and synaptic plasticity. Therefore, the possibility exists that downregulation of the β-arrestin isoform(s) specifically involved in G-protein-independent signaling at $mGlu_5$ may restore normal translation in the absence of FMRP.

1.14: Breaking down Lithium: GSK3α and GSKβ.

Inhibition of GSK3α/β with either lithium or non-specific GSK3 inhibitors has shown promise in treating pathogenic phenotypes in the *Fmr1* KO mouse model (see Table 1.3) and in an open-label clinical trial, FX patients chronically treated with lithium showed moderate improvements in a number of outcomes (Berry-Kravis, Sumis et al. 2008). Although GSK3α and GSK3β are commonly referred to as isoforms, they are actually paralogs, derived from different genes. GSK3α and GSK3β share 85% overall sequence homology and 98% amino acid sequence identity within their kinase domains; however, GSK3α has an extended N-terminal region (Woodgett 1990, Dajani, Fraser et al. 2001). Both GSK3α and GSK3β are highly expressed in the mouse hippocampus postnatally (Figure 1.6, Allen Brain Atlas), in both neurons and glia (Woodgett 1990, Ferrer, Barrachina et al. 2002, Yao, Shaw et al. 2002, Perez-Costas, Gandy et al. 2010). Paralog-specific GSK3 KO animals have been generated. GSK3β KO mice die late in development, however GSK3β heterozygous mice are viable and have been extensively characterized (Hoeflich, Luo et al. 2000, Beaulieu, Sotnikova et al. 2004, O'Brien, Harper et al. 2004). GSK3α KO mice are viable and exhibit similar deficits as GSK3β heterozygous mice, most notably an anti-depressant like state, similar to the effects of lithium, as well as memory impairments (Beaulieu, Sotnikova et al. 2004,

O'Brien, Harper et al. 2004, MacAulay, Doble et al. 2007, Bersudsky, Shaldubina et al. 2008, Kimura, Yamashita et al. 2008, Kaidanovich-Beilin, Lipina et al. 2009). Importantly, there are notable differences in the contribution of GSK3α and GSK3β, especially in the involvement of neuropsychiatric disease. Case in point, GSK3α KO mice exhibit impaired social interaction (Kaidanovich-Beilin, Lipina et al. 2009). Additionally, in the Disc1-L100P mouse, which models schizophrenia-related behaviors, genetic reduction of GSK3α specifically reverses pre-pulse inhibition (Cooper, Coe et al.) and normalizes the hyperactivity phenotype and spine development abnormalities observed in the Disc1-L100P mutant (Lee, Kaidanovich-Beilin et al. 2011, Lipina, Kaidanovich-Beilin et al. 2011). Intriguingly, the *Fmr1* KO mouse shares similar deficits in PPI, hyperactivity and spine abnormalities (Table 1.1), suggesting that paralog-specific inhibition of GSK3 could offer enhanced therapeutic benefit by specifically targeting the paralog which is relevant to the pathophysiology of FX. It was once hypothesized that development of paralog-specific small molecule inhibitors would be a near impossibility due to the high sequence identity of the GSK3α and GSK3β kinase domains (Kaidanovich-Beilin and Woodgett 2011). In fact, most currently available GSK3 inhibitors lack true selectivity, most often non-specifically acting on cyclin-dependent kinases as well (O'Leary and Nolan 2015). Recently however, highly selective inhibitors of both GSK3α and GSK3β have been developed, as Chapter 3 reveals, allowing us to probe the specific contribution of each paralog in the pathophysiology of FX.

1.15: Polygenic causes of autism and intellectual disability: 16p11.2 CNVs.

Although monogenic causes of ID offer a unique opportunity to probe the contribution of a single gene to cognitive function, estimates suggest that ~15% of cases of ID are caused by polygenic copy number variants (CNVs) > 400 kb in length (Cooper, Coe et al. 2011). Variation at human chromosome 16p11.2 is one of the most common of these and accounts for approximately 0.5-1% of all ASD cases (Malhotra and Sebat 2012). 16p11.2 CNVs, which include either deletion or duplication of a ~600 kb region, are highly penetrant causes of intellectual impairment and diagnosable

psychiatric disorders that include ASD (Zufferey, Sherr et al. 2012). In deletion carriers, full scale IQ is decreased by ~2 standard deviations, such that 70% have an IQ < 85 (Figure 1.7) (Zufferey, Sherr et al. 2012). In addition to ASD, individuals with 16p11.2 CNVs have a higher prevalence of other disorders that include epilepsy, mood and anxiety disorders, learning disabilities, linguistic impairments, schizophrenia, bipolar disorder, obesity, asthma and dysmorphic features (Shimojima, Inoue et al. 2009, Ciuladaite, Kasnauskiene et al. 2011, Bassuk, Geraghty et al. 2013, Castro-Gago, Perez-Gay et al. 2013, Weber, Kohler et al. 2013). Clinical studies have indicated that patients with the microdeletion CNV tend to exhibit more severe symptoms, commonly associated with ASD, ID and obesity compared to patients with the duplication, which is more commonly associated with schizophrenia (Weiss, Shen et al. 2008). The affected region harbors 27 annotated protein-coding genes, most of which are expressed in the brain, and more specifically, the CA1 region of the hippocampus (Christian, Brune et al. 2008, Kumar, KaraMohamed et al. 2008, Weiss, Shen et al. 2008). In addition to ASD, patients with CNVs at chromosome 16p11.2 have a higher risk for other developmental and psychiatric conditions such as schizophrenia, bipolar disorder, and ID (Weiss, Shen et al. 2008, Bijlsma, Gijsbers et al. 2009, McCarthy, Makarov et al. 2009, Zufferey, Sherr et al. 2012). Although the development of three mouse models of 16p11.2 deletion syndrome and two mouse models of 16p11.2 duplication syndrome have led to a number of important findings, the mechanism by which microdeletion or duplication at chromosome 16p11.2 causes cognitive and anatomical impairments is largely unknown. Moreover, little is known about how CNVs, as a distinct group of genetic abnormalities, contribute to ASD and ID.

1.16: Animal models of 16p11.2 deletion and duplication syndromes.

Two independent mouse models of the human 16p11.2 duplication (16p11.2 *dp/+* mice) and three models of the human 16p11.2 deletion (16p11.2 *df/+* mice) have been established and characterized (Horev, Ellegood et al. 2011, Portmann, Yang et al. 2014, Arbogast, Ouagazzal et al. 2016). These mice all carry highly similar (with subtle differences in regional overlap) heterozygous deletion or duplication of mouse

chromosome 7qF3, the syntenic region of human chromosome 16p11.2 (Figure 1.8). While humans with 16p11.2 deletion syndrome are prone to obesity, all three 16p11.2 *df/+* mouse models are underweight compared with WT controls. Despite inconsistent effects on body size, MRI analysis of the seminal 16p11.2 *df/+* and 16p11.2 *dp/+* mouse models revealed that deletion or duplication of the syntenic region of 16p11.2 led to macrocephaly and microcephaly in mice respectively, which mirrors anatomical abnormalities identified in the respective human conditions (Horev, Ellegood et al. 2011). In zebrafish it has been shown that deletion or duplication of only *Kctd13* (a single gene in the 16p11.2 region) mirrors neuroanatomical macro and microcephaly characteristics of 16p11.2 CNVs. However it is also important to note that manipulation of either *Mvp* or *Mapk3* in addition to *Kctd13* exacerbated these anatomical defects (Golzio, Willer et al. 2012). Human 16p11.2 deletion carriers tend to exhibit significantly more impairment than carriers of the regional duplication. Similar to this, 16p11.2 *df/+* mice show behavioral and cognitive phenotypes that are more severe compared with 16p11.2 *dp/+* mice (Horev, Ellegood et al. 2011). Similar to the *Fmr1* KO mouse, 16p11.2 *df/+* mice are hyperactive and show severe impairments in hippocampus-dependent cognitive tasks, including passive avoidance and context-dependent memory tests (Horev, Ellegood et al. 2011, Portmann, Yang et al. 2014, Tian, Stoppel et al. 2015, Arbogast, Ouagazzal et al. 2016). All three 16p11.2 *df/+* mouse models show deficient novelty detection in an object recognition memory task. Interestingly 16p11.2 *dp/+* mice show enhanced novelty detection (Horev, Ellegood et al. 2011, Portmann, Yang et al. 2014, Arbogast, Ouagazzal et al. 2016). Although comparisons between 16p11.2 *df/+* and 16p11.2 *dp/+* mice have revealed largely reciprocal phenotypes, it is interesting that both 16p11.2 *df/+* and 16p11.2 *dp/+* mice show impairments in social interaction assays, consistent with the observation that both human deletion and duplication carriers are at higher risk for ASD (Arbogast, Ouagazzal et al. 2016).

Synaptic function of 16p11.2 *dp/+* mice has not been extensively investigated. 16p11.2 *dp/+* mice show elevated levels of ERK1/2 protein and as such, increased bulk ERK1, and ERK2 phosphorylation. This is to be expected as *Mapk3*, which encodes ERK1 is in the duplicated region. This was accompanied by increased dendritic

arborization in cortical pyramidal neurons which was reversed by inhibition of ERK1/2 with U0126 (Blizinsky, Diaz-Castro et al. 2016). Two groups of researchers have independently investigated ERK1/2 signaling in 16p11.2 *df/+* mice. Interestingly, one group observed elevated activity of both ERK1 and ERK2 in cortical lysates (Pucilowska, Vithayathil et al. 2015). Despite this observed hyperactivity of ERK signaling, total levels of ERK1/2 phosphorylation in hippocampal slices remains reduced in 16p11.2 *df/+* mice due to the heterozygous deletion of *Mapk3* and thus reduction of total ERK1 (Tian, Stoppel et al. 2015). In addition to implications that altered ERK signaling is pathogenic in 16p11.2 *df/+* and 16p11.2 *dp/+* mice, other interesting similarities between 16p11.2 *df/+* and *Fmr1* KO have been observed. Despite observations that protein synthesis is deficient in 16p11.2 *df/+* mice, likely due to a global reduction in ERK1/2 activity, induction and maintenance of mGluR-LTD in CA1 of the hippocampus is unaltered. Intriguingly, this form of synaptic plasticity persists in the absence of *de novo* protein synthesis, possibly as a result of elevated synaptic Arc, which phenocopies the *Fmr1* KO mouse. Similarly, chronic treatment with the mGlu5 negative allosteric modulator CTEP corrects deficits in a passive avoidance task, which has also been observed in *Fmr1* KO mice (Michalon, Sidorov et al. 2012, Tian, Stoppel et al. 2015).

1.17: Convergence at $mGlu_5$: FX and 16p11.2 CNVs.

An obvious and urgent question is whether these polygenic causes of psychiatric illness have overlapping pathophysiology with the single-gene disorders. Two genes in the 16p11.2 region, *MAPK3* and *MVP* are directly involved in signaling pathways downstream of $mGlu_5$ signaling, and several other genes in this region are targets of FMRP (Kolli, Zito et al. 2004, Paspalas, Perley et al. 2008, Crepel, Steyaert et al. 2011). *MAPK3* codes for the ERK1 isoform protein product, which, as discussed previously, is an integral protein in the pathway that leads to the production of synaptic proteins necessary for mGluR LTD. Conversely, Major Vault Protein (*MVP*) is thought to be a negative regulator of ERK1/2 (Kolli, Zito et al. 2004), and a rare inherited deletion in the 16p11.2 region confined to *MVP*, *CDIPT1*, *SEZ6L2*, *ASPHD1*, and *KCTD13* has been

shown to be associated with ASD (Crepel, Steyaert et al. 2011). Although 16p11.2 *df/+* mice exhibit normal induction and maintenance of mGluR-LTD, the pathogenic loss of the protein-synthesis dependence of this form of synaptic plasticity, as well as increased expression of the plasticity protein Arc, phenocopies the *Fmr1* KO mouse. Evidence that 16p11.2 *df/+* mice have deficient translational regulation suggest that disruption of the synaptic control of protein synthesis could be a cause of cognitive impairment in 16p11.2 CNV carriers, similar to patients with FX. If this is indeed the case, then disease-modifying treatments that are currently in development for FX may provide benefit to 16p11.2 CNV carriers as well.

1.18: Conclusions

An overarching theme that is highlighted in this literature review, is a need to refine the mGluR theory of FX to specify modulation of only the disease-relevant signaling pathways and target molecules downstream of $mGlu_5$ that are pathogenic to the core dysfunctions in FX (and possibly 16p11.2 CNVs as well). However, in order to do so, further investigation into which target(s) mechanistically link $mGlu_5$ activation to the translational initiation machinery at the synapse is needed. Chapter 2 evaluates the possibility that β-arrestins may recruit the Ras-ERK signaling pathway and mediate *de novo* protein synthesis at the synapse upon $mGlu_5$ receptor activation. Furthermore, it validates downregulation of β-arrestin-biased signaling at $mGlu_5$ as a fruitful strategy in treating FX dysfunction. Chapter 3 probes the isoform-specific contribution of GSK3α and/or GSK3β in the synaptic pathophysiology of the *Fmr1* KO mouse model and evaluates isoform-specific inhibition as a potential therapeutic avenue in FX. Chapter 4 investigates synaptic dysfunction in mouse models of 16p11.2 deletion and duplication syndromes. Moreover, chapter 4 investigates the possibility that the $GABA_B$ agonist R-baclofen, which has shown therapeutic benefit in pre-clinical and clinical studies for FX, may be efficacious in reversing phenotypes associated with the 16p11.2 deletion mouse model, thereby evaluating the hypothesis there may be convergence at the synapse between two separate known genetic causes of ASD and ID at the synapse.

Identified Prevalence of Autism Spectrum Disorder

ADDM Network 2000 – 2012
Combing Data from All Sites

Surveillance Year	Birth Year	Number of ADDM Sites Reporting	Prevalence per 1,000 Children (Range)	Approximately 1 in X children
2000	1992	6	6.7 (4.5-9.9)	1 in 150
2002	1994	14	6.6 (3.3-10.6)	1 in 150
2004	1996	8	8.0 (4.6-9.8)	1 in 125
2006	1998	11	9.0 (4.2-12.1)	1 in 110
2008	2000	14	11.3 (4.8-21.2)	1 in 88
2010	2002	11	14.7 (5.7-21.9)	1 in 68
2012	2004	11	14.6 (8.2-24.6)	1 in 68

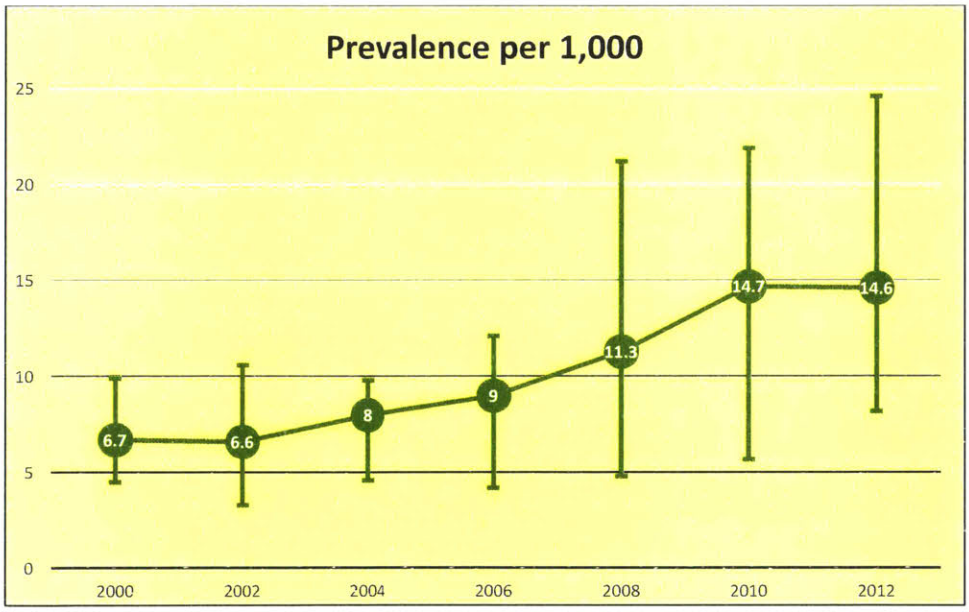

Figure 1.1: Prevalence of ASD from 2000-2012.

Estimates of the prevalence of Autism Spectrum Disorder in children age 8 taken at regular intervals from 2000 to 2012 indicate a trend towards steadily increased prevalence over time. Data obtained from the CDC.

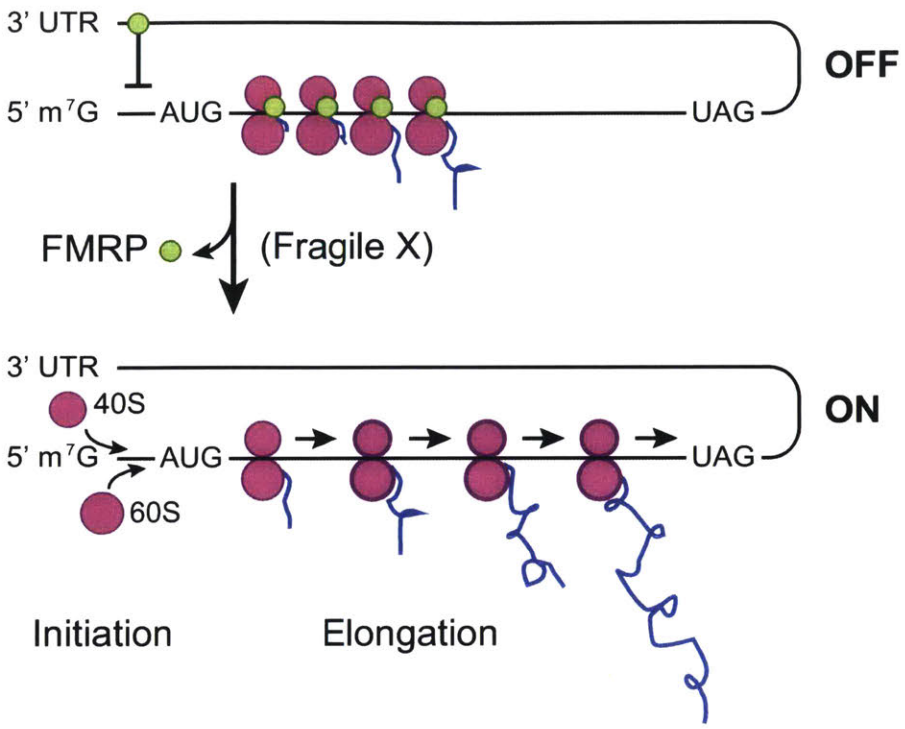

Figure 1.2: FMRP regulates mRNA translation.

In a normal neuron, where FMRP (green) is functional, it can be found bound to regions of mRNA in association with stalled ribosome complexes, supporting its role in suppression of the elongation step of translation. It can also be found bound to the 3'UTRs in association with the machinery for translation initiation, supporting a separate role for FMRP in translation initiation. In neurons that lack FMRP, a translational brake is lifted, as FMRP does not block the initiation of ribosome assembly, nor does it stall the elongation of actively translating ribosomes. Taken together, loss of this translational break leads to excessive protein synthesis, known to be pathogenic in FX. Adapted from Bhakar, Dolen, and Bear, *Annu. Rev. Neurosci.* 2012.

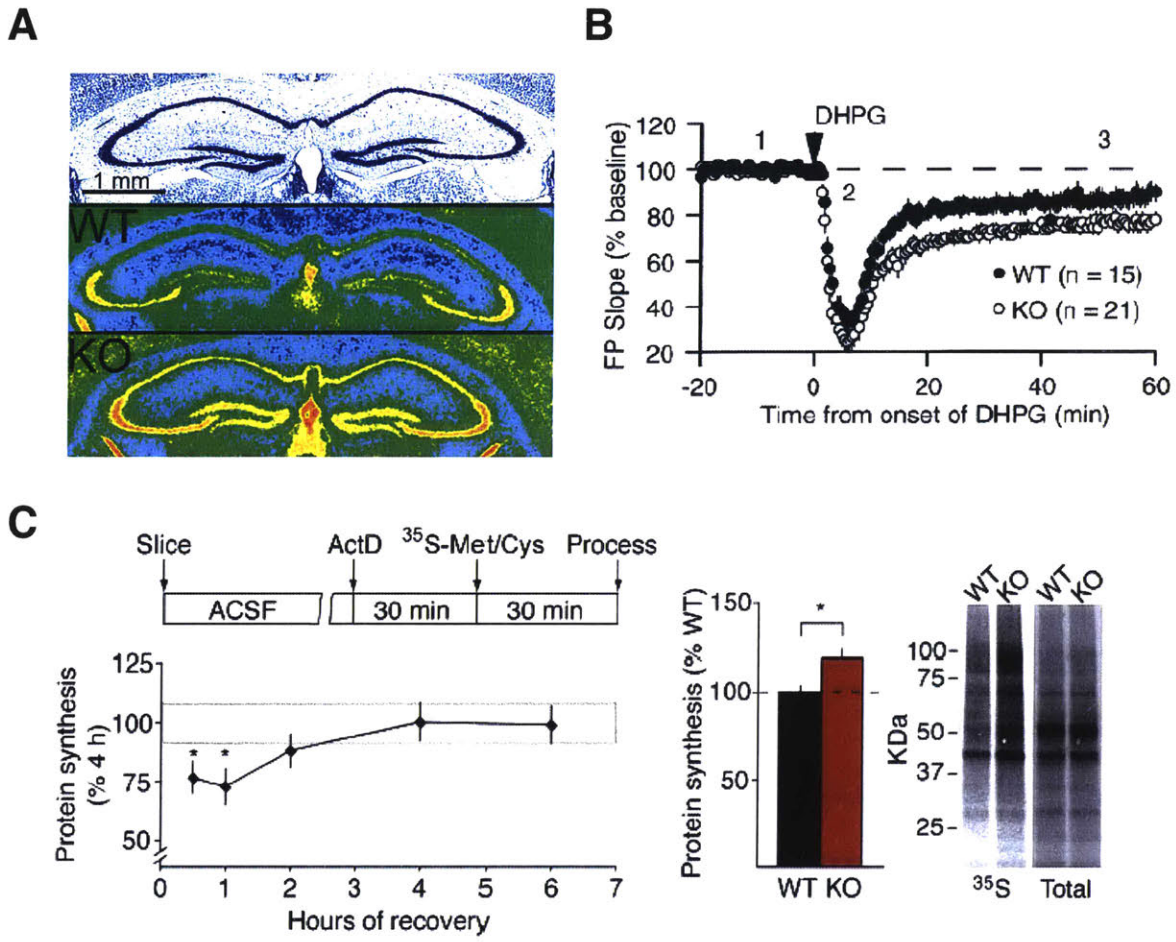

Figure 1.3: Exaggerated protein synthesis and mGluR-LTD in the *Fmr1* KO mouse.

(**A**) Nissl-stained coronal sections (top) and their corresponding pseudocolored autoradiograms (middle and bottom) show quantitative increases in translation rates throughout the hippocampus of 6-month-old *Fmr1* KO mice *in vivo* (bottom) compared with WT controls (middle). Images courtesy of C.B. Smith (Qin et al.2005), adapted from Bhakar, Dolen, and Bear, *Annu. Rev. Neurosci.* 2012. (**B**) The magnitude of mGluR-LTD, a form of synaptic plasticity that is dependent on *de novo* protein synthesis, is exaggerated in the *Fmr1* KO mouse compared with WT controls in CA1 of the hippocampus. (Huber et al., 2002). (**C**) Metabolic labeling of slices prepared under conditions modeling slice electrophysiology experiments reveals rates of protein synthesis in the hippocampus are maximal 4-6 hours after slicing. Similar to observations *in vivo* in (A), metabolic labeling of hippocampal slices reveal elevated protein synthesis in the *Fmr1* KO mouse compared to WT mice (Osterweil et al., 2010).

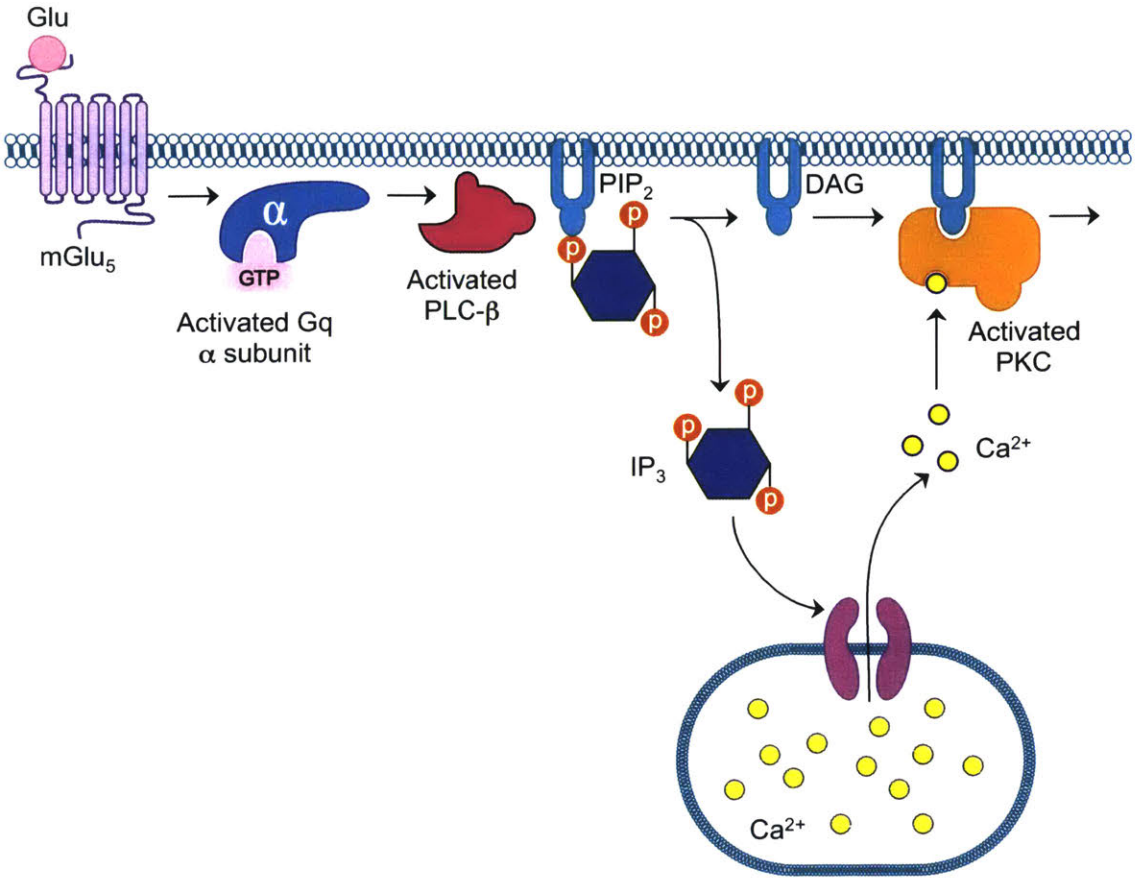

Figure 1.4: $mGlu_5$ is a G_q-protein coupled receptor.

Canonically, $mGlu_5$ signaling occurs through the G_q-dependent activation of PLC-β, which hydrolyzes PIP_2, leading to increases in DAG, which subsequently activates PKC (and PKD, not shown), and IP_3, whose receptor activation leads to release of Ca^{2+} from intracellular stores. Abbreviations: $[Ca^{2+}]$, calcium release from intracellular stores; PLC-β, phospholipase C beta; PIP_2, phosphatidylinositol (4,5)-bisphosphate; DAG, diacyl glycerol; PKC, protein kinase C; P_3, inositol triphosphate.

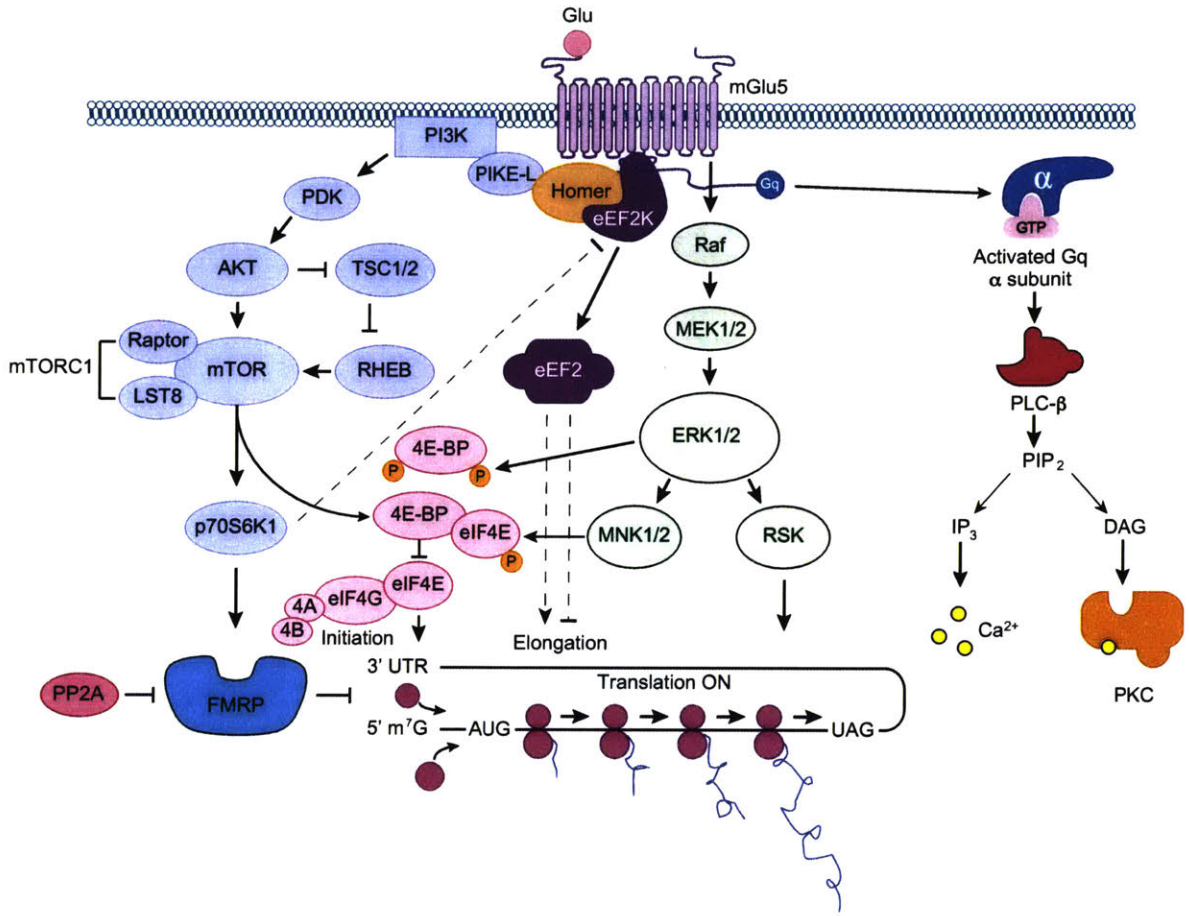

Figure 1.5: Signaling pathways mediate synaptic translation upon $mGlu_5$ activation.

Glutamate binding to $mGlu_5$ activates three main pathways that couple the receptors to translational regulation: (1) the PLC/PKC pathway (2) the mTOR pathway (blue ovals), and (3) the ERK pathway (green ovals). Key regulatory components of translation initiation are shown in light pink. Key regulatory components of translation elongation are shown in purple. $mGlu_5$ may also inhibit FMRP (teal) function to regulate translation through a fourth pathway requiring stimulation of PP2A (dark pink). Arrows indicate a positive consequence on downstream components; perpendicular lines indicate an inhibitory consequence. Abbreviations: $[Ca^{2+}]$, calcium release from intracellular stores; eEF2, eukaryotic elongation factor 2; eIF4, eukaryotic initiation factor 4; ERK, extracellular signal–regulated kinase; FMRP, fragile X mental retardation protein; ($G\alpha q$) heterotrimeric G proteins; IP_3, inositol-1,4,5-triphosphate; mGlu5, metabotropic glutamate receptor 5; mTOR, mammalian target of rapamycin; PLC, phospholipase C; PP2A, protein phosphatase 2A; Raptor, regulatory-associated protein of mTOR. TSC, tuberous sclerosis complex.

Fragile X phenotype (vs. WT)	mGluR5 manipulation	Reference(s)
Exaggerated mGluR-LTD	*Grm5*$^{+/-}$ cross CTEP	Dolen et al. 2007 Michalon et al. 2012
Increased AMPAR internalization	MPEP	Nakamoto et al. 2007
Impaired spontaneous EPSCs in juvenile hippocampus	MPEP	Meredith et al. 2011
Increased protein synthesis	*Grm5*$^{+/-}$ cross MPEP CTEP	Dolen et al. 2007 Osterweil et al. 2010 Michalon et al. 2012
Decreased number of mRNA granules in whole brain	MPEP	Aschrafi et al. 2005
Increased glycogen synthase kinase-3 activity	MPEP	Min et al. 2009
Increase beta amyloid	MPEP	Malter et al. 2010
Increased ERK and mTOR signaling	CTEP	Michalon et al. 2012
Increased dendritic spine/filopodia density	*Grm5*$^{+/-}$ cross Fenobam MPEP AFQ056 CTEP	Dolen et al. 2007 De Vrij et al. 2008 Su et al. 2011 Levenga et al. 2011 Michalon et al. 2012
Altered visual cortical plasticity	*Grm5*$^{+/-}$ cross	Dolen et al. 2007
Prolonged epileptiform discharges in hippocampus	MPEP	Chuang et al. 2005
Increased persistent activity states in neocortex	MPEP, *Grm5*$^{+/-}$ cross	Hays et al. 2011
Impaired presynaptic function in the amygdala	MPEP	Suvrathan et al. 2010
Exaggerated inhibitory avoidance extinction	*Grm5*$^{+/-}$ cross	Dolen et al. 2007
Associative motor-learning deficit	Fenobam	Veloz et al. 2012
Impaired eyelid conditioning	MPEP	Koekkoek et al. 2005
Increased audiogenic seizure	*Grm5*$^{+/-}$ cross MPEP CTEP	Dolen et al. 2007 Thomas et al. 2012, Yan et al. 2005 Michalon et al. 2012
Defective prepulse inhibition of acoustic startle	MPEP AFQ056 CTEP	De Vrij et al. 2008 Levenga et al. 2011 Michalon et al. 2012
Avoidance behavior deficits	Fenobam	Veloz et al. 2012
Decreased initial performance on rotorod	MPEP	Thomas et al. 2012
Increased open-field activity	MPEP CTEP	Min et al. 2009, Yan et al. 2005
Abnormal social interaction with unfamiliar mouse	*Grm5*$^{+/-}$ cross	Thomas et al. 2011
Increased marble burying (repetitive behavior)	MPEP	Thomas et al. 2012
Macroorchidism	CTEP (partial rescue)	Michalon et al. 2012
Pubertal increase in body weight	*Grm5*$^{+/-}$ cross	Dolen et al. 2007

Table 1.1: FX phenotypes corrected by $mGlu_5$ manipulation.

Abbreviations: AMPAR, α-amino-3-hydroxy-5-methyl-4-isoxazolepropionic acid receptor; CTEP, 2-chloro-4-((2,5-dimethyl-1-(4-(trifluoromethoxy)phenyl)-1H-imidazol-4-yl)ethynyl)pyridine; EPSC, excitatory postsynaptic currents; FX, fragile X; mGluR; LTD, long-term depression; mGluR, metabotropic glutamate receptor; MPEP, 2-methyl-6-(phenylethynyl)-pyridine; mRNA, messenger RNA; WT, wild type.
MPEP, Fenobam, CTEP, AFQ056 = $mGlu_5$ negative allosteric modulators.

Fragile X phenotype (vs. WT)	ERK pathway manipulation	Reference(s)
Exaggerated mGluR-LTD	Lovastatin (Ras farnesylation)	Osterweil et al. 2013
Increased protein synthesis	U0126 (ERK) Lovastatin (Ras farnesylation)	Osterweil et al. 2010 Osterweil et al. 2013
Altered visual cortical excitability	Lovastatin (Ras farnesylation)	Osterweil et al. 2013
Prolonged epileptiform discharges in hippocampus	Lovastatin (Ras farnesylation)	Osterweil et al. 2013
Increased audiogenic seizure	U0126 (ERK) Lovastatin (Ras farnesylation)	Osterweil et al. 2010 Osterweil et al. 2013

Fragile X phenotype (vs. WT)	mTOR pathway manipulation	Reference(s)
Exaggerated mGluR-LTD	S6K1 KO cross (p70 S61 Kinase)	Battacharya et al. 2012
Increased protein synthesis	*Tsc2*$^{+/-}$ cross (TSC2) PF-4708671 (p70 S61 Kinase) FS-115 (p70 S61 Kinase)	Auerbach et al. 2011 Battacharya et al. 2016 Battacharya et al. 2016
Impaired signaling and protein expression	S6K1 KO cross (p70 S61 Kinase)	Battacharya et al. 2012
Deficits in the elevated plus maze	Temsirolimis (mTOR)	Busquets-Garcia et al. 2013
Deficits in open field activity	Temsirolimis (mTOR)	Busquets-Garcia et al. 2013
Impaired novel object recognition	Temsirolimis (mTOR) S6K1 KO cross (p70 S61 Kinase)	Busquets-Garcia et al. 2013 Battacharya et al. 2012
Increased dendritic spine/filopodia density	S6K1 KO cross (p70 S61 Kinase) PF-4708671 (p70 S61 Kinase) FS-115 (p70 S61 Kinase)	Battacharya et al. 2012 Battacharya et al. 2016 Battacharya et al. 2016
Decreased initial performance on rotorod	S6K1 KO cross (p70 S61 Kinase)	Battacharya et al. 2012
Deficits in the Y maze	S6K1 KO cross (p70 S61 Kinase) PF-4708671 (p70 S61 Kinase) FS-115 (p70 S61 Kinase)	Battacharya et al. 2012 Battacharya et al. 2016 Battacharya et al. 2016
Pubertal increase in body weight	S6K1 KO cross (p70 S61 Kinase) FS-115 (p70 S61 Kinase)	Battacharya et al. 2012 Battacharya et al. 2016
Macroorchidism	S6K1 KO cross (p70 S61 Kinase) PF-4708671 (p70 S61 Kinase) FS-115 (p70 S61 Kinase)	Battacharya et al. 2012 Battacharya et al. 2016 Battacharya et al. 2016
Deficits in marble burying	FS-115 (p70 S61 Kinase)	Battacharya et al. 2016
Impaired social interaction	PF-4708671 (p70 S61 Kinase) FS-115 (p70 S61 Kinase)	Battacharya et al. 2016 Battacharya et al. 2016
Impaired contextual fear conditioning	*Tsc2*$^{+/-}$ cross (TSC2)	Auerbach et al. 2011
Increased audiogenic seizure	Rapamycin (mTOR, partial rescue) Temsirolimis (mTOR)	Osterweil et al., 2010 Busquets-Garcia et al. 2013

Table 1.2: FX phenotypes corrected by ERK or mTOR pathway manipulation.

Fragile X phenotype (vs. WT)	GSK3 manipulation	Reference(s)
Exaggerated mGluR-LTD	Lithium	Choi et al. 2011
Impaired signaling	Lithium	Liu et al. 2012
LTP, reduced stead-state depolarization in the dentate gyrus	Lithium, CT99021	Franklin et al. 2014
Increased protein synthesis	Lithium	Liu et al. 2012
Impaired L-LTP in the anterior cingulate cortex	CT99021, SB415286	Chen et al. 2014
Increased glycogen synthase kinase-3 activity	Lithium SB415286	Min et al. 2009, Yuskaitis et al. 2010, Liu et al. 2011 Guo et al. 2012
Adult hippocampal neurogenesis and maturation deficits	SB415286	Guo et al. 2012
Increased dendritic spine/filopodia density	Lithium	Liu et al. 2011
Exaggerated inhibitory avoidance extinction	Lithium	Liu et al. 2011, Yuskaitis et al. 2010
Impaired trace fear memory and/or AMPAR GluA1 upregulation	CT99021 SB415286	Chen et al. 2014 Guo et al. 2012
Increased audiogenic seizure	Lithium	Yuskaitis et al. 2010
Deficits in categorical and/or spatial processing tasks	TDZD-8, VP0.7 Lithium	Franklin et al. 2014 King and Jope, 2013
Deficits in the elevated plus maze	Lithium	Yuskaitis et al. 2010, Liu et al. 2011, Chen et al. 2013
Impaired novel object recognition	TDZD-8, VP0.7	Franklin et al. 2014, King and Jope, 2013
Increased open-field activity	Lithium	Min et al. 2009, Yuskaitis et al. 2010, Liu et al. 2011, Chen et al. 2013
Abnormal social interaction with unfamiliar mouse	Lithium	Liu et al. 2011, Mines et al. 2010
Macroorchidism	Lithium (partial rescue)	Liu et al. 2011

Table 1.3: FX phenotypes corrected by GSK3α/β manipulation.

Abbreviations: LTP, long term potentiation; L-LTP, late-long term potentiation; GluA1, glutamate ionotropic receptor AMPA type subunit 1.
Lithium = direct and indirect inhibitory action at GSK3; CT99021, SB415286 = ATP-competitive GSK3 inhibitors; TDZD-8, VP0.7 = non-competitive ATP binding site inhibitors.

Fragile X phenotype (vs. WT) corrected by R-baclofen	Reference(s)
Impaired signaling	Qin et al. 2015
Elevated AMPAR internalization	Henderson et al. 2012
Increased protein synthesis	Henderson et al. 2012, Qin et al. 2015
Increased dendritic spine/filopodia density	Henderson et al. 2012
Increased audiogenic seizure	Pacey et al. 2009 Pacey et al. 2011 Henderson et al. 2012
Abnormal social interaction with unfamiliar mouse	Qin et al. 2015

Table 1.4: FX phenotypes corrected by treatment with the $GABA_B$ agonist R-baclofen.

A

GSK3α

B

GSK3β

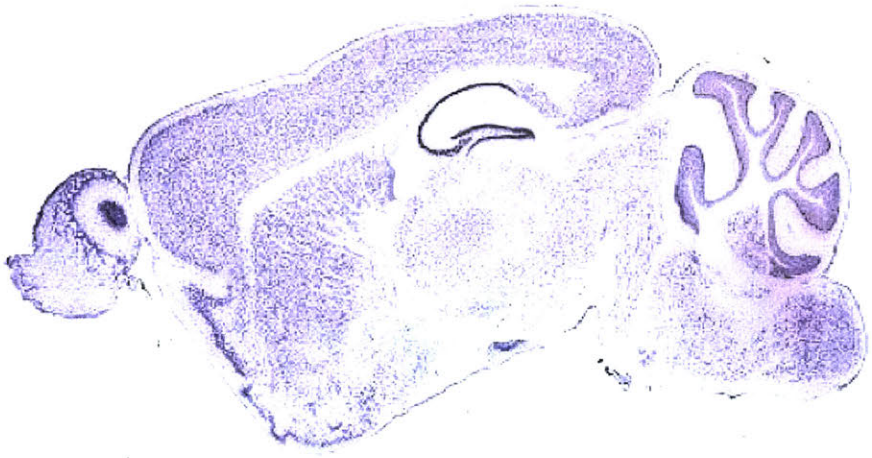

Figure 1.6: Expression of GSK isoforms in the mouse hippocampus.

(**A**, **B**) In situ hybridization shows that GSK3α and GSK3β (A and B, respectively) are both highly expressed in the mouse hippocampus. ISH images were obtained from the Allen Brain Atlas.

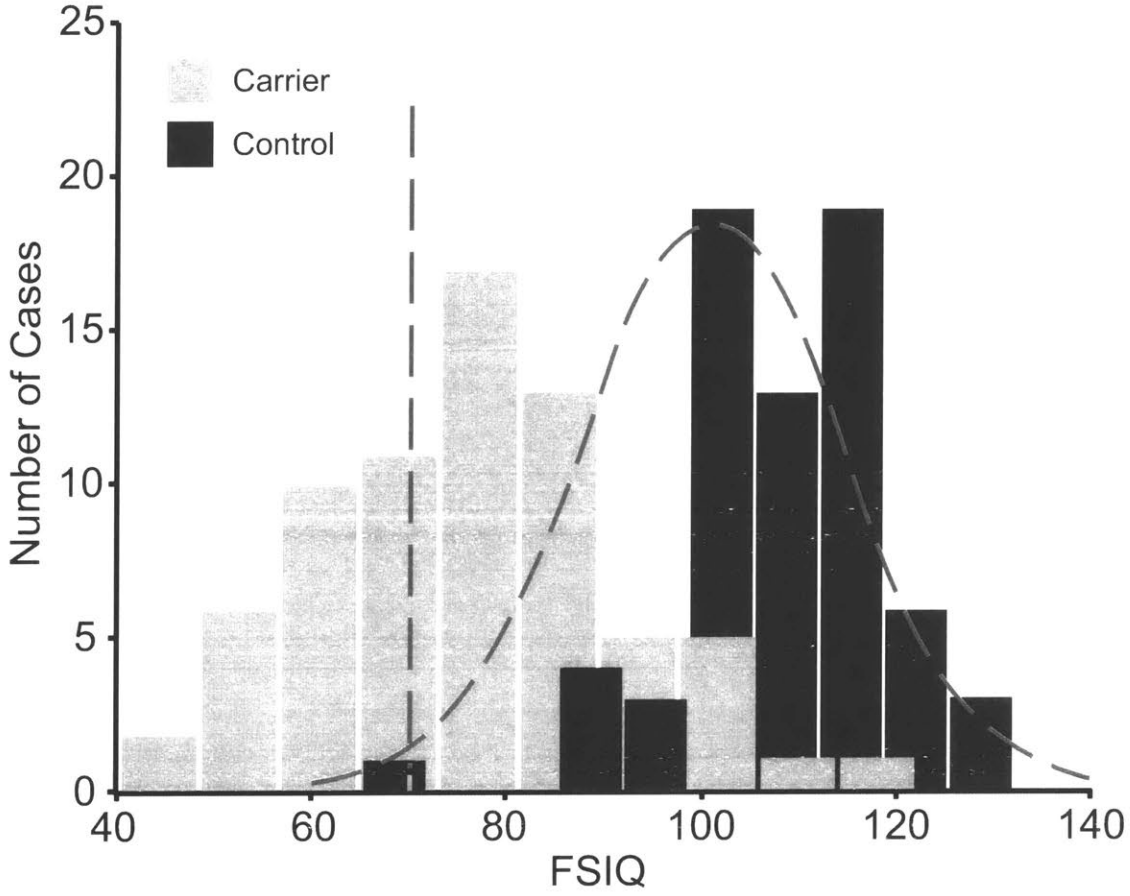

Figure 1.7: Distribution of IQ in 16p11.2 deletion carriers.

Distribution of full scale intelligence quotient (FSIQ) in 16p11.2 BP4-BP5 deletion carriers (grey bars), intrafamilial non-carrier relatives (control, black bars), and general population (dashed curve). The dashed vertical line represents the FSIQ threshold (70) for intellectual disability. Mean FSIQ is 32 points lower in carriers when compared to non-carrier relatives. Adapted from Zufferey et al. (2012).

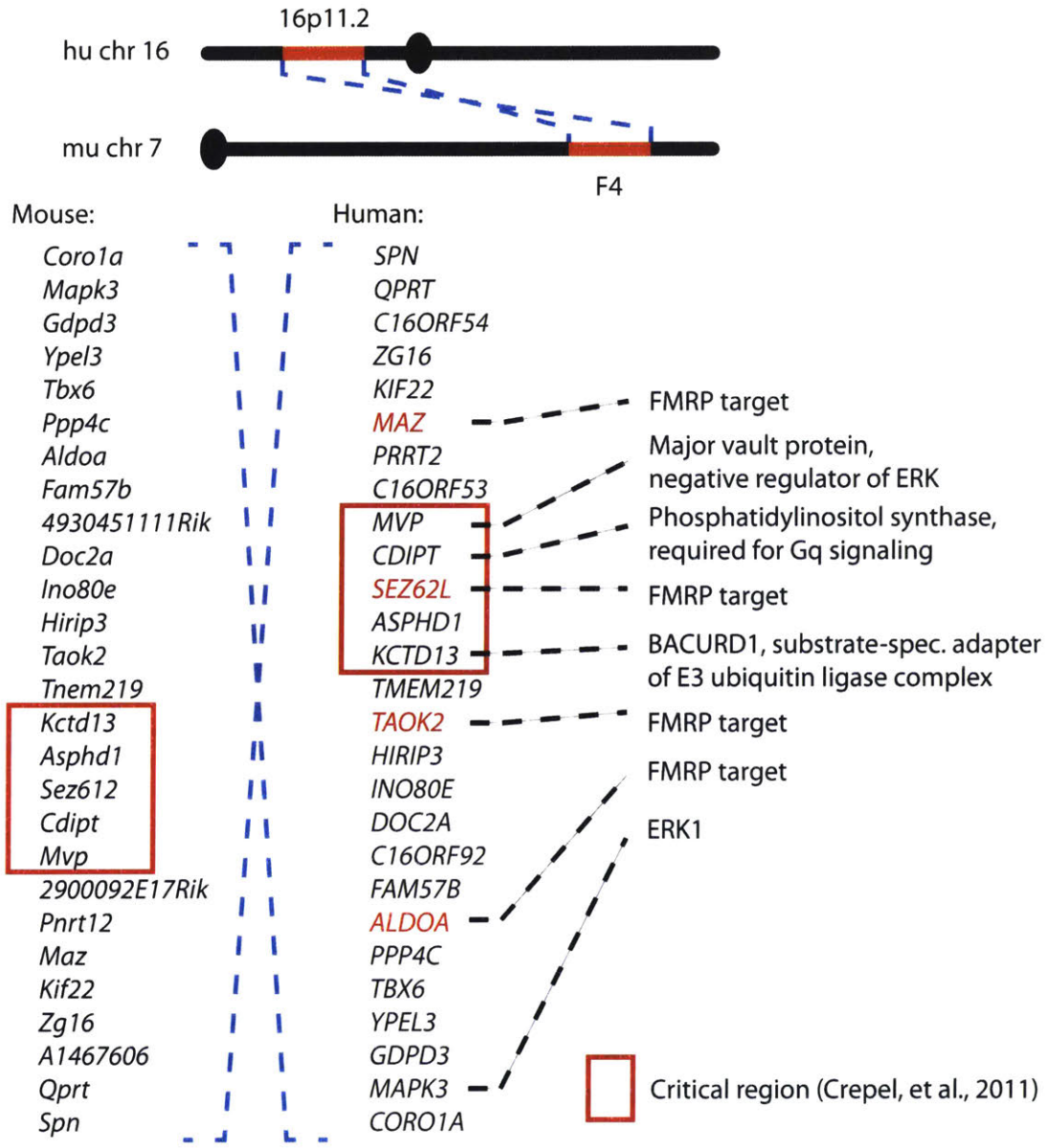

Figure 1.8: Human 16p11.2 is syntenic to mouse chromosome 7qF3.

Mouse chromosome 7qF3 and human chromosome 16p11.2 are syntenic, as described in Weiss et al. (2008). 4 of the ~27 genes within the affected region are targets of FMRP (as identified by Darnell et al. 2011). Others are important for signaling downstream of $mGlu_5$.

Chapter 2

β-Arrestin2 couples $mGlu_5$ to FMRP-regulated protein synthesis and is a novel target for the treatment of Fragile X

Portions of this chapter have been submitted for review:

Stoppel LJ, Auerbach BD, Senter RK, Preza AR, Lefkowitz RJ, Bear MF. β-Arrestin2 couples metabotropic glutamate receptor 5 to synaptic protein synthesis in Fragile X (in submission)

2.1: Abstract

The primary pathogenic cause of Fragile X Syndrome (FX) is dysregulated synaptic protein synthesis downstream of metabotropic glutamate receptor 5 ($mGlu_5$) activation. Therapies targeting this dysregulation, however, have failed in clinical trials, due in part to our incomplete understanding of the signaling pathways that couple $mGlu_5$ activation to neuronal translation. Here, we demonstrate that β-arrestin2 is a critical link between $mGlu_5$ activation and FMRP-mediated translation and synaptic plasticity. Heterozygous deletion of β-arrestin2 severely blunts $mGlu_5$-stimulated protein synthesis, ERK activation, and mGluR-LTD while preserving canonical G_q signaling. Interestingly, genetic reduction of β-arrestin2 in the *Fmr1* KO mouse is sufficient to correct many recognized deficits, including exaggerated protein synthesis and mGluR-LTD as well as many cognitive and behavioral impairments. Importantly, this reduction in β-arrestin2 does not induce the same psychotomimetic side effects associated with full $mGlu_5$ inhibitors, indicating that targeting β-arrestin2-mediated signaling may be a more selective approach to the treatment of FX.

2.2: Introduction

2.2.1: Dysfunction at $mGlu_5$, a regulator of protein synthesis, is core to the pathophysiology of FX.

Numerous genetic and molecular studies have demonstrated that poorly regulated synaptic protein synthesis downstream of metabotropic glutamate receptor 5 ($mGlu_5$) contributes to the pathophysiology of Fragile X (FX), a genetic cause of intellectual disability (ID) and autism spectrum disorder (ASD) (Pop, Gomez-Mancilla et al. 2014). This work suggests that targeting $mGlu_5$ or its downstream effectors may be a fruitful approach for improving the course of FX and other genetic syndromes with shared pathophysiology (Bozdagi, Sakurai et al. 2010, Auerbach, Osterweil et al. 2011, Aguilar-Valles, Matta-Camacho et al. 2015, Barnes, Wijetunge et al. 2015, Tian, Stoppel et al. 2015, Wenger, Kao et al. 2016).

2.2.2: Targeting $mGlu_5$: failure in the clinic.

Although $mGlu_5$-based therapies have been immensely successful at correcting many neurophysiological and behavioral deficits in animal models of FX (Bhakar, Dolen et al. 2012), to date, however, the results of human clinical trials in FX using $mGlu_5$ negative allosteric inhibitors (NAMs) have been disappointing (Scharf, Jaeschke et al. 2015, Berry-Kravis, Des Portes et al. 2016). Although many factors contribute to the challenge of translating findings from animal models to humans, one factor that is common to all drug trials is the therapeutic window—the range of doses that can treat disease pathophysiology without causing negative side effects. In humans, for example, it has been reported that inhibition of $mGlu_5$ produces dose-limiting psychotomimetic effects (Pecknold, McClure et al. 1982, Porter, Jaeschke et al. 2005, Abou Farha, Bruggeman et al. 2014). The first-generation $mGlu_5$ NAMs were identified based on their ability to inhibit canonical G_q signaling mediated by phosphoinositide hydrolysis and release of Ca^{2+} from intracellular stores (Gasparini, Lingenhohl et al. 1999, Cosford,

Tehrani et al. 2003, Lindemann, Jaeschke et al. 2011). However, available data suggest alternative signaling pathways are central to the regulation of synaptic protein synthesis by $mGlu_5$ (Osterweil, Krueger et al. 2010, Bhakar, Dolen et al. 2012, Richter, Bassell et al. 2015). Thus, it is possible that therapeutic effects can be enhanced and separated from side effects by selectively targeting the coupling of $mGlu_5$ to disease-relevant signaling pathway(s).

2.2.3: Honing in on disease-relevant targets: pathway-specific manipulation.

One pathway that is known to be central to mGlu5 stimulated protein synthesis and fragile X pathophysiology culminates in activation of ERK1/2 and the phosphorylation of proteins involved in the regulation of cap-dependent mRNA translation (Banko, Hou et al. 2006, Osterweil, Krueger et al. 2010, Osterweil, Chuang et al. 2013). Activation of this pathway by $mGlu_5$ can occur independently of canonical G-protein signaling, but how this is achieved has yet to be elucidated. As is the case for many seven-transmembrane domain receptors, G-protein signaling of ligand-bound $mGlu_5$ is terminated by recruitment of β-arrestin to the carboxyl tail of the receptor. In recent years it has become clear that β-arrestin recruitment can also trigger activation of alternative signaling cascades. Of particular relevance is the observation that β-arrestin2 recruitment to the angiotensin II receptor (which like mGlu5 is also G_q-coupled) stimulates the ERK1/2 pathway and increases mRNA translation rates in both human embryonic kidney 293 and rat vascular smooth muscle cells (DeWire, Kim et al. 2008, Ahn, Kim et al. 2009). We therefore hypothesized that β-arrestin2 may comprise the missing link between $mGlu_5$ and protein synthesis in neurons.

2.3: Results

2.3.1: β-arrestin2, but not β-arrestin1, is involved in ERK-mediated synaptic protein synthesis.

To test the hypothesis that β-arrestins couple $mGlu_5$ activity to synaptic translation, we stimulated hippocampal slices from male *Arrb1*$^{+/-}$, *Arrb2*$^{+/-}$, and wild-type (WT) littermates with a selective positive allosteric modulator of $mGlu_5$, 3-Cyano-N- (1,3-diphenyl-1H-pyrazol-5-yl)benzamide (CDPPB, 10 μM, 30 minutes), and measured the incorporation of ^{35}S-methionine/cysteine into new protein. We found that $mGlu_5$ activation caused a parallel increase in protein synthesis (Figure 2.1A) and ERK1/2 phosphorylation (Figure 2.1B) in WT slices, which were both absent in slices from *Arrb2*$^{+/-}$ mice. This blunted response to $mGlu_5$ stimulation occurred in the absence of differences in basal protein synthesis rates or ERK phosphorylation levels (Figure 2.1). We failed to observe a comparable effect on stimulated protein synthesis in *Arrb1*$^{+/-}$ mice (Figure 2.2), suggesting that β-arrestin2 is the relevant isoform for $mGlu_5$ signaling. From a therapeutic standpoint, it is noteworthy that mGlu5 stimulated protein synthesis is abrogated in mice lacking a single allele of *Arrb2*; a full knockout is not required to see an effect.

2.3.2: AKT-mTOR signaling downstream of $mGlu_5$ is intact in both *Arrb1*$^{+/-}$ and *Arrb2*$^{+/-}$ hippocampal slices.

β-arrestins have also been shown to participate in additional signaling cascades, including the Akt-mTOR pathway that has been implicated in the regulation of protein synthesis (DeWire, Ahn et al. 2007). Consistent with previous studies performed in hippocampal slices (Osterweil, Krueger et al. 2010), however, we found that $mGlu_5$ activation failed to increase phosphorylation of Akt or ribosomal protein S6, an accepted readout of mTOR activity (Bhattacharya, Mamcarz et al. 2016), in WT mice. These measures of mTOR pathway activity were also unaffected in slices prepared from *Arrb1*$^{+/-}$ and *Arrb2*$^{+/-}$ mice (Figure 2.3). These results suggest that loss of β-arrestin2

decreases $mGlu_5$-stimulated protein synthesis by specifically uncoupling $mGlu_5$ activation from ERK signaling, while leaving other signaling cascades intact.

2.3.3: G_q signaling is unaltered in *Arrb2*$^{+/-}$ hippocampal slices.

To assay the integrity of G_q signaling in the *Arrb2*$^{+/-}$ mice, we examined $mGlu_5$-mediated calcium mobilization in hippocampal slices from WT and *Arrb2*$^{+/-}$ animals using the cell-permeable calcium fluorescent dye Fluo4-AM, a commonly used read-out for G-protein dependent $mGlu_5$ activity during drug screening efforts. We found that a brief application of the orthosteric $mGlu_5$ agonist S-3,5-dihydroxyphenylglycine (DHPG, 25 μM, 1 min) to slices resulted in a rapid increase in Ca^{2+}-mediated fluorescence that was not significantly different between WT and *Arrb2*$^{+/-}$ slices (Figure 2.4). These DHPG-induced changes in calcium fluorescence were completely blocked by pretreatment with the phospholipase C inhibitor, U73122 (data not shown). These results indicate that a partial reduction in β-arrestin2 does not result in aberrant G_q signaling in response to $mGlu_5$ activation. Moreover, they suggest that modulation of $mGlu_5$ receptor-mediated protein synthesis can be dissociated from G-protein dependent signaling via manipulation of β-arrestin2.

2.3.4: *Arrb2*$^{+/-}$ slices lack the protein synthesis-dependent component of $mGlu_5$-dependent LTD.

Activation of $mGlu_5$ results in a form of synaptic long-term depression (LTD) in the hippocampus that requires rapid *de novo* synaptic protein synthesis (Huber, Kayser et al. 2000). We therefore investigated the functional relevance of the observed biochemistry by determining if genetic reduction of *Arrb2* also alters the expression and/or protein synthesis-dependency of LTD induced with DHPG (25 μM, 5 min) (Huber, Roder et al. 2001). Basal synaptic transmission was normal (Figure 2.6A) but LTD magnitude was significantly reduced in *Arrb2*$^{+/-}$ slices compared to WT (Figure 2.5A,B). Consistent with previous observations, LTD in WT slices was significantly diminished in the presence of the protein synthesis inhibitor cycloheximide (CHX, 60 μM). In contrast, the residual LTD in slices from *Arrb2*$^{+/-}$ animals was unaffected by CHX

(Figure 2.5C,D). Therefore, we conclude that the protein synthesis-dependent component of $mGlu_5$-dependent LTD is absent in the *Arrb2*$^{+/-}$ hippocampus.

2.3.5: *Arrb2*$^{+/-}$ mice have normal basal synaptic transmission, pre-synaptic mGlu-LTD and NMDAR-LTD.

In WT mice, the LTD that remains when DHPG is applied in the presence of CHX is expressed via a presynaptic mechanism, revealed by a change in the paired-pulse ratio (Auerbach, Osterweil et al. 2011). This change in paired-pulse ratio after DHPG was similarly observed in *Arrb2*$^{+/-}$ mice, indicating that this presynaptic, protein synthesis-independent mechanism of LTD is unaffected by reducing signaling through β-arrestin2 (Figure 2.6B). Another, mechanistically distinct form of hippocampal LTD can be induced by stimulating NMDA receptors. This type of LTD is expressed postsynaptically, but does not require ERK1/2 or immediate translation of mRNA. We found that it is also unaffected by genetic reduction of β-arrestin2 in the hippocampus (Figure 2.6C). Taken together, these results suggest that the diminished LTD magnitude observed in *Arrb2*$^{+/-}$ animals is likely a specific consequence of impaired $mGlu_5$-stimulated mRNA translation at the synapse.

2.3.6: Genetic reduction of β-arrestin2 in *Fmr1* KO mice restores aberrant protein synthesis and mGlu-LTD to WT levels.

Our results indicate that β-arrestin2 couples $mGlu_5$ activation to ERK-dependent protein synthesis and LTD. Aberrantly increased $mGlu_5$-dependent protein synthesis has been shown to be pathogenic in *Fmr1* KO mice (Dolen, Osterweil et al. 2007, Bhakar, Dolen et al. 2012). Therefore, we investigated whether a genetic reduction of *Arrb2* in *Fmr1* KO mice could correct fragile X phenotypes. We crossed *Arrb2*$^{+/-}$ male mice to *Fmr1*$^{x/-}$ female mice and found that both the increased synaptic protein synthesis (Figure 2.7A,B) and exaggerated mGlu-LTD (Figure 2.7 characteristic of *Fmr1*$^{-/y}$ mice were restored to WT levels in *Arrb2*$^{+/-}$ x *Fmr1*$^{-/y}$ mice.

2.3.7: Two wrongs make a right, yet again. Cognitive impairments in a

hippocampus-associated aversive learning task in both *Fmr1* KO and *Arrb2*$^{+/-}$ mice are corrected in *Arrb2*$^{+/-}$ x *Fmr1*$^{-/y}$ mice.

We next investigated the possibility that restoration of normal protein synthesis and $mGlu_5$-dependent synaptic plasticity in *Arrb2*$^{+/-}$ x *Fmr1*$^{-/y}$ mice could lead to improvements in cognitive and behavioral assays previously shown to be impaired in *Fmr1*$^{-/y}$ mice. We assayed inhibitory avoidance, a hippocampus-dependent behavior that is known to be disrupted in *Fmr1*$^{-/y}$ mice (Qin, Kang et al. 2002, Dolen, Osterweil et al. 2007) (Figure 2.8A). Memory strength was measured as the latency to enter the dark side of a box that was associated with a foot shock. We discovered that *Arrb2*$^{+/-}$ as well as *Fmr1*$^{-/y}$ mice failed to form a strong association between the context and foot shock (between time 0 and 6 hours) indicating impaired memory acquisition. This is consistent with previous results showing that bidirectional changes in hippocampal synaptic protein synthesis can actually manifest as similar impairment at the behavior level (Auerbach, Osterweil et al. 2011). Remarkably, however, *Arrb2*$^{+/-}$ x *Fmr1*$^{-/y}$ mice were indistinguishable from WT and exhibited normal memory acquisition and extinction over the course of 48 hours (Figure 2.8B).

2.3.8: Genetic reduction of β-arrestin2 in *Fmr1* KO mice corrects loss of novelty detection and alleviates susceptibility to audiogenic seizure.

We also investigated non-aversive object recognition memory. Mice were first allowed to explore an arena with two identical objects for two sessions and then, the next day, one of the familiar objects was replaced with a novel object (Figure 2.9A). While *Fmr1*$^{-/y}$ mice explored both the novel and familiar objects to an equal degree, indicating a severe impairment in novelty detection, *Arrb2*$^{+/-}$ x *Fmr1*$^{-/y}$ mice as well as *Arrb2*$^{+/-}$ single mutants showed a strong preference for the novel object similar to WT mice (Figure 2.9B). To ensure that this effect was not due to differential interest in overall exploration, we scored total time spent sniffing the two familiar objects during habituation session 1, and found no significant difference in exploration of either object, or cumulative exploration, across genotypes (Figure 2.9C). In an additional series of behavioral experiments we investigated audiogenic seizures (AGS), as increased

susceptibility to AGS is a hallmark phenotype in *Fmr1*$^{-/y}$ mice. Genetic reduction of *Arrb2* in *Fmr1* KO mice significantly attenuated seizure incidence (Figure 2.10) very similar to what has been observed using $mGlu_5$ and ERK-pathway inhibitors (Yan, Rammal et al. 2005, Dolen, Osterweil et al. 2007, Osterweil, Krueger et al. 2010).

2.3.9: Dose-limiting side effects seen with full $mGlu_5$ inhibitors are not apparent in *Arrb2*$^{+/-}$ mice.

Our data suggest that the $mGlu_5$ signaling relevant to FX pathophysiology specifically passes through β-arrestin2 to activate ERK and protein synthesis. If this conclusion is correct, then modulators that specifically target mGlu5 coupling to β-arrestin2 might avoid side effects that arise from inhibition of canonical G_q and/or mTOR pathway signaling. First-generation $mGlu_5$ NAMs, identified based on inhibition of G_q signaling, have been shown to act synergistically with the non-competitive NMDA receptor blocker MK801 to induce hyper-locomotion in mice (Homayoun, Stefani et al. 2004, Pietraszek, Gravius et al. 2005). MK801 is psychotomimetic in humans, and hyper-locomotion in mice is believed to be relevant to the mechanism(s) that cause derealization and visual hallucinations in people treated with mGlu5 NAMs (Pecknold, McClure et al. 1982, Porter, Jaeschke et al. 2005, Abou Farha, Bruggeman et al. 2014). We confirmed that pretreatment with the selective $mGlu_5$ inhibitor 3-[(2-Methyl-1,3-thiazol-4-yl)ethynyl]-pyridine (MTEP) (Cosford, Tehrani et al. 2003) significantly potentiates MK801-induced hyper-locomotion in WT mice. However, we found that baseline locomotor activity was the same in *Arrb2*$^{+/-}$ and WT mice, as was the synergistic effect of MTEP pretreatment (Figure 2.11). The fact that MTEP continues to exacerbate hyper-locomotion in mice that lack $mGlu_5$-regulated protein synthesis suggests that the psychotomimetic effects of the NAM are mediated by inhibition of pathways unrelated to FX pathophysiology.

2.4: Discussion

2.4.1: β-arrestin2 facilitates ERK1/2-dependent synaptic protein synthesis.

The primary purpose of this study was to establish a role for β-arrestin2 in $mGlu_5$-mediated signaling in the hippocampus. We found that $mGlu_5$-dependent ERK activation and protein synthesis are deficient in *Arrb2*$^{+/-}$ mice. Additionally, we found no differences in the recruitment of other signaling pathways in *Arrb2*$^{+/-}$ mice, including canonical Gq signaling or the AKT-mTOR pathway, suggesting that β-arrestin2 selectively couples $mGlu_5$ activation to the ERK cascade. The disruption in ERK activation appears to have functional consequences as well, as *Arrb2*$^{+/-}$ hippocampal slices exhibit diminished mGlu-LTD, likely due to the loss of the protein synthesis-dependent component of this form of plasticity. Our finding that β-arrestin2 acts as a signaling scaffold facilitating Ras-ERK pathway activation and mRNA translation is consistent with the role of β-arrestin2 at the angiotensin II receptor, which is similarly coupled to G_q signaling and activation of phospholipase C (DeWire, Kim et al. 2008, Ahn, Kim et al. 2009).

2.4.2: There is a functional divergence of β-arrestin isoforms in $mGlu_5$ function.

We have presented compelling evidence that β-arrestin1 and β-arrestin2 perform functionally distinct roles at the $mGlu_5$ receptor. While β-arrestin2 appears to be directly coupled to translation in a manner that is independent from canonical G_q signaling pathways, β-arrestin1 does not appear to be necessary for *de novo* protein synthesis. While the obvious hypothesis would be that β-arrestin1 plays a crucial role in $mGlu_5$ internalization and desensitization, further investigation is necessary to confirm that this is the case. Furthermore it is notable, that while a heterozygous deletion of β-arrestin2 does not yield quantifiable changes in calcium mobilization, that is not to say that β-arrestin2 is not involved in G_q signaling. In fact, we would likely expect that full deletion of β-arrestin2 might lead to enhanced $mGlu_5$ signaling as a result of reduced $mGlu_5$ endocytosis and diminished receptor desensitization. Indeed, preliminary evidence suggests that there is enhanced G_q activation in *Arrb2*$^{-/-}$ mice (data not shown).

Nonetheless, we are not the first to report a divergence of function between the two β-arrestin isoforms, and in fact, β-arrestin1 and β-arrestin2 show functional specialization at a plethora of GPCRs, often taking on contradictory roles at different receptors (Srivastava, Gupta et al. 2015).

2.4.3: $mGlu_5$-specific β-arrestin2-biased negative allosteric modulation could be a viable pharmacological target for the treatment of Fragile X in humans.

Inhibitors of $mGlu_5$ and the Ras-ERK pathway have been successful in combating the excessive protein synthesis known to be pathogentic in the mouse model of Fragile X (Dolen, Osterweil et al. 2007, Michalon, Sidorov et al. 2012, Osterweil, 2013 #4). In order to validate the therapeutic benefit of reducing β-arrestin2 signaling in the Fragile X mouse model we employed a genetic reduction strategy. While we have demonstrated that β-arrestin2 is a viable target in correcting the pathophysiology of Fragile X, our strategy was merely a "proof of principle" attempt. The ideal pharmacological intervention would involve developing a β-arrestin2-biased negative allosteric modulator of $mGlu_5$ (Figure 2.12). Allosteric modulation allows precise dose-dependent control over receptor function by acting as a "dimmer" of orthosteric ligand binding rather than introducing competition for the orthosteric binding site (or ligand traps) associated with traditional receptor antagonism (Conn, Christopoulos et al. 2009). There is compelling evidence that it is possible to develop compounds that have receptor-targeted signaling-pathway-specificity (Sheffler, Gregory et al. 2011, Iacovelli, Felicioni et al. 2014, Hathaway, Pshenichkin et al. 2015). However, considering the high degree of sequence and structural similarity of β-arrestin isoforms, achieving such specificity at $mGlu_5$ is likely to be challenging (Srivastava, Gupta et al. 2015).

2.4.4: Avoiding dose-limiting side-effects- the advantage of specificity.

One of the downfalls of $mGlu_5$ inhibitors in the clinic, are the dose-limiting side effects of global $mGlu_5$ receptor inhibition, including drug tolerance and off-target inhibition of NMDARs, leading to psychotomimetic tendencies leading to visual

hallucinations (Pecknold, McClure et al. 1982, Porter, Jaeschke et al. 2005, Abou Farha, Bruggeman et al. 2014). While our genetic reduction strategy did not allow us to evaluate drug tolerance (see Chapter 3), we did find evidence that MK801-mediated hyperlocomotion associated with $mGlu_5$ inhibitors was not apparent in *Arrb2*$^{+/-}$ mice. Furthermore, when we inhibited $mGlu_5$ with MTEP in *Arrb2*$^{+/-}$ mice, we were able to induce the same potentiated hyperlocomotion seen in WT mice pre-treated with MTEP, indicating that this finding was not a consequence of some form of adaptation. We believe that this is concrete evidence, in addition to the finding that *Arrb2*$^{+/-}$ mice show normal NMDAR-LTD, that NMDAR function is unaffected by reduction of β-arrestin2 signaling, that β-arrestin2-targeted negative allosteric modulation of $mGlu_5$ could yield clinically significant improvements over $mGlu_5$ inhibitors that failed to meet safety and efficacy endpoints in clinical trials.

2.4.5: Conclusion

G-protein coupled receptors respond to a wide variety of signals and initiate a large number of distinct cellular signaling pathways. This versatility has made these receptors attractive targets for pharmacological therapies, and over 50% of the current drugs used clinically target these receptors (Insel, Tang et al. 2007). The finding that β-arrestin- and G protein-dependent cellular signaling are pharmacologically separable has opened a new avenue for the treatment of disease. For some disorders, modulation of only one of these signaling pathways may be therapeutically beneficial, while the other(s) could mediate undesirable and possibly conflicting outcomes (Whalen, Rajagopal et al. 2011). Our findings suggest that $mGlu_5$ modulators for the treatment of fragile X may be a case in point. There is little doubt that β-arrestin-biased allosteric modulators of mGlu receptors are feasible (Sheffler, Gregory et al. 2011, Iacovelli, Felicioni et al. 2014, Hathaway, Pshenichkin et al. 2015), and their development could lead to the next generation of drugs for the treatment of fragile X and several other genetically defined causes of ID and ASD (Bozdagi, Sakurai et al. 2010, Auerbach, Osterweil et al. 2011, Aguilar-Valles, Matta-Camacho et al. 2015, Barnes, Wijetunge et al. 2015, Tian, Stoppel et al. 2015, Wenger, Kao et al. 2016).

2.5: Methods

2.5.1: Animals

Arrb2$^{+/-}$ male and female mutant mice on the C57Bl/6J clonal background were bred together to produce the WT and *Arrb2*$^{+/-}$ offspring used in this study. *Fmr1*$^{-/x}$ female mice (Jackson Labs) were crossed with *Arrb2*$^{+/-}$ mice to generate double mutant animals. All experimental animals were age-matched male littermates, and were studied with the experimenter blind to genotype and treatment condition. Animals were group housed and maintained on a 12:12 hour, light: dark cycle. The Institutional Animal Care and Use Committee at MIT approved all experimental techniques and all animals were treated in accordance with NIH and MIT guidelines.

2.5.2: Reagents

(S)-3,5-dihydroxyphenylglycine (S-DHPG) was purchased from Tocris. Fresh bottles of DHPG were prepared as a 100x stock in H_2O, divided into aliquots, and stored at -80°C. Fresh stocks were made once a week. Cycloheximide (Sigma) was prepared daily at 100x stock in H_2O. Actinomycin D (Tocris) was prepared as a stock solution of 1mg/mL in 0.01% DMSO and aCSF and stored at -20°C. CDPPB (Tocris) was prepared daily at 75 mM stock in DMSO. U73122 (Tocris) was prepared as a 5 mM stock in DMSO. MK801 (Sigma) was prepared in H_2O daily and .3 mg/kg was injected i.p. at a dosing volume of 10 ml/kg. MTEP (Tocris) was prepared in H_2O daily and 10 mg/kg was injected i.p. at a dosing volume of 10 ml/kg.

2.5.3: Electrophysiology

Slices were prepared as described previously (Dolen, Osterweil et al. 2007). Acute hippocampal slices were prepared from P28-35 animals in ice-cold dissection buffer containing (in mM): NaCl 87, Sucrose 75, KCl 2.5, NaH_2PO_4 1.25, $NaHCO_3$ 25, $CaCl_2$ 0.5, $MgSO_4$ 7, Ascorbic acid 1.3, and D-glucose 10 (saturated with 95% O_2 / 5% CO_2). Immediately following slicing the CA3 region was removed. Slices were recovered in

artificial cerebrospinal fluid (aCSF) containing (in mM): NaCl 124, KCl 5, NaH_2PO_4 1.23, $NaHCO_3$ 26, $CaCl_2$ 2, $MgCl_2$ 1, and D-glucose 10 (saturated with 95% O_2/5% CO_2) at 32.5°C for ≥ 3 hours prior to recording. Field recordings were performed in a submersion chamber, perfused with aCSF (2-3 ml/min) at 30°C. Field EPSPs (fEPSPs) were recorded in CA1 stratum radiatum with extracellular electrodes filled with aCSF. Baseline responses were evoked by stimulation of the Schaffer collaterals at 0.033 Hz with a 2-contact cluster electrode (FHC) using a 0.2 ms stimulus yielding 40-60% of the maximal response. fEPSP recordings were filtered at 0.1 Hz - 1 kHz, digitized at 10 kHz, and analyzed using pClamp9 (Axon Instruments). The initial slope of the response was used to assess changes in synaptic strength. Data were normalized to the baseline response and are presented as group means ± SEM. The input output function was examined by stimulating slices with incrementally increasing current and recording the fEPSP response. Paired pulse facilitation was induced by applying two pulses at different interstimulus intervals. Facilitation was measured by the ratio of the fEPSP slope of stimulus 2 to stimulus 1. NMDAR-dependent LTD was induced by delivering 900 test pulses at 1 Hz. mGlu-LTD was induced by S-3,5-Dihydroxyphenylglycine (S-DHPG, 25 μM) for 5 minutes. In order to determine the protein synthesis dependency of mGlu-LTD, slices were incubated with the protein synthesis inhibitor cycloheximide (60 μM) for at least 10 minutes prior to recording and throughout the entire experiment. The magnitude of LTD was measured by comparing the average response 55-60 minutes post DHPG/LFS application to the average of the last 5 minutes of baseline. Statistical significance for input-output function, paired-pulse facilitation, and mGlu- or NMDAR-dependent plasticity was determined by two-way ANOVA and post-hoc Student's t-tests.

2.5.4: Fluorescence-based calcium imaging in brain slices

Hippocampal slices (350 μm thick) were recovered in aCSF for 2 hours at 32°C. Slices were then moved to a small recovery chamber and incubated in oxygenated aCSF containing 20 μM fluo-4-acetoxymethyl ester (fluo-4 AM; ThermoFisher) and 0.1% Pluronic F-127 (ThermoFisher) for 1 hour in the dark. After 1 hour, slices were then

washed with oxygenated aCSF containing 1 μM tetrodotoxin (Abcam) and 50 μM D-AP5 (Tocris) for 20 minutes in a recording chamber. A low-powered (4X) objective was used to identify the brain region of interest. CA1 pyramidal neurons were visualized using a 40X water immersion objective and a Nikon Eclipse E600FN microscope. Changes in Ca^{2+} fluorescence were monitored in the presence of 1 μM tetrodotoxin and 50 μM D-AP5 using a Hamamatsu ORCA-100 camera, HCImage software (Hamamatsu), and a mercury arc-lamp and power supply (Nikon). After a 10 second baseline, 25 μM (S)-3,5-DHPG was bath applied. For a subset of experiments, slices were pre-treated with 10 μM U73122 during the wash period to block phospholipase C activity. Data were analyzed using Image J software. Increases in Ca^{2+} mobilization in hippocampal neurons were reported as changes in relative fluorescence divided by the baseline fluorescence ($\Delta F/F$).

2.5.5: Metabolic labeling

Metabolic labeling of new protein synthesis was performed as previously described (Osterweil, Krueger et al. 2010). Male P28-P32 littermate mice were anesthetized with isoflurane and the hippocampus was rapidly dissected into ice-cold aCSF (in mM: 124 NaCl, 3 KCl, 1.25 NaH_2PO_4, 26 $NaHCO_3$, 10 dextrose, 1 $MgCl_2$, 2 $CaCl_2$, saturated with 95% O_2 and 5% CO_2). Hippocampal slices (500 μm) were prepared using a Stoelting Tissue Slicer and transferred into 32.5°C aCSF (saturated with 95% O_2 and 5% CO_2) within 5 min. Slices were incubated in aCSF undisturbed for 3.5-4 h to allow for recovery of basal protein synthesis. Actinomycin D (25 μM) and vehicle or CDPPB (10 μM) was then added to the recovery chamber for 30 min to inhibit transcription and stimulate mGlu receptors, respectively after which slices were transferred to fresh aCSF containing ~10 mCi/ml [^{35}S] Met/Cys (Perkin Elmer) for an additional 30 min. Slices were then homogenized, and labeled proteins isolated by TCA precipitation. Samples were read with a scintillation counter and subjected to a protein concentration assay (Bio-Rad). Data was analyzed as counts per minute per microgram of protein, normalized to the [^{35}S] Met/Cys aCSF used for incubation and the average incorporation

of all samples analyzed and then normalized to percent WT for each experiment. Statistical significance was determined using unpaired t-tests.

2.5.6: Immunoblotting

Hippocampal slices were prepared and recovered as described in metabolic labeling experiments. Sets of slices were stimulated with CDPPB (10 μM) for 30 minutes and then flash frozen in liquid nitrogen immediately after stimulation, prior to processing. Yoked unstimulated slices were also processed to assess basal signaling levels. Immunoblotting was performed according to established methods using primary antibodies to p-ERK1/2 (Thr202/Tyr204) (Cell Signaling Technology), ERK1/2 (Cell Signaling Technology), p-Akt (Ser473) (Cell Signaling Technology), Akt (Cell Signaling Technology), pS6 240/44 (Cell Signaling Technology) and S6 (Cell Signaling Technology). Protein levels were measured by densitometry (Quantity One), and quantified as the densitometric signal of phospho-protein divided by the total protein signal in the same lane.

2.5.7: Inhibitory avoidance extinction

Inhibitory avoidance experiments were performed as previously described (Dolen, Osterweil et al. 2007). On the day of testing, P56-P76 animals were placed into the dark compartment of an IA training box (a two-chambered Perspex box consisting of a lighted safe side and a dark shock side separated by a trap door) for 30 seconds followed by 90 seconds in the light compartment for habituation. Following the habituation period, the door separating the two compartments was opened and animals were allowed to enter the dark compartment. Latency to enter following door opening was recorded ("baseline", time 0, 8-9am); animals with baseline entrance latencies of greater than 120 seconds were excluded. After each animal stepped completely into the dark compartment with all four paws, the sliding door was closed and the animal received a single scrambled foot-shock (0.5mA, 2.0 sec) via electrified steel rods in the floor of the box. This intensity and duration of shock consistently caused animals to vocalize and jump. Animals remained in the dark compartment for 15 sec following the

shock and were then returned to their home cages. Six to seven hours following IA training, mice received a retention test ("post-acquisition", time 6 hours, 2p.m.-3p.m.). During post-acquisition retention testing each animal was placed in the lit compartment as in training; after a 90 second delay, the door opened, and the latency to enter the dark compartment was recorded (cut-off time 537 sec). For inhibitory avoidance extinction (IAE) training, animals were allowed to explore the dark compartment of the box for 200 seconds in the absence of foot-shock (animals remaining in the lit compartment after the cutoff were gently guided, using an index card, into the dark compartment); following IAE training animals were returned to their home cages. Twenty-four hours following initial IA training, mice received a second retention test ("post-extinction 1", time 24 hours, 8a.m-9a.m.). Animals were tested in the same way as at the six hour time point, followed by a second 200 second extinction trial in the dark side of the box; following training animals were again returned to their home cages. Forty-eight hours following avoidance training, mice received a third and final retention test ("post-extinction 2", time 48 hours, 8a.m.- 9a.m.).

2.5.8: Audiogenic seizures

AGS experiments were performed as previously described (Dolen, Osterweil et al. 2007). Animals at P19-25 (immediately following weaning) were habituated to the behavioral chamber (28x17.5x12 cm transparent plastic box) for 1 minute prior to stimulus onset. AGS stimulus was a 125 db at 0.25 m siren (modified personal alarm, Radioshack model 49-1010, powered from a DC converter). Seizures were scored for incidence during a 2-minute stimulus presentation or until animal reached AGS endpoint (wild running, status epilepticus, respiratory arrest or death were all scored as seizure activity).

2.5.9: Object recognition

The object recognition task was adapted from experiments previously described (Leger, Quiedeville et al. 2013). Animals at P56-70 were habituated to a 40 cm x 40 cm x 40 cm box during 2 x 15 minute sessions, spaced 1-2 hours apart. Animals were returned

to their home cage in between sessions. 24 hours post habituation animals were exposed to two identical objects for 2 x 10 minute exploration sessions in the same box, spaced 1-2 hours apart. Animals were required to explore each object for at least 10 seconds (for a total of at least 20 seconds) in the first session to be included in the subsequent sessions. 24 hours post object exploration, one object was replaced with a novel object and the animals were allowed to explore the objects for 10 minutes. Time spent sniffing was recording during this exploration period and was characterized by sniffing within 2 cm of each object or directly touching the objects. Time spent climbing or on top of the objects was not included. Familiar and novel object and side placement was randomly assigned, by animal. Discrimination index was calculated as [(time spent exploring novel object) / (time spent exploring novel object + time spent exploring familiar object)].

2.5.10: MK801-induced hyperlocomotion

To determine the effects of genotype on MK801-induced hyperlocomotion, mice were habituated in the open field (40 cm x 40 cm x 40 cm box) for 60 min, followed by the administration of vehicle or MK801 and locomotor activity was recorded for another 60 min. To determine the effects of MTEP by genotype on MK801-induced hyperlocomotion, mice were habituated in the open field for 30 min, followed by the intraperitoneal (i.p.) administration of MTEP (10 mg/kg at a dosing volume of 10 ml/kg). After an additional 30 min, MK801 (0.3 mg/kg at a dosing volume of 10 ml/kg) was administered i.p. and locomotor activity was recorded for another 60 min. The time course of drug-induced changes in ambulation was expressed as cm traveled/5 min over the 120-min session. Sessions were recorded using Plexon's *CinePlex*® Studio and analyzed using Plexon's *CinePlex*® Editor and code written in MATLAB. MK801-induced locomotor activity was scored and analyzed using the average of the final 5 minutes (minute 115-120) per cohort.

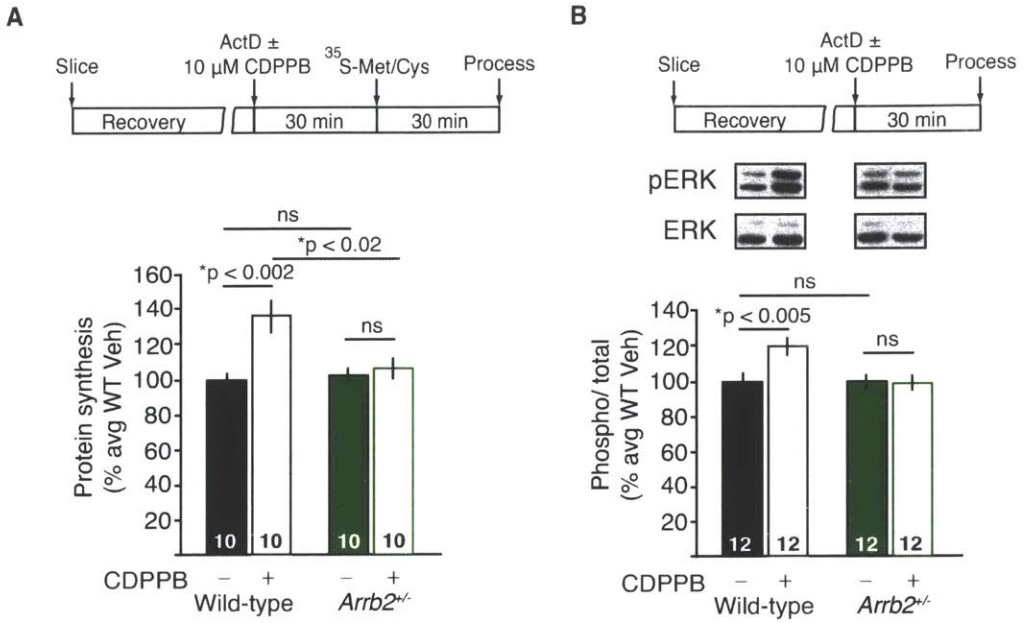

Figure 2.1: β-Arrestin2 is necessary for protein synthesis-dependent mGlu-LTD and ERK1/2 activation.

(**A**) Schematic illustrates experimental timeline. Protein synthesis was elevated in WT slices stimulated with CDPPB compared with vehicle whereas treatment had no effect in *Arrb2*$^{+/-}$ slices (two-way ANOVA, genotype vs. treatment, *p = 0.012). (**B**) Representative immunoblots of ERK1/2 phosphorylation and total ERK protein from hippocampal slices ± CDPPB stimulation from WT and *Arrb2*$^{+/-}$ mice. WT slices stimulated with CDPPB show elevated ERK1/2 phosphorylation compared with vehicle, whereas no change is observed in *Arrb2*$^{+/-}$ mice (two-way ANOVA, genotype vs. treatment, *p = 0.015).

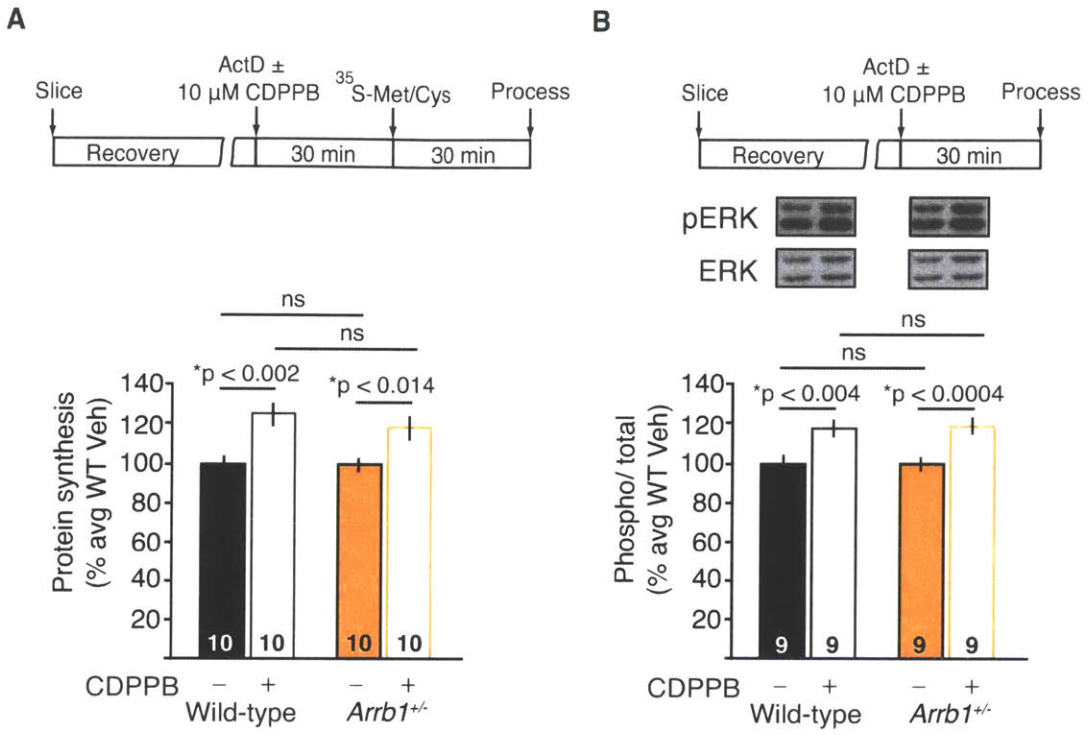

Figure 2.2: β-Arrestin1 is not necessary for protein synthesis-dependent ERK1/2 activation.

(**A**) Schematic illustrates experimental timeline. Protein synthesis was similarly elevated in WT slices and *Arrb1*$^{+/-}$ slices stimulated with CDPPB compared to vehicle-treated slices of both genotypes (two-way ANOVA, genotype vs. treatment, $p = 0.589$). (**B**) Schematic illustrates experimental timeline. Representative immunoblots of ERK1/2 phosphorylation and total ERK protein from hippocampal slices ± 10µM CDPPB stimulation from WT and *Arrb1*$^{+/-}$ mice. WT and *Arrb1*$^{+/-}$ slices stimulated with CDPPB show elevated ERK1/2 phosphorylation compared with vehicle, (two-way ANOVA, genotype vs. treatment, $p = 0.786$).

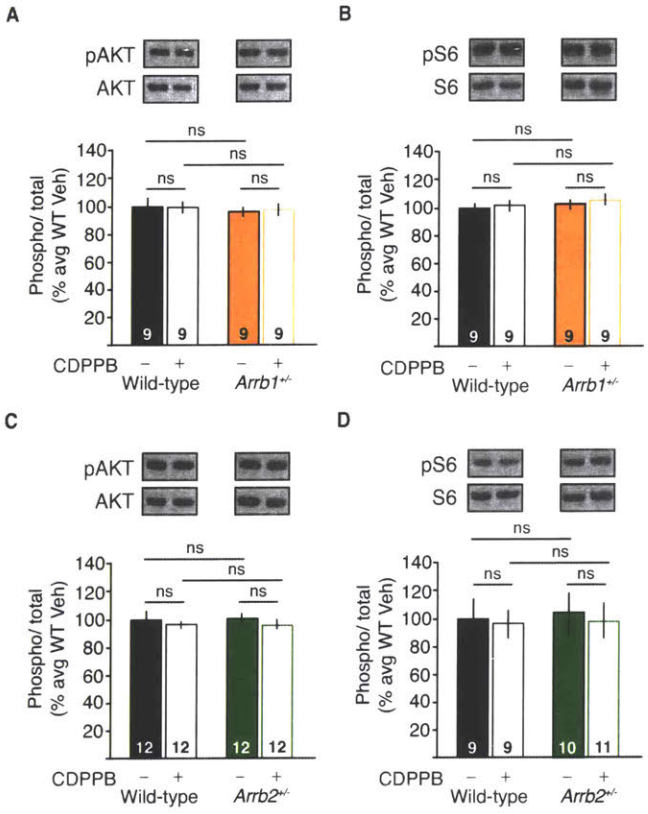

Figure 2.3: The AKT-mTOR pathway is not activated by CDPPB in WT, *Arrb1*$^{+/-}$ or *Arrb2*$^{+/-}$ mice.

(**A**) Representative immunoblots of AKT phosphorylation and total AKT protein from hippocampal slices ± 10μM CDPPB stimulation from WT and *Arrb1*$^{+/-}$ mice. Neither WT nor *Arrb1*$^{+/-}$ slices stimulated with CDPPB show elevated AKT phosphorylation compared with vehicle, (two-way ANOVA, genotype vs. treatment, p = 0.727). (**B**) Representative immunoblots of ribosomal protein S6 phosphorylation and total S6 protein from hippocampal slices ± 10μM CDPPB stimulation from WT and *Arrb1*$^{+/-}$ mice. Neither WT nor *Arrb1*$^{+/-}$ slices stimulated with CDPPB show elevated S6 phosphorylation compared with vehicle, (two-way ANOVA, genotype vs. treatment, p = 0.945). (**C**) Representative immunoblots of AKT phosphorylation and total AKT protein from hippocampal slices ± 10μM CDPPB stimulation from WT and *Arrb2*$^{+/-}$ mice. Neither WT nor *Arrb2*$^{+/-}$ slices stimulated with CDPPB show elevated AKT phosphorylation compared with vehicle, (two-way ANOVA, genotype vs. treatment, p = 0.894). (**D**) Representative immunoblots of ribosomal protein S6 phosphorylation and total S6 protein from hippocampal slices ± 10μM CDPPB stimulation from WT and *Arrb2*$^{+/-}$ mice. Neither WT nor *Arrb2*$^{+/-}$ slices stimulated with CDPPB show elevated S6 phosphorylation compared with vehicle, (two-way ANOVA, genotype vs. treatment, p = 0.920).

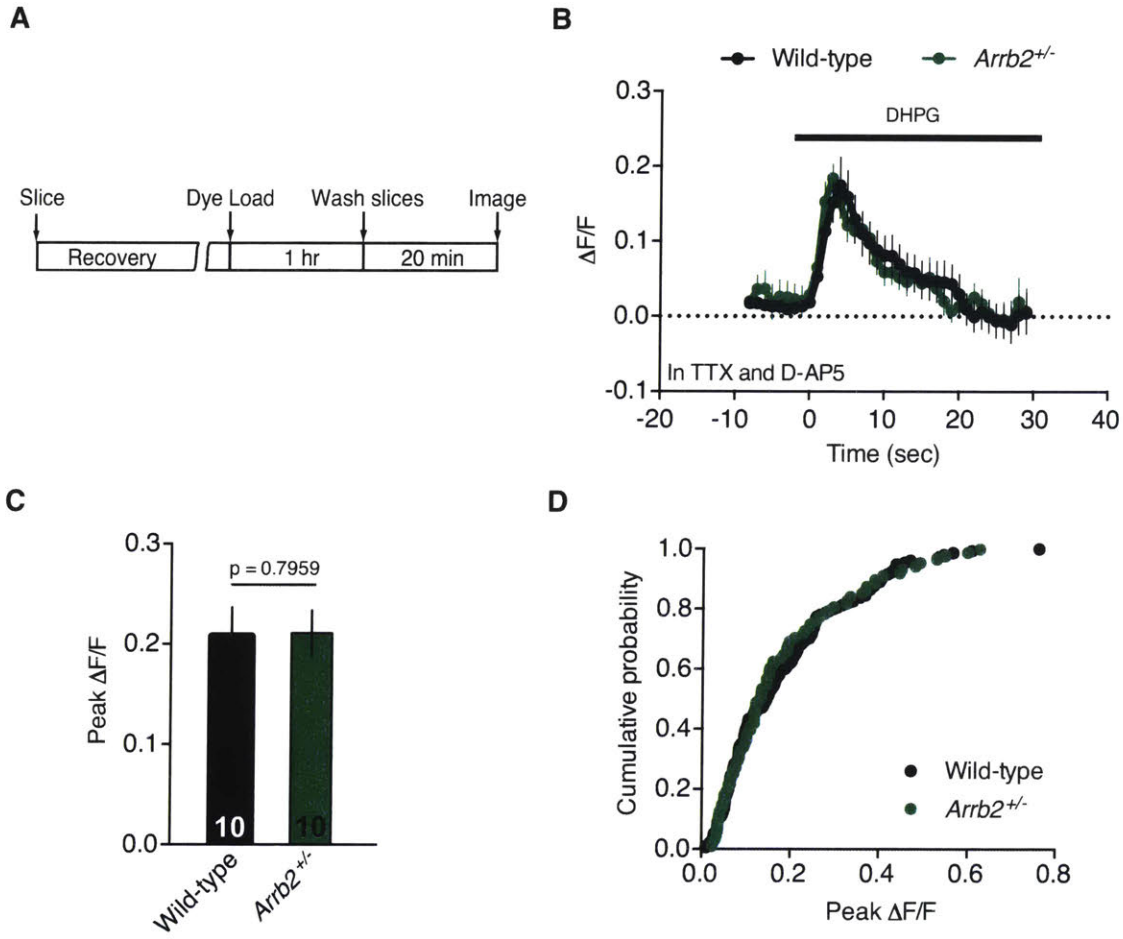

Figure 2.4: Genetic reduction in β-Arrestin2 does not alter G_q-coupled calcium mobilization in area CA1 of the hippocampus.

(**A**) Schematic illustrates experimental timeline: WT and *Arrb2*$^{+/-}$ hippocampal slices were recovered in aCSF at 32 °C for 2 hours, incubated with 20 µM Fluo-4 AM dye and 0.1% pluronic F-127 for 1 hour in the dark prior to imaging. Slices were washed with aCSF containing 1 µM tetrodotoxin and 50 µM D-AP5 for 20 minutes. After a 10 second baseline, 25 µM (S)-3,5-DHPG was added and changes in calcium fluorescence were recorded. (**B**) Quantification of calcium fluorescence over time in WT and *Arrb2*$^{+/-}$ slices. Data are normalized as ΔF/F as detailed in the materials and methods. (**C**) There is no significant difference in the peak calcium fluorescence measured between WT and *Arrb2*$^{+/-}$ slices (Mann-Whitney test, p = 0.7959). N represents individual animals, where 3-4 slices per animal were analyzed. (**D**) The cumulative probability of peak fluorescence for all cells analyzed is not different between WT and *Arrb2*$^{+/-}$ slices. (Experiments conducted by Rebecca Senter).

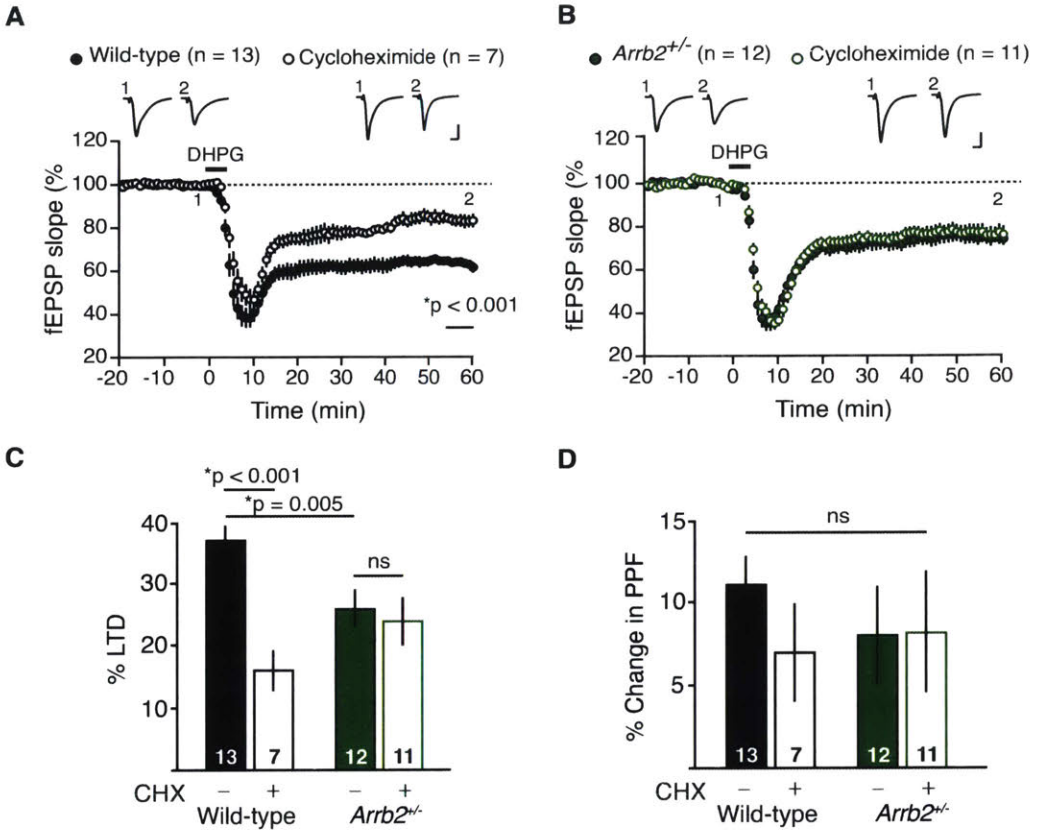

Figure 2.5: LTD is impaired and independent of *de novo* protein synthesis in *Arrb2*$^{+/-}$ mice.

(**A**) LTD is significantly attenuated by pretreatment with the protein synthesis inhibitor cycloheximide (CHX, 60 μM) in slices from WT animals (*p < 0.001). (**B**) CHX treatment has no effect on DHPG-LTD in slices from *Arrb2*$^{+/-}$ mice. (**C**) The magnitude of protein-synthesis-dependent post-synaptic mGlu-LTD is greatly diminished in slices from *Arrb2*$^{+/-}$ mice compared with WT mice (two-way ANOVA, genotype vs. treatment, *p = 0.003). (**D**) There is no significant difference in paired pulse facilitation between WT and *Arrb2*$^{+/-}$ mice. In this and subsequent figures, representative field excitatory postsynaptic potential (fEPSP) traces (average of ten sweeps) were taken at the times indicated by numerals. Scale bars equal 0.5 mV, 5 ms. N represents number of animals (1-2 slices) per group. All data are plotted as mean ± s.e.m. (Experiments conducted by Benjamin Auerbach).

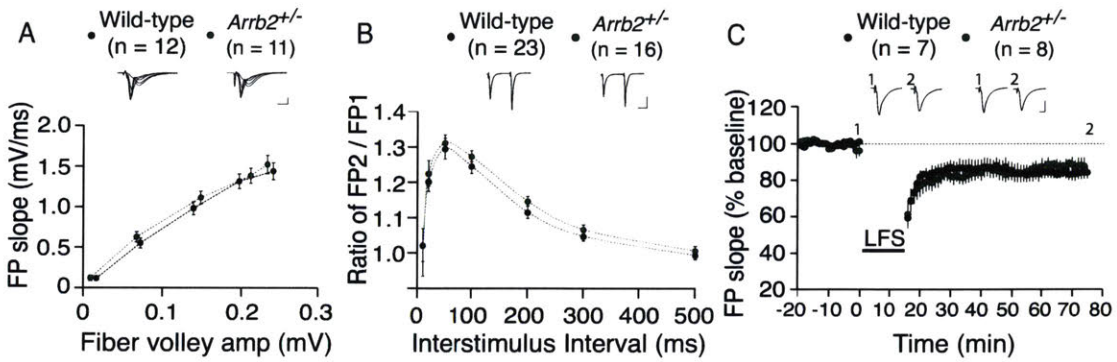

Figure 2.6: *Arrb2*$^{+/-}$ mice have normal basal synaptic function and NMDAR-dependent LTD.

(**A**) Basal synaptic transmission (plotted as fEPSP amplitude against presynaptic fiber volley amplitude) does not differ between genotypes. Scale bars equal 0.5 mV, 20 ms for representative field potential traces. (**B**) Paired pulse facilitation is normal across several inter-stimulus intervals (20, 30, 50, 100, 200, 300, 500 ms) in *Arrb2*$^{+/-}$ slices. Scale bars equal 0.5 mV, 20 ms. (**C**) The magnitude of NMDA receptor-dependent LTD evoked by low frequency stimulation (LFS, 900 pulses at 1 Hz) does not differ between genotypes ($p = 0.610$). Representative field potential traces (average of 10 sweeps) were taken at times indicated by numerals. Scales bars equal 0.5 mV, 5 ms. (Experiments conducted by Benjamin Auerbach).

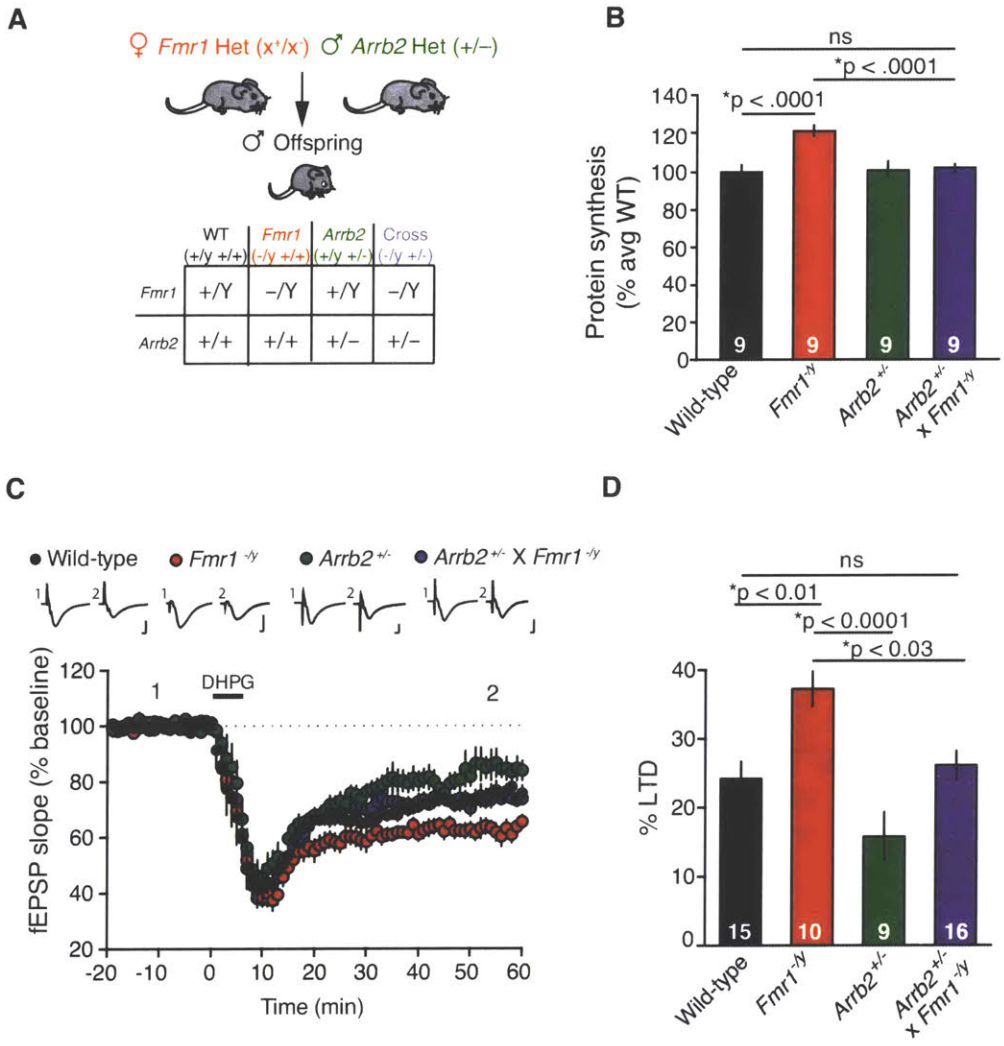

Figure 2.7: Genetic reduction of β-arrestin2 in *Fmr1*$^{-/y}$ mice corrects exaggerated protein synthesis and mGlu-LTD.

(**A**) Genetic rescue strategy. (**B**) Basal protein synthesis is significantly increased in slices from *Fmr1*$^{-/y}$ mice (*p < 0.0001) compared with WT slices. Basal protein synthesis is comparable in slices from *Arrb2*$^{+/-}$ x *Fmr1*$^{-/y}$ mice and WT mice. (**C**) The magnitude of DHPG-induced LTD in slices from *Arrb2*$^{+/-}$ x *Fmr1*$^{-/y}$ mice is significantly different from *Fmr1*$^{-/y}$ slices (*p < 0.03), and is indistinguishable from WT slices. Representative field potential traces (average of 10 sweeps) were taken at times indicated by numerals. Scales bars equal 0.5 mV, 2 ms. (**D**) Summary of LTD data. Bar graphs, percentage decrease from baseline in fEPSP slope. (Experiments in panels C and D were conducted by Benjamin Auerbach and Rebecca Senter).

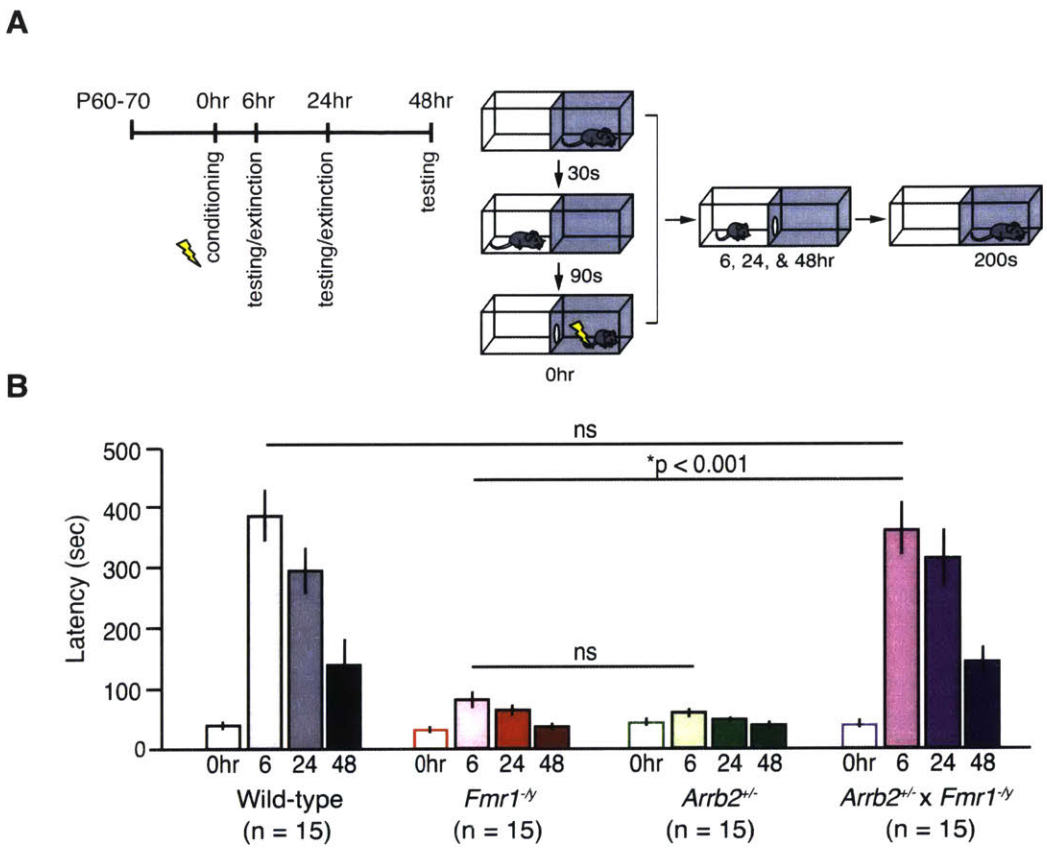

Figure 2.8: Genetic reduction of β-arrestin2 in *Fmr1*$^{-/y}$ mice corrects impaired memory in a single-trial, hippocampus-associated learning task.

(**A**) Experimental design of inhibitory avoidance learning task. (**B**) *Fmr1*$^{-/y}$ mice and *Arrb2*$^{+/-}$ mice show impaired acquisition of inhibitory avoidance learning compared to WT mice (two-way ANOVA, *p < 0.001 for each comparison, WT vs. *Fmr1*$^{-/y}$, WT vs. *Arrb2*$^{+/-}$). *Arrb2*$^{+/-}$ x *Fmr1*$^{-/y}$ mice show comparable acquisition and extinction of inhibitory avoidance to WT mice (two-way ANOVA, p = 0.916). There is a statistically significant interaction between genotype and time point across groups (repeated measures two-way ANOVA, *p = < 0.001).

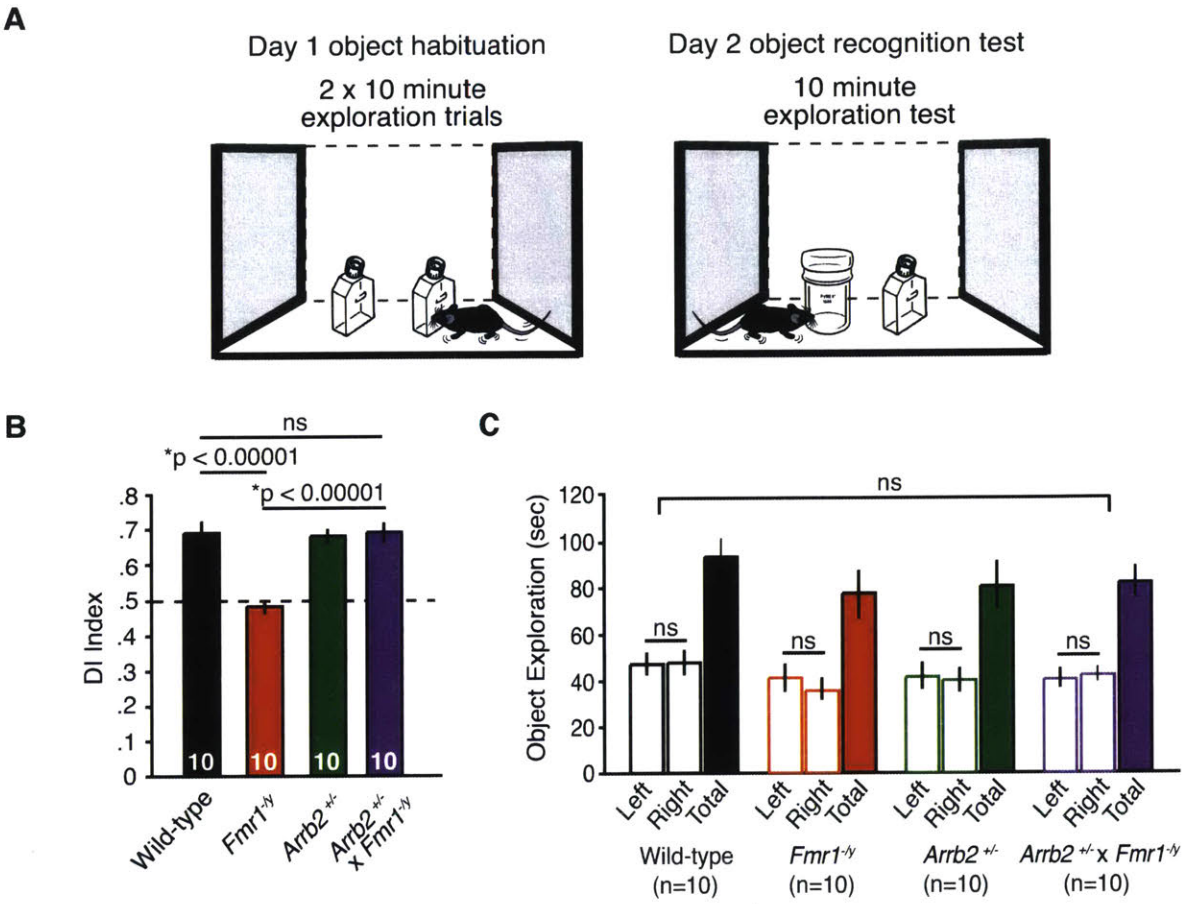

Figure 2.9: Genetic reduction of β-arrestin2 in *Fmr1*$^{-/y}$ mice corrects impaired familiar object recognition memory.

(**A**) Experimental design of familiar object recognition task. (**B**) *Fmr1*$^{-/y}$ mice show impaired novelty detection on experimental test day 2 when presented with a familiar and novel object compared to WT (*$p < 0.00001$). In comparison, *Arrb2*$^{+/-}$ x *Fmr1*$^{-/y}$ show a discrimination index that is not significantly different from WT mice (Student's two-tailed t-test, $p = 0.9598$). (**C**) There is no significant difference in time spent exploring each of two identical objects during the first object habituation session in any genotype, nor is there any significant difference in total time spent exploring during habituation session one.

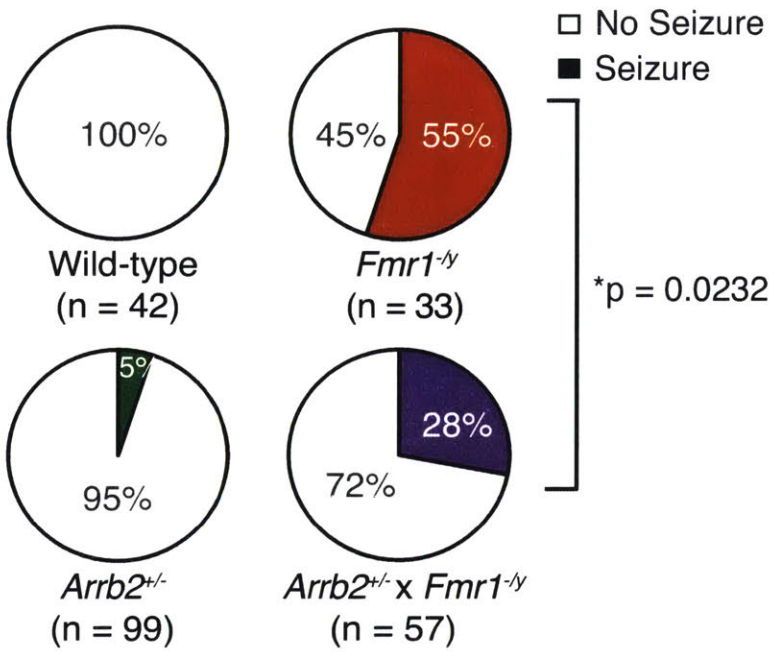

Figure 2.10: Genetic reduction of β-arrestin2 in *Fmr1*$^{-/y}$ mice alleviates the susceptibility to audiogenic seizures.

Fmr1$^{-/y}$ mice exhibit increased susceptibility to audiogenic seizure activity compared to WT (two-tailed Fisher's exact test, *p = 0.0001) and *Arrb2*$^{+/-}$ mice (*p = 0.0001). Genetic reduction of *Arrb2* in *Fmr1*$^{-/y}$ mice significantly reduces the incidence of seizure activity (*p = 0.0232).

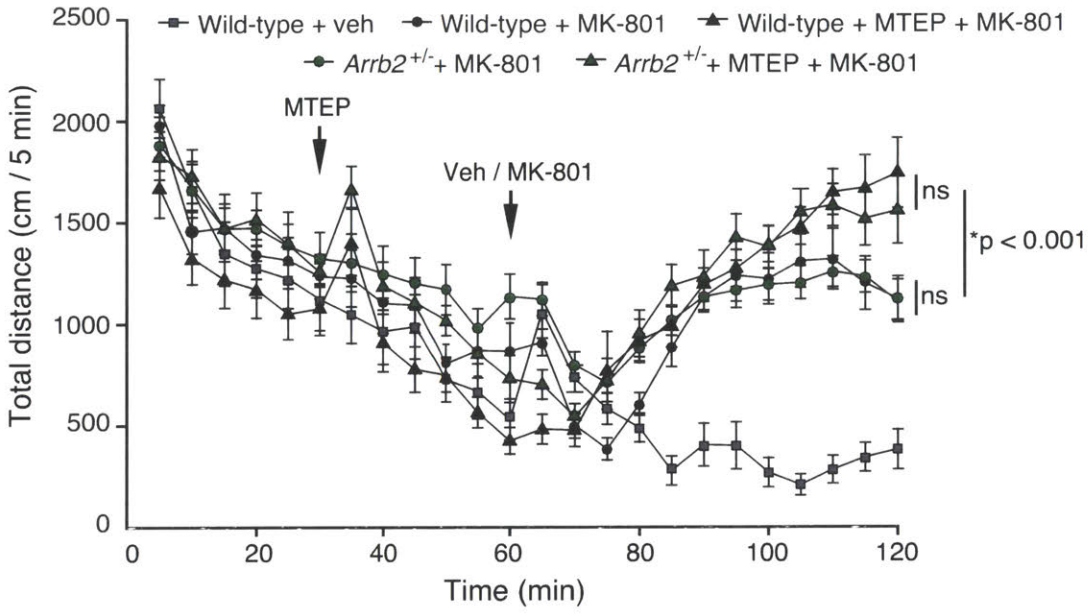

Figure 2.11: Genetic reduction in β-arrestin2 does not potentiate the psychotomimetic effects of MK801.

WT and *Arrb2*$^{+/-}$ mice injected intraperitoneally with the NMDAR antagonist MK801 (0.3 mg/kg) show comparable hyperlocomotion 60 minutes post-treatment compared to vehicle (N = 10 mice per group). Data points represent distance travelled in cm over 5 minute bins, averaged as pooled animals per treatment group. Pre-treatment with MTEP (10 mg/kg, i.p.) potentiates hyperlocomotion in both WT and *Arrb2*$^{+/-}$ mice (N = 9 mice per group). Two-way ANOVA for genotype: $p = 0.499$ and for treatment: $^*p < 0.001$, no significant interaction between genotype and treatment. Student's two-tailed t-test WT + MK801 vs. WT + MTEP + MK801: $^*p = 0.009$. Student's two-tailed t-test *Arrb2*$^{+/-}$ + MK801 vs. *Arrb2*$^{+/-}$ + MTEP + MK801 $^*p = 0.037$.

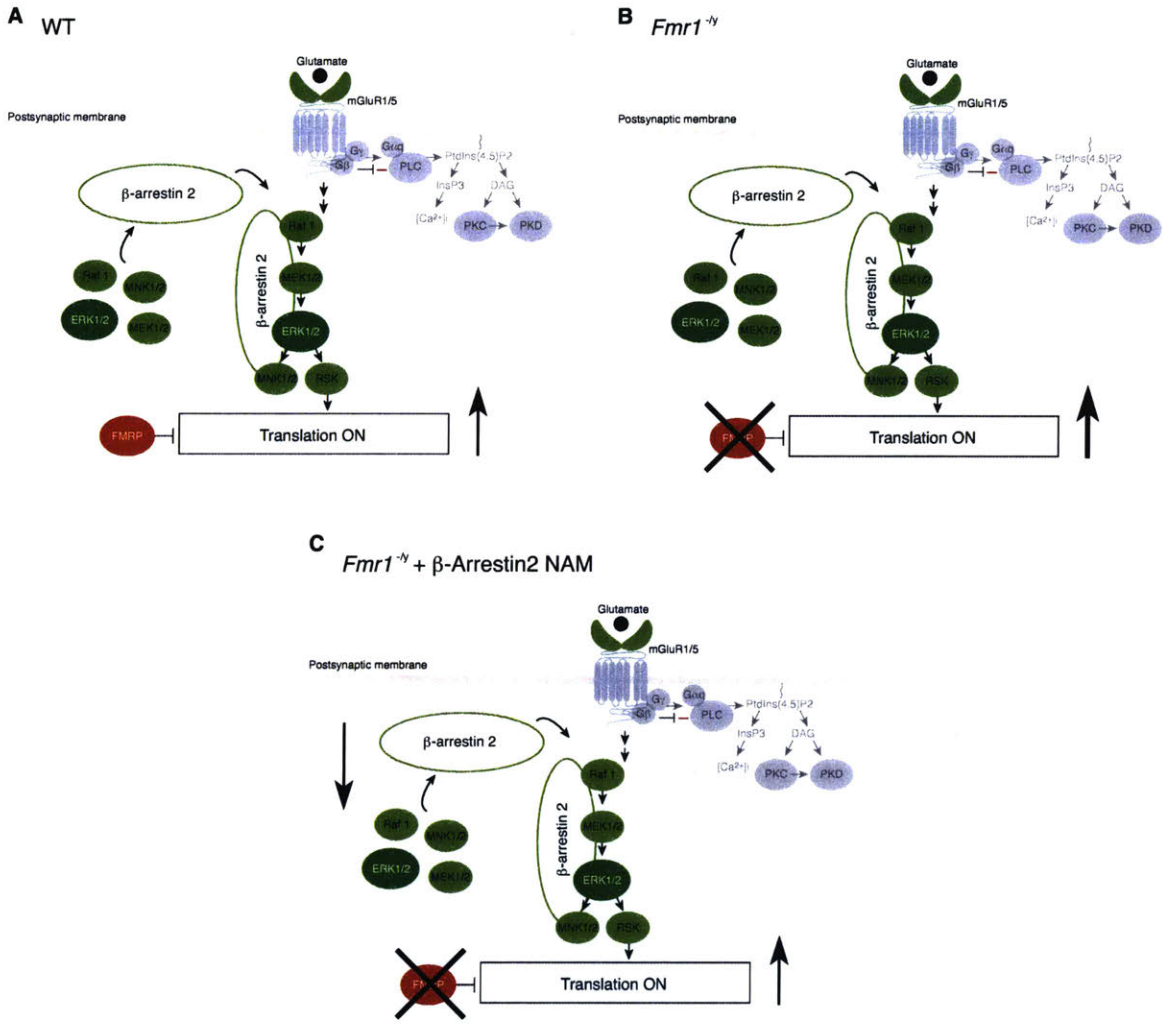

Figure 2.12: β-arrestin2-biased negative allosteric modulation could be beneficial in the treatment of FX

(**A**) In WT mice, β-arrestin2 acts as a signaling scaffold for the Ras-ERK pathway, -coupling $mGlu_5$ activation to synaptic translation that is kept in check by FMRP. (**B**) In *Fmr1*$^{-/y}$ mice, loss of FMRP releases the brake on translation leading to a hyperactive response to $mGlu_5$ activation and ERK1/2 activity, leading to pathogenic exaggerated protein synthesis. (**C**) Proposed model: in *Fmr1*$^{-/y}$ mice, genetic reduction of β-arrestin2, or more therapeutically relevant, β-arrestin2-biased negative allosteric modulation at $mGlu_5$, prevents hyperactive signaling through the Ras-ERK pathway leading to restoration of translation back to WT levels.

Chapter 3

Selective inhibition of GSK3α but not GSK3β corrects many phenotypes associated with a mouse model of Fragile X

3.1: Abstract

Several lines of evidence point to dysregulated synaptic protein synthesis downstream of metabotropic glutamate receptor 5 ($mGlu_5$) as a primary pathogenic culprit in Fragile X Syndrome (FX). Therapies designed to correct this dysregulation, however, have failed in clinical trials, due in part to our incomplete understanding of the signaling pathways that couple $mGlu_5$ activation to the translational machinery at the synapse. Dual inhibition of the glycogen synthase kinase 3 paralogs (GSK3α and GSK3β) has been a promising therapeutic avenue, correcting a plethora of aberrant phenotypes in a mouse model of FX. Likewise, the drug lithium which non-specifically inhibits GSK3α/β has been used clinically to improve mood dysregulation in individuals with FX. However, these potential therapies have been plagued by dose-limiting toxicities driven by dual inhibition of both GSK3 paralogs. Recent development of two highly-selective inhibitors of GSK3α or GSK3β has allowed us to probe paralog-specific contribution to the pathophysiology of FX. Surprisingly, inhibition of GSK3α but not GSK3β corrected excessive synaptic translation in a mouse model of FX, and reversed many impairments including cortical hyperexcitability, susceptibility to audiogenic seizures, and deficits in learning and memory. Importantly, GSK3α-specific inhibition did not result in the pharmacodynamic tolerance or psychotomimetic activity associated with $mGlu_5$ inhibitors. Thus, our data implicates GSK3α as the disease-relevant paralog in FX and suggests that GSK3α-specific inhibitors may offer significant advantages over first-generation $mGlu_5$ inhibitors for the treatment of FX and related disorders.

3.2: Introduction

Fragile X syndrome (FX) is the most prevalent inherited monogenic cause of autism and intellectual disability, affecting 1:4000 males and 1:4000-6000 females (Turner, Webb et al. 1996, Song, Barton et al. 2003, Bailey, Raspa et al. 2008, Hagerman, Berry-Kravis et al. 2009, Budimirovic and Kaufmann 2011). Evidence from molecular and behavioral suggests that targeting $mGlu_5$ or its downstream effectors may be a fruitful approach to treating FX. Indeed, $mGlu_5$-based therapies have been immensely successful at "correcting" FX in animal models (Table 1.1). However, in contrast to pre-clinical studies, safety and efficacy results in clinical trials have been disappointing, largely due to unexpected off-target effects (as discussed in Chapter 1). This is likely due to the fact that global manipulation of $mGlu_5$ also affects processes unrelated to FX pathophysiology, resulting in side effects that sharply limit the utility of this approach. In particular, $mGlu_5$ antagonists have been shown to induce psychotomimetic effects in humans and potentiate MK801-driven psychotomimetic-like behaviors in mice, likely due to cross talk between G-protein-dependent signaling downstream of $mGlu_5$ and NMDA receptors (Homayoun, Stefani et al. 2004, Chen, Liao et al. 2011, Abou Farha, Bruggeman et al. 2014, Gould, Amato et al. 2016). As such, ideal pharmacological treatments should specifically interfere with the signaling pathways that regulate FMRP-mediated translation proximal to the translational machinery to minimize dose-limiting side effects. This led us to explore targets that are not known to directly affect $mGlu_5$ activity or Ras-ERK1/2 signaling, that may be successful in alleviating FX phenotypes in the *Fmr1* KO mouse.

3.2.1: Lithium as a therapeutic for FX.

The mood stabilizer lithium, more commonly used in the treatment of Bipolar Disorder, has been validated in studies of the *Fmr1* KO mouse as a possible intervention in the treatment of FX (Min, Yuskaitis et al. 2009, Mines, Yuskaitis et al. 2010, Yuskaitis, Mines et al. 2010, Choi, Schoenfeld et al. 2011, Liu, Chuang et al.

2011, Liu, Huang et al. 2012, King and Jope 2013, Franklin, King et al. 2014). While promising results from a pilot open-label clinical trial reinforce this notion (Berry-Kravis, Sumis et al. 2008), a relatively high side effect rate sharply limits the potential of lithium as a therapeutic in children and adolescents with FX and other autism spectrum disorders (Siegel, Beresford et al. 2014).

3.2.2: GSK3α/β is overactive in the *Fmr1* KO mouse.

Accumulating evidence suggests that the disease-relevant action of lithium is inhibition of glycogen synthase kinase 3 (GSK3). GSK3 has two paralogs, GSKα and GSKβ, which are derived from different genes (Woodgett 1990). Despite sharing 85% overall sequence homology and 98% amino acid sequence identity within their kinase domains, differential actions of GSK3α and GSK3β have been identified (Woodgett 1990, Dajani, Fraser et al. 2001, Kaidanovich-Beilin and Woodgett 2011). Paralog-specific contribution of GSK3 to the pathophysiology of FX has not been examined. GSK3β is a target of FMRP (Darnell, Van Driesche et al. 2011), and the inhibitory serines of both GSK3α (at Ser9) and GSK3β (at Ser21) are hypoactive in the *Fmr1* KO mouse, implicating overactive GSK3α/β is core to the pathogenesis of FX (Min, Yuskaitis et al. 2009, Yuskaitis, Mines et al. 2010, Liu, Chuang et al. 2011, Guo, Murthy et al. 2012). Evidence from genetic and molecular studies has demonstrated that dysregulated synaptic protein synthesis downstream of metabotropic glutamate receptor 5 ($mGlu_5$) contributes to the pathophysiology of FX (Qin, Kang et al. 2005, Dolen, Osterweil et al. 2007). GSK3 can be regulated by $mGlu_5$ and acute inhibition of $mGlu_5$ reduces aberrant GSK3 signaling in the *Fmr1* KO mouse (Liu, Gong et al. 2005, Yuskaitis, Mines et al. 2010). Furthermore, inhibition of GSK3α/β with either lithium or non-specific GSK3 inhibitors corrects excessive protein synthesis and many other protein-synthesis dependent deficiencies in the *Fmr1* KO mouse, suggesting that GSK3α/β is either directly or indirectly coupled to translation (Min, Yuskaitis et al. 2009, Mines, Yuskaitis et al. 2010, Yuskaitis, Mines et al. 2010, Choi, Schoenfeld et al. 2011, Liu, Chuang et al. 2011, Guo, Murthy et al. 2012, Liu, Huang et al. 2012, Chen, Sun et al. 2013, King and Jope 2013, Chen, Lu et al. 2014, Franklin, King et al. 2014).

3.2.3: Paralog-specific contribution to FX has not been investigated.

Non-specific GSK3 inhibitors have failed in clinical trials for other indications due to dose-limiting toxicities driven by dual inhibition of both GSK3 paralogs (Gupta, Gulen et al. 2012, Lo Monte, Kramer et al. 2013, McCubrey, Steelman et al. 2014). In fact, evidence suggests that there may be notable differences in the contribution of GSK3α and GSK3β to neuropsychiatric disease (Lee, Kaidanovich-Beilin et al. 2011, Lipina, Kaidanovich-Beilin et al. 2011) Kaidanovich-Beilin, Lipina et al. 2009). It was once hypothesized that development of paralog-specific small molecule inhibitors would be unlikely due to the high sequence identity of the GSK3α and GSK3β kinase domains (Kaidanovich-Beilin and Woodgett 2011). Case in point, currently available GSK3 inhibitors lack true kinome selectivity, most often non-specifically acting on structurally similar kinases as well (O'Leary and Nolan 2015).

Taking advantage of an Asp133 → Glu196 "switch" in the hinge binding region, GSK3α/β, GSK3α, and GSK3β-selective inhibitors with exquisite kinase-specificity have been synthesized. The recent development of these highly-selective inhibitors of GSK3α or GSK3β have allowed us to evaluate paralog-specific contribution to the pathophysiology of FX. Much to our surprise, inhibition of GSK3α but not GSK3β abrogated excessive protein synthesis in *Fmr1* KO mice, as well as the amelioration of cortical hyperexcitability, susceptibility to audiogenic seizures, and deficits in learning and memory without exhibiting dose-limiting pharmacological properties and off-target adverse consequences that have limited the potential success of $mGlu_5$ inhibitors in the clinic.

3.3: Results

3.3.1: Development of paralog-specific inhibitors of GSK3α and GSK3β.

Inhibitors with exquisite selectivity for either GSK3α, GSK3β, or pan GSK3α/β were made available to us through a collaboration with the Stanley Center for Psychiatric Research at the Broad Institute of MIT and Harvard University. Exploiting an Asp133 → Glu196 "switch" in the hinge binding region of the adenosine triphosphate (ATP) binding sites between GSK3α and GSK3β, these first-in-class small molecule inhibitors exhibit high paralog specificity for either GSK3α (BRD0705) or GSK3β (BRD3731). A third compound inhibits both GSK3α and GSK3β (BRD0320) with high specificity (Figure 3.1A). Importantly, all three compounds demonstrate high selectivity for GSK3 without binding to similar off-target kinase domains (Figure 3.1B). The availability of these inhibitors allowed us to probe the involvement of each gene independently in the *Fmr1* KO mouse and investigate paralog-specific inhibition as a potential therapeutic target in the treatment of FX.

3.3.2: Acute inhibition of GSK3α but not GSK3β ameliorates seizure susceptibility in *Fmr1* KO mice.

In order to evaluate the therapeutic potential of GSK3α and GSK3β-specific inhibition in FX, we acutely dosed *Fmr1* KO mice and WT littermate controls with either vehicle (10% DMSO, 45% PEG400, 45% normal saline) or 30mg/kg BRD0705, BRD3731 or BRD0320 intraperitoneally (i.p.) 1 hr prior to exposure to a 125 dB alarm. *Fmr1* KO mice treated with vehicle were significantly more likely to exhibit seizure activity in response to the alarm compared with WT controls. 30mg/kg BRD0705, BRD3731 or BRD0320 did not affect seizure incidence in WT mice. To our surprise, only inhibition of GSK3α with BRD0705 or dual inhibition of GSK3α/β with BRD0320 significantly reduced audiogenic seizure susceptibility in *Fmr1* KO mice. Importantly, GSK3β-specific inhibition with BRD3731 yielded no significant change in seizure activity, with BRD3731-treated *Fmr1* KO mice exhibiting a high incidence of seizure

activity that was indistinguishable from vehicle-treated animals (Figure 3.2). Taken together, this data suggested to us that GSK3α but not GSK3β may be the relevant paralog contributing to the disease pathophysiology seen in *Fmr1* KO mice.

3.3.3: *Fmr1* KO mice do not develop drug-tolerance to chronic administration of BRD0705.

Global inhibition of $mGlu_5$ has demonstrated similar attenuation of seizure activity in the *Fmr1* KO mouse (Yan, Rammal et al. 2005, Dolen, Osterweil et al. 2007, Michalon, Sidorov et al. 2012, Thomas, Bui et al. 2012). Consistent with these reports, we found that acute administration of the $mGlu_5$ negative allosteric modulator CTEP ameliorates audiogenic seizures in the *Fmr1* KO mouse (Figure 3.3A), to a similar extent as inhibition of GSK3α or GSK3α/β. An important caveat to the apparent benefit of global manipulation of $mGlu_5$ is the observation that *Fmr1* KO mice develop tolerance to chronic delivery of $mGlu_5$ inhibitors. Case in point, the observed benefit of CTEP in reducing susceptibility to seizures in *Fmr1* KO mice is completely lost after 5 days of consecutive drug delivery (Figure 3.3B). In order to evaluate drug tolerance upon chronic administration of BRD0705, we delivered 5 consecutive systemic doses of 30mg/kg BRD0705 or vehicle daily to WT and *Fmr1* KO mice littermates (Figure 3.4A). We did not observe any loss of drug efficacy as a result of multiple dosing, with chronic administration of BRD0705 yielding an analogous reduction of seizure incidence in *Fmr1* KO mice (Figure 3.4B) as acutely delivered BRD0705 (Figure 3.2).

3.3.4: Acute inhibition of GSK3α but not GSK3β corrects elevated protein synthesis in *Fmr1* KO mice.

A previous study showed that chronic dietary lithium reduced elevated rates of cerebral protein synthesis in *Fmr1* KO mice (Liu, Huang et al. 2012). To examine the consequence of GSK3α and GSK3β inhibition on synaptic translation, we performed metabolic labeling on WT and *Fmr1* KO hippocampal slices in the presence of 10 μM BRD0705 or BRD3731. We found that BRD0705 (Figure 3.5) but not BRD3731 (Figure 3.6) corrected elevated protein synthesis in slices from *Fmr1* KO mice, suggesting that

GSK3α but not GSK3β is coupled to translation at the synapse. Inhibition of neither GSK3 paralog had an effect on protein synthesis in WT slices.

3.3.5: BRD0705 attenuates evoked hyperexcitability in the *Fmr1* KO mouse visual cortex.

Increased excitability in the cortex is a robust and reproducible phenotype observed in *Fmr1* KO mice. Excitingly, this hyperexcitability can be dampened by inhibition of $mGlu_5$ of downstream signaling pathways coupled to translation (Hays et al., 2011). To investigate whether BRD0705 could also reduce cortical hyperexcitability, we prepared acute slices of the visual cortex from WT and *Fmr1* KO animals and measured evoked activity in layer V pyramidal neurons. Electrical stimulation was delivered once every 30 seconds to the white matter, with action potentials recorded by placing a glass recording electrode in layer 5. Responses were collected for 30 minutes in vehicle followed by an additional 30 minutes in the presence of 10 μM BRD0705 (Figure 3.7A). We found that the number of action potentials evoked in *Fmr1* KO slices was significantly greater compared to WT slices in vehicle conditions (Figure 3.7B, C, D), however, application of BRD0705 significantly dampened this activity in *Fmr1* KO slices (Figure 3.7B, C, D).

3.3.6: BRD0705 attenuates spontaneous hyperexcitability in the *Fmr1* KO mouse visual cortex.

In addition to the action potentials generated in response to electrical stimulation of the underlying white matter, we also observed a significant amount of spontaneous activity in *Fmr1* KO slices that was present spontaneously, prior to any electrical stimulation. In order to determine if *Fmr1* KO slices also displayed enhanced spontaneous activity in this region, we recorded events occurring in between electrical stimulations in addition to our evoked spiking. These events occur spontaneously and are not dependent upon electrical stimulation. We observed a significantly more spontaneous events in *Fmr1* KO slices compared to wild-type slices (Figure 3.8A). We were therefore motivated to determine if application of BRD0705 would similarly dampen this hyperexcitability in *Fmr1* KO slices. *Fmr1* KO slices displayed significantly

more spontaneous events compared to WT slices, and, excitingly, this hyperexcitability was significantly dampened by BRD0705 (Figure 3.8B, C).

3.3.7: Evoked spiking in layer V visual cortex is protein-synthesis dependent.

We have shown that GSK3α-specific inhibition with BRD0705 can normalize protein synthesis in the hippocampus as well as reduce hyperexcitable spiking in layer V of the visual cortex in *Fmr1* KO slices. In order to investigate whether a reduction in cortical hyperexcitability could be a direct consequence of the restoration of normal synaptic translation, we treated cortical slices from WT and *Fmr1* KO mice with the protein synthesis inhibitor cycloheximide (CHX; 60 μM) and measured evoked activity in layer V pyramidal neurons using the same induction paradigm described above. We compared baseline evoked spiking activity during the first 30 minutes prior to washing in CHX and the second 30 minutes following wash-in of CHX (Figure 3.9A). We found that CHX blocked evoked spiking in WT slices and diminished prolonged firing in *Fmr1* KO slices to WT-vehicle levels (Figure 3.9B-D). We conclude that evoked spiking in layer V of visual cortex is dependent on *de novo* protein synthesis. Furthermore, inhibition of protein synthesis blocks the induction of evoked firing in WT slices, but not *Fmr1* KO slices, although it does significantly attenuate prolonged firing to physiologically normal levels. Therefore, it is likely that the observed attenuation of cortical hyperexcitability by BRD0705 is a functional result of restored protein synthesis at the synapse.

3.3.8: Chronic inhibition of GSK3α restores learning and memory in *Fmr1* KO mice on an inhibitory avoidance task.

We next investigated the possibility that restoration of normal synaptic translation by inhibition of GSK3α could lead to improvements in an assay of learning and memory previously shown to be impaired in *Fmr1* KO mice. We investigated inhibitory avoidance, which is thought to be reliant on the hippocampus as well as protein synthesis and $mGlu_5$-dependent (Qin, Kang et al. 2002, Dolen, Osterweil et al. 2007, Sherry, Milsome et al. 2010, Gieros, Sobczuk et al. 2012). We administered 30 mg/kg BRD0705 or vehicle i.p. to adult WT or *Fmr1* KO littermates for 5 consecutive days prior to conditioning. In order to minimize stress and behavioral modifications associated

with the i.p. injection itself, we administered "sham" saline injections once daily for 20 consecutive days prior to the first vehicle or BRD0705 injection (Figure 3.10A). Memory strength was measured as the latency to enter the dark side of a box that was associated with a foot shock. Consistent with previous findings, we observed that *Fmr1* KO mice failed to form a strong association between the context and foot shock (between time 0 and 6 hours) indicating impaired memory acquisition. Remarkably, however, the behavior of *Fmr1* KO mice chronically treated with BRD0705 was indistinguishable from either vehicle or BRD0705-treated WT mice, exhibiting normal memory acquisition and extinction over the course of 48 hours (Figure 3.10B).

3.3.9: Dose-limiting side effects seen with the $mGlu_5$ inhibitor MTEP are not induced by the GSK3α inhibitor BRD0705.

Administration of the non-competitive NMDA receptor blocker MK801 is known to induce hyper-locomotion in mice (Carlsson and Carlsson 1989, Kuribara, Asami et al. 1992). Because $mGlu_5$ itself indirectly couples to NMDA receptors, modulation of $mGlu_5$ activity is known to have off-target impact on the modulation of NMDA receptors as well (Chen, Liao et al. 2011, Cleva and Olive 2011). First-generation $mGlu_5$ NAMs, identified based on inhibition of G_q signaling, have been shown to act synergistically with MK801 to potentiate the hyper-locomotive response to the NMDA receptor antagonist in mice (Homayoun, Stefani et al. 2004, Pietraszek, Gravius et al. 2005). MK801 is also known to be psychotomimetic in humans, and hyper-locomotion in mice is believed to be relevant to the mechanism that causes derealization and visual hallucinations in people treated with $mGlu_5$ NAMs (Pecknold, McClure et al. 1982, Porter, Jaeschke et al. 2005, Abou Farha, Bruggeman et al. 2014). We confirmed that pretreatment with the selective $mGlu_5$ inhibitor 3-[(2-Methyl-1,3-thiazol-4-yl)ethynyl]-pyridine (MTEP) (Cosford, Tehrani et al. 2003) significantly potentiates MK801-induced hyper-locomotion in WT mice. Importantly, WT mice pretreated with BRD0705 did not exhibit the same potentiation of the hyper-locomotive response to MK801 (Figure 3.11), implying that GSK3α does not have parallel interactions with NMDARs.

3.3.10: GSK3α is coupled to the translational machinery downstream of ERK1/2.

Excessive translation pathological to FX is thought to be, in part, a result of hypersensitivity of the translational machinery in response to activation of $mGlu_5$ and extracellular signal-regulated kinase (ERK1/2). In addition to $mGlu_5$ NAMs, inhibition of ERK1/2 itself, or upstream effectors of ERK1/2, have been explored, but have been met with cautious hesitation, as therapeutic targets for FX (Osterweil, Krueger et al. 2010, Bhattacharya, Kaphzan et al. 2012, Busquets-Garcia, Gomis-Gonzalez et al. 2013, Bhattacharya, Mamcarz et al. 2016, Berry-Kravis, Levin et al. 2015). We observed a reduction in aberrant protein synthesis in hippocampal slices from *Fmr1* KO mice as a result of GSK3α-specific inhibition. However, the mechanism by which GSK3α couples to synaptic translation downstream of $mGlu_5$ is not known. To investigate this, we pre-treated WT and *Fmr1* KO slices with either vehicle or BRD0705 and then probed phosphorylation of key targets known to be coupled to translation in response to $mGlu_5$ activation. We stimulated $mGlu_5$ by initially priming the slice with the $mGlu_5$ positive allosteric modulator CDPPB for 30 minutes followed by stimulation with the group 1 mGluR agonist 3,5-dihydroxyphenylglycine (DHPG) for 5 minutes in order to achieve maximal receptor activation which we hypothesized might augment subtle changes in phosphorylation of targets (Figure 3.12A). We did not observe activation of the AKT-mTOR pathway in WT or *Fmr1* KO slices that had received either stimulation or vehicle, in either the presence or absence of BRD0705 (Figure 3.12C, D). In comparison, we saw robust activation of ERK1/2 upon $mGlu_5$ stimulation, in WT and *Fmr1* KO slices receiving either vehicle or BRD0705 pre-treatment (Figure 3.12B). The magnitude of ERK1/2 was comparable in both WT and *Fmr1* KO slices, reinforcing previous findings suggesting that basal ERK1/2 activation is normal (Osterweil, Krueger et al. 2010, Osterweil, Chuang et al. 2013). This evidence suggests that although protein synthesis is attenuated by inhibition of GSK3α, ERK1/2 activation is not affected, implying that GSK3α couples to translation at a target that is downstream of ERK1/2.

3.4: Discussion

3.4.1: The effects of BRD0705 and BRD3731 on phosphorylation of GSK3α/β are unknown.

Taken together, these results support a role for GSK3α in synaptic translation, via an unknown mechanism, either downstream of ERK1/2 signaling or through another pathway altogether. It has been shown that GSK3α and GSK3β are overactive in the *Fmr1* KO mouse, a consequence of hypo-phosphorylation of the inhibitory serines that negatively regulate GSK3 activity. Interestingly, one study showed that GSK3α but not GSK3β is pathogenically overactive in the *Fmr1* KO mouse hippocampus which may be consistent with our finding that selective inhibition of GSK3α led to the reversal of hippocampus-associated cognitive impairments in these mice. We did not evaluate the effects of BRD0705 or BRD3731 on phosphorylation of the inhibitory serines of GSK3α and GSK3β as these small molecule inhibitors directly inhibit their targets by competing for binding at the ATP binding site of each paralog-specific kinase domain. Nonetheless, it is possible that these inhibitors may have indirect effects on these inhibitory phosphorylation sites.

3.4.2: Selective inhibition of GSK3α but not GSK3β corrects pathological phenotypes in the *Fmr1* KO mouse.

Although selective inhibition of GSK3β had no effect on seizure incidence, inhibition of GSK3α as well as dual inhibition of GSK3α/β induced a significant reduction in the propensity to seize in *Fmr1* KO mice. One might infer that the observed benefits attributed to dual inhibition of GSK3α/β may, in fact, be exclusively driven by inhibition of GSK3α. Several studies have concluded that direct and/or indirect inhibitors of GSK3 correct a wide variety of pathological phenotypes in the *Fmr1* KO mouse (Min, Yuskaitis et al. 2009, Mines, Yuskaitis et al. 2010, Yuskaitis, Mines et al. 2010, Choi, Schoenfeld et al. 2011, Liu, Chuang et al. 2011, Guo, Murthy et al. 2012, Liu, Huang et al. 2012, Chen, Sun et al. 2013, King and Jope 2013, Chen, Lu et al. 2014, Franklin, King et al.

2014). The pharmacological interventions used to inhibit GSK3 in these previous manipulations included lithium, CT99021, SB415286, TDZD-8, and VP0.7. While all of these compounds either directly and/or indirectly inhibit GSK3, they are all known to act on other kinases as well, confounding conclusions which attribute therapeutic benefit to inhibition of GSK3 alone. More egregiously, many studies have misattributed phenotypic improvements in response to treatment with lithium or other non-specific compounds to inhibition of GSK3β, despite a total lack of evidence demonstrating that GSK3β alone is the disease-relevant paralog (Chiu and Chuang 2011, Guo, Murthy et al. 2012, Liu, Huang et al. 2012, Chen, Sun et al. 2013). All evidence collected in the present series of experiments suggests that inhibition of GSK3α but not GSK3β provides therapeutic benefit in the *Fmr1* KO mouse.

3.4.3: Normalization of synaptic protein synthesis: a key mechanism in many phenotypes.

Elevated cerebral protein synthesis is a hallmark of the pathophysiology of FX. We have shown previously, that global inhibition of either $mGlu_5$ or the Ras-ERK pathway is sufficient to correct this pathogenic phenotype in the *Fmr1* KO mouse (Figure 3.13). Interestingly, these same genetic and pharmacological interventions that normalized protein synthesis were also effective in reducing susceptibility to audiogenic seizures in *Fmr1* KO mice, suggesting that audiogenic seizures could be a pathophysiological consequence of elevated synaptic translation (Dolen, Osterweil et al. 2007, Osterweil, Krueger et al. 2010, Michalon, Sidorov et al. 2012, Osterweil, Chuang et al. 2013). Consistent with this hypothesis, the same pharmacological manipulations that corrected aberrant protein synthesis and seizure susceptibility also abrogated cortical hyperexcitability in the *Fmr1* KO mouse (Hays, Huber et al. 2011, Osterweil, Chuang et al. 2013). We have shown here that evoked spiking activity in layer V of the visual cortex is protein synthesis-dependent. *Fmr1* KO mice also show deficits in memory consolidation, reconsolidation, and memory recall on an inhibitory avoidance task. We have observed that memory reconsolidation in this task is blocked by systemic delivery of the protein synthesis inhibitor cycloheximide (data not shown). It has been

shown that memory reconsolidation and retrieval on a similar passive avoidance task is $mGlu_5$-dependent (Gieros, Sobczuk et al. 2012). A central theme, consistent with the mGluR theory of FX (Bear, Huber et al. 2004), suggests that phenotypic deficits associated with the loss of FMRP, a translational repressor, can be attributed to pathological dysregulation of protein synthesis at the synapse. GSK3α-specific inhibition normalizes protein synthesis to WT levels in the *Fmr1* KO mouse, thereby correcting audiogenic seizure activity, cortical hyperexcitability, and cognitive impairments in our studies. Importantly, inhibition of GSK3α does not alter normal protein synthesis in WT slices. This suggests that mechanistically, BRD0705 is correcting a pathology specific to FX without altering some other process necessary for normal functioning.

3.4.4: GSK3α couples to the translational machinery by an unknown mechanism.

Although we have collected compelling evidence suggesting that GSK3α is involved in the regulation of synaptic translation, a mechanism has not yet been revealed. All previous manipulations that have abrogated altered protein synthesis (Figure 3.13) in the *Fmr1* KO mouse did so by normalizing signaling through ERK1/2 specifically. We show that activation of the Ras-ERK1/2 pathway is not affected by inhibition of GSK3α suggesting that it acts downstream of this signaling pathway, possibly directly targeting the initiation or elongation steps of translation. This is exciting, as it might avoid potential adverse consequences of altering ERK1/2, which plays crucial roles in the brain unrelated to synaptic translation. Similarly, it does not seem likely that GSK3α is acting within or upstream of the AKT-mTOR signaling pathway known to be coupled to translation initiation. Elucidating the role of GSK3α in translation will be key to the advancement and development of targeted therapeutics in FX and other related disorders of troubled translation.

3.4.5: Pre-clinical evidence that GSK3α is a better target than global $mGlu_5$.

Manipulation of various targets within the $mGlu_5$ pathway have shown great promise in pre-clinical studies including components of the Ras-ERK1/2 pathway and

$mGlu_5$ itself. Despite the success and relative ease of correcting a number of pathophysiologies in the *Fmr1* KO mouse model, these targeted-strategies have failed to translate to the clinic thus far. Observations from pre-clinical studies have identified concerns that could be predictive of limitations of these compounds in clinical trials investigating safety and efficacy. Chronic administration of the $mGlu_5$ negative modulators CTEP and MPEP demonstrated a loss of therapeutic benefit in the audiogenic seizure assay in *Fmr1* KO mice, presumably due to development of drug tolerance in these mice over time (Yan, Rammal et al. 2005, Min, Yuskaitis et al. 2009). A similar development of tolerance was previously seen in *Fmr1* KO mice chronically treated with GSK3 inhibitors, with the noteworthy exception of lithium (Min, Yuskaitis et al. 2009). Importantly, mice receiving chronic BRD0705 treatment did not appear to exhibit any drug tolerance.

Another liability associated with global negative modulation of $mGlu_5$ is a consequential predisposition to psychotomimetic tendencies which manifest as hyper-locomotion in mice. Specifically, WT mice pre-treated with the $mGlu_5$ antagonist MTEP or MPEP prior to administration of the NMDA receptor antagonist MK-801 often demonstrate a potentiated locomotor response compared with WT mice that did not receive pre-treatment with MTEP or MPEP (Homayoun, Stefani et al. 2004, Gould, Amato et al. 2016). This increased tendency to exhibit psychotomimetic locomotion is reminiscent of visual hallucinations experienced by individuals treated with $mGlu_5$ antagonists and is thought to be caused by off-target inhibition of NMDA receptors. Mice pre-treated with BRD0705 did not show any propensity to psychotomimetic tendencies or potentiated hyper-locomotion in response to MK-801 treatment suggesting that GSK3α does not directly or indirectly regulate NMDA receptor activation.

3.4.6: GSK3 paralog specificity in neuropsychiatric disease.

GSK3 paralog-specific contribution to neuropsychiatric disease has been studied previously (Kaidanovich-Beilin and Woodgett 2011), although not in the context of FX. Paralog-specific GSK3 knock-out (KO) animals have been generated, and although

GSK3α KO mice are viable, GSK3β KO mice die late in development so conclusions about paralog function have been attributed to heterozygous deletion of GSK3β rather than full knockout of gene function (Hoeflich, Luo et al. 2000, Beaulieu, Sotnikova et al. 2004, O'Brien, Harper et al. 2004). Both mouse models show learning and memory impairments as well as a comparable anti-depressant-like state, which presumably models the mood-stabilizing effects of lithium (Beaulieu, Sotnikova et al. 2004, O'Brien, Harper et al. 2004, MacAulay, Doble et al. 2007, Bersudsky, Shaldubina et al. 2008, Kimura, Yamashita et al. 2008, Kaidanovich-Beilin, Lipina et al. 2009). Interestingly, evidence suggests that GSK3α KO mice exhibit impaired social interaction (Kaidanovich-Beilin, Lipina et al. 2009). Additionally, in the Disc1-L100P mouse, which models schizophrenia-related behaviors, genetic reduction of GSK3α specifically reverses pre-pulse inhibition (Cooper, Coe et al.) and normalizes the hyperactivity phenotype and spine development abnormalities of Disc1-L100P mutants (Lee, Kaidanovich-Beilin et al. 2011, Lipina, Kaidanovich-Beilin et al. 2011). Intriguingly, the *Fmr1* KO mouse shares similar deficits in PPI, hyperactivity and spine abnormalities (Yan, Rammal et al. 2005, Dolen, Osterweil et al. 2007, de Vrij, Levenga et al. 2008, Min, Yuskaitis et al. 2009, Levenga, Hayashi et al. 2011, Michalon, Sidorov et al. 2012), suggesting that paralog-specific inhibition of GSK3 could offer enhanced therapeutic benefit by specifically targeting the paralog which is relevant to the pathophysiology of FX. In particular, evidence presented here supports the conclusion that although both GSK3α and GSK3β are dysregulated in FX, selective inhibition of GSK3α may be the disease-relevant therapeutic target.

3.5: Methods

3.5.1: Animals

Fmr1$^{-/x}$ female mice (Jackson Labs) were crossed WT C57BL/6J male mice to generate WT and *Fmr1*$^{-/y}$ male offspring. All experimental animals were age-matched male littermates, and were studied with the experimenter blind to genotype and treatment condition. Animals were group housed and maintained on a 12:12 hour, light: dark cycle. The Institutional Animal Care and Use Committee at MIT approved all experimental techniques and all animals were treated in accordance with NIH and MIT guidelines.

3.5.2: Reagents

GSK3 inhibitors BRD0320, BRD3731, BRD0705 were all synthesized at the Broad Institute and generously gifted to us. All compounds for acute and chronic AGS, Inhibitory Avoidance, and MK-801-induced hyperlocomotion were administered at a dose of 30 mg/kg in a vehicle of 10% DMSO, 45% PEG400, 45% normal saline. For chronic AGS and Inhibitory Avoidance, vehicle and drug were delivered intraperitoneally (i.p.) at a dosing volume of 10 ml/kg. For MK-801-induced hyperlocomotion, vehicle and drug were delivered i.p. at a dosing volume of 2 ml/kg with a needle with precision for small volumes, utilized due to gastrointestinal complications and impact on locomotion at higher doses of the DMSO and PEG400 vehicle. For slice experiments, all GSK3 inhibitors were prepared as 50 mM stocks in DMSO and stored in aliquots at -20°C. (S)-3,5-dihydroxyphenylglycine (S-DHPG) was purchased from Tocris. Fresh bottles of DHPG were prepared as a 100x stock in H_2O, divided into aliquots, and stored at -80°C. Fresh stocks were made once a week. Actinomycin D (Tocris) was prepared as a stock solution of 1mg/mL in 0.01% DMSO and aCSF and stored at -20°C. CDPPB (Tocris) was prepared daily at 75 mM stock in DMSO. MK801 (Sigma) was prepared in H_2O daily and .3 mg/kg was injected i.p. at a dosing volume of 10 ml/kg. MTEP (Tocris) was prepared in H_2O daily and 10 mg/kg was injected i.p. at a dosing

volume of 10 ml/kg. CTEP was formulated as a microsuspension in vehicle (0.9% NaCl, 0.3% Tween-80). Chronic treatment consisted in one dose every 48 hours at 2 mg/kg (i.p.) in a volume of 10 ml/kg.

3.5.3: Audiogenic seizures

AGS experiments were performed as previously described in Chapter 2 (Dolen, Osterweil et al. 2007). For acute dosing, animals were animals at injected with either vehicle or drug 1-2 hours prior to exposure to the alarm in a separate room. For chronic dosing, animals were injected for four consecutive days prior to testing and received a final (fifth) injection 1-2 hours prior to testing. All animals were run at P23-25 (immediately following weaning) and were habituated to the behavioral chamber (28x17.5x12 cm transparent plastic box) for 1 minute prior to stimulus onset. AGS stimulus was a 125 db at 0.25 m siren (modified personal alarm, Radioshack model 49-1010, powered from a DC converter). Seizures were scored for incidence during a 2-minute stimulus presentation or until animal reached AGS endpoint (wild running, status epilepticus, respiratory arrest or death were all scored as seizure activity).

3.5.4: Metabolic labeling

Metabolic labeling of new protein synthesis was performed as previously described in Chapter 2 (Osterweil, Krueger et al. 2010). Male P28-P32 littermate mice were anesthetized with isoflurane and the hippocampus was rapidly dissected into ice-cold aCSF (in mM: 124 NaCl, 3 KCl, 1.25 NaH_2PO_4, 26 $NaHCO_3$, 10 dextrose, 1 $MgCl_2$, 2 $CaCl_2$, saturated with 95% O_2 and 5% CO_2). Hippocampal slices (500 μm) were prepared using a Stoelting Tissue Slicer and transferred into 32.5°C aCSF (saturated with 95% O_2 and 5% CO_2) within 5 min. Slices were incubated in aCSF undisturbed for 3 h to allow recovery of basal protein synthesis and then transferred to either aCSF containing vehicle (DMSO) or drug, which was present for the remainder of the experiment. After 3.5-4 h recovery, Actinomycin D (25 μM) was then added to the chamber for 30 min to inhibit transcription after which slices were transferred to fresh aCSF containing ~10 mCi/ml [^{35}S] Met/Cys (Perkin Elmer) for an additional 30 min.

Slices were then homogenized, and labeled proteins isolated by TCA precipitation. Samples were read with a scintillation counter and subjected to a protein concentration assay (Bio-Rad). Data was analyzed as counts per minute per microgram of protein, normalized to the [^{35}S] Met/Cys aCSF used for incubation and the average incorporation of all samples analyzed and then normalized to percent WT for each experiment. Statistical significance was determined using a two-way ANOVA for genotype and treatment. Pairwise comparisons of significance were made using Student's two-tailed t-tests.

3.5.5: Evoked and spontaneous spiking in visual cortex LV

Slices of visual cortex were prepared from P16-P21 wild-type or Fmr1 KO male animals. Slices were recovered for 30 minutes at 32°C and then for an additional 2.5 hours at room temperature in a modified aCSF containing (in mM): 124 NaCl, 3.5 KCl, 1.25 NaH_2PO_4, 26 $NaHCO_3$, 10 glucose, 0.8 $MgCl_2$, and 1 $CaCl_2$, saturated with 95%/5% O_2/CO_2. Action potentials were evoked by electrical stimulation of the white matter (clustered bipolar tungsten, FHC) and recorded by placing a glass recording electrode (~1 MΩ resistance when filled with aCSF) in layer V of the visual cortex. A single, 0.2 ms duration, electrical stimulation was delivered every 30 seconds using a stimulus intensity between 35-80 μA. Evoked extracellular recordings were first collected in vehicle conditions for 30 minutes (60 trials total), followed by 30 additional minutes in the presence of 10 μM BRD0705. All recordings were made using a Multiclamp 700B amplifier (Molecular Devices), amplified 1000 times, filtered between 0.3 and 3 Hz, and digitized at 25 kHz. Evoked responses were measured for the first 3.2 seconds following electrical stimulation. Spontaneous events were characterized as those occurring between 3.2 seconds and 30 seconds after stimulation. To determine the protein synthesis dependence of both the evoked and spontaneous activity in layer V, a subset of slices were subjected to bath application of 60 μM cyclohexamide (CHX) for 30 minutes after an initial 30 minute baseline recording in aCSF. A third 30 minute recording was also collected to fully capture the effect of CHX on spiking.

3.5.6: Inhibitory avoidance extinction

Inhibitory avoidance experiments were performed as previously described (Dolen, Osterweil et al. 2007). On the day of testing, P56-P76 animals were placed into the dark compartment of an IA training box (a two-chambered Perspex box consisting of a lighted safe side and a dark shock side separated by a trap door) for 30 seconds followed by 90 seconds in the light compartment for habituation. Following the habituation period, the door separating the two compartments was opened and animals were allowed to enter the dark compartment. Latency to enter following door opening was recorded ("baseline", time 0, 8-9am); animals with baseline entrance latencies of greater than 120 seconds were excluded. After each animal stepped completely into the dark compartment with all four paws, the sliding door was closed and the animal received a single scrambled foot-shock (0.5mA, 2.0 sec) via electrified steel rods in the floor of the box. This intensity and duration of shock consistently caused animals to vocalize and jump. Animals remained in the dark compartment for 15 sec following the shock and were then returned to their home cages. Six to seven hours following IA training, mice received a retention test ("post-acquisition", time 6 hours, 2p.m.-3p.m.). During post-acquisition retention testing each animal was placed in the lit compartment as in training; after a 90 second delay, the door opened, and the latency to enter the dark compartment was recorded (cut-off time 537 sec). For inhibitory avoidance extinction (IAE) training, animals were allowed to explore the dark compartment of the box for 200 seconds in the absence of foot-shock (animals remaining in the lit compartment after the cutoff were gently guided, using an index card, into the dark compartment); following IAE training animals were returned to their home cages. Twenty-four hours following initial IA training, mice received a second retention test ("post-extinction 1", time 24 hours, 8a.m-9a.m.). Animals were tested in the same way as at the six hour time point, followed by a second 200 second extinction trial in the dark side of the box; following training animals were again returned to their home cages. Forty-eight hours following avoidance training, mice received a third and final retention test ("post-extinction 2", time 48 hours, 8a.m.- 9a.m.).

3.5.7: MK801-induced hyperlocomotion

To determine the effects of genotype on MK801-induced hyperlocomotion, mice were habituated in the open field (40 cm x 40 cm x 40 cm box) for 60 min, followed by the administration of vehicle or MK801 and locomotor activity was recorded for another 60 min. To determine the effects of MTEP and BRD0705 by genotype on MK801-induced hyperlocomotion, mice were habituated in the open field for 30 min, followed by the intraperitoneal (i.p.) administration of MTEP (10 mg/kg at a dosing volume of 10 ml/kg) or BRD0705 (30 mg/kg at a dosing volume of 2 ml/kg). After an additional 30 min, MK801 (0.3 mg/kg at a dosing volume of 10 ml/kg) was administered i.p. and locomotor activity was recorded for another 60 min. The time course of drug-induced changes in ambulation was expressed as cm traveled/5 min over the 120-min session. Sessions were recorded using Plexon's *CinePlex*® Studio and analyzed using Plexon's *CinePlex*® Editor and code written in MATLAB. MK801-induced locomotor activity was scored and analyzed using the average of the final 5 minutes (minute 115-120) per cohort.

2.5.8: Immunoblotting

Hippocampal slices were prepared and recovered as described in metabolic labeling experiments. Sets of slices were stimulated with CDPPB (10 μM) for 30 minutes followed by DHPG (50 μM) for 5 minutes and then flash frozen in liquid nitrogen immediately after stimulation, prior to processing. Yoked unstimulated slices were also processed to assess basal signaling levels. Immunoblotting was performed according to established methods using primary antibodies to p-ERK1/2 (Thr202/Tyr204) (Cell Signaling Technology), ERK1/2 (Cell Signaling Technology), p-Akt (Ser473) (Cell Signaling Technology), Akt (Cell Signaling Technology), p-S6 240/44 (Cell Signaling Technology) and S6 (Cell Signaling Technology). Protein levels were measured by densitometry (Quantity One), and quantified as the densitometric signal of phospho-protein divided by the total protein signal in the same lane.

A

	IC_{50} (μM)	
	GSK3α	GSK3β
BRD0320	0.008 ± 0.005	0.005 ± 0.003
BRD3731	0.215 ± 0.186	0.015 ± 0.011
BRD0705	0.066 ± 0.044	0.515 ± 0.257

B

Kinase	% Inhibition BRD0705 10μM	IC50 (μM)	Fold Selectivity
GSK3α	100.8	0.079	
GSK3β	96.5	0.488	6.2
CDK2/CycA2	65.3	6.87	86.9
CDK2/CycE1	53.4	9.43	119.3
CDK3/CycE1	52.8	9.74	123.3
CDK5/p25	52.0	9.20	116.4
PAK4	33.8		
ROS	31.3		
EPHA3	25.2		
FLT3	25.0		
FGFR4(N535K)	22.1		
CDC2/CycB1	17.2		
HGK	14.9		
EPHB4	14.7		
EPHA5	12.7		
MST3	11.7		
MAP3K4_Cascade	11.6		
COT_Cascade	11.2		
PDHK4	11.0		
LOK	9.6		
PAK5	9.3		
CDK9/CycT1	8.4		
CDK7/CycH/MAT1	8.3		
YES	7.9		
BRAF_Cascade	7.8		
DYRK3	7.7		
RAF1_Cascade	7.5		
EPHA6	7.4		
AurC	7.3		

Figure 3.1: GSK3 inhibitors with exquisite paralog-specificity.

(**A**) GSK3 inhibitors synthesized at the Broad Institute show highly specific affinity for GSK3α/β (BRD0320), GSK3β but not GSK3α (BRD3731) and GSK3α but not GSK3β (BRD0705) allowing for investigation of paralog-specific contribution to Fragile X pathology. (**B**) Selectivity panel for other kinases showing that BRD0705 is highly specific for GSK3α. (Compounds were synthesized and evaluated for specificity by Florence Wagner at the Broad Institute and generously provided to us in collaboration).

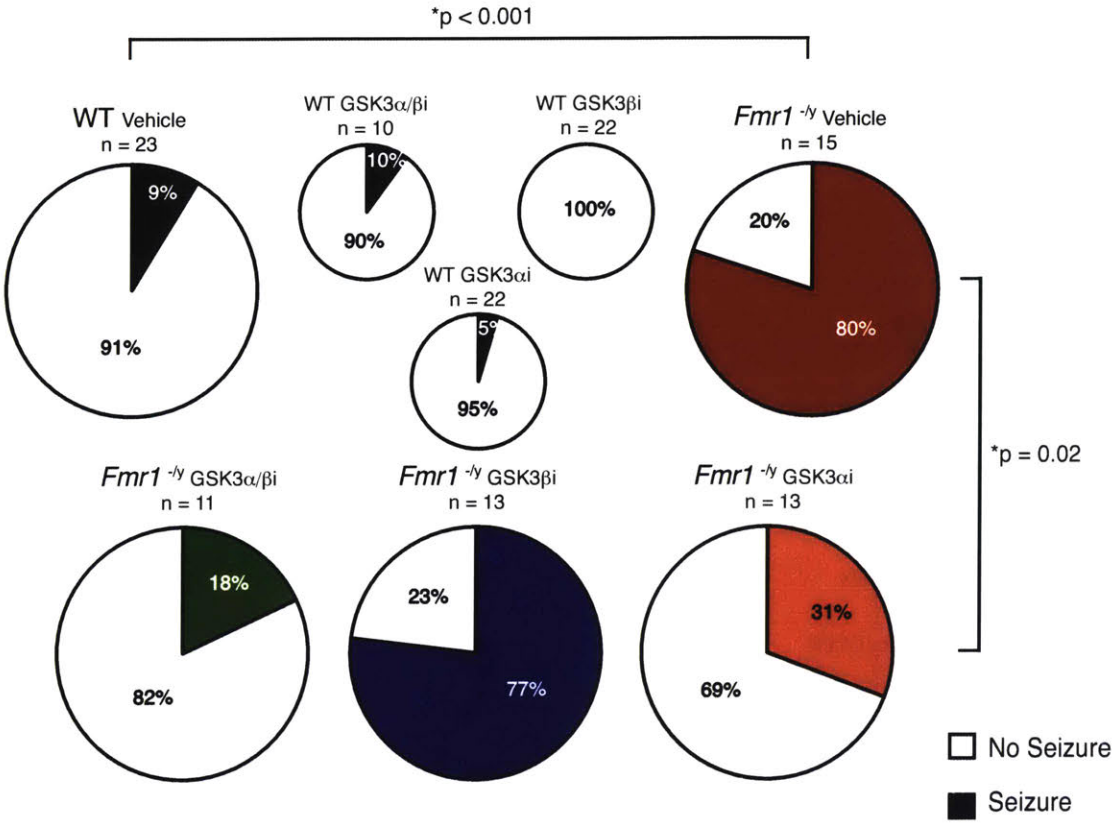

Figure 3.2: Acute inhibition of GSK3α/β and GSK3α, but not GSK3β, alleviates audiogenic seizure susceptibility in *Fmr1* KO mice.

Acute treatment (30 mg/kg) with three GSK3 specific inhibitors reveals paralog-specificity in the alleviation of susceptibility to audiogenic seizures in *Fmr1* KO mice. Vehicle-treated (10% DMSO, 45% PEG400, 45% normal saline) WT mice were not prone to seizures, with 2/23 animals exhibiting seizure activity in response to an auditory alarm. In WT animals, acute treatment with BRD0705 (GSK3α-inhibitor), BRD3731 (GSK3β-inhibitor) or BRD0320 (GSK3α/β-inhibitor) did not show a significant effect on seizure incidence compared with vehicle; two-tailed Fisher's exact test: p = 1.0; p = 0.4889; p = 1.0, respectively. Vehicle-treated *Fmr1* KO mice exhibit significantly enhanced susceptibility to seizure in response to an auditory alarm compared with WT controls; *p < 0.001. *Fmr1* KO mice given an acute dose of either BRD0705 or BRD0320 (GSK3α or GSK3α/β-inhibitors), but not BRD3731 (GSK3β-inhibitor) reduce this heighted susceptibility to seizures compared with vehicle-treated *Fmr1* KO mice; *p = 0.002; *p = 0.0043; *p = 1.0. Taken together, this suggests that GSK3α but not GSK3β is relevant to enhanced hyperexcitability and audiogenic seizure impairments in *Fmr1* KO mice. (Experiments testing BRD0320 were conducted by Michael Lewis and Arnold Heynen).

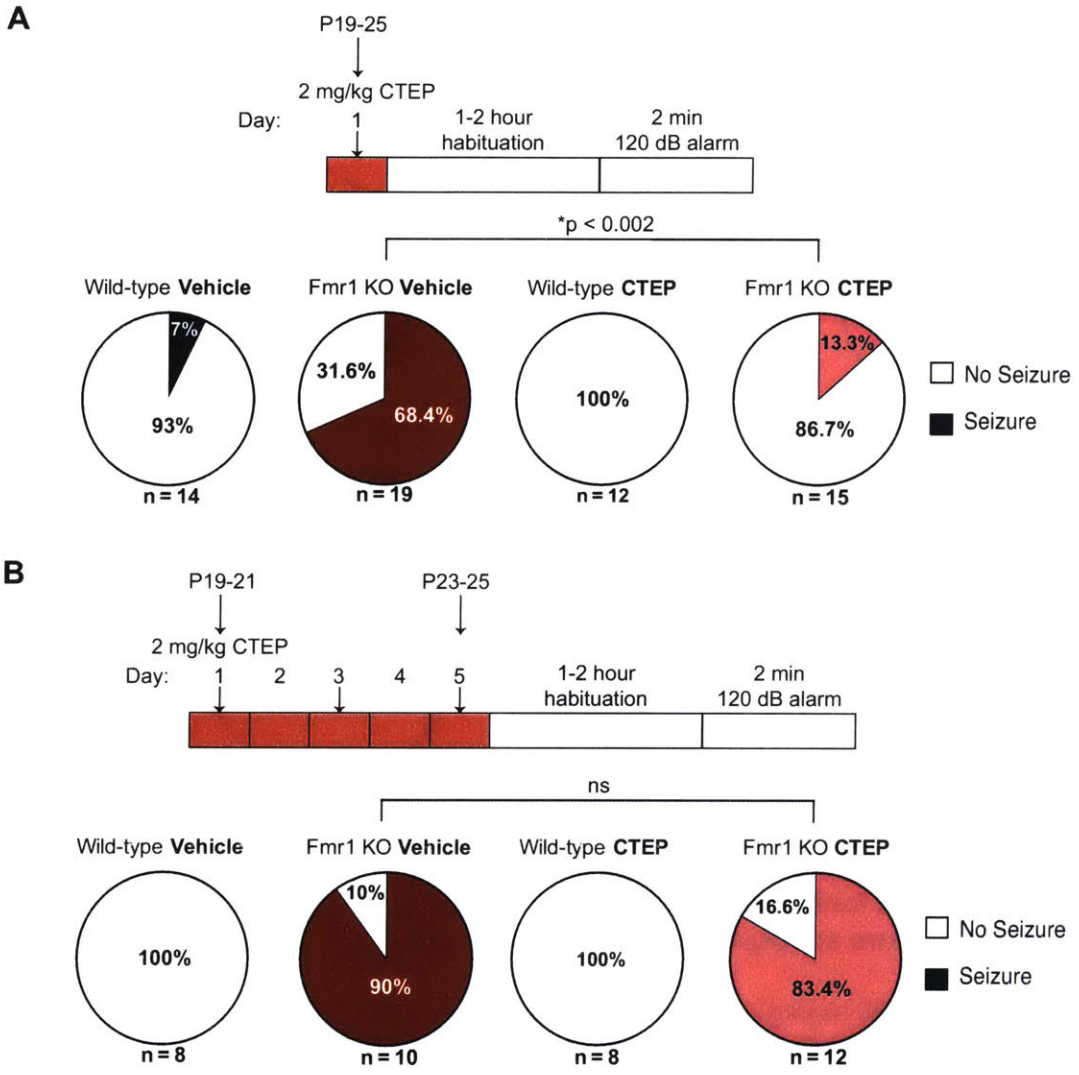

Figure 3.3: *Fmr1* KO mice develop tolerance to CTEP in AGS upon chronic administration.

(**A**) Schematic shows acute dose schedule and AGS timeline. Fmr1 KO mice treated with vehicle (DMSO) exhibit increased susceptibility to audiogenic seizures compared to WT treated with vehicle; two-tailed Fisher's exact test, *p = 0.0009. An acute dose with 2 mg/kg of the $mGlu_5$ negative allosteric modulator CTEP significantly reduces the incidence of audiogenic seizure in *Fmr1* KO mice; *p = 0.0019. (**B**) Schematic shows chronic dosing schedule and AGS timeline. Chronic treatment with 2 mg/kg CTEP no longer alleviates susceptibility to audiogenic seizures, indicating that mice develop tolerance to multiple doses of CTEP over 5 days. Two-tailed Fisher's exact test, *Fmr1* KO vehicle treated vs. CTEP treated: p = 1.0. (Experiments were conducted by Rebecca Senter and Amanda Coronado).

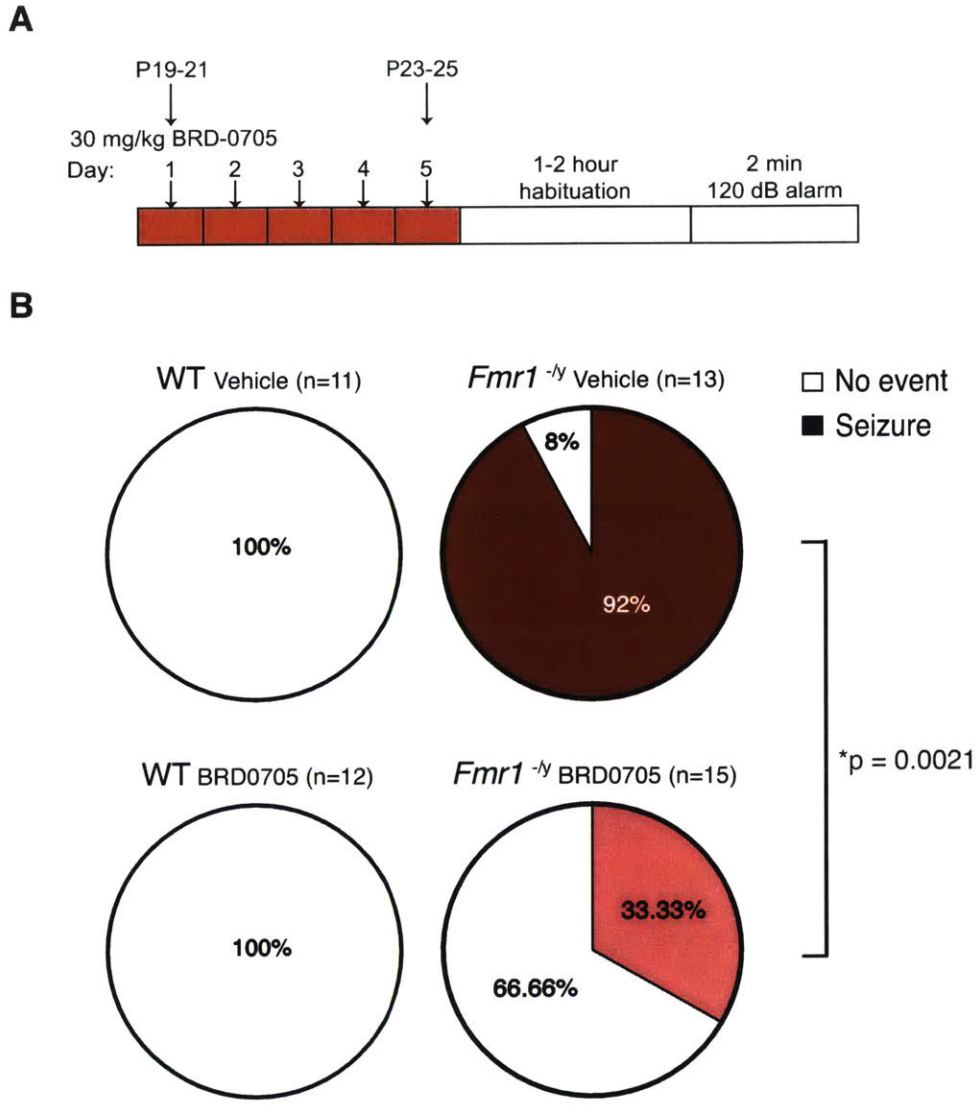

Figure 3.4: No evidence of drug tolerance in AGS with chronic BRD0705 treatment.

(**A**) Schematic shows chronic dosing schedule and AGS timeline. (**B**) *Fmr1*$^{-/y}$ mice treated with vehicle exhibit increased susceptibility to audiogenic seizure activity compared to WT treated with vehicle (two-tailed Fisher's exact test, *$p < 0.0001$). Chronic (5 day) dosing with 30 mg/kg BRD0705 has no effect on WT mice but significantly reduces the incidence of audiogenic seizure in *Fmr1*$^{-/y}$ mice (*$p = 0.0021$).

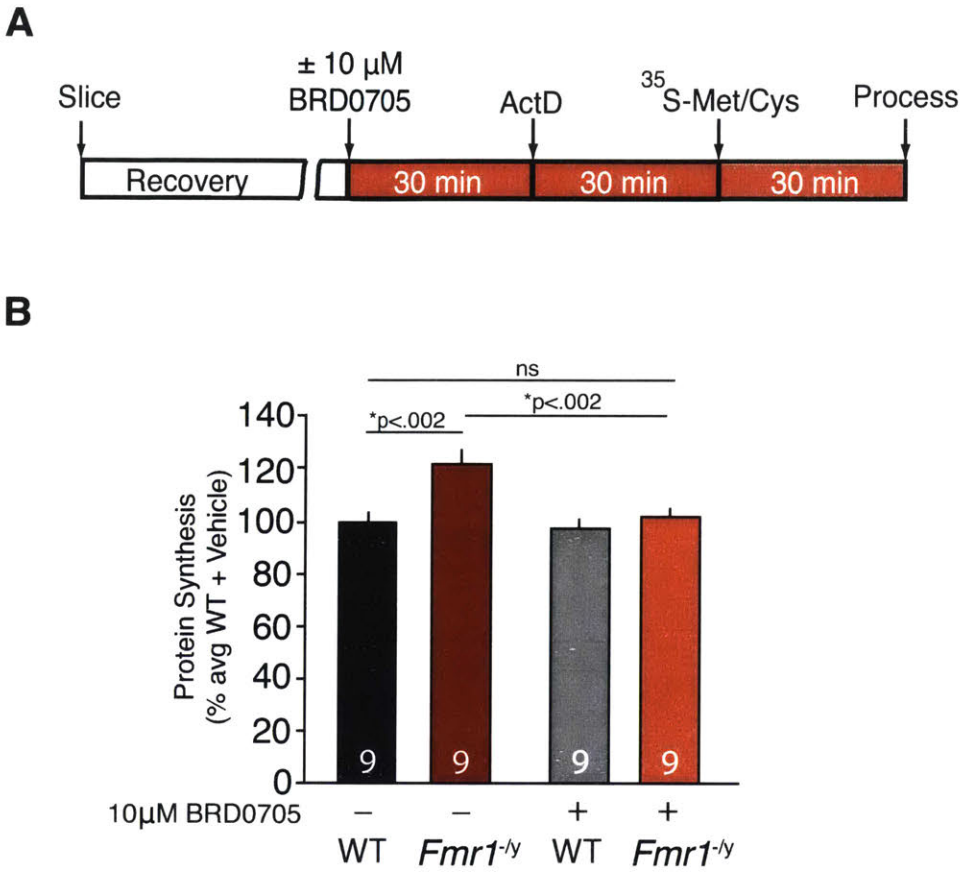

Figure 3.5: Excess protein synthesis in *Fmr1* KO mice is corrected by GSK3α inhibition.

(**A**) Schematic illustrates experimental timeline. (**B**) Basal protein synthesis is significantly increased in slices from *Fmr1*$^{-/y}$ mice (Student's two-way t-test; *$p < 0.002$) compared with WT slices. Treatment with BRD0705, an inhibitor GSK3α significantly reduces elevated protein synthesis in *Fmr1*$^{-/y}$ mice back to wild-type levels (Student's two-way t-test *Fmr1*$^{-/y}$ vehicle vs. *Fmr1*$^{-/y}$ drug: *$p < 0.002$; WT vehicle vs. *Fmr1*$^{-/y}$ drug: $p = 0.805$). There is a significant interaction between genotype and treatment (Two-way ANOVA; $p = 0.012$).

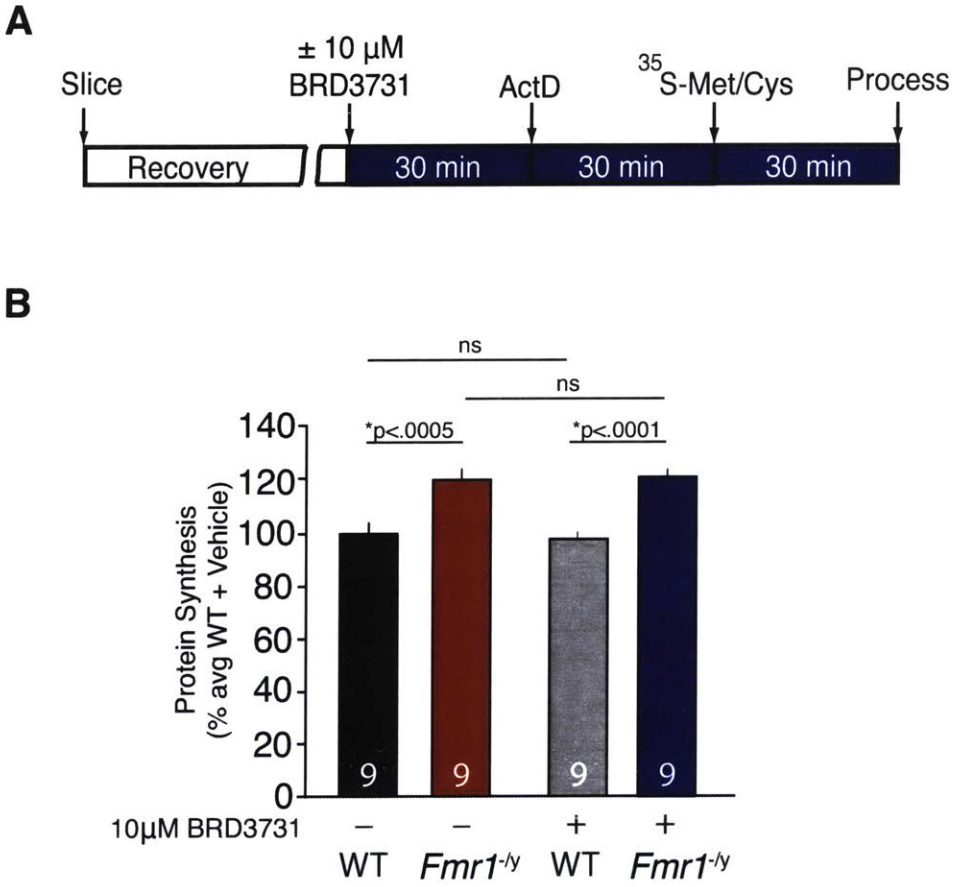

Figure 3.6: Inhibition of GSK3β does not correct excessive protein synthesis in *Fmr1* KO mice.

(**A**) Schematic illustrates experimental timeline. (**B**) Basal protein synthesis is significantly increased in vehicle-treated slices from *Fmr1*$^{-/y}$ mice (Student's two-way t-test; *$p < 0.0005$) compared with vehicle-treated WT slices. Treatment with BRD3731, an inhibitor GSK3β does not affect elevated protein synthesis in *Fmr1*$^{-/y}$ mice compared with WT slices (*$p < 0.001$). There is no significant interaction between genotype and treatment (Two-way ANOVA; $p = .617$).

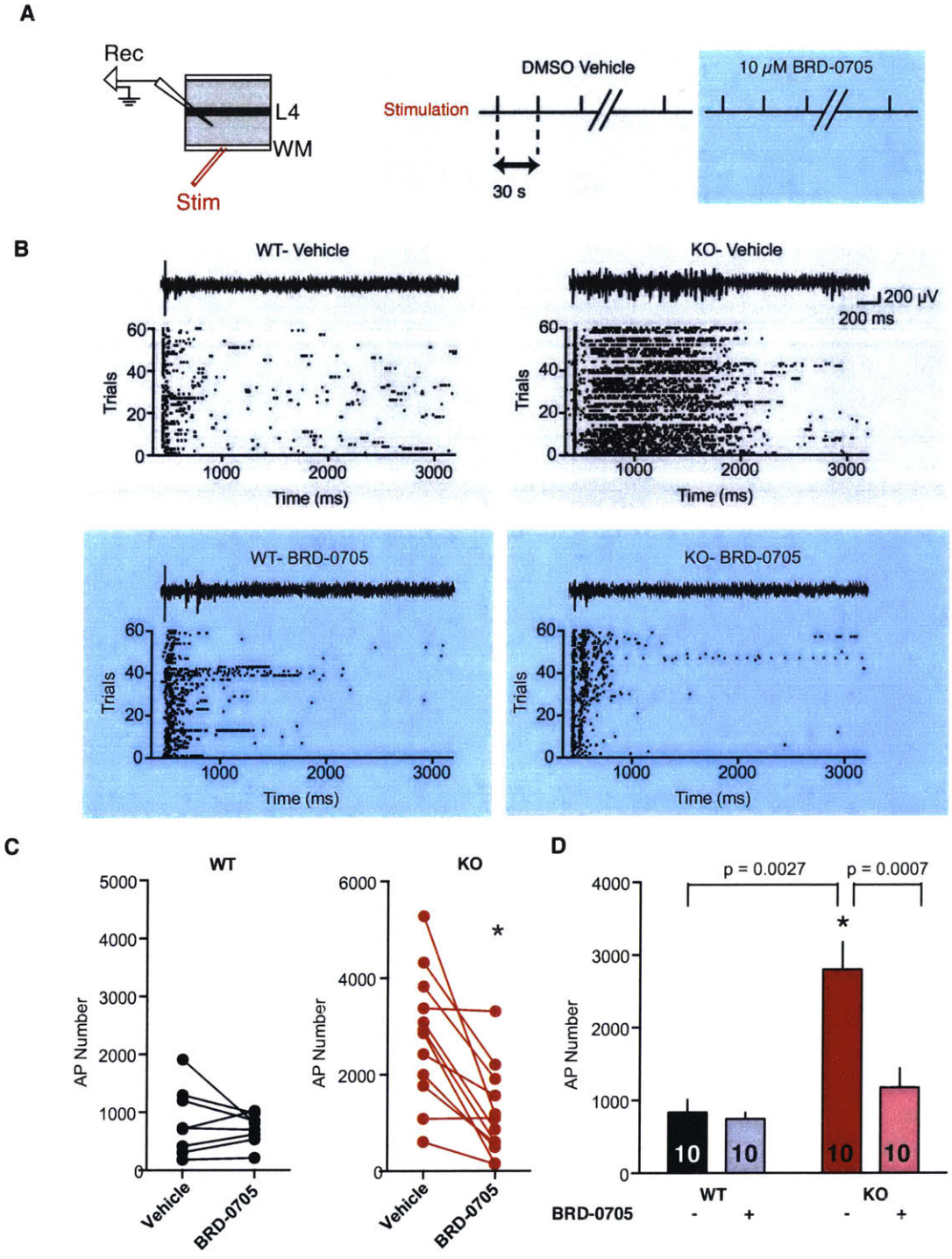

Figure 3.7: BRD0705 reduces evoked hyperexcitability in the *Fmr1* KO visual cortex.

(**A**) Extracellular recordings were performed in layer V of the visual cortex. Action potentials were generated every 30 seconds with white matter stimulation for a total of 60 trials in vehicle, followed by 60 trials in 10 μM BRD0705. (**B**) Representative rastor plots and traces from both wild-type (WT) and *Fmr1* KO slices show prolonged firing in the *Fmr1* KO, which is corrected by BRD0705 treatment. (**C**) BRD0705 significantly reduces the number of action potentials (AP) in *Fmr1* KO slices (paired t-test, $p = 0.007$). (**D**) The mean number of action potentials is significantly greater in *Fmr1* KO slices and can be corrected by application of 10 μM BRD0705 (two-way repeated measures ANOVA, genotype x treatment, $p = 0.0017$, WT vehicle vs. *Fmr1* KO vehicle, $p = 0.0027$, *Fmr1* KO vehicle vs. *Fmr1* KO + BRD0705, $p = 0.0007$). (Experiments were conducted by Rebecca Senter).

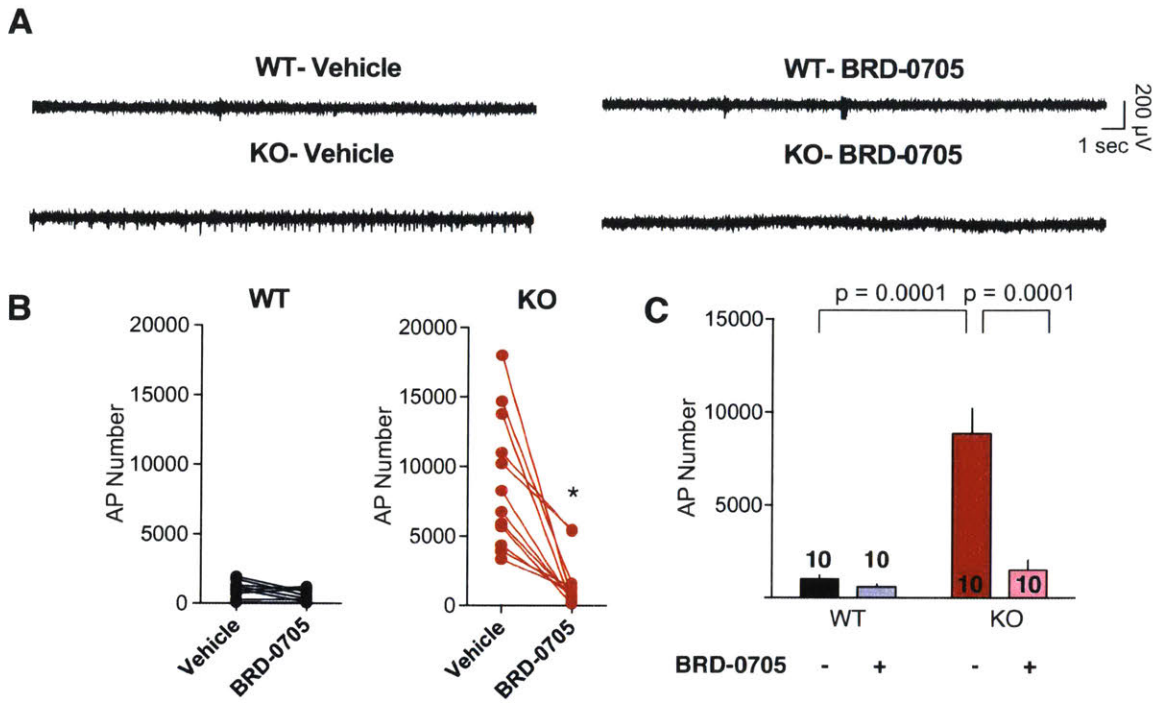

Figure 3.8: BRD0705 reduces spontaneous hyperexcitability in the *Fmr1* KO visual cortex.

(**A**) Extracellular recordings were performed in layer V of the visual cortex and the number of spontaneous action potentials was measured over 30 minutes in vehicle, followed by 30 minutes in 10 μM BRD0705. (**B**) BRD0705 significantly reduces the number of spontaneous action potentials (AP) in *Fmr1* KO slices (paired t-test, p = 0.0003). (**C**) The mean number of spontaneous action potentials is significantly greater in *Fmr1* KO slices and can be corrected by application of 10 μM BRD0705 (two-way repeated measures ANOVA, genotype x treatment, p = 0.0004, WT vehicle vs. *Fmr1* KO vehicle, p = 0.0001, *Fmr1* KO vehicle vs. *Fmr1* KO + BRD0705, p = 0.0001). (Experiments were conducted by Rebecca Senter).

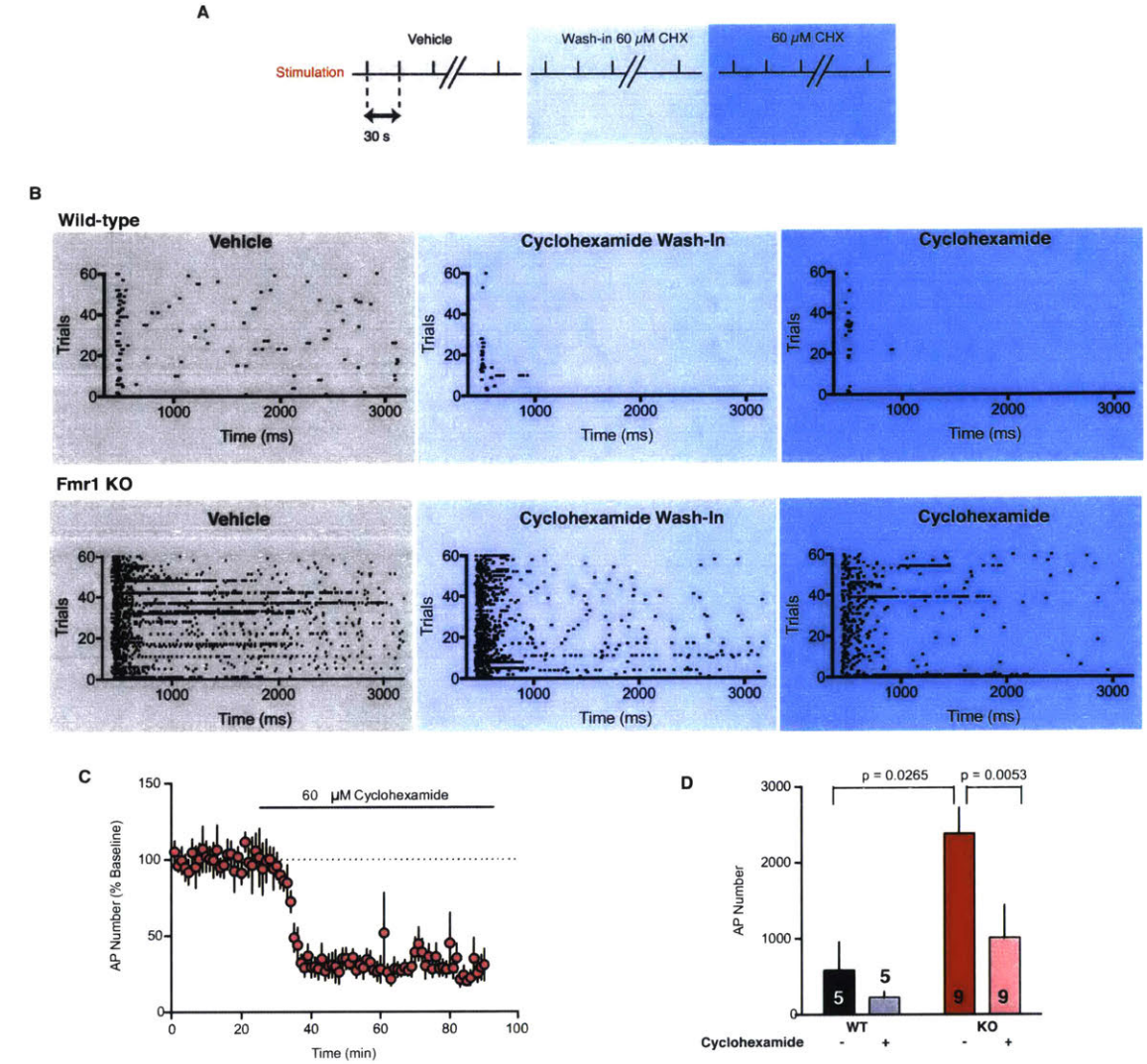

Figure 3.9: Evoked spiking in layer V visual cortex is protein synthesis-dependent.

(**A**) Evoked extracellular action potentials were recorded for 30 minutes in aCSF (vehicle), followed by a 30 minute wash-in of 60 μM cyclohexamide (CHX). After the wash-in period, an additional 30 minutes of recordings were collected in CHX. (**B**) Representative rastor plots from both WT and *Fmr1* KO slices showing prolonged firing in *Fmr1* KO slices, which is reduced by application of CHX. (**C**) Time course of the averaged number of action potentials in response to application of CHX in *Fmr1* KO slices. Data are represented as % baseline action potential number. (**D**) The mean number of action potentials is significantly greater in *Fmr1* KO slices and can be corrected by application of CHX (two-way repeated measures ANOVA, genotype x treatment, WT vehicle vs. *Fmr1* KO vehicle, $p = 0.0265$, *Fmr1* KO vehicle vs. *Fmr1* KO + CHX, $p = 0.0053$. (Experiments were conducted by Rebecca Senter).

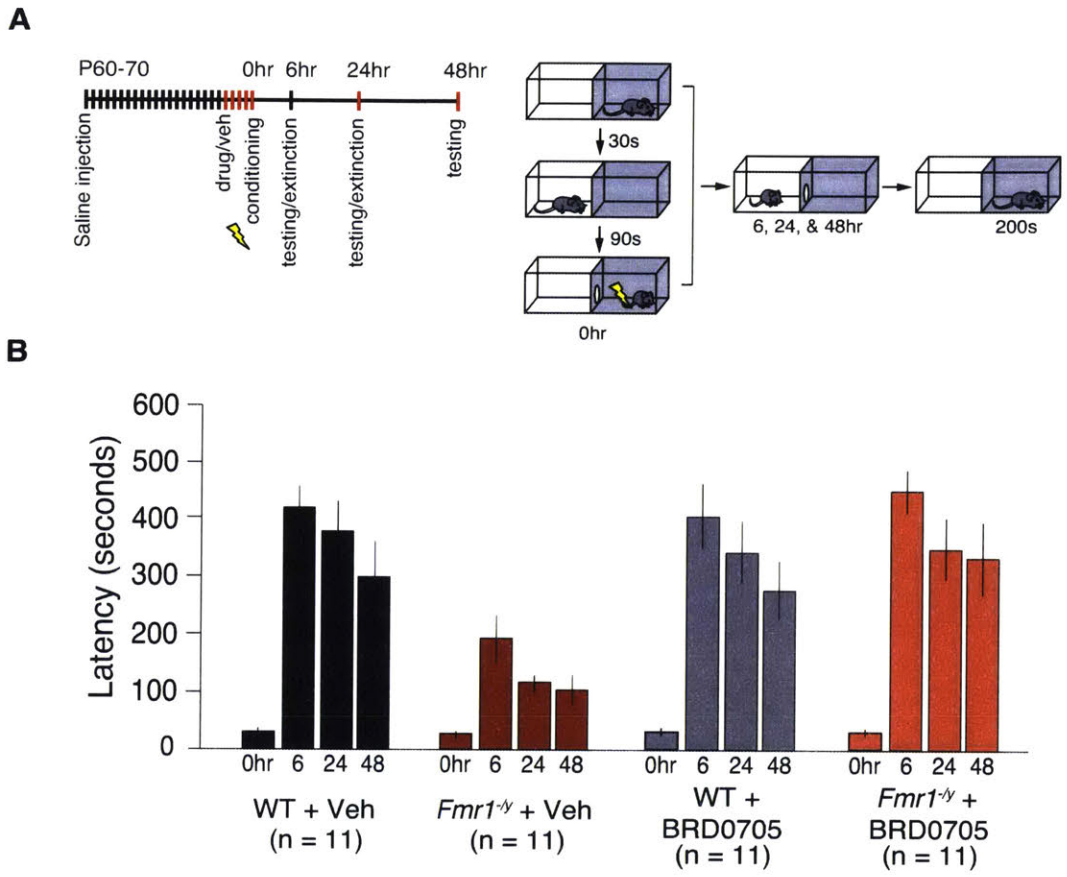

Figure 3.10: Inhibition of GSK3α in *Fmr1*$^{-/y}$ mice corrects impaired memory in an inhibitory avoidance learning task.

(**A**) Experimental design of dosing schedule and inhibitory avoidance learning task. Animals were dosed with saline for 20 days prior to vehicle or drug in order to habituate to the injection. After 5 days of vehicle or drug, animals began the IA task, receiving a daily dose throughout the remainder of the experiment. (**B**) Vehicle treated *Fmr1*$^{-/y}$ mice show impaired acquisition of inhibitory avoidance learning compared to vehicle treated WT mice (two-tailed ANOVA, *$p < 0.001$). BRD0705 treated *Fmr1*$^{-/y}$ mice show comparable acquisition and extinction of inhibitory avoidance to vehicle and R-baclofen-treated WT mice (two-way ANOVA, $p = 0.859$, $p = 0.844$, respectively). There is a statistically significant interaction between genotype and time point across treatments (repeated measures two-way ANOVA, *$p = < 0.001$).

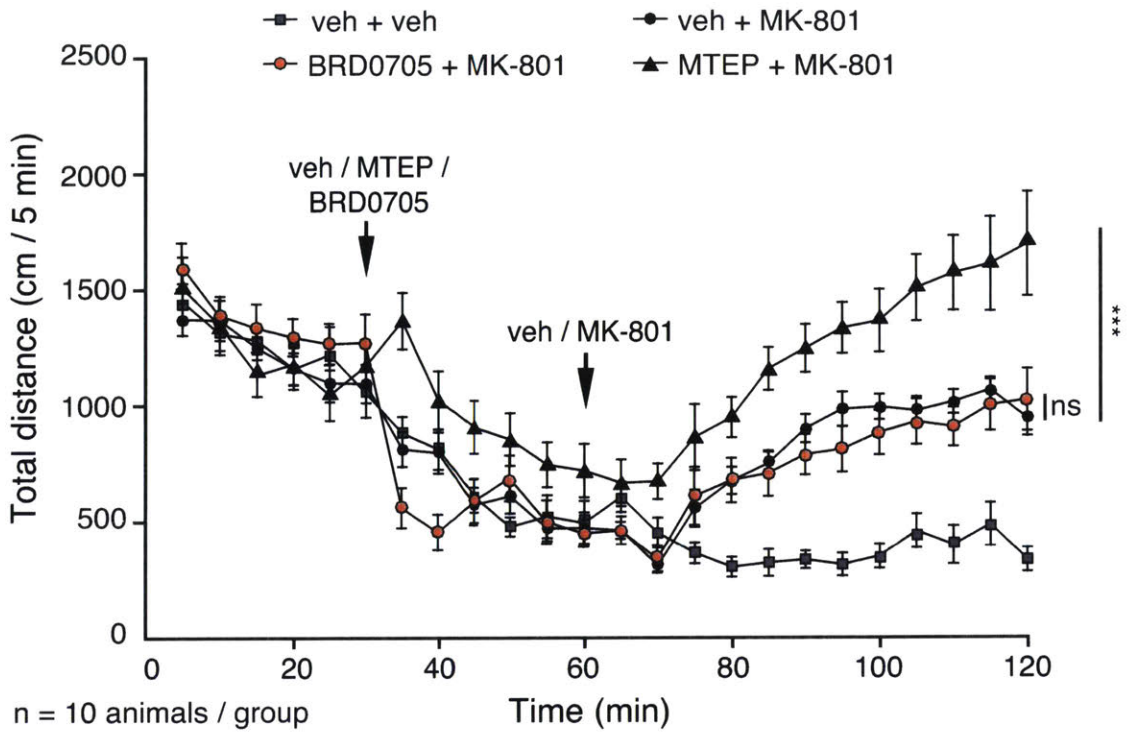

Figure 3.11: Inhibition of GSK3α does not potentiate the psychotomimetic effects of MK801.

WT mice pre-treated with BRD0705 injected intraperitoneally with the NMDAR antagonist MK801 (0.3 mg/kg) show comparable hyperlocomotion 60 minutes post-treatment compared to mice pre-treated with vehicle (N = 10 mice per group). Student's two-tailed t-test vehicle + MK801 vs. BRD0705 + MK801: $p = 0.633$. Data points represent distance travelled in cm over 5 minute bins, averaged as pooled animals per treatment group. Comparatively, pre-treatment with MTEP (10 mg/kg, i.p.) potentiates hyperlocomotion (N = 10 mice per group) compared to either BRD0705 or vehicle. ANOVA on ranks: $^*p = 0.006$. Holm-Sidak pairwise multiple comparisons: veh vs. BRD0705: not significant, veh vs. MTEP: $^*p < 0.05$; BRD0705 vs. MTEP: $^*p < 0.05$.Student's two-tailed t-test vehicle + MK801 vs. MTEP + MK801: $^*p = 0.0075$; BRD0705 + MK801 vs. MTEP + MK801 $^*p = 0.025$.

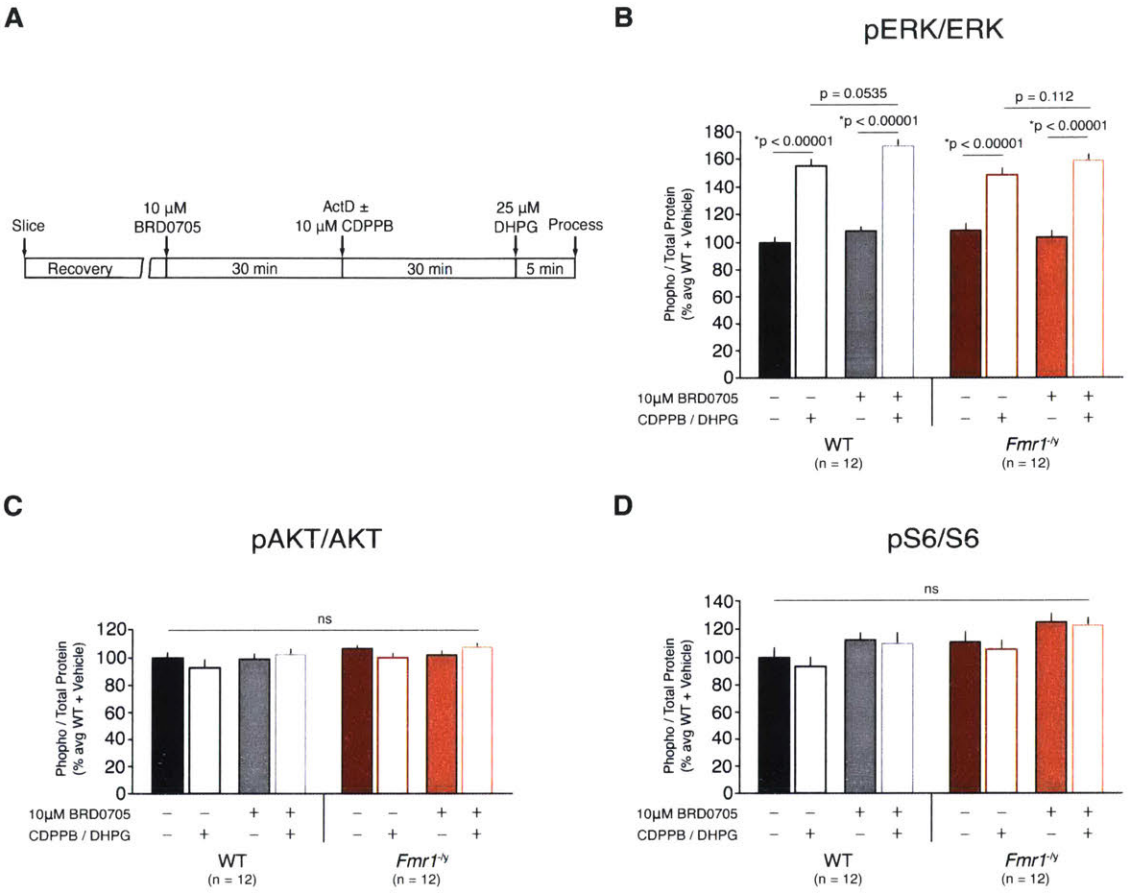

Figure 3.12: Inhibition of GSK3α does not affect $mGlu_5$-stimulated ERK1/2, AKT, or mTOR activation.

(**A**) Schematic illustrates experimental timeline. (**B**) Activation of $mGlu_5$ causes a robust activation of ERK1/2 across all conditions (stats represented are Student's unpaired two-way t-tests). There is no significant interaction between genotype and stimulation (two-way ANOVA: $p = 0.067$). There is no significant interaction between genotype and drug treatment (two-way ANOVA: $p = 0.067$). There is no significant interaction between genotype and stimulation among drug treated slices (two-way ANOVA: $p = 0.503$). This suggests that BRD0705 does have any affect $mGlu_5$-stimulated ERK1/2 activation. (**C**) Neither activation of $mGlu_5$ nor treatment with BRD0705 leads to changes in AKT activation. There is no significant interaction between genotype and stimulation (two-way ANOVA: $p = 0.916$). There is no significant interaction between genotype and drug treatment (two-way ANOVA: $p = 0.620$). There is no significant interaction between genotype and stimulation among drug treated slices (two-way ANOVA: $p = 0.746$). This suggests that BRD0705 does have any affect $mGlu_5$-stimulated AKT activation. (**D**) Neither activation of $mGlu_5$ nor treatment with BRD0705

leads to changes in S6 (a readout of mTOR) activation. There is no significant interaction between genotype and stimulation (two-way ANOVA: $p = 0.958$). There is no significant interaction between genotype and drug treatment (two-way ANOVA: $p = 0.857$). There is no significant interaction between genotype and stimulation among drug treated slices (two-way ANOVA: $p = 0.990$). This suggests that BRD0705 does have any affect $mGlu_5$-stimulated S6 activation.

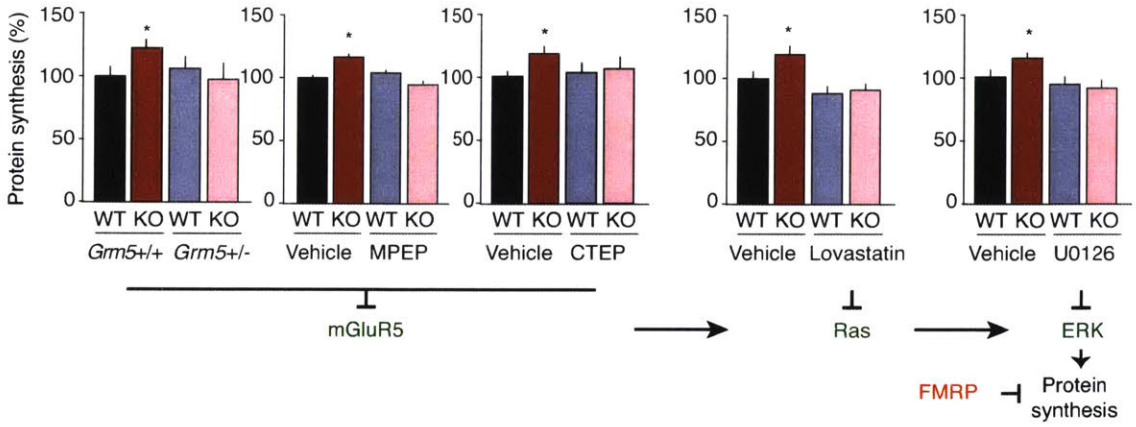

Figure 3.13: Pharmacological interventions which normalize mGluR-mediated signaling rescue basal protein synthesis in *Fmr1* KO mice.

Genetic reduction of $mGlu_5$ or pharmacological inhibition with MPEP, a non-competitive antagonist of $mGlu_5$ or CTEP, a negative allosteric modulator of $mGlu_5$ restores basal protein synthesis to WT levels in *Fmr1* KO hippocampal slices. Lovastatin, an inhibitor of Ras-ERK signaling, and U0126, a direct inhibitor of ERK1/2, similarly correct elevated protein synthesis in the *Fmr1* KO mouse. Figure adapted from Dolen et al. (2007), Michalon et al. (2012), Osterweil et al. (2010) and Osterweil et al. (2013).

Chapter 4

Selective activation of $GABA_B$ receptors with R-baclofen corrects several cognitive and behavioral deficits in a 16p11.2 CNV mouse model

Portions of this chapter have been published:

Tian D, Stoppel LJ, Heynen AJ, Lindemann L, Jaeschke G, Mills AA, Bear MF. Contribution of mGluR5 to pathophysiology in a mouse model of human chromosome 16p11.2 microdeletion. *Nature Neuroscience* 2015 Feb;18 (2):182-4

4.1: Abstract

Human chromosome 16p11.2 microdeletion is the most common gene copy number variation (CNV) in autism, affecting an estimated 3 in 10,000 people. Caused by a single copy deletion of ~27 genes, people with 16p11.2 microdeletion syndrome often exhibit impaired communication and socialization skills as well as intellectual disability. Studies on animal models of human 16p11.2 microdeletion disorder have revealed morphological, behavioral and electrophysiological deficits. In particular, we found that neuronal dysfunction downstream of metabotropic glutamate receptor 5 ($mGlu_5$) contributes to cognitive deficits in mouse model of 16p11.2 microdeletion disorder and may be a point of convergence in the synaptic pathophysiologies of this and other genetic causes of autism including Fragile X Syndrome. Recently, R-baclofen, a $GABA_B$ receptor agonist, was shown to correct many disease-related pathologies in a mouse model of Fragile X Syndrome including cognitive impairments, and has shown promising outcomes in clinical trials with patients with autism and Fragile X Syndrome. We investigated the efficacy of R-baclofen to treat cognitive deficits in heterozygous 16p11.2 deletion mice. We chronically administered R-baclofen to 8-12 week old group-housed 16p11.2 *df/+* and WT male littermates for 2 weeks prior to behavioral testing. We found that vehicle-treated 16p11.2 *df/+* mice exhibited profound deficits in a familiar object recognition task and contextual fear discrimination task, similar to previous reports. Additionally, we found that 16p11.2 *df/+* mice exhibit hyperactivity, spend more time in the center in the open field and fail to habituate across testing sessions. Importantly, chronic R-baclofen treatment corrected deficits in object recognition and contextual fear discrimination and restored normal habituation and behavior in the open field. Our results indicate that inhibition of $GABA_B$ receptors with R-baclofen may be a promising treatment avenue for patients with 16p11.2 microdeletion disorder and other genetic causes of autism with similar dysfunction. Additionally, we also examined basal protein synthesis, ERK1/2 activation, as well as habituation to an open field and novelty detection in mice harboring a duplication of the

16p11.2-syntenic region on chromosome 7. We found that 16p11.2 *dp/+* animals tend to exhibit reciprocal phenotypes to those of 16p11.2 *df/+* mice, including increased basal protein synthesis, ERK1/2 activation and enhanced novelty detection.

4.2: Introduction

4.2.1: 16p11.2 CNVs cause neuropsychiatric disorders and intellectual disability in humans.

Chromosomal copy number variations (CNVs) have been associated with 5-10% of patients with ASD (Levy, Ronemus et al. 2011, Pinto, Darvishi et al. 2011, Malhotra and Sebat 2012). Variation at human chromosome 16p11.2 is the most common of these and accounts for approximately 0.5-1% of all ASD cases (Malhotra and Sebat 2012). The common clinical presentations in individuals carrying the 16p11.2 microdeletion are language impairment, intellectual disability (ID), ASD, anxiety, attention deficit hyperactive disorder (ADHD), and epilepsy (Hanson, Nasir et al. 2010, Zufferey, Sherr et al. 2012). Clinical studies have indicated that patients with the microdeletion CNV tend to exhibit more severe symptoms, commonly associated with ASD, ID and obesity compared to patients with the duplication, which is more commonly associated with schizophrenia (Weiss, Shen et al. 2008).

4.2.2: Several genes within the affected 16p11.2 region are implicated in FX.

The 16p11.2 region includes ~27 annotated protein-coding genes, many of which are expressed in the mouse brain, and specifically, in CA1 of the hippocampus (Horev, Ellegood et al. 2011). Two of these genes, *MAPK3* and *MVP* are directly involved in signaling pathways downstream of $mGlu_5$ signaling, and several other genes in this region are targets of FMRP (Kolli, Zito et al. 2004, Paspalas, Perley et al. 2008, Crepel, Steyaert et al. 2011). *MAPK3*, which codes for the ERK1 isoform protein product, is an integral protein in the pathway that leads to the production of synaptic proteins necessary for mGluR-LTD. Interestingly, evidence indicates that Major Vault Protein (*MVP*) is a negative regulator of MAPK (ERK1/2) (Kolli, Zito et al. 2004), and a rare inherited deletion in the 16p11.2 region confined to *MVP*, *CDIPT1*, *SEZ6L2*, *ASPHD1*, and *KCTD13* has been shown to be associated with ASD (Crepel, Steyaert et al. 2011). The net effect of allelic variation of these and other genes in the 16p11.2 region on

synaptic protein synthesis and function remains to be fully determined, but considering the identity of the genes in this area, it would be surprising if variation in this region did not cause synaptic pathophysiology on the same axis that is disrupted in FX. Specifically, we hypothesize that disruption of the synaptic control of protein synthesis may contribute to cognitive impairment in 16p11.2 CNV carriers, similar to patients with FX.

4.2.3: Animal models of 16p11.2 CNVs reveal cognitive, behavioral, and synaptic deficits.

Mouse models of both the human 16p11.2 duplication (16p11.2 *dp/+*) and deletion (16p11.2 *df/+*) have been established (Horev, Ellegood et al. 2011, Portmann, Yang et al. 2014). The first published mouse models of the 16p11.2 CNVs carry either deletion or duplication of the region spanning mouse genes *Slx1b-Sept1*, ~30 genes in total (Horev, Ellegood et al. 2011). A subsequent 16p11.2 *df/+* mouse model spans ~24 genes, from *Coro1a-Spn*. Interestingly, despite harboring the shortest regional deletion, overlapping with both other deletion models, these mice are deaf, whereas no other 16p11.2 *df/+* model shows auditory deficits (Portmann, Yang et al. 2014). Another pair of 16p11.2 *df/+* and 16p11.2 *dp/+* mouse models, which models the BP4-BP5 human interval, corresponds to a region in mice ranging from the genes *Sult1a1* to *Spn*, approximately 26 genes (Arbogast, Ouagazzal et al. 2016).

Characterization of the first 16p11.2 CNV mouse models indicated that similar to the human CNV phenotypes, deletion or duplication led to macrocephaly or microcephaly, respectively, with behavioral phenotypes associated with the deletion being more severe than the duplication (Horev, Ellegood et al. 2011). At this time, surprisingly, much remains unknown regarding the synaptic pathophysiology and accompanying cognitive deficits in these mice, with only a handful of studies characterizing animal models of these CNVs. In zebrafish it has been shown that deletion or duplication of only *KCTD13* (a single gene in the 16p11.2 region, which functions as an E3 Ubiquitin-ligase adaptor) mirrors neuroanatomical macro and microcephaly characteristics of 16p11.2 CNVs. Interestingly, manipulation of either *MVP*

or *MAPK3* in addition to *KCTD13* exacerbated these anatomical defects (Golzio, Willer et al. 2012).

A second mouse model of 16p11.2 *df/+* was more recently characterized and recapitulated many of the gross anatomical and motor phenotypes previously published(Horev, Ellegood et al. 2011, Portmann, Yang et al. 2014). Investigation of the second 16p11.2 *df/+* mouse model revealed dysfunction in the basal ganglia circuitry, specifically elevated dopamine-sensitive cells in the striatum of 16p11.2 *df/+* mice, despite fewer cells with dopamine receptors compared with controls in deeper layers of the cortex. These researchers found no deficits in social interaction or anxiety while there was a robust deficit in recognition of familiar objects, indicating a complete lack of habituation in these mice(Portmann, Yang et al. 2014). Consistent with this notion, the same group looked at ultrasonic vocalizations (USVs) as a readout of the response to social cues in this mouse model and found a deficiency in 16p11.2 *df/+* mice in initial USV responses to novel social cues(Yang, Mahrt et al. 2015).

Most recently, a study confirmed a similar deficit in familiar object recognition in the original mouse model of 16p11.2 microdeletion.(Horev, Ellegood et al. 2011) They also observed deficient habituation in an open field task as well anxiolytic tendencies in the open field and elevated plus maze(Pucilowska, Vithayathil et al. 2015). An investigation of embryonic 16p11.2 *df/+* tissue has revealed abnormal progenitor cell dynamics, consistent with what was previously reported in an ERK2 deficient mouse model(Pucilowska, Puzerey et al. 2012), implying that the loss of *MapK3* (ERK1 isoform) in 16p11.2 *df/+* mice strongly contributes to the observed anatomical and cognitive deficits in these mice (Pucilowska, Vithayathil et al. 2015).

4.2.4 Investigation of 16p11.2 *df/+* and 16p11.2 *dp/+* mouse models have revealed largely reciprocal phenotypes.

16p11.2 *df/+* and 16p11.2 *dp/+* mice harboring the human BP4-BP5 mutation (the most recent models to be generated) have been extensively compared, revealing largely reciprocal phenotypes (Arbogast, Ouagazzal et al. 2016). Notably, opposite phenotypes were observed in locomotor activity, with 16p11.2 *df/+* mice being

hyperactive compared with WT controls and 16p11.2 *dp/+* mice being hypoactive. 16p11.2 *df/+* mice demonstrated greater repetitive behavior, as measured by rearing, jumping and climbing, while 16p11.2 *dp/+* mice exhibited reduced climbing compared to WT littermates. 16p11.2 *df/+* mice also showed impaired memory in a novel object recognition task, while 16p11.2 *dp/+* demonstrated superior performance compared to WT, as measured by time spent attending to a novel object versus a familiar object. Interestingly, both 16p11.2 *df/+* and 16p11.2 *dp/+* mice showed impairments in social interaction, providing some face validity to these models, as human carriers of both the microdeletion and microduplication are at higher risk for developing ASD, although the latter is notably more prone to schizophrenia (Weiss, Shen et al. 2008). Although preliminary comparisons of hippocampal synaptic transmission and LTP have been investigated between 16p11.2 *df/+* and 16p11.2 *dp/+* mice (Arbogast, Ouagazzal et al. 2016), no one has explored translational control at the synapse.

4.2.5: FX and 16p11.2 CNVs: convergence at $mGlu_5$.

As mentioned previously, two genes within the affected 16p11.2 region either directly or indirectly impact the ERK signaling pathway, known to be pathogenic in FX. Several other genes are targets of FMRP (Kolli, Zito et al. 2004, Paspalas, Perley et al. 2008, Crepel, Steyaert et al. 2011). Given the important role of ERK in synaptic translation and plasticity, we hypothesize that 16p11.2 *df/+* and/or 16p11.2 *dp/+* mice may phenocopy the *Fmr1* KO mouse and share similar synaptic deficits. Similarly, interventions that have been successful in rescuing phenotypes in the *Fmr1* KO mouse may be effective in correcting deficits associated with 16p11.2 CNV mouse models. Chronic or acute treatment with the $mGlu_5$ negative allosteric modulator CTEP corrected elevated protein synthesis and impaired mGluR-LTD as well as hippocampus-associated cognitive deficits in *Fmr1* KO mice (Michalon, Sidorov et al. 2012). Additionally, reducing glutamatergic signaling through $mGlu_5$ by chronic treatment with the $GABA_B$ agonist R-baclofen was also useful in correcting elevated protein synthesis and mGluR-LTD in *Fmr1* KO mice, and has showing promising preliminary results in clinical trials FX (El Idrissi, Ding et al. 2005, D'Hulst, De Geest et al. 2006, Selby, Zhang

et al. 2007, Centonze, Rossi et al. 2008, Curia, Papouin et al. 2009, D'Hulst, Heulens et al. 2009, Pacey, Heximer et al. 2009, Adusei, Pacey et al. 2010, Olmos-Serrano, Paluszkiewicz et al. 2010, Pacey, Tharmalingam et al. 2011, Henderson, Wijetunge et al. 2012, Heulens, D'Hulst et al. 2012, He, Nomura et al. 2014, Martin, Corbin et al. 2014, Braat, D'Hulst et al. 2015, Qin, Huang et al. 2015, Wahlstrom-Helgren and Klyachko 2015, Zhao, Wang et al. 2015, Martin, Martinez-Botella et al. 2016).

4.2.6: Characterization and correction of synaptic and cognitive deficits in 16p11.2 *df/+* and 16p11.2 *dp/+* mice.

We obtained the original 16p11.2 *df/+* and 16p11.2 *dp/+* mouse models, generated in Alea Mills' lab at Cold Spring Harbor, which contain a ~30 gene deletion or duplication spanning a region from mouse genes *Slx1b-Sept1* (Horev, Ellegood et al. 2011). We found that 16p11.2 *df/+* mice (and to a lesser extent, 16p11.2 *dp/+* mice) exhibit synaptic and cognitive deficits that overlap with the *Fmr1* KO mouse model. Furthermore, we observed that chronic treatment with the $mGlu_5$ negative allosteric modulator CTEP, as well as the $GABA_B$ agonist R-baclofen, is efficacious in correcting a number of these impairments.

4.3: Results

4.3.1: Steady decline of transmission rate of the 16p11.2 *df/+* allele.

Mutant 16p11.2 deletion mice mice (16p11.2 *df/+*), engineered to be heterozygous null at the region of chromosome 7qF3 that is syntenic to human chromosome 16p11.2 (Horev, Ellegood et al. 2011), were back-crossed for 5-10 generations to C57BL/6J mice (Charles River) to allow a comparison of synaptic physiology with previous studies(Auerbach, Osterweil et al. 2011, Michalon, Sidorov et al. 2012). As noted previously (Horev, Ellegood et al. 2011), loss of the genes in this region can compromise survival, and we found that this effect was amplified in successive generations on the C57BL/6J (Figure 4.1). As a result of this phenomenon, animals were particularly limited for this study; however, all data was generated using group-housed littermates, age-matched whenever possible.

4.3.2: Basal synaptic transmission is normal in 16p11.2 *df/+* mice.

We first characterized basal synaptic transmission at the Schaffer collateral–CA1 synapse using hippocampal slices from 4-5 week old mice and found no difference from wild type (WT) in input-output or paired-pulse facilitation (PPF) (data not shown). To investigate NMDA receptor-dependent synaptic plasticity, we induced long-term potentiation (LTP) with theta-burst stimulation (TBS), and long-term depression (LTD) with low-frequency (1 Hz) stimulation (LFS). Again, there was no difference from WT (Figure 4.2A, B), suggesting basic excitatory synaptic transmission and plasticity mechanisms are intact in the mutant mice.

4.3.3: There is deficient postsynaptic regulation of protein synthesis in 16p11.2 *df/+* mice.

We next assayed $mGlu_5$ mediated long-term depression (mGluR-LTD). mGluR-LTD was induced either by brief application of the mGluR1/5 agonist S-3,5-dihydrozyphenylglycine (DHPG) or by applying a series of paired pulses at 50 ms

interval (PP-LFS-LTD) (Huber, Gallagher et al. 2002). We again found no difference between WT and the 16p11.2 *df/+* mutant with either induction protocol (Figure 4.2C-F).

A distinctive property of mGluR-LTD in WT animals is a requirement for mRNA translation at the time of induction (Huber, Gallagher et al. 2002). In slices from *Fmr1*$^{-/y}$ mice, however, mGluR-LTD is unaffected by translation inhibitors such as cycloheximide (CHX) (Hou, Antion et al. 2006, Nosyreva and Huber 2006) because basal synaptic synthesis of LTD-regulatory proteins such as Arc(Waung, Pfeiffer et al. 2008, Jakkamsetti, Tsai et al. 2013, Wilkerson, Tsai et al. 2014) is elevated downstream of constitutive $mGlu_5$ activity due to loss of the translational repressor FMRP (Osterweil, Krueger et al. 2010). We were therefore compelled to investigate the protein synthesis-dependence of mGluR LTD in the 16p11.2 *df/+* mice, and discovered a striking difference from WT. Like FX model mice, mGluR-LTD in the 16p11.2 *df/+* mice was unaffected by CHX using either the chemical or electrical induction protocols (Figure 4.2D,F).

As reported previously in WT animals, DHPG induces LTD via two mechanisms: a postsynaptic reduction in AMPA receptors and a presynaptic reduction in glutamate release probability. Only the postsynaptic mechanism is CHX sensitive (Auerbach, Osterweil et al. 2011). To test whether the different sensitivity of LTD to CHX in the mutant was due to a qualitatively different expression mechanism, we analyzed PPF at the beginning and end of each DHPG-LTD experiment. No difference was observed between the WT and mutant slices (data not shown). These findings point to a deficiency in postsynaptic regulation of protein synthesis in the 16p11.2 *df/+* mice.

4.3.4: 16p11.2 *df/+* mice show significant cognitive impairment in two aversive-learning tasks.

Evidence indicating that mGluR-LTD was protein synthesis independent in 16p11.2 *df/+* mice is reminiscent of similar findings in the *Fmr1* KO mouse. This prompted us to test the mutant mice in two hippocampus-dependent behavioral assays, contextual fear conditioning (CFC) and inhibitory avoidance (IA), which have been shown in previous studies to reveal cognitive impairments in *Fmr1*$^{-/y}$ mice (Auerbach,

Osterweil et al. 2011, Michalon, Sidorov et al. 2012). CFC requires intact $mGlu_5$ signaling (Lu, Jia et al. 1997) and new protein synthesis at the time of conditioning (Stiedl, Palve et al. 1999). In this assay, mice are exposed to a distinctive environmental context in which a foot-shock is delivered, and 24 h later the mice are returned to either the same (familiar) or a different (novel) context (Figure 4.3A). WT mice expressed fear memory by freezing in the familiar context, and demonstrated an ability to discriminate different contexts by freezing less in the novel context. In contrast, the mutant mice showed significantly less freezing in the familiar context, and were unable to distinguish between the familiar and novel context (Figure 4.3B). To determine if this deficit was due to reduced sensitivity to foot-shock, we measured the distance each animal traveled during and immediately after the shock(Mauceri, Freitag et al. 2011) (Figure 4.3C). We found the shock elicited comparable movement in the two genotypes, suggesting the difference in freezing at 24 h was due to an impairment in memory formation in the mutant mice.

In the IA assay, mice received a foot shock upon entry into the dark side of a two-chamber box (Figure 4.3D). Memory strength and extinction were measured as the latency to enter the dark side when given the opportunity at 6, 24, and 48 h intervals(Dolen, Osterweil et al. 2007, Michalon, Sidorov et al. 2012). The 16p11.2 *df/+* mice showed impaired acquisition and extinction of IA memory.

4.3.5: Chronic treatment with $mGlu_5$ NAM CTEP reverses cognitive deficits in inhibitory avoidance learning.

We next investigated the possibility that chronic post-adolescent treatment with the $mGlu_5$ NAM CTEP could ameliorate the IA deficits. WT and mutant mice were treated every second day with CTEP (2 mg/kg *p.o.*) or vehicle for 4 weeks(Michalon, Sidorov et al. 2012) and were then tested in the IA assay as described above. Although treatment had no effect in the WT mice, it corrected the deficits in the mutants both in terms of acquisition and extinction (Figure 4.3E).

4.3.6: 16p11.2 *df/+* mice exhibit deficient basal protein synthesis, which is accompanied by an increase in Arc protein levels.

The mGluR-LTD deficit and the correction of cognitive deficits with an $mGlu_5$ NAM bear a striking resemblance to what has been shown previously in the FX mouse model. We were motivated to investigate the possibility of shared pathophysiology for several reasons, including the fact that four deleted genes are targets of FMRP (*MAZ*, *SEZ62L*, *TAOK2*, *ALDOA*) (Darnell, Van Driesche et al. 2011) and disruption of several genes in this region are predicted to affect $mGlu_5$ signaling (*MVP*, *CDIPT*, *MAPK3*) or protein turnover (*KCTD13*) (Golzio, Willer et al. 2012). The most straightforward prediction from our results is that synaptic protein synthesis downstream of $mGlu_5$ is exaggerated by the 16p11.2 microdeletion, and this gives rise to cognitive impairment. In the *Fmr1*$^{-/y}$ mouse, bulk protein synthesis in hippocampal slices is elevated and corrected by manipulations of $mGlu_5$ (Dolen, Osterweil et al. 2007, Osterweil, Krueger et al. 2010). In contrast, we found reduced basal protein synthesis in hippocampal slices in the 16p11.2 *df/+* mice, possibly explained by the decrease in ERK pathway activity (Figure 4.4). However, immunoblots for Arc protein showed a significant increase. The $mGlu_5$-dependent synthesis of Arc protein normally gates LTD and synapse elimination(Waung, Pfeiffer et al. 2008, Jakkamsetti, Tsai et al. 2013, Wilkerson, Tsai et al. 2014). Therefore, constitutive elevation of Arc could render mGluR-LTD insensitive to acute inhibition of protein synthesis and contribute to cognitive impairment.

4.3.7: Investigation of the therapeutic implications of chronic R-baclofen treatment on 16p11.2 *df/+* mice.

Based on our finding that chronic CTEP administration ameliorated some of the cognitive deficits associated with 16p11.2 *df/+* mice (Figure 4.3E), we were compelled to investigate the effect of R-baclofen, a $GABA_B$ receptor agonist, on these mice. Recently, R-baclofen, was shown to correct many disease-related pathologies in a mouse model of Fragile X Syndrome including cognitive impairments, and has shown promising outcomes in clinical trials with patients with autism and Fragile X Syndrome (Berry-Kravis, Hessl et al. 2012, Henderson, Wijetunge et al. 2012, Qin, Huang et al.

2015). We hypothesized that R-baclofen may show efficacy in treating many of the cognitive and behavioral phenotypes associated with 16p11.2 *df/+* mice based on the aforementioned similarities between the synaptic pathophysiology of 16p11.2 *df/+* and *Fmr1* KO mice. In order to investigate this hypothesis, we treated WT and 16p11.2 *df/+* group-housed littermates with either vehicle (drinking water obtained from the mouse facility) or R-baclofen (0.5 mg/ml in drinking water from the same source) chronically for 12 days prior to the first day of behavioral testing. Dosing continued for the remainder of the study and water was changed daily for both vehicle and drug-treated animals. Animals were subjected to a behavioral battery consisting of an open field habituation test followed by an object recognition task, concluding with a context discrimination (aversive stimulus) task followed by one week of recovery from an aversive stimulus. One week post-context discrimination testing, one brain hemisphere was Golgi-stained and the other hemisphere was dissected with the hippocampus, visual cortex, and frontal cortex being prepared for Western Blot analysis (Figure 4.5). A separate cohort of mice received the same 12-day chronic dosing schedule of either vehicle or drug prior to testing, but was only subject to the context discrimination task, as the task design dictated a much larger cohort of animals.

4.3.8: Habituation deficits in the open field are normalized by chronic R-baclofen treatment in 16p11.2 *df/+* mice.

We measured the total distance traveled by WT and 16p11.2 *df/+* mice as an indicator of hyperactivity in a 40cm x 40cm behavior arena across two 15-minute habituation sessions, spaced 1-2 hours apart. Vehicle treated 16p11.2 *df/+* mice traveled a significantly greater distance in the arena across both habituation sessions, indicative of a generalized hyperactivity in these mice. Chronic administration of 0.5 mg/ml R-baclofen had no effect on locomotion in these mice, but rather induced hyperactivity in WT mice, to a similar magnitude as both vehicle and R-baclofen treated 16p11.2 *df/+* mice (Figure 4.6). During each habituation session, we monitored the time spent in three pre-defined zones (outer, middle, and center) of the arena (Figure 4.7A). Vehicle-treated WT mice spend significantly more time near the walls in the outer zone

of the arena across both sessions combined (30 minutes total), whereas 16p11.2 *df/+* mice spend roughly equal time exploring the outer and inner (middle + center) zones of the arena. Interestingly, chronic R-baclofen administration does not affect exploration patterns of WT mice, but restores normal exploration in 16p11.2 *df/+* mice, leading to increased time spent in the outer zone and decreased time spent exploring the inner zones (Figure 4.7B). We then analyzed each habituation session independently in all four treatment groups. WT and 16p11.2 *df/+* mice spent indistinguishably similar percentages of time exploring each zone (with a moderate but significant preference for the outer zone) during the first 15-minute habituation session, regardless of treatment (Figure 4.7C). Interestingly, during the second 15-minute habituation session, vehicle-treated WT mice spent significantly more time in the outer zone than 16p11.2 *df/+* mice (82.6% +/- 3.29 vs. 53.1% +/- 3.84, Student's two-tailed t-test: $^*p < 0.0001$) (Figure 4.7D). We hypothesized that this may indicative of a deficit in habituation in 16p11.2 *df/+* mice from session 1 to session 2. While WT mice spend significantly more time in the outer zone and less time in the inner zones of the arena during session 2 compared with session 1 (Figure 4.7E), 16p11.2 *df/+* mice behavior that is indistinguishable across habituation sessions (Figure 4.7F). Intriguingly, chronic R-baclofen treatment corrected this habituation deficit in 16p11.2 *df/+* mice, while the behavior of WT mice treated with R-baclofen was unaffected (Figures 4.7C-F).

4.3.9: Chronic R-baclofen restores novelty detection and associative memory deficits in 16p11.2 *df/+* mice.

We next examined the effects of chronic R-baclofen treatment on the performance of WT and 16p11.2 *df/+* mice in a non-aversive object recognition memory task. Mice were first allowed to explore an arena with two identical objects for two sessions and then, the next day, one of the familiar objects was replaced with a novel object (Figure 4.8A). Similar to previous reports, we observed a severe deficit in novelty detection in vehicle-treated 16p11.2 *df/+* mice, reminiscent of what we observed in the *Fmr1* KO mouse in the same task (see Chapter 2). Chronic treatment with R-baclofen had no effect on preference for a novel object in WT mice, but completely restored

novelty detection in 16p11.2 *df/+* mice. Finally, mice were subjected to an aversive context-recognition task. Confirming previous observations (Figure 4.3B) vehicle-treated 16p11.2 *df/+* exhibited profound memory deficits on the testing day, as evidenced by lack of freezing in the familiar context where they had previously received a foot shock (Figure 4.9). 16p11.2 *df/+* mice treated with R-baclofen froze significantly more in the familiar context on testing day, comparable to WT mice treated with either vehicle or R-baclofen, demonstrating that R-baclofen restored the ability to both acquire and recall the association between context and an aversive event (Figure 4.9B).

4.3.10: Acute R-baclofen restores deficient protein synthesis in hippocampal slices from 16p11.2 *df/+* mice *in vitro*.

Previously, we reported deficits in *de novo* translation at the synapse in 16p11.2 *df/+* mice (Figure 4.4A). In order to investigate the effects of R-baclofen on protein synthesis in WT and 16p11.2 *df/+* mice, we pre-incubated hippocampal slices from P28-P32 animals in either vehicle (DMSO) or 10 μM R-baclofen in ACSF for 1 hour prior to measuring rates of basal protein synthesis with a metabolic labeling assay (Figure 4.10A). Recapitulating our previous observerations, vehicle-treated 16p11.2 *df/+* slices had significantly impaired translation compared to vehicle-treated WT slices. Astonishingly, we found that pre-treatment with R-baclofen significantly elevated rates of protein synthesis in 16p11.2 *df/+* slices, such that they were indistinguishable from vehicle-treated WT slices. Interestingly, WT slices pre-treated with R-baclofen also showed elevated rates of protein synthesis compared to vehicle-treated slices (Figure 4.10B).

4.3.11: Chronic R-baclofen does not impact ERK1/2 signaling in hippocampus, visual cortex, or frontal cortex.

We hypothesized that deficient rates of protein synthesis in 16p11.2 *df/+* mice were largely a result of deficent ERK1/2 signaling, shown to be reduced in respose to a hemizygous loss of *Mapk3*, the gene that codes for the ERK1 protein (Boulton, Yancopoulos et al. 1990). We measured basal activity of ERK1/2 in the hippocampus,

visual cortex, and frontal cortex in WT and 16p11.2 *df/+* animals that had been chronically treated with vehicle or R-baclofen to determine whether enhancing $GABA_B$ signaling impacted aberrant ERK1/2 signaling in 16p11.2 *df/+* mice. We observed significantly elevated ERK1/2 and ERK1-isoform-specific phosphorylation normalized to total ERK and ERK1 protein in the hippocampus of vehicle-treated 16p11.2 *df/+* mice that does appear to be impacted by R-baclofen treatment (Figure 4.11A). However, we do not attribute the significant improvement in 16p11.2 *df/+* mice on cognitive and behavioral tasks after R-baclofen treatment to changes in ERK activity, as no significant interactions were found (two-way ANOVA) between genotype and treatment in any brain region evaluated for either isoform of ERK (Figures 4.11, 4.12, 4.13).

4.3.12: Chronic R-baclofen treatment restores elevated Arc in 16p11.2 *df/+* mice, but has no effect on c-fos.

We previously reported elevated expression of the activity-regulated "plasticity" protein Arc in the hippocampus of 16p11.2 *df/+* mice, which we rationalized may contribute to the finding that mGluR-LTD was independent of *de novo* protein synthesis in these mice. We measured Arc expression in the hippocampus, visual cortex, and frontal cortex in WT and 16p11.2 *df/+* animals that had been chronically treated with vehicle or R-baclofen. Consistent with our previous findings, we observed elevated basal Arc in the hippcocampus of 16p11.2 *df/+* mice compared with WT, and expanded this observation to incude the visual cortex and frontal cortex as well. Chronic R-baclofen treatment normalized Arc to WT levels in 16p11.2 *df/+* mice, having no impact on Arc expression in WT mice (Figure 4.14A). Because Arc expression can be regulated by activity and exposure to the environment, we measured expression of another activity-regulated protein, c-fos, to determine if the observed changes in Arc expression were merely reflecting changes in activity of the mice. We observed significantly upregulated expression of c-fos in the hippocampus, visual cortex, and frontal cortex of vehicle-treated 16p11.2 *df/+* mice, as well as R-baclofen-treated WT and 16p11.2 *df/+* compared with WT mice treated with vehicle (Figure 4.14B). This is consistent with our observations that 16p11.2 *df/+* mice are hyperactive compared with

WT mice, and that R-baclofen treatment induced hyperactivity in WT mice, while having no impact on 16p11.2 *df/+* mice (Figure 4.6). Based on the finding that elevations in c-fos mirror elevated locomotor activity in WT and 16p11.2 *df/+* mice, but expression of Arc does not, we hypothesize that the correction of elevated Arc signaling in 16p11.2 *df/+* mice treated with R-baclofen is not due to changes in locomotion. Therefore, one possible explanation for the observed therapeutic benefits of chronic R-baclofen treatment in 16p11.2 *df/+* mice could be that increased $GABA_B$ signaling corrects augmented production of Arc at the synapse, thus restoring normal synaptic plasticity leading to improvements in learning and memory in 16p11.2 *df/+* mice.

4.3.13: 16p11.2 *dp/+* mice have elevated basal rates of hippocampal protein synthesis, elevated ERK1/2 phosphorylation and increased total ERK1.

We have shown that deletion of the syntenic-16p11.2 region in mice results in deficient synaptic translation in hippocampal slices (Figures 4.4A, 4.10B). We therefore hypothesized that a duplication of the same region may result in aberrant protein synthesis as well. We measured basal protein synthesis rates in hippocampal slices from WT and 16p11.2 *dp/+* mice and observed a reciprocal significant elevation in protein synthesis in 16p11.2 *dp/+* slices compared with WT controls (Figure 4.15A). We hypothesized that this elevation was possibly a consequence of enhanced ERK1/2 activity, as the gene encoding ERK1 is duplicated in this region. We measured basal phosphorylation of ERK1 and ERK2 (as well as total ERK1/2 activity) in hippocampal slices and found that ERK1/2 is overactive in 16p11.2 *dp/+* slices (Figure 4.15B). As expected, total ERK1 protein is significantly elevated in 16p11.2 *dp/+* mice; however, phosphorylation rates of ERK1 are unaffected, although it important to note that total pERK1 is elevated due to elevated total ERK1 protein. Surprisingly, we found elevated rates of ERK2 phosphorylation, which we hypothesize may contribute to the observed elevated rate of translation in these animals (Figure 4.15C).

4.3.14: 16p11.2 *dp/+* mice show enhanced novelty detection, a phenotype reciprocal to impairments observed in 16p11.2 *df/+* mice.

Based on the finding that protein synthesis is augmented in 16p11.2 *dp/+* mice, which appears to be pathogenic in other mouse models of intellectual disability (most notably the *Fmr1* KO mouse model), we hypothesized that 16p11.2 *dp/+* mice may exhibit behavioral and cognitive impairments. To our surprise, 16p11.2 *dp/+* mice were indistinguishable from WT mice in the open field, demonstrating a strong preference for the outer zone near the walls of the arena, across both sessions. We also observed no difference between WT and 16p11.2 *dp/+* mice in total distance traveled during the task, a measure of overall locomotor activity (Figure 4.16). Additionally we found that 16p11.2 *dp/+* show normal memory acquisition and recall in an aversive-contextual memory task (data not shown). Interestingly, we observed that 16p11.2 *dp/+* mice perform better than WT mice in a familiar object recognition task, spending significantly more time exploring a novel object during the test session (Figure 4.17). Overall, our data indicate that compared with a deletion of the syntenic-16p11.2 region, duplication of the same region in mice results in largely reciprocal phenotypes.

4.4: Discussion

4.4.1: A mouse model of human 16p11.2 microdeletion reveals deficits in translational regulation at the synapse.

Investigation of 16p11.2 *df/+* mice, a mouse model harboring a ~30 gene deletion (Horev, Ellegood et al. 2011), modeling a similar deletion found in humans at the 16p11.2 loci, has identified significant synaptic deficits that may be pathogenic in this disorder. 16p11.2 *df/+* mice have deficient hippocampal synaptic translation which may be a result of the deletion of one copy of the gene encoding the protein ERK1, an important protein coupled to synaptic protein synthesis. Reduced ERK1 protein expression results in an overall reduction of ERK1 activation. Others have shown that ERK1 and ERK2 may be hyperactive as a result of the missing copy of *Mapk3* (Pucilowska, Vithayathil et al. 2015); however, quantification of total phosphorylated ERK1/2 remains significantly decreased compared with WT controls (Tian, Stoppel et al. 2015). Interestingly, although bulk basal protein synthesis is decreased, protein expression of the plasticity protein Arc is elevated in the hippocampus. Arc has been implicated as a critical protein for the induction and maintenance of long-term depression, a form of synaptic plasticity that is dependent on *de novo* protein synthesis at the synapse (Waung, Pfeiffer et al. 2008, Jakkamsetti, Tsai et al. 2013). Interestingly, elevated Arc expression is also implicated in the pathophysiology of the *Fmr1* KO mouse (Busquets-Garcia, Gomis-Gonzalez et al. 2013). Although we did not observe deficits in basal synaptic transmission or the magnitude of mGluR-LTD (or other forms of synaptic plasticity) in 16p11.2 *df/+* mice, the protein synthesis-dependence of mGluR-LTD was absent in these mice, presumably a consequence of abundant Arc at the synapse. Similarly, mGluR-LTD is maintained-independent of new protein synthesis-in the *Fmr1* KO mouse, consistent with shared pathophysiology between these two animal models.

4.4.2: 16p11.2 *df/+* mice exhibit profound cognitive and behavioral abnormalities, consistent with highly penetrant ID in human deletion carriers.

Investigation of the 16p11.2 *df/+* mouse model has revealed multiple behavioral and cognitive impairments. 16p11.2 *df/+* mice failed to form the association between an adverse event (footshock) and a context in two hippocampus-dependent tasks. They also perform poorly on a non-aversive task, designed to measure novelty detection. They demonstrate dysfunction in habituation to a novel environment, with an enhanced tendency to explore the center of the environment, indicative of reduced anxiety (or more likely, increased impulsivity). Notably, 16p11.2 *df/+* mice also display extreme hyperactivity. While face validity of the 16p11.2 mouse models remains controversial, our observations demonstrate striking similarities between mouse models of 16p11.2 CNVs and human carriers, most notably impaired cognitive function. Intellectual disability is highly penetrant in carriers of the 16p11.2 microdelection (Zufferey, Sherr et al. 2012). Intriguingly, all of the identified behavioral and cognitive deficits characteristic of 16p11.2 *df/+* mice phenocopy *Fmr1* KO mice. Taken together, our findings suggest that dysfunctional translational control may be important in the pathogenesis of these deficits.

4.4.3: Shared pathophysiology between 16p11.2 CNVs and FX may inform potential therapeutic interventions for 16p11.2 carriers.

The GABAergic system as well as $mGlu_5$-mediated signaling are known to be altered in the *Fmr1* KO mouse. Although GABA function has not been examined in 16p11.2 *df/+* mice, *MAZ*, a gene in the deleted region, is a target of FMRP and directly regulates genes involved in GABA signaling (Murakami, Matsuda et al. 2006). Furthermore, observations that aberrant $mGlu_5$ signaling may contribute to pathophysiology in 16p11.2 CNV mouse models suggests that the same pharmacological interventions that have been useful in correcting deficits in the *Fmr1* KO mouse may translate to models of 16p11.2 CNVs as well. Our results thus far support this hypothesis. Chronic administration of the $mGlu_5$ negative allosteric modulator CTEP restored memory acquisition in a passive avoidance task. Chronic administration of the drug R-baclofen, a $GABA_B$ agonist, restores normal novelty detection, habituation and memory acquisition in 16p11.2 *df/+* mice as well.

One important caveat to our theory- that common phenotypes shared between the *Fmr1* KO mouse and 16p11.2 *df/+* mice stem from shared deficits in translational control, is the finding that protein synthesis is elevated in *Fmr1* KO mice yet deficient in 16p11.2 *df/+* mice. Although others have shown that defective protein synthesis can lead to cognitive dysfunction in many of these same assays (Auerbach, Osterweil et al. 2011, Liu, Ma et al. 2015), compelling evidence suggests that both CTEP and R-baclofen reduce elevated rates of translation in the *Fmr1* KO mouse (Henderson, Wijetunge et al. 2012, Michalon, Sidorov et al. 2012, Qin, Huang et al. 2015). One possibility that is supported by our data would be that shared impairments in learning and memory between the *Fmr1* KO mouse and 16p11.2 *df/+* mice are a consequence of elevated synthesis of specific proteins important for plasticity rather than elevation of bulk protein synthesis. Specifically, elevated translation of the "plasticity protein" Arc is similarly observed in both FX and 16p11.2 microdeletion mouse models. Chronic R-baclofen treatment resulted in a normalization of elevated Arc in the hippocampus, frontal cortex, and visual cortex of 16p11.2 *df/+* mice. Although no one has investigated the effects of $GABA_B$ agonism on Arc in the *Fmr1* KO mouse, a parallel correction of pathogenic Arc over-expression could explain the comparable phenotypic improvements between these two mouse models.

Another possibility arises from the recent observation that administration of R-baclofen in WT mice causes an *increase* in bulk protein synthesis *in vivo*, despite a contradictory *decrease* in *Fmr1* KO littermates (Qin, Huang et al. 2015). Notably, we observe a similar effect on protein synthesis in WT slices in our preparation *in vitro*. Furthermore, the same group found variable doses of R-baclofen to have widely different effects on locomotion, with lower-threshold doses actually inducing hyperactivity in WT mice while higher doses reduced activity, more predictive of increased inhibition (Qin, Huang et al. 2015). We observed baseline hyperactivity in 16p11.2 *df/+* mice that was not affected by chronic administration of 0.5 mg/ml R-baclofen. WT mice became hyperactive as a result of chronic R-baclofen treatment, which would be consistent with what has been previously seen with lower-dose

treatment. Thus, it may be important to investigate whether the observed improvements in cognition with R-baclofen treatment are dose-dependent.

4.4.4: 16p11.2 *df/+* and 16p11.2 *dp/+* mice exhibit many reciprocal phenotypes consistent with differences observed between human deletion and duplication carriers.

Consistent with previous reports, we found 16p11.2 *df/+* mice to be significantly more impaired that 16p11.2 *dp/+* mice. Interestingly, we found phenotypes of these two mice to be largely reciprocal. While 16p11.2 *df/+* mice lacked novelty detection, exhibited impaired protein synthesis and decreased ERK1 activation, 16p11.2 *dp/+* mice showed enhanced novelty detection, exaggerated protein synthesis and elevated ERK1 phosphorylation. 16p11.2 microdeletion disorder is more associated with ASD and intellectual disability in humans, while microduplication carriers are at a heightened risk for schizophrenia. Schizophrenia has been characterized by a heightened awareness of sensory stimuli, thus enhanced novelty detection in 16p11.2 *dp/+* mice may be consistent with this clinical observation. Similarly, multiple learning and memory impairments observed in 16p11.2 *df/+* mice are reminiscent of severe intellectual disability in human deletion carriers, suggesting that these 16p11.2 CNV mouse models may have high predictive validity as models of disease.

4.4.5: Conclusion

16p11.2 *df/+* mice appear to share common phenotypes with the *Fmr1* KO mouse, most notably, impairments in learning and memory as a consequence of altered signaling at $mGlu_5$. Further investigation into the exact mechanism by which R-baclofen reduces Arc expression and corrects multiple impairments in 16p11.2 *df/+* mice, including deficient protein synthesis and behavioral and cognitive impairments, is warranted. Clinical trials examining the safety and efficacy of R-baclofen in patients with FX have shown promising results and could potentially lead to the first FDA-approved intervention for this disorder. Therefore, based on our observations that deficits common to both the *Fmr1* KO mouse and 16p11.2 *df/+* mice can be corrected

by chronic R-baclofen treatment, we suggest that R-baclofen may ameliorate behavioral and cognitive impairment in human 16p11.2 CNV carriers.

4.5: Methods

4.5.1: Animals

A mouse line carrying a microdeletion of mouse chromosome 7qF3, the syntenic region of human chr16p11.2, was generously provided by Professor Alea Mills from the Cold Spring Harbor Laboratory prior to publication (Horev, Ellegood et al. 2011). In the present study F3 heterozygous 16p11.2 *df/+* male mice on a mixed 129/C57BL/6 background were backcrossed greater than 3 generations to C57BL/6J mice from Charles River Laboratory. Mice carrying a microduplication of mouse chromosome 7qF3 re-derived on a C57/BL/6J background was acquired from Jackson Laboratory. All mice were group-housed on a 12 hour on/12 hour off light/dark cycle. All experiments were conducted in accordance with the rules and regulations of The Institutional Animal Care and Use Committee at MIT. During backcrossing 16p11.2 *df/+* mice we observed a steady decline in the percentage of heterozygous 16p11.2 *df/+* mice, indicating a non-Mendelian transmission of the 16p11.2 *df/+* allele. All experiments were performed by an experimenter blind to genotype and treatment.

4.5.2: Reagents

S-3,5-dihydrozyphenylglycine (S-DHPG) was purchased from Sigma-Aldrich. Aliquots of DHPG were prepared in H_2O as 100x stock (50 mM) and used within 7 days of preparation. Cycloheximide (CHX) was purchased from Sigma-Aldrich, prepared fresh in H_2O as 100x (60 mM) stock and used on the same day of preparation. CTEP, [2-chloro-4-((2,5-dimethyl-1-(4-(trifluoromethoxy)phenyl)-1H-imidazol-4-yl)ethynyl)pyridine], was synthesized at Hoffmann-La Roche, formulated as a micro-suspension prepared in 0.9% saline/0.3% Tween-80, and administered by oral gavage at a dose of 2 mg/kg. R-baclofen, a gift from the Simon's foundation, was dissolved at 0.5 mg/ml in drinking water acquired from the animal facility daily in regular water bottles. Dissolving required mild heating and water was cooled to room temperature

before administration. Vehicle (drinking water) and R-baclofen treated water were given *ad libitum* and changed daily for the duration of the experiment.

4.5.3: Hippocampal electrophysiology

Electrophysiological experiments were performed at the Schaffer collateral-CA1 synapse of dorsal hippocampal slices (400 μm thick) prepared from p28-35 male mice using experimental protocols previously described(Auerbach, Osterweil et al. 2011). Input-output functions were determined by incrementally (10 μA to 100 μA) stimulating the Schaffer collaterals and recording the resulting fEPSP response. Paired-pulse facilitation was conducted by applying two stimulus pulses (stimulus 1 and 2) at varying inter-stimulus-intervals (Sidorov, Krueger et al.). Facilitation was measured by taking the ratio of the fEPSP slope in response to stimulus 2 to that of stimulus 1. Long-term potentiation (LTP) was induced using theta-burst stimulation (TBS) delivered in two trains with a 30 sec interval. Each train was composed of 50 ms bursts of stimuli (100 Hz) delivered at 5 Hz for 1 sec. NMDA receptor dependent long-term depression (LTD) was elicited with low-frequency stimulation (LFS) comprised of 900 pulses at 1 Hz. For DHPG-LTD, slices were incubated in artificial cerebrospinal fluid (aCSF) in the presence or absence of the protein synthesis inhibitor cycloheximide (± CHX, 60 μM, 40 min), and $mGlu_5$ was activated by bath application of DHPG (50 μM, 5 min). Synaptic responses were followed for an additional 60 min following DHPG application. Paired pulse facilitation was assessed 30 min prior to, and 60 min following DHPG application in all slices used in DHPG-LTD experiments (see Figure 4.2C, D). For paired-pulse low frequency stimulation (PP-LFS), slices were incubated in aCSF containing APV (50 μM) ± CHX for 30 min mGluR-LTD was then induced by application of 1200 paired-pulse stimulation (50 ms ISI) at 1Hz, and synaptic responses were recorded for an additional 60 min in the presence of APV. Statistical significance was determined using repeated measures two-way ANOVA and *post hoc* Bonferroni tests.

4.5.4: Contextual discrimination task

Context discrimination was performed in a Freezeframe Chamber (Coulbourn Instrument) as previously described (Ehninger, Han et al. 2008, Auerbach, Osterweil et al. 2011). Briefly, 6 to 12 week-old wildtype and 16p11.2 *df/+* male mice were fear conditioned on day 1 and the subsequent percentage of time spent freezing in either the familiar or a novel context was determined 24 hr later. On the day of conditioning, animals were allowed to explore the behavioral chamber for 3 min, followed by delivery of a 2 sec, 0.8 mA foot-shock. Mice remained in the context for 15 sec after the shock before returning to their home cages. Fear response was assessed 24 hr later. To determine context specificity of the conditioned response, mice trained on day 1 were separated into two groups on day 2: one group was tested in the same training context (familiar context), and the other tested in a novel context. The novel context was created by varying spatial cues, floor material, and lighting of the testing chamber. The percentage of time a mouse spent freezing during a testing session of 4 min on day 2 was the behavioral readout. To determine if WT and 16p11.2 *df/+* mice had the same sensitivity to foot-shock, the distance traveled by each subject during the 2 sec foot-shock and 1 sec immediately following was recorded. Statistical significance was determined using repeated measures two-way ANOVA and *post hoc* Student's t-tests.

4.5.5: Inhibitory avoidance extinction

Inhibitory avoidance tests were performed with a passive avoidance apparatus (Ugo Basile Passive Avoidance Apparatus, Step-through model for mouse) as previously described with modification (Dolen, Osterweil et al. 2007). In all IA tests, a mouse was subjected to one training session (0 hr) and three subsequent testing sessions (6, 24 and 48 hr). In each session, a mouse was first placed in a LED-illuminated "START" compartment of a two-compartment test apparatus for 30 sec prior to the partition door opening. Upon entering the dark compartment the door was closed immediately. The subject remained in the dark compartment for 60 sec before being taken out. During the training session, a 2 sec foot-shock of 0.4 mA was delivered. No shock was delivered in the three testing sessions. The latency to enter the dark compartment was recorded to assess baseline level (0 hr), acquisition of fear memory (6 hr), and memory extinction

(24 hr and 48 hr). Male mice 6-10 weeks of age were used in IA tests without drug treatment. In IA tests with CTEP treatment, 4-6 week old male mice were divided into four groups according to genotype (WT or 16p11.2 *df/+*) and drug treatment (vehicle or CTEP). Administration of vehicle or CTEP (2 mg/kg) was initiated at the age of 4-6 weeks, given as one dose every 48 hr by oral gavage, and continued for 4 weeks prior to IA testing by an experimenter blind to both genotype and drug condition. Statistical significance was determined using repeated measures two-way ANOVA and *post hoc* Student's t-tests.

4.5.6: Metabolic labeling

Metabolic labeling of new protein synthesis was performed as previously described (Osterweil et al. 2010). Male P28-P32 littermate WT and 16p11.2 *df+/-* mice were anesthetized with isoflurane and the hippocampus was rapidly dissected into ice-cold artificial cerebral spinal fluid (aCSF) (in mM: 124 NaCl, 3 KCl, 1.25 NaH_2PO_4, 26 $NaHCO_3$, 10 dextrose, 1 $MgCl_2$, 2 $CaCl_2$, saturated with 95% O_2 and 5% CO_2). Hippocampal slices (500 μM) were prepared using a Stoelting Tissue Slicer and transferred into 32.5°C aCSF (saturated with 95% O_2 and 5% CO_2) within 5 min. Slices were incubated in aCSF undisturbed for 3.5–4 h to allow for recovery of basal protein synthesis (Sajikumar et al., 2005, Osterweil et al., 2010). Actinomycin D (25μM) was then added to the recovery chamber for 30 min to inhibit transcription after which slices were transferred to fresh aCSF containing ~10 mCi/ml [^{35}S] Met/Cys (Perkin Elmer) for another 30 min. Vehicle (DMSO) or R-baclofen (10 μM) treated slices were incubated in vehicle or drug 30 minutes prior to the addition of Actinomycin D and remained in vehicle or drug for the duration of the experiment. Slices were then homogenized, and labeled proteins isolated by TCA precipitation. Samples were read with a scintillation counter and subjected to a protein concentration assay (Bio-Rad). Data was analyzed as counts per minute per microgram of protein, normalized to the [^{35}S] Met/Cys aCSF used for incubation and the average incorporation of all samples analyzed and then normalized to percent WT for each experiment.

4.5.7: Immunoblotting

Tissue for immunoblotting was harvested from slices used in metabolic labeling as well as gross dissection of the hippocampus, visual cortex, and frontal cortex of animals chronically treated with vehicle or R-baclofen. Immunoblotting was performed according to established methods using primary antibodies to ARC (Osterweil, Krueger et al.), p-ERK1/2 (Thr202/Tyr204) (Cell Signaling Technology), ERK1/2 (Cell Signaling Technology), MVP (Abcam), and cFOS (Cell Signaling Technology). ARC, cFOS, MVP, ERK1 and ERK2, as well as ERK1 and ERK2 phosphorylation were measured by densitometry (Quantity One), and quantified as the densitometric signal of each protein divided by the total protein signal (determined by Memcode staining) in the same lane. Statistical significance was determined using unpaired Student's two-way t tests.

4.5.8: Open field habituation

Open field habituation task was performed in a 40 cm x 40 cm x 40 cm box during 2 x 15 minute habituation sessions, spaced 1-2 hours apart. Animals at 8-12 weeks of age were placed in the behavior box and allowed to explore freely for each habituation session. Sessions were recorded and locomotor activity was tracked using Plexon's *CinePlex*® Studio and analyzed using Plexon's *CinePlex*® Editor and code written in MATLAB. For analysis, the box was divided into three zones: a "center" zone (containing the inner 20 x 20 cm center square), an "outer" zone (the outermost area 5 cm from the walls) and a "middle" zone (the 5 cm thick space between the center and outer zones). The center and middle zones were pooled to become the "inner" zone for some analyses. Total distance traveled was computed as the sum of distance covered over the course of each habituation session. Statistical significance was determined using Student's two-way t tests for each comparison.

4.5.9: Object recognition

Object recognition task was adapted from experiments previously described (Leger, Quiedeville et al. 2013). Animals at 8-12 weeks of age were habituated to a 40 cm x 40 cm x 40 cm box during 2 x 15 min sessions, spaced 1-2 hours apart. Animals were

returned to their home cage in between session. 24 hours post habituation animals were exposed to two identical objects for 2 x 10 min exploration sessions in the same box, spaced 1-2 hours apart. Animals were required to explore each object for at least 10 seconds (for a total of at least 20 seconds) in the first session to be included in the subsequent sessions. 24 hours post object exploration, one object was replaced with a novel object and the animals were allowed to explore the objects for 10 minutes. Time spent exploring was recording during this exploration period and was characterized by sniffing within 2 cm of each object or directly touching the objects. Time spent climbing or on top of the objects was not included. Familiar and novel object and side placement was randomly assigned, by animal. Discrimination index was calculated as [(time spent exploring novel object) / (time spent exploring novel object + time spent exploring familiar object)].

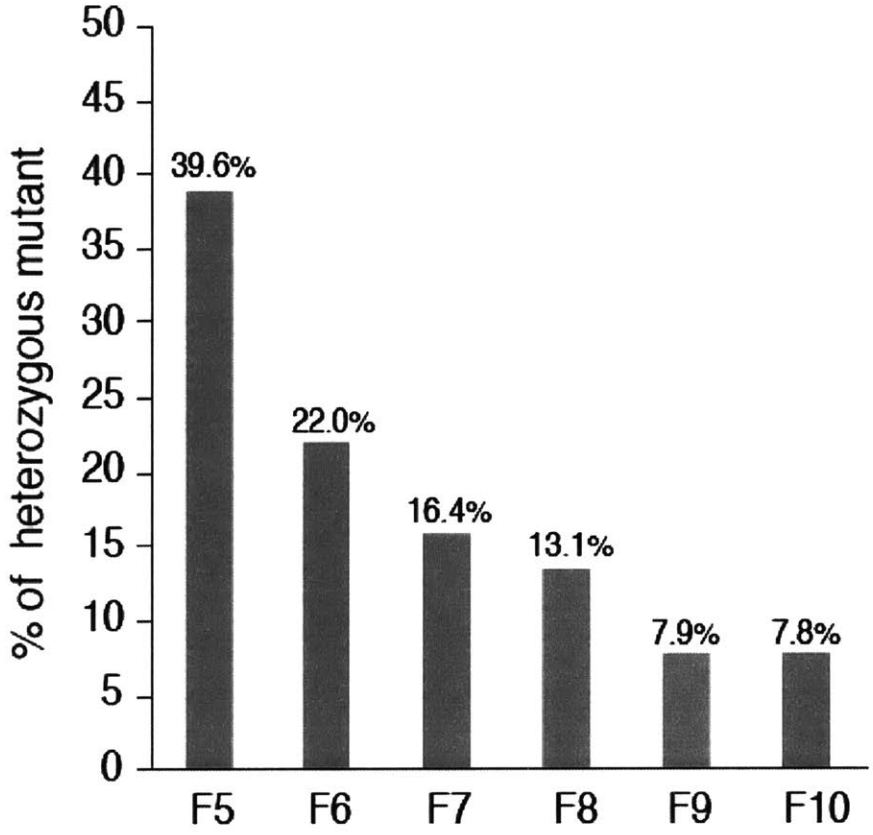

Figure 4.1: Steady decline of transmission rate of the 16p11.2 *df/+* allele.

The percentage of the heterozygous 16p11.2 *df/+* mutant mice, including both male and female, gradually declines across multiple generations during backcrossing to C57BL/6J. The number of positive and total mice for each generation are: F5: 21/53, F6: 26/118, F7: 41/250, F8: 57/434, F9:16/202, and F10: 8/102. (Data tracked and analyzed by Di Tian).

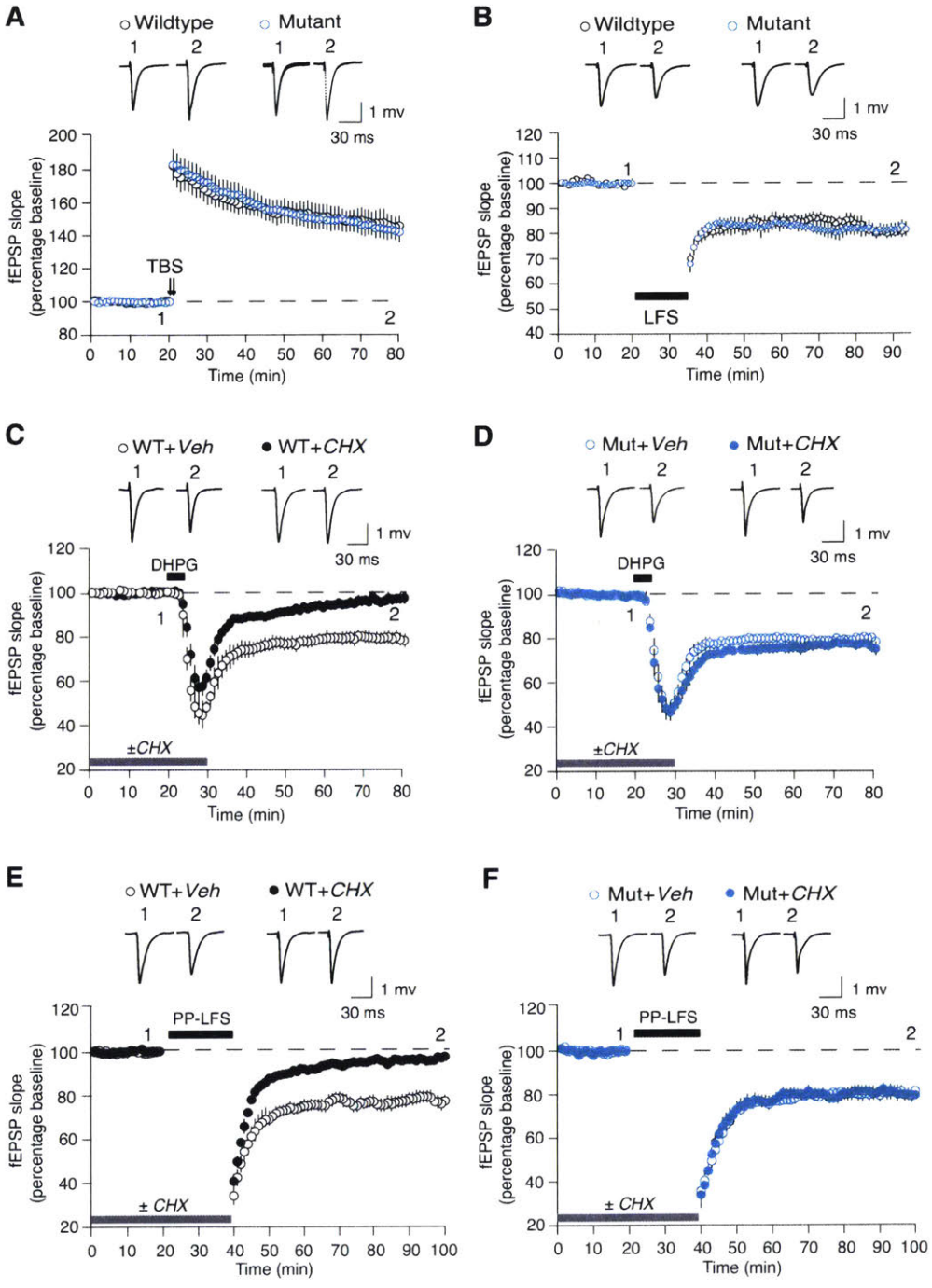

Figure 4.2: mGluR-LTD is protein synthesis independent in 16p11.2 *df/+* mice.

(**A**) TBS-LTP is unchanged in the 16p11.2 *df/+* (n = 9 animals, 17 slices) as compared

with WT (n =10 animals, 19 slices) mice. (**B**) LFS-LTD remains unchanged in 16p11.2 *df/+* (n = 7 animals, 13 slices) as compared with WT (n = 9 animals, 15 slices) mice. (**C, D**) The magnitude of DHPG-LTD is comparable in hippocampal slices from the WT (WT, n = 17 animals, 23 slices) and 9 16p11.2 *df/+* (16p11.2 *df/+*, n = 17 animals, 26 slices) mice in the absence of CHX. However, CHX blocks DHPG-LTD in WT (WT, n = 17 animals, 25 slices) but not 16p11.2 *df/+* slices (16p11.2 *df/+*, n = 17 animals, 23 slices) (Two-way ANOVA, genotype x CHX, p = 0.0074). (**E, F**) The magnitude of PP-LFS-LTD is comparable in hippocampal slices from the WT (n = 12 animals, 17 slices) and 16p11.2 *df/+* (n = 7 animals, 12 slices) mice in the absence of CHX. CHX significantly attenuates PP-LFS-LTD in the WT (WT, n = 12 animals, 15 slices) but not 16p11.2 *df/+* slices (16p11.2 *df/+*, n = 7 animals, 15 slices) (Two-way ANOVA, genotype x CHX, p = 0.013). Representative fEPSP traces (average of 10 sweeps) were taken at the times indicated by numerals. All data are plotted as mean ± SEM. (Experiments conducted by Di Tian)

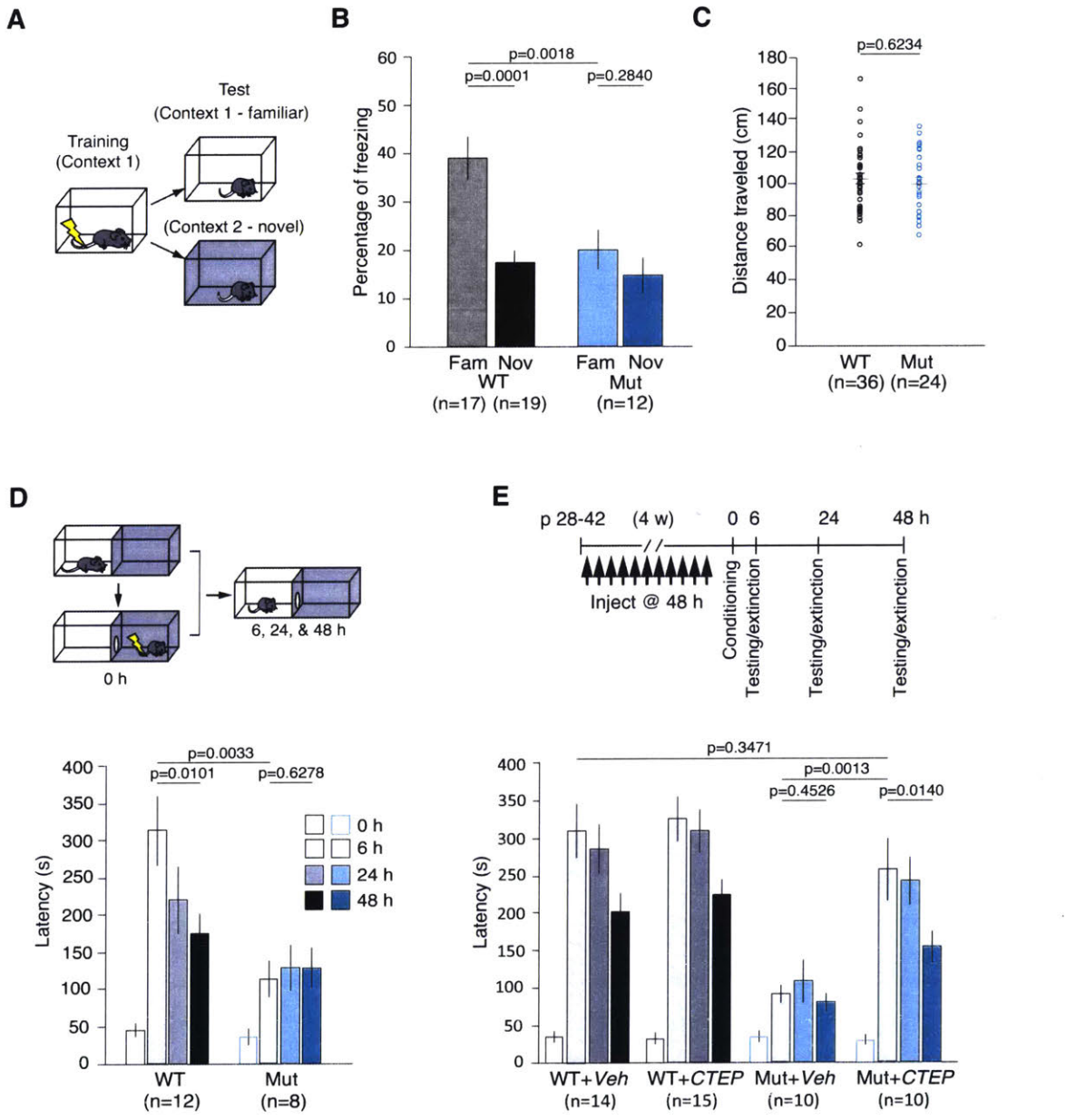

Figure 4.3: 16p11.2 *df/+* mice exhibit deficits in hippocampal-associated context discrimination task and inhibitory avoidance (IA).

(**A**) Context discrimination task experimental design. (**B**) 16p11.2 *df/+* mice show significantly less freezing in the familiar context compared with WT (unpaired t-test, p = 0.0018). While WT mice are able to distinguish a novel from familiar context (unpaired t-test, p < 0.0001), the 16p11.2 *df/+* mice are impaired (unpaired t-test, p = 0.284). Two-way ANOVA, genotype x context, p = 0.0193. (**C**) 16p11.2 *df/+* and WT mice have the

same running response to foot-shock during the training session (unpaired t-test, p = 0.92). (**D**) 16p11.2 *df/+* mice are impaired in IA acquisition (WT vs 16p11.2 *df/+*, 0 hr vs 6 hr, repeated measures two-way ANOVA, p = 0.0108; WT vs 16p11.2 *df/+* at 6 hr, post-hoc Student's t-test, p = 0.0033). Unlike WT (WT, 6 hr vs 48 hr, post-hoc paired t-test, p = 0.0101), the 16p11.2 *df/+* mice show no extinction of fear memory (WT vs 16p11.2 *df/+*, 6 hr vs 48 hr, repeated measures two-way ANOVA, p = 0.0197; 16p11.2 *df/+*, 6 hr vs 48 hr, post-hoc paired t-test, p = 0.6278). (**E**) CTEP treatment ameliorates behavioral deficits in 16p11.2 *df/+* mice in IA. In 16p11.2 *df/+* mice, CTEP treatment enhances acquisition (16p11.2 *df/+* +Veh vs 16p11.2 *df/+* + CTEP, 0 hr vs 6 hr, repeated measures two-way ANOVA, p = 0.0011; 16p11.2 *df/+* +Veh vs 16p11.2 *df/+* + CTEP at 6 hr, post-hoc paired t-test, p = 0.0013) and extinction of fear memory (16p11.2 *df/+* + Veh vs 16p11.2 *df/+* + CTEP, 6 hr vs 48 hr, repeated measures two-way ANOVA, p = 0.0016; 16p11.2 *df/+* + Veh, 6 hr vs 48 hr, post-hoc paired t-test, p = 0.4281; 16p11.2 *df/+*+CTEP, 6 hr vs 48 hr, post-hoc paired t-test, p = 0.014). There is no statistically significant difference between WT + Veh and 16p11.2 *df/+* + CTEP at 6 hr (unpaired t=test, p = 0.6088). In WT mice, CTEP has no effect on either acquisition (WT + Veh vs. WT+CTEP, 0 hr vs. 6 hr, repeated measures two-way ANOVA, p = 0.6564) or extinction of fear memory (WT + Veh vs. WT+CTEP, 6 hr vs. 48 hr, repeated measures two-way ANOVA, p = 0.9882). All data are plotted as mean ± SEM. (Experiments conducted by Di Tian and Arnold Heynen)

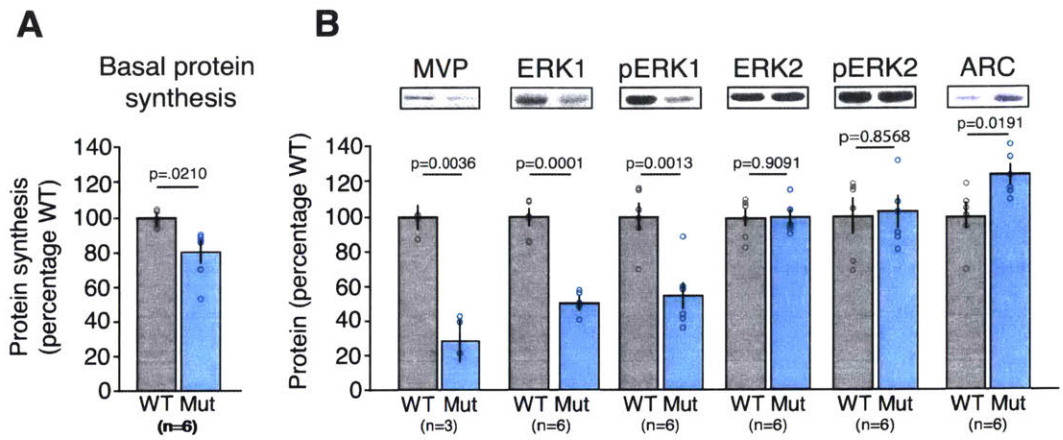

Figure 4.4: 16p11.2 *df/+* mice exhibit a decrease in basal protein synthesis, which is accompanied by an increase in Arc protein levels.

(**A**) Metabolic labeling of hippocampal slices reveals a significant reduction of basal protein synthesis in 16p11.2 *df/+* as compared to WT mice. (**B**) MVP, ERK1 and pERK1 are decreased in 16p11.2 *df/+* mice as compared to WT mice, whereas ERK2 and pERK2 levels are comparable between 16p11.2 *df/+* and WT mice. Arc protein levels are significantly increased in 16p11.2 *df/+* mice as compared to WT mice. All data are plotted as mean ± SEM; n indicates number of animals.

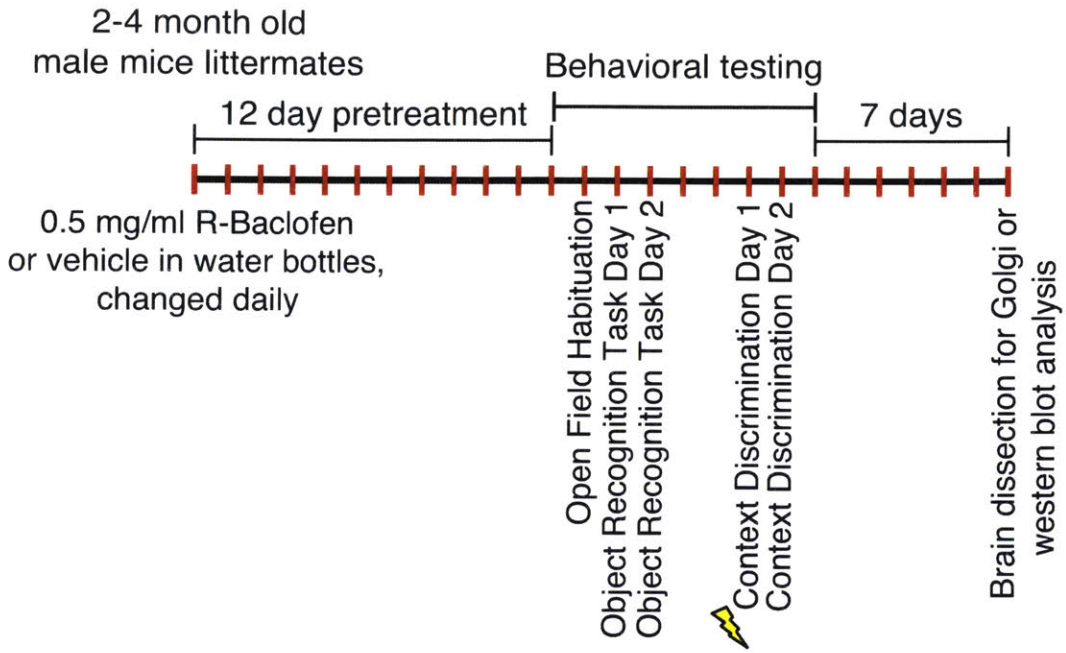

Figure 4.5: R-baclofen treatment schedule and behavioral test battery timeline.

Schematic illustrates experimental timeline. WT and 16p11.2 *df/+* group-housed male littermate animals 8-16 weeks of age were treated for 12 days prior to testing with either vehicle (drinking water) or 0.5 mg/mL R-baclofen in standard issue water bottles obtained from the animal facility, changed daily. Animals were run through a battery of behavioral tests, beginning with open field habituation, an object recognition task, followed by a context discrimination task. Open completion of the behavioral battery, animals received 7 more days of vehicle or drug prior to euthanasia. Brains were extracted after 7 days and one hemisphere was Golgi stained while the other hemisphere was dissected and the hippocampus, visual cortex, and frontal cortex were saved for western blot analysis.

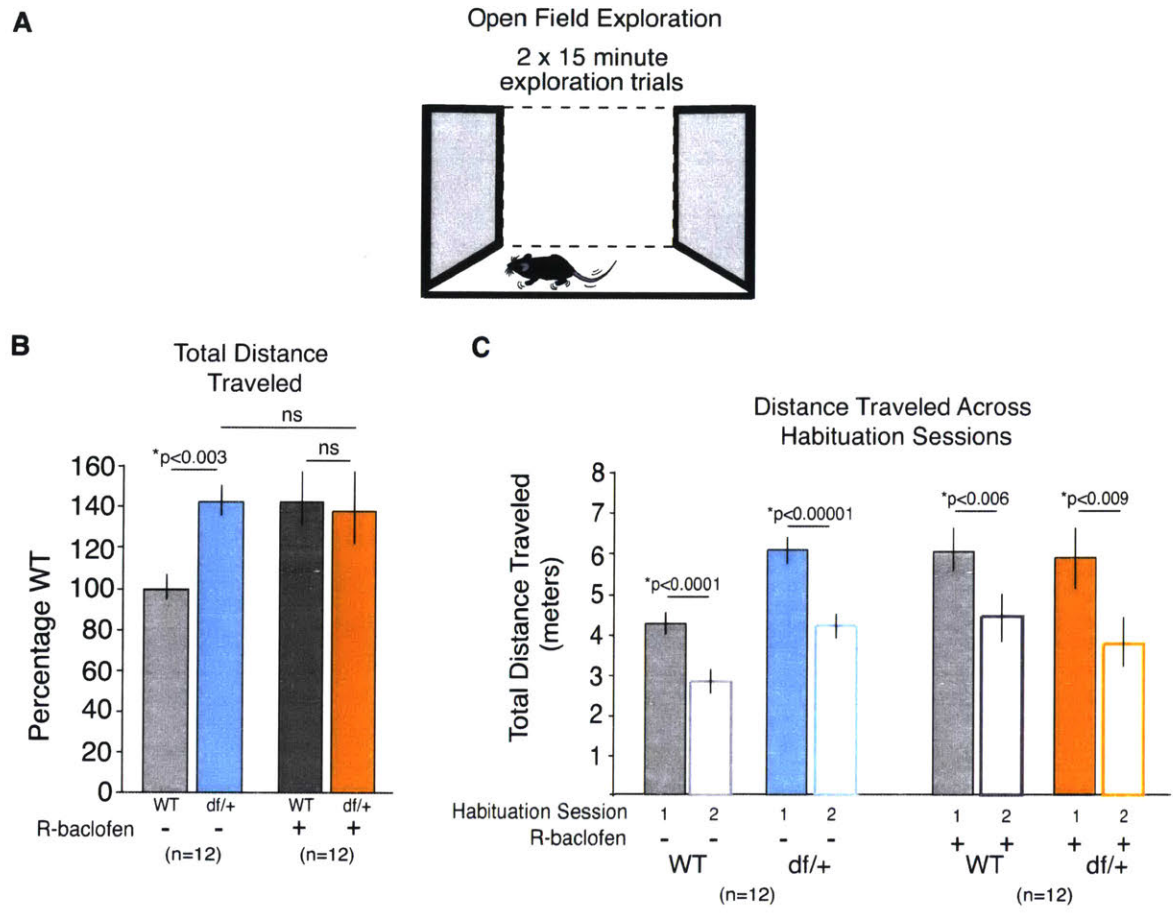

Figure 4.6: R-baclofen treatment does not reverse a hyperactivity phenotype in 16p11.2 *df/+* mice.

(**A**) Experimental design of open field habituation task. (**B**) 16p11.2 *df/+* mice treated with vehicle show statistically significant hyperactivity compared with WT animals treated with vehicle in the open field as indicated by distance traveled over the course of both habituation sessions (Student's two-way t-test, *$p < 0.003$). WT animals treated with R-baclofen show significantly increased locomotion compared with vehicle treated animals (*$p < 0.01$). There is no statistical significance between: 16p11.2 *df/+* animals treated with vehicle or R-baclofen ($p = 0.504$); WT animals treated with R-baclofen and 16p11.2 *df/+* animals treated with vehicle ($p = 0.992$) or WT animals and 16p11.2 *df/+* treated with R-baclofen ($p = 0.839$). (**C**) Across genotypes and treatments, animals travel a greater distance in the first habituation session compared with the second habituation session (Student's two-way t-tests, WT vehicle: *$p < 0.0001$; 16p11.2 *df/+* vehicle: *$p < 0.0001$; WT R-baclofen: *$p < 0.006$; 16p11.2 *df/+* R-baclofen: *$p < 0.009$). All data are plotted as mean ± SEM; n indicates number of animals.

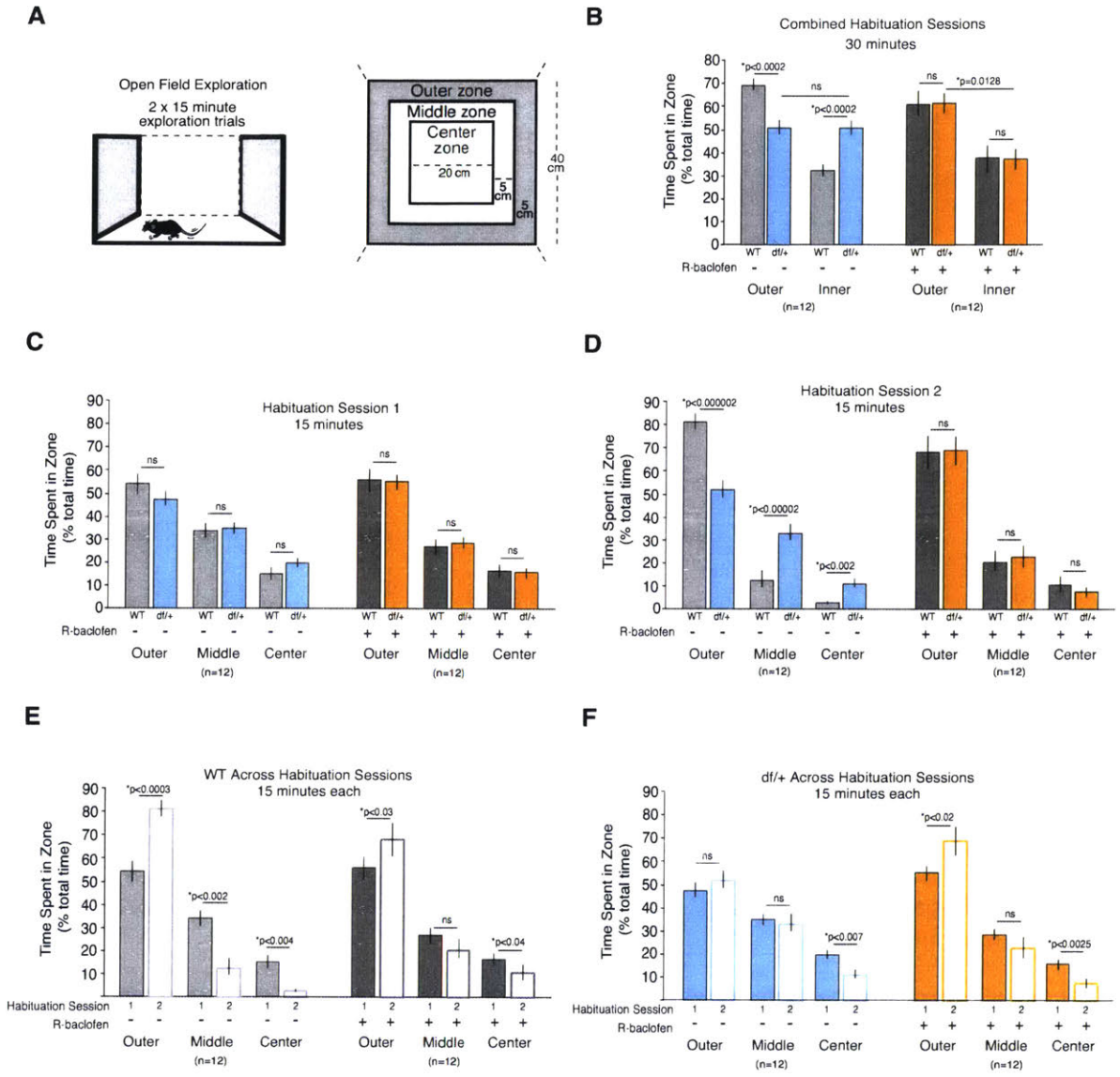

Figure 4.7: 16p11.2 *df/+* mice show habituation deficits in an open field task, which is reversed by chronic R-baclofen treatment.

(**A**) Experimental design of open field habituation task. (**B**) R-baclofen treatment restores preference for the outer zone in 16p11.2 *df/+* mice. Pooling both habituation sessions, 16p11.2 *df/+* mice treated with vehicle spend an equal time in the inner (center + middle) zone of the box whereas WT mice treated with vehicle spend significantly more time in the outer zone than the inner zone (Student's paired two-way t-tests; $p = 0.944$; $^*p < 0.0001$, respectively). In comparison, WT and 16p11.2 *df/+* mice treated with R-baclofen spend significantly more time in the outer zone than the inner zone (Student's paired two-way t-tests; $^*p < 0.007$; $^*p < 0.0001$, respectively). There is no significant difference between time spent in either the inner or the outer zone

between WT and 16p11.2 *df/+* mice treated with R-baclofen ($p = 0.984$; $p = 0.981$, respectively). (**C**) WT and 16p11.2 *df/+* mice exhibit similar zone exploration during habituation session 1, regardless of treatment. (**D**) WT mice treated with vehicle spend significantly more time in the outer zone than 16p11.2 *df/+* mice during habituation session 2 and significantly less time in the middle and center zones (unpaired Student's t-tests, $*p < 0.000002$; $*p < 0.00002$; $*p < 0.002$, respectively). There is no significant difference between time spent in any zone (outer, middle, center) between WT and 16p11.2 *df/+* mice treated with R-baclofen (unpaired Student's t-tests, $p = 0.899$; $p = 0.728$; $p = 0.485$, respectively. (**E**, **F**) Shows the data in C and D plotted by genotype and treatment across habituation sessions. Figure emphasizes that 16p11.2 *df/+* mice treated with vehicle show little habituation to the environment across sessions 1 and 2. This apparent lack of habituation is restored to WT levels (WT habituation is unaffected by treatment) with R-baclofen administration.

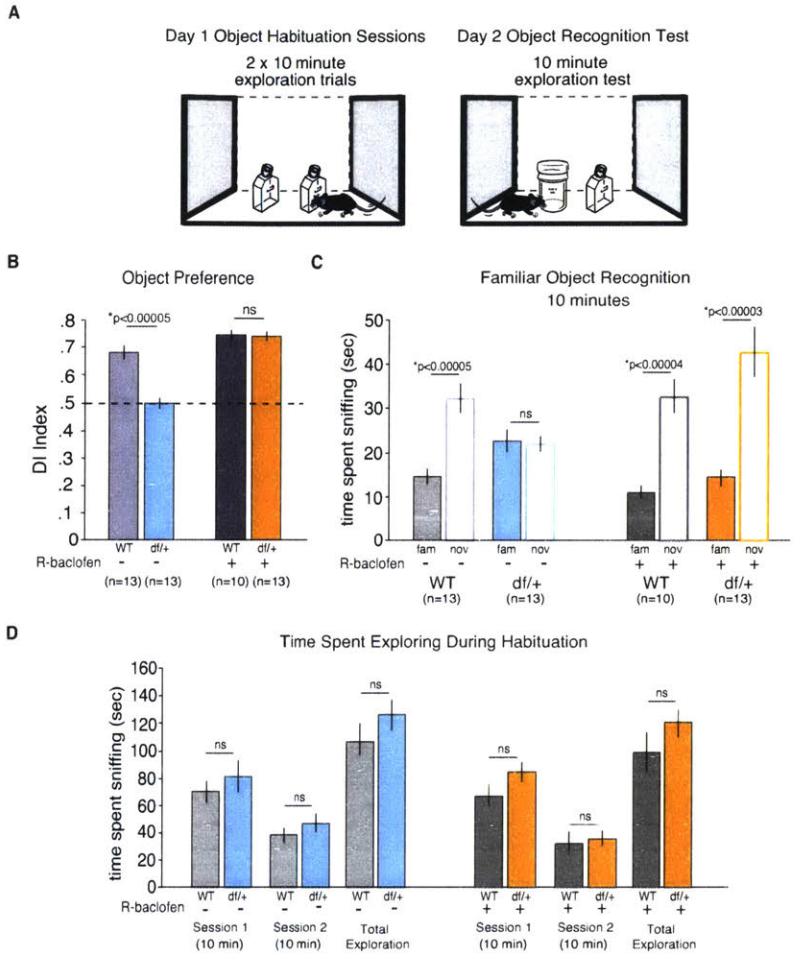

Figure 4.8: Chronic R-baclofen treatment restores novelty detection deficits in an object recognition task in 16p11.2 *df/+* mice.

(**A**) Experimental design of familiar object recognition task. (**B**) Vehicle treated 16p11.2 *df/+* mice show impaired novelty detection on experimental test day 2 when presented with a familiar and novel object compared to vehicle treated WT (*$p < 0.00005$). Chronic R-baclofen treatment restores novelty detection in 16p11.2 *df/+* mice, making them indistinguishable from WT mice (Student's two-tailed t-test; $p = 0.950$). (**C**) As depicted in (B), WT vehicle, WT R-baclofen, and 16p11.2 *df/+* R-baclofen treated mice show significantly more exploration of a novel object compared with a familiar object. In comparison, vehicle treated 16p11.2 *df/+* mice show no preference for the novel or familiar object, exploring each approximately equally. (**D**) There is no significant difference in time spent exploring each of two identical objects during the first object habituation session in either genotype regardless of treatment, nor is there any significant difference in total time spent exploring during either habituation session.

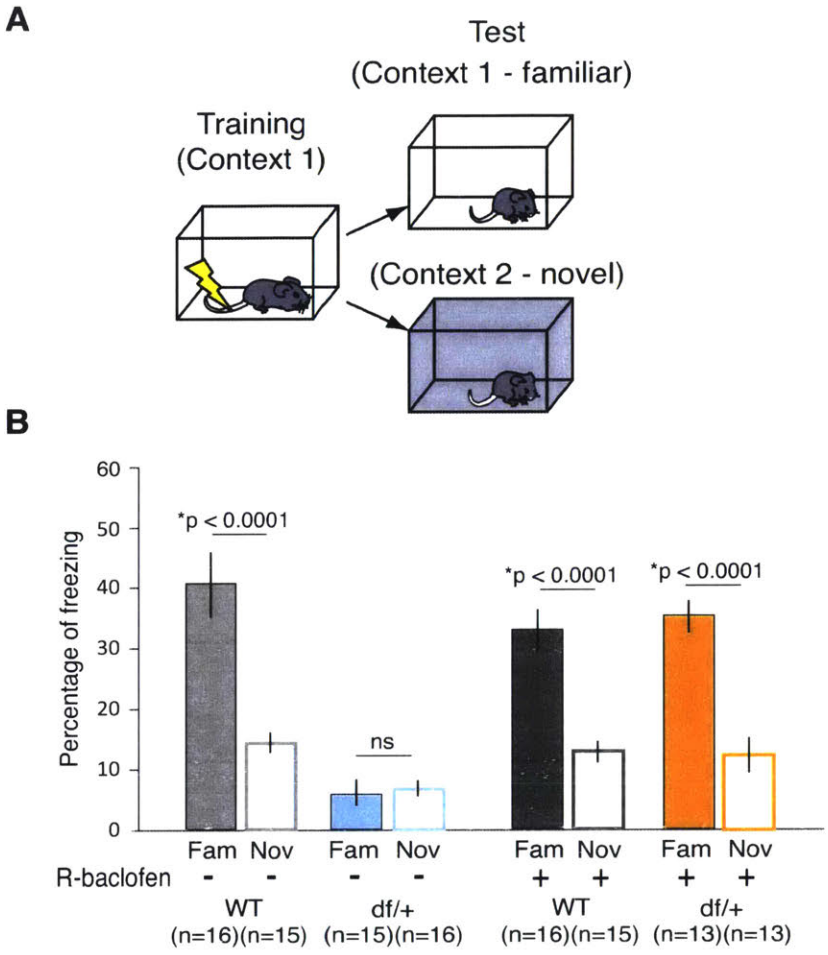

Figure 4.9: Chronic R-baclofen treatment restores memory deficits in a context-dependent aversive learning task in 16p11.2 *df/+* mice.

(**A**) Experimental design of context-dependent discrimination task. (**B**) Smiiar to what was previously found (Figure 4.3B), vehicle-treated 16p11.2 *df/+* mice show significantly less freezing in the familiar context compared with WT mice (unpaired two-tailed t-test, $p < 0.0001$). Vehicle and R-baclofen treated WT mice are able to distinguish a novel from familiar context (unpaired two-tailed t-test, $^*p < 0.0001$, $^*p < 0.0001$). Upon chronic treatment with R-baclofen, 16p11.2 *df/+* mice are able to distinguish a novel from familiar context as indicated by significantly increased freezing in the familiar context compared with novel context (unpaired two-tailed t-test, $p < 0.0001$). Two-way ANOVA, genotype x context, WT vehicle: $^*p < 0.001$; 16p11.2 *df/+* vehicle: $p = 0.885$; WT R-baclofen: $^*p < 0.001$; 16p11.2 *df/+* R-baclofen: $^*p < 0.001$.

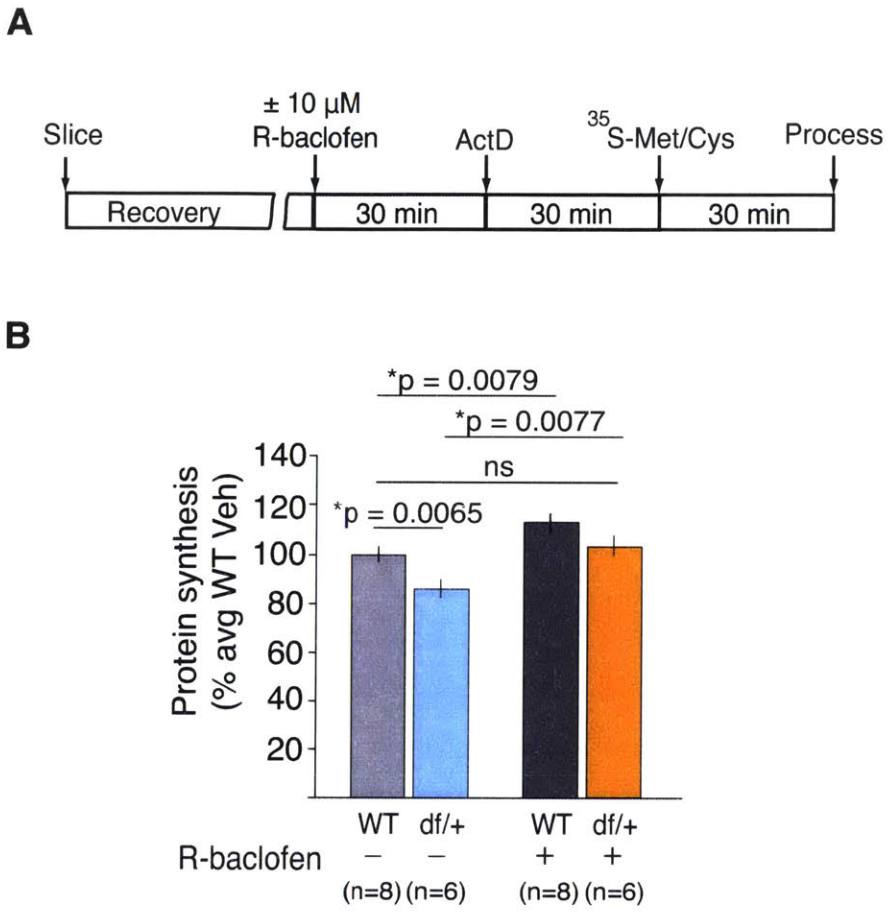

Figure 4.10: Deficient protein synthesis in 16p11.2 *df/+* mice is restored to WT levels by R-baclofen.

(**A**) Schematic illustrates experimental timeline. (**B**) Basal protein synthesis is significantly decreased in slices from 16p11.2 *df/+* mice (Student's two-way t-test; *p = 0.0065) compared with WT slices. Treatment with R-baclofen, a $GABA_B$ agonist significantly increases protein synthesis in both WT and 16p11.2 *df/+* mice (Student's two-way t-test WT + vehicle vs. WT + R-baclofen: *p = 0.0079; df vehicle vs. 16p11.2 *df/+* + R-baclofen: *p = 0.0077). There is no significant difference between rates of protein synthesis in WT slices treated with vehicle and 16p11.2 *df/+* slices treated with R-baclofen.

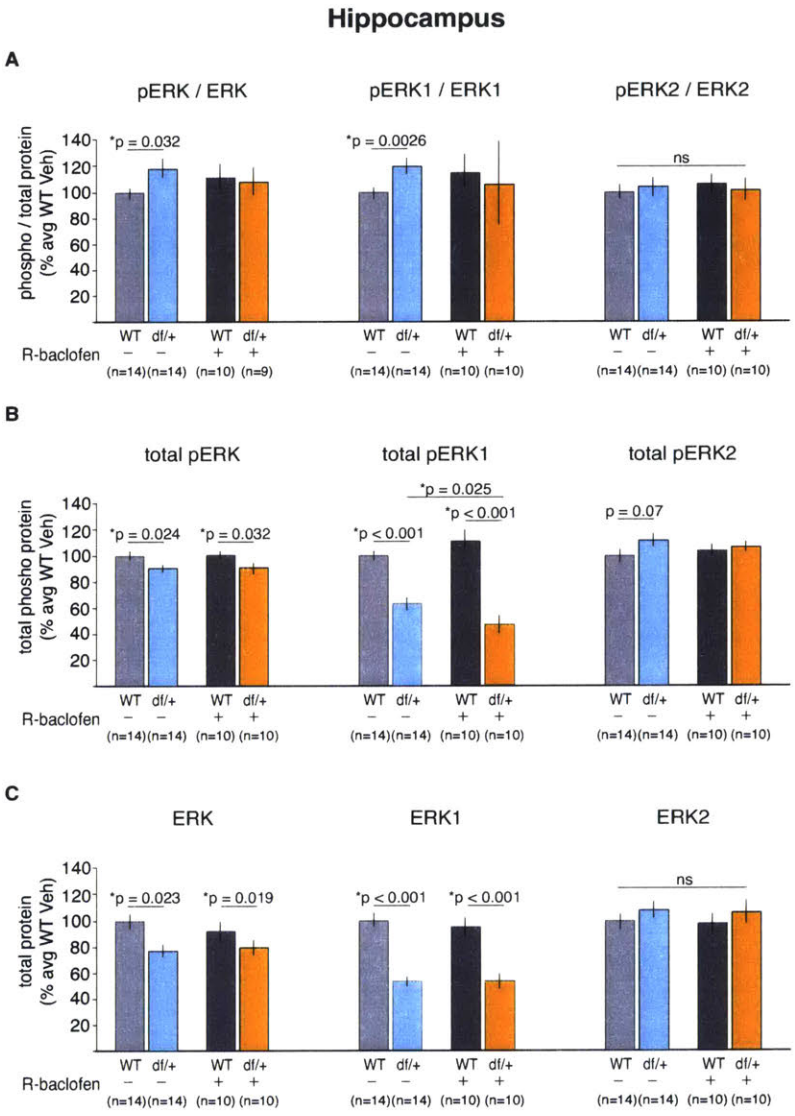

Figure 4.11: R-baclofen treatment does not affect ERK1/2 activation in the hippocampus.

Chronic R-baclofen treatment does not have an effect on ERK1, ERK2, or total ERK1/2 protein expression, or overall ERK activity in the hippocampus of WT and 16p11.2 *df/+* mice. Two-tailed ANOVAs fail to show significant interaction between genotype and treatment for any parameter measured, with the exception of total pERK1: (**A**) pERK/ERK: $p = 0.578$; pERK1/ERK1: $p = 0.941$; pERK2/ERK2: $p = 0.355$. (**B**) total pERK: $p = 0.315$; total pERK1: $p = 0.006$; total pERK2: $p = 0.589$. (**C**) total ERK: $p = 0.516$; total ERK1: $p = 0.313$; total ERK2: $p = 0.870$.

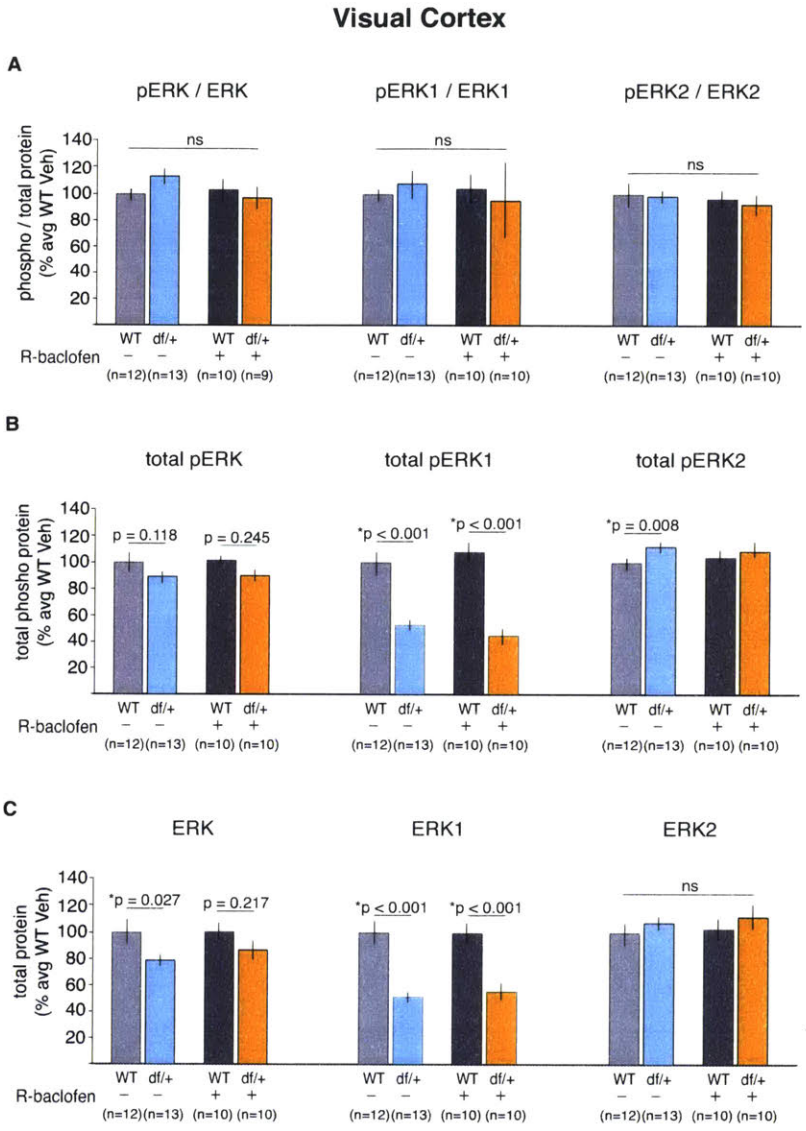

Figure 4.12: R-baclofen treatment does not affect ERK1/2 activation in visual cortex.

Chronic R-baclofen treatment does not have an effect on ERK1, ERK2, or total ERK1/2 activity or protein expression in the visual cortex of WT and 16p11.2 *df/+* mice. Two-tailed ANOVAs fail to show significant interaction between genotype and treatment for any parameter measured: (**A**) pERK/ERK: p = 0.180; pERK1/ERK1: p = 0.934; pERK2/ERK2: p = 0.545. (**B**) total pERK: p = 0.573; total pERK1: p = 0.222; total pERK2: p = 0.671. (**C**) total ERK: p = 0.840; total ERK1: p = 0.479; total ERK2: p = 0.971.

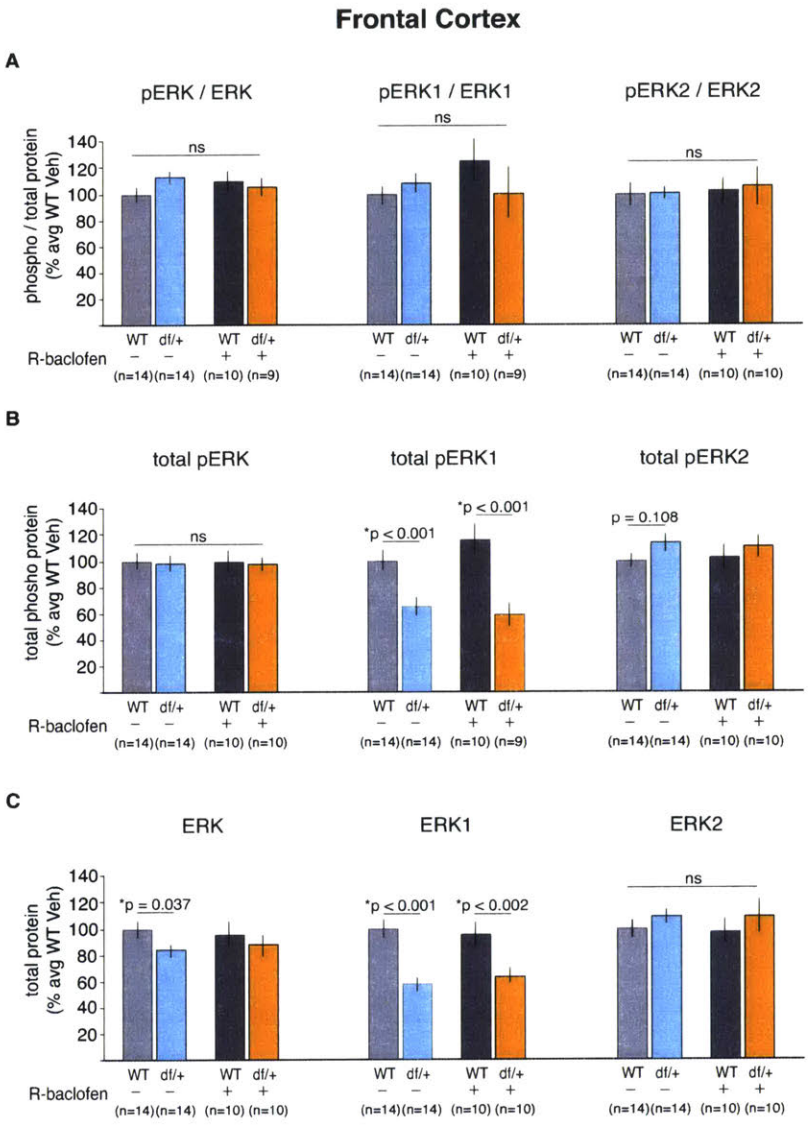

Figure 4.13: R-baclofen treatment does not affect ERK1/2 activation in frontal cortex.

Chronic R-baclofen treatment does not have an effect on ERK1, ERK2, or total ERK1/2 activity or protein expression in the frontal cortex of WT and 16p11.2 *df/+* mice. Two-tailed ANOVAs fail to show significant interaction between genotype and treatment for any parameter measured: (**A**) pERK/ERK: $p = 0.260$; pERK1/ERK1: $p = 0.900$; pERK2/ERK2: $p = 0.549$. (**B**) total pERK: $p = 0.189$; total pERK1: $p = 0.201$; total pERK2: $p = 0.413$. (**C**) total ERK: $p = 0.888$; total ERK1: $p = 0.708$; total ERK2: $p = 0.862$.

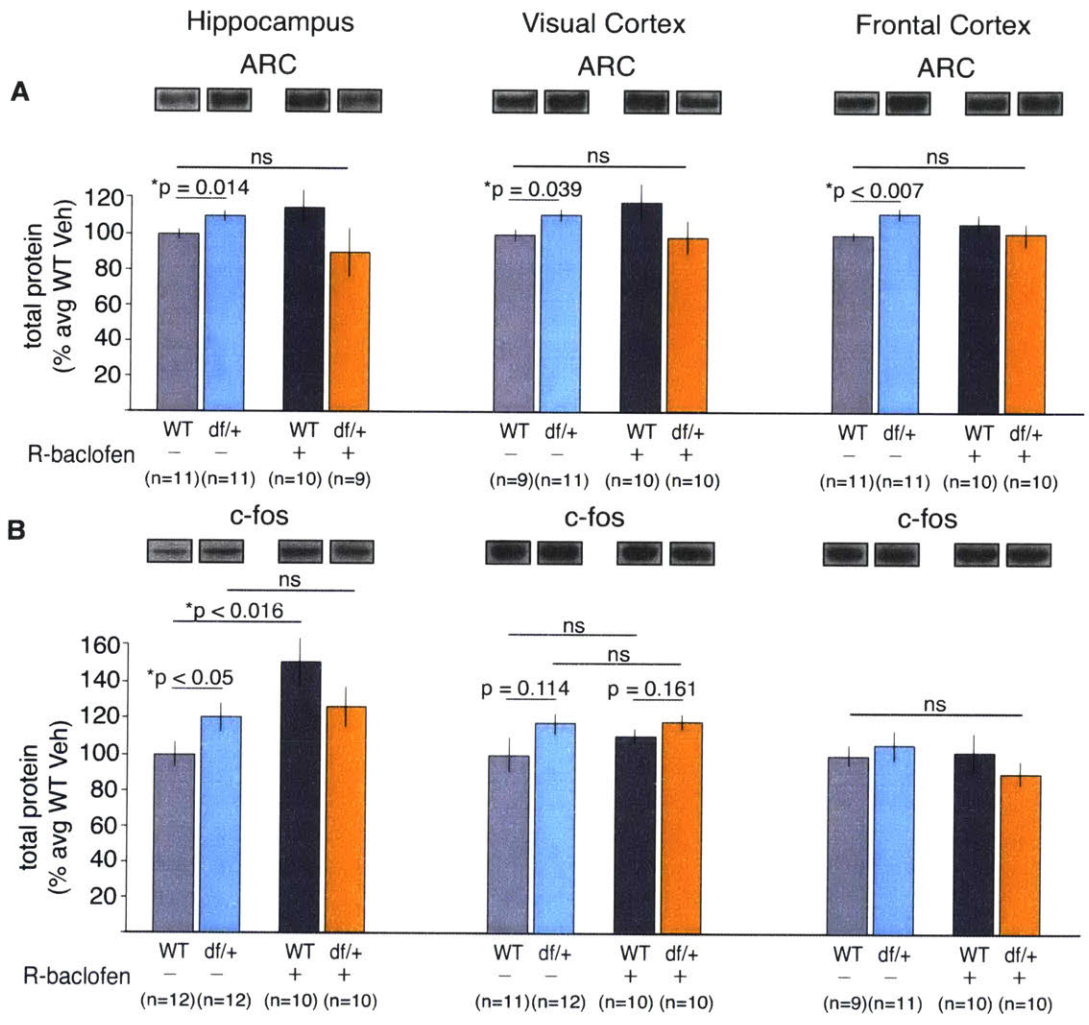

Figure 4.14: Arc is restored to WT levels in 16p11.2 *df/+* mice treated with R-baclofen.

(**A**) Arc is elevated in the hippocampus, visual cortex, and frontal cortex of vehicle treated 16p11.2 *df/+* mice compared with WT (Student's two-tailed t-test; *p = 0.014, *p = 0.039, *p < 0.007, respectively by region). Chronic R-baclofen administration led to an overall increase in Arc protein expression in WT yet a paradoxical decrease in 16p11.2 *df/+* mice to WT-vehicle-treated levels. Two-tailed ANOVA for genotype and treatment: hippocampus- *p = 0.026; visual cortex- *p = 0.034; frontal cortex- *p = 0.044. (**B**) Changes in Arc protein expression do not appear to be a result of increased locomotor activity, as reflected by changes in c-fos expression. In the hippocampus, but not the visual cortex or frontal cortex, chronic R-baclofen treatment led to increased c-

fos expression in WT mice compared with vehicle (Student's two-tailed t-test; *p < 0.016), reflecting increased activity in these mice (Figure 4.6B). Vehicle and R-baclofen-treated 16p11.2 *df/+* mice express comparable levels of c-fos protein but elevated compared with vehicle-treated WT mice, reflecting baseline hyperactivity in these mice which is unaffected by R-baclofen treatment. Two-tailed ANOVA for genotype and treatment: hippocampus- *p = 0.021; visual cortex- *p = 0.454; frontal cortex- *p = 0. 282.

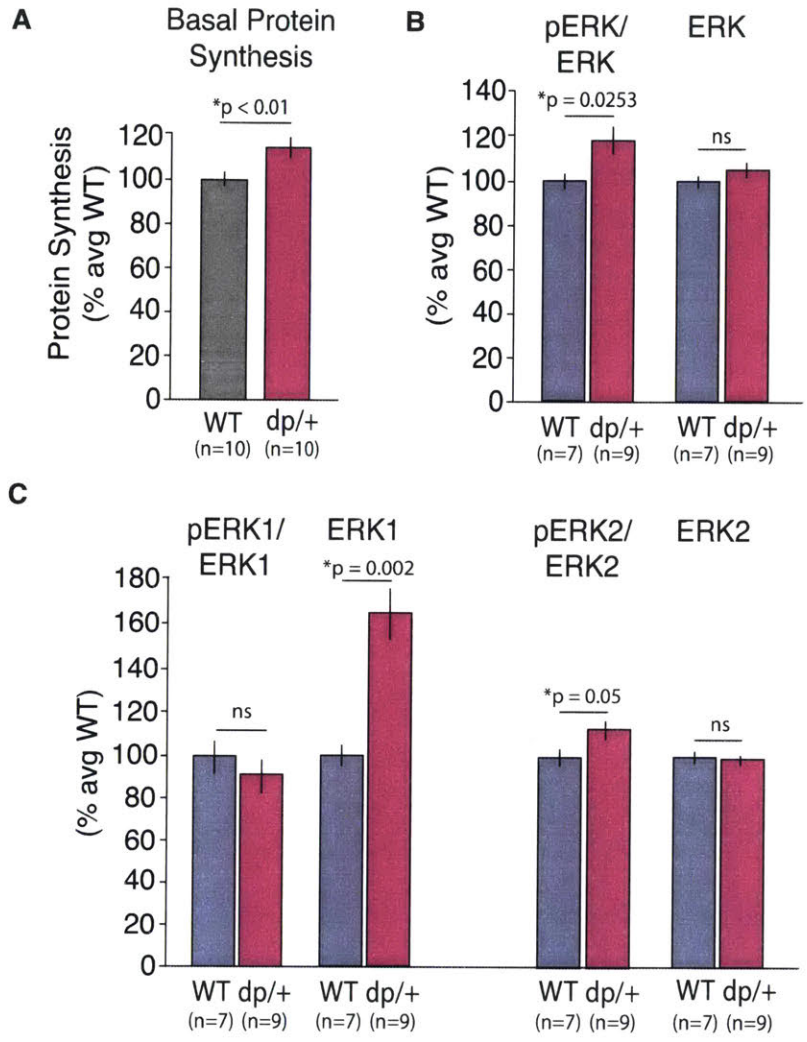

Figure 4.15: 16p11.2 *dp/+* mice have elevated basal hippocampal protein synthesis, elevated ERK1/2 phosphorylation and total ERK1 protein.

(**A**) Hippocampal slices from 16p11.2 *dp/+* mice show elevated basal protein synthesis compared to WT slices (Student's two-way t-test; *p < .01). (**B**) 16p11.2 *dp/+* mice show elevated phosphorylation of ERK1/2 but no significant different in total ERK1/2 levels (*p = 0.0253, p = .210, respectively). (**C**) 16p11.2 *dp/+* mice have significantly elevated levels of total ERK1 protein with no difference in ERK1 activation compared to WT slices (*p = 0.002, p = 0.398, respectively). There is elevated ERK2 activity in 16p11.2 *dp/+* slices compared to WT (*p = 0.05) but no difference in total ERK2 protein between WT and 16p11.2 *dp/+* slices (p = 0.516), likely accounting for the overactive ERK1/2 phosphorylation in (B).

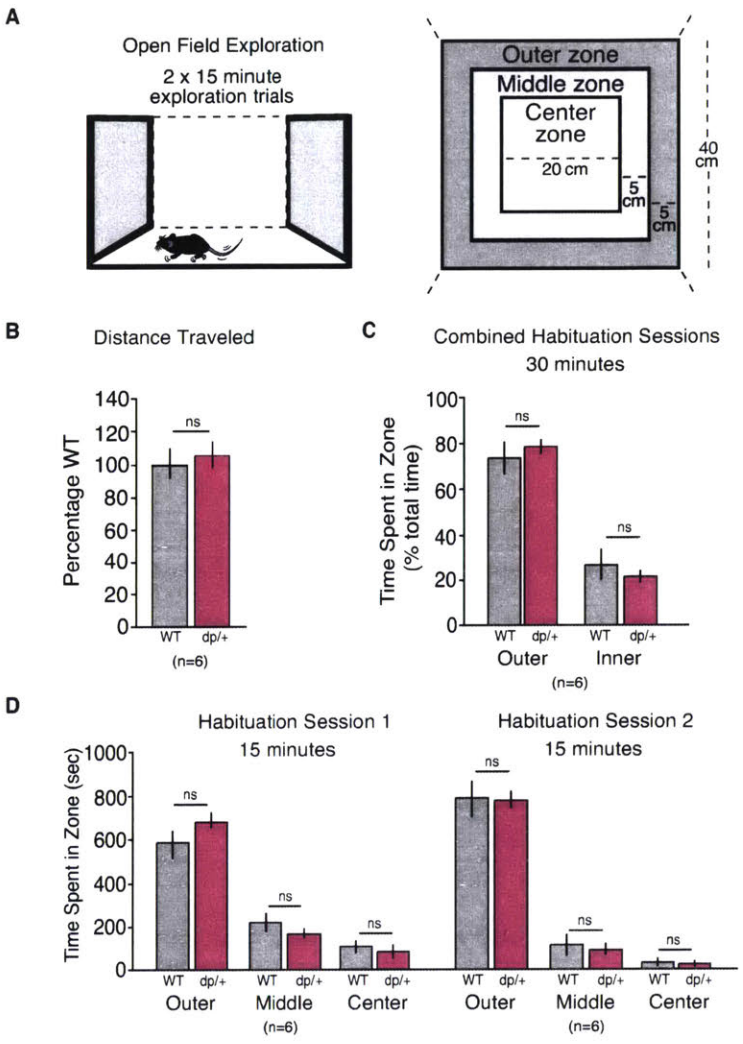

Figure 4.16: 16p11.2 *dp/+* mice show normal behavior in an open field.

(**A**) Experimental design of open field habituation task. (**B**) There is no difference in total distance traveled across sessions between WT and 16p11.2 *dp/+* mice (unpaired Student's two-way t-test; $p = 0.640$). (**C**) There is no difference in time spent in either the outer or inner (center and middle combined) zones of the arena between WT and *dp/+* mice ($p = 0.572$, $p = 0.453$, respectively), with both genotypes showing a strong preference for the outer zone over the inner zone (paired Student's t-test; $^*p = 0.0164$, $^*p < 0.0002$, respectively). (**D**) There is no significant difference between WT and 16p11.2 *dp/+* mice in any zone in either habituation session.

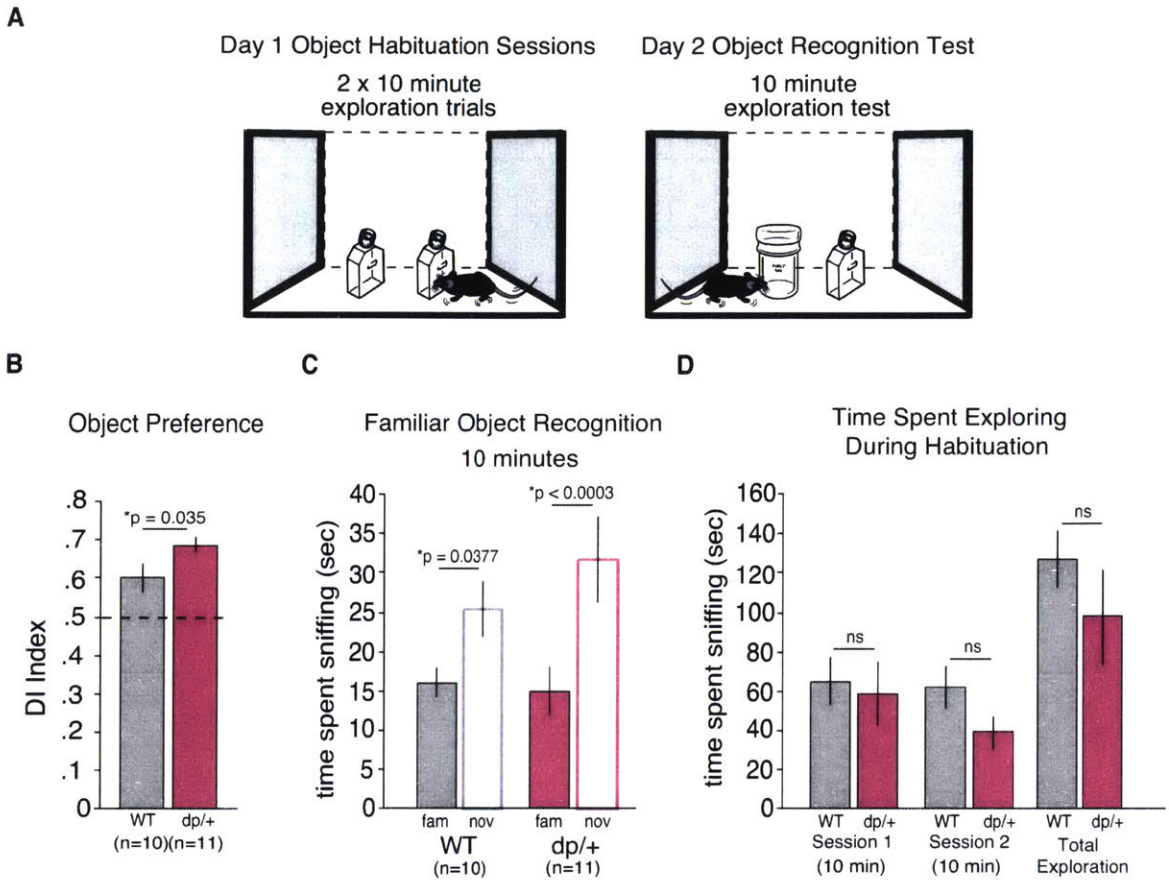

Figure 4.17: 16p11.2 *dp/+* mice show enhanced novelty detection in an object recognition task.

(**A**) Experimental design of Object Recognition task. (**B**) 16p11.2 *dp/+* mice show an enhanced preference for the novel object compared with WT mice (unpaired Student's two-way t-test; *p = 0.035). (**C**) Both WT and 16p11.2 *dp/+* mice spend more time exploring a novel object than a familiar object, which they were previously exposed to (paired Student's two-way t-test; *p = 0.0377; *p < 0.0003, respectively). (**D**) There is no difference in total exploration in any session, or combined across both habituation sessions between WT and 16p11.2 *dp/+* mice.

Chapter 5

Implications and Future Directions

5.1: Introduction

Our understanding of autism has evolved considerably since it was first hypothesized to be a consequence of emotional deprivation caused by negligent "refrigerator mothers" (Kanner and Eisenberg 1957). More than half a century later, an overwhelming breadth of evidence now supports the hypothesis that ASDs and intellectual disability (ID) are predominantly rooted in genetic perturbations, albeit heterogeneous in nature. Advancements in whole-genome sequencing have led to the identification of a diversity of monogenic and polygenic modifications that are known to confer risk for ASD and ID. One hypothesis, which has garnered a great deal of support from human brain transcriptome mapping studies, suggests that ASDs and ID may be a common consequence of disorders diverse in genetic origin but related in synaptic dysfunction. It is overly simplistic to assert that dysfunction downstream of $mGlu_5$ is *the* point of convergence shared amongst *all* genetic causes of ASD and ID. More likely, impaired $mGlu_5$ signaling may be one of many processes disrupted in these disorders. However, $mGlu_5$ is a known modulator of protein synthesis and synaptic plasticity at the synapse (Huber, Roder et al. 2001, Simonyi, Schachtman et al. 2005, Osterweil, Krueger et al. 2010) and has been implicated in the synaptic pathophysiology of many distinct monogenic and polygenic causes of ASDs and ID in mouse models (Dolen, Osterweil et al. 2007, Auerbach, Osterweil et al. 2011, Michalon, Sidorov et al. 2012, D'Antoni, Spatuzza et al. 2014, Pignatelli, Piccinin et al. 2014, Barnes, Wijetunge et al. 2015, Ebrahimi-Fakhari and Sahin 2015, Tian, Stoppel et al. 2015, Zantomio, Chana et al. 2015, Gogliotti, Senter et al. 2016). Therefore, we and others have hypothesized that restoring normal $mGlu_5$ signaling may be sufficient for correcting aberrant phenotypes known to be a consequence of altered synaptic translation in mouse models of disease (Bear, Huber et al. 2004). Indeed, studies of the *Fmr1* KO mouse have garnered overwhelming evidence supporting this postulation (Dolen, Osterweil et al. 2007, Michalon, Sidorov et al. 2012). Many others have investigated the efficacy of targeting other mediators of translation downstream of $mGlu_5$ signaling (see Chapter 1). These attempts have largely been met with great success. Despite the enormous body of evidence supporting modulation of $mGlu_5$ or downstream signaling pathways as

promising therapeutic avenues in the treatment of FX and other ASDs, outcomes from clinical trials have not been as optimistic. In this thesis, we have examined the possibility that refining the therapeutic target- to selectively modulate translation, while leaving other important cellular processes intact- may avoid dose-limiting adverse consequence associated with global inhibitors of $mGlu_5$. Although we have gathered significant evidence suggesting that these strategies may be more successful in minimizing unintended outcomes, a realistic possibility is that these approaches may present their own limitations. In this chapter, we consider the benefits of honing in on disease relevant targets in ASDs and ID and discuss potential limitations on translatability between mouse models of disease and human disorders.

5.2: At the heart of it all: troubled translation is a hallmark of FX and 16p11.2 CNVs.

When the mGluR theory of FX was first proposed, it was known that impairments in protein synthesis-dependent forms of plasticity at $mGlu_5$ were core to the synaptic pathophysiology of FX. Given the known role of FMRP as a translational repressor, it was assumed, although not yet confirmed, that synaptic protein synthesis would be altered in the mouse model of FX. Similarly, it was hypothesized that pathogenic phenotypes associated the *Fmr1* KO mouse, such a susceptibility to audiogenic seizures, were rooted in abnormal translation. Because the role of synaptic protein synthesis in the *Fmr1* KO mouse had not fully been explored, the mGluR theory of FX focused on modulating $mGlu_5$ rather than selectively targeting the signaling pathways specific to synaptic translation downstream of $mGlu_5$. As we begin to decipher how receptor activation is coupled to protein synthesis, we can now appreciate that activation of $mGlu_5$ catalyzes a variety of important cellular processes unrelated to synaptic translation, predominantly as result of G protein coupled signaling. As such, although global modulation of $mGlu_5$ may successfully restore normal translation, it could also lead to adverse modulation of processes that were not pathogenic in FX. In light of the wealth of knowledge uncovered over the past 12 years since the reveal of the mGluR theory of FX, it seems important to revise some of the details. In particular,

emphasis should be put on the notion that potential therapeutics for FX should specifically aim to restore normal translation of specific aberrantly expressed mRNAs known to be pathogenic in FX but leave other signaling arms downstream of $mGlu_5$ intact.

5.2.1 Treating troubled translation with β-arrestin2-biased negative allosteric modulation at $mGlu_5$.

In Chapter 2 we presented evidence suggesting that β-arrestin2 mediates the Ras-ERK signaling pathway that is coupled to translation at $mGlu_5$ and known to be pathogenic in FX. Importantly, a genetic reduction of β-arrestin2 in the *Fmr1* KO mouse restores normal rates of protein synthesis and corrects a number of pathological phenotypes associated with FX. Although our "proof of principle" approach did not allow us to evaluate the potential translatability of pharmacological reduction of β-arrestin2-biased signaling at $mGlu_5$ for FX, evidence indicates that receptor-specific "biased ligands" are feasible and well tolerated, thus far (Sheffler, Gregory et al. 2011, Iacovelli, Felicioni et al. 2014, Hathaway, Pshenichkin et al. 2015).

5.2.2 Treating troubled translation with GSK3α-selective inhibition.

In Chapter 3 we examined the selective involvement of both GSK3α and GSK3β independently in the *Fmr1* KO mouse. Previous evidence suggested that both GSK3α and GSK3β were overactive in the *Fmr1* KO mouse, although interestingly, GSK3α seemed to be altered in the mouse hippocampus (Yuskaitis, Mines et al. 2010). Conversely, only GSK3β has been identified as a target of FMRP (Darnell, Van Driesche et al. 2011). We found that GSK3α-specific inhibition but not GSK3β-specific inhibition alleviated many of the phenotypes associated with FX pathology. Exciting to us, and consistent with the "revised" mGluR theory of FX, selective inhibition of GSK3α abrogated excessive protein synthesis in the *Fmr1* KO mouse. Furthermore, we determined that cortical hyperexcitability, thought to be pathogenic to sensory hyperexcitability and thus hypersensitivity seen in both the *Fmr1* KO mouse and individuals with FX, is protein synthesis-dependent. Furthermore, hyperexcitability persists in the *Fmr1* KO mouse, even in the presence of protein synthesis inhibitors, consistent with similar observations in the protein synthesis-dependent form of synaptic

plasticity, mGluR-LTD. Evidence suggesting that selective inhibition of GSK3α is sufficient to correct protein synthesis-dependent phenotypes associated with the *Fmr1* KO mouse is groundbreaking. Therapeutics that inhibit GSK3, including lithium, have been plagued by dose-limiting toxicities driven by dual inhibition of both GSK3 paralogs. GSK3 plays integral cellular functions that are not involved in $mGlu_5$ signaling. GSK3 is a key regulatory kinase in the WNT pathway, and as such, a major concern in the clinical application of dual GSK3α/β inhibitors is potential oncogenic consequences due to dysregulation of β-catenin, a direct substrate of GSK3 phosphorylation (Gupta, Gulen et al. 2012, Lo Monte, Kramer et al. 2013, McCubrey, Steelman et al. 2014). Paralog-specific inhibition allows us to modulate only the paralog relevant to FX (GSK3α) while keeping WNT signaling and subsequent degradation of β-catenin by GSK3 intact (Doble, Patel et al. 2007). While our evaluation of the efficacy of these novel targets were limited to the *Fmr1* KO mouse model, we suspect they may have therapeutic potential in other mouse models of ASDs and ID characterized by similar perturbations in synaptic translation.

5.2.3: Troubled translation in other models of ASDs and ID: 16p11.2 CNVs.

Supporting the hypothesis that impaired translation at $mGlu_5$ could be a common hub of dysfunction in multiple distinct genetic causes of ID and ASDs, we found protein synthesis to be altered in both 16p11.2 *df/+* mice and 16p11.2 *dp/+* mice, models of 16p11.2 microdeletion and microduplication disorder, respectively, in humans. While 16p11.2 *dp/+* mice had elevated rates of protein synthesis, reminiscent of the *Fmr1* KO mouse (Dolen, Osterweil et al. 2007, Osterweil, Krueger et al. 2010), 16p11.2 *df/+* mice had deficient translation, more reminiscent of a mouse model of Tuberous Sclerosis (Auerbach, Osterweil et al. 2011). Despite this, 16p11.2 *df/+* mice exhibited significantly impaired cognition and hyperactivity, phenocopying *Fmr1* KO mice, while 16p11.2 *dp/+* mice showed remarkable performance on a cognitive assay, exhibiting enhanced novelty detection compared with their WT littermates. In support of this, chronic administration with the $mGlu_5$ NAM CTEP corrected impairments in a passive avoidance task in 16p11.2 *df/+* mice, consistent with similar observations in *Fmr1* KO mice treated with CTEP. Offering a hypothesis to explain this perplexity, we found Arc, an activity

regulated immediate early gene that is known to be important for changes in synaptic plasticity, to be upregulated in 16p11.2 *df/+* mice, despite deficient bulk protein synthesis. Furthermore, chronic application of the $GABA_B$ agonist R-baclofen corrected many cognitive and habituation impairments in 16p11.2 *df/+* mice which we believe may be attributed to restoration of physiological levels of Arc. This presents the possibility that convergence of synaptic dysfunction across multiple genetic models of disease may be more exquisite than initially expected. To this point, we may not be able to capture an accurate snapshot of dysfunction by examining gross changes in (for example) protein synthesis or synaptic plasticity. It may be necessary to examine protein or kinase-specific changes of targets (for example, the "plasticity protein" Arc) known to be imperative in important processes at the synapse.

5.2.4: The axis of troubled translation- bidirectional impairments with similar consequences.

It has been theorized that mutations defining syndromic autism define an axis of synaptic pathophysiology (Auerbach, Osterweil et al. 2011). In particular, this is based on the observation that two disorders that have reciprocal alterations in synaptic translation manifest similar cognitive and behavioral impairments. Indeed, investigation of a variety of mouse models of neuropsychiatric disease (including but not limited to FX, Tuberous Sclerosis, 16p11.2 CNVs, Rett Syndrome, Phelan McDermid Syndrome, and Syngap1 Syndrome) would all adequately fit on such an axis and support this notion. One caveat to this hypothesis, highlighted above in the discussion about convergence between FX and 16p11.2 CNVs is that global changes may be misleading. Based on the defective rate of protein synthesis in the 16p11.2 *df/+* mouse model, we would likely place this syndrome on the opposite side of the axis as FX. However, as previously discussed, we can appreciate that more likely, these two syndromes should be placed in the vicinity of each other, as they share a similar pathophysiology, likely due to parallel increases in Arc protein expression. Therefore, it may be more useful to re-define such an axis to reflect aberrations in expression of "plasticity proteins" known to be core to dysfunctional regulation of changes in synaptic strength in response to stimuli.

5.3: Do 'autistic' mice exist? The importance of semantics.

I have continually been reminded throughout my PhD that "there is no such thing as an autistic mouse. Mice don't have autism, people do." A consistent misnomer used liberally in the FX (and 16p11.2) animal model literature (and likely this thesis) is the claim that our studies investigate "mouse models of ASD". In order to receive a diagnosis of ASD, an individual must show (1) impairments in social communication, language, and related cognitive skills and behavioral and emotional regulation and (2) the presence of restricted, repetitive behaviors (Volkmar and Reichow 2013). The *Fmr1* KO mouse does exhibit behaviors that may be reminiscent of DSM-5 criterion (1) and (2). Consistent with criterion (1), *Fmr1* KO mice show impairments in social interaction (Spencer, Alekseyenko et al. 2005), deficient pup isolation-induced ultrasonic vocalizations (USVs) (Lai, Sobala-Drozdowski et al. 2014), and deficient behavior in a resident-intruder assay of social aggression (Mineur, Huynh et al. 2006). Others have found that, consistent with criterion (2), the *Fmr1* KO mouse shows increased repetitive behavior in a marble burying assay (Spencer, Alekseyenko et al. 2011). We did not evaluate these behaviors in our analyses, as the gap between "social interaction" in mice and humans is vast, and is thought to lack predictive validity. Therefore, when we refer to our study of the *Fmr1* KO mouse as a "mouse model of ASD", our claim is misleading. It would be more valid to refer to the *Fmr1* KO as a "mouse that has been engineered to model a genetic mutation that confers risk for ASD in humans." Throwing caution (and semantics) to the wind, we are often guilty of incorrectly claiming to study something that we are, in fact, not evaluating. Perhaps (negligibly) less misleading, we also make claims that the *Fmr1* KO mouse is a "mouse model of ID". We, and others, have found the *Fmr1* KO mouse (and 16p11.2 *df/+* mouse) to exhibit strongly impaired learning and memory. Although we cannot measure the IQ of a mouse, poor performance on cognitive tasks has proven to be a reasonable (and reproducible) indicator of ID in mouse models and can be corrected by pharmacological intervention. To this point, in the case of both FX and 16p11.2 CNVs, ID is highly penetrant- much

more so than ASDs in individuals with these mutations supporting the claim that these mutant mice are "models of ID".

5.4: Limitations of animal models in studying human disease.

Humans diverged from mice approximately ~75 million years ago (Zhao, Shetty et al. 2004), yet the protein-coding regions of the mouse and human genomes are 85% identical (Emes, Goodstadt et al. 2003). Despite this, since the lineages originally split, new genes in the mouse genome have disproportionately affected the reproductive system, whereas in the human lineage, expression of new genes are overwhelmingly skewed in the brain, in particular the neocotex (Zhang, Landback et al. 2011). Due to the enormous disparity between cognitive potential in mice and humans, the translatability of using animal models to study function (and more importantly dysfunction) in the human brain has been called into question.

5.4.1: Construct, face, and predictive validity.

As originally proposed by McKinney and Bunney (1969), an archetypal animal model of disease should mimic the human condition in its etiology, symptomatology, biochemistry, and treatment, thus laying the foundation for the concept of construct, face, and predictive validity of animal models (McKinney and Bunney 1969, Willner 1984, Blanchard, Summers et al. 2013). As it pertains to mouse models of neuropsychiatric disease, construct validity refers to the theoretical rationale of the mouse model. It requires that the model be generated with the same underlying biological or genetic cause (for example, a genetic mutation or particular neuroanatomical abnormality). Face validity refers to the similarities between symptoms that define a disease in humans and phenotypes or deficits observed in the mouse model (for example epilepsy and seizure disorders in individuals with FX and susceptibility to audiogenic seizures in mouse models of FX). Finally, predictive validity requires that treatments that are efficacious for improving pathological phenotypes in mouse models should be predictive of similar success in the human condition in clinical trials.

5.4.2: Validity of the Fmr1 KO mouse.

In Chapters 2 and 3 we evaluated novel targets as potential treatments for FX. Taking advantage of either a "proof of principle" approach in which we manipulated β-arrestin2 genetically, or a pharmacological approach were we inhibited GSK3 with paralog-selective inhibitors, we assessed the efficacy of our strategies in the *Fmr1* KO mouse. As a model of disease, the *Fmr1* KO mouse is considered to have reasonable construct and face validity making it a valuable tool for studying the synaptic pathophysiology of FX. In individuals with FX, an epigenetic silencing of the *FMR1* gene leads to either complete or nearly complete elimination of the protein product FMRP, with full loss of FMRP leading to the most severe cases of FX (Pieretti, Zhang et al. 1991, Verkerk, Pieretti et al. 1991, Devys, 1993 #62, Devys, Lutz et al. 1993, Fu, Kuhl et al. 1991, Pieretti, Zhang et al. 1991). Although this implies that the *Fmr1* KO mouse might have more construct validity as a model of FX patients with fully silenced FMRP, it is generally accepted that knocking out *Fmr1* effectively models methylation-mediated silencing of *Fmr1.* Of interesting note, attempts to model the CGG repeat instability that leads to hypermethylation and epigenetic silencing of the *FMR1* gene in humans have failed result in functional loss of FMRP in mice (Lavedan, Grabczyk et al. 1998).

Knocking out *Fmr1* in mice leads to a number of phenotypes that share common features with symptoms and impairments seen in individuals with FX. The *Fmr1* KO mouse is prone to audiogenic seizures, exhibits hyperactivity, shows impairments in social interaction, exhibits repetitive behavior in a marble burying task, as well as a number of deficits on tasks evaluating learning and memory (see Table 1.1). Individuals with FX exhibit similar characteristics including co-morbid seizure disorders and epilepsy, attention deficit hyperactivity disorder, ASD, obsessive compulsive disorder and ID (Bhakar, Dolen et al. 2012). At the cellular level, similar to observations in *Fmr1* KO mice, patients with FX show increased levels of pERK and pAKT in platelets and increased density of immature spines (Wisniewski, Segan et al. 1991, Comery, Harris et al. 1997, Irwin, Galvez et al. 2000, Irwin, Patel et al. 2001, Osterweil, Krueger et al. 2010, Pellerin, Caku et al. 2016). Based on a plethora of shared phenotypes and

impairments, the *Fmr1* KO mouse model exhibits face validity as an animal model of FX.

Despite demonstrating strong construct and face validity, the *Fmr1* KO mouse has not yet established predictive validity as a translatable model of disease. Countless manipulations have fully reversed aberrant phenotypes in the *Fmr1* KO mouse yet these same strategies have failed in clinical trials. The projects in Chapters 2 and 3 of this thesis are dedicated to refining our hypotheses and honing in on targets that may optimize therapeutic benefit while minimizing off-target effects. In this way, we hope that the *Fmr1* KO mouse will be substantiated as an animal model with predictive validity.

5.4.3: Validity of 16p11.2 CNV mouse models.

As discussed in Chapter 4, the construct validity of 16p11.2 *df/+* and 16p11.2 *df/+* animal models is a point of contention. Significantly fewer studies have investigated the face validity of mouse models of 16p11.2 CNVs. Face validity may be difficult to evaluate due to the wide phenotypic range associated with these disorders in human carriers. Furthermore, to our knowledge the predictive validity of these models has not yet been challenged. Three 16p11.2 *df/+* mouse models and two reciprocal 16p11.2 *dp/+* models differ by the size and span of the altered region. In humans, the affected region harbors ~25 genes with another 4 genes located in the segmentally duplicated regions that flank this region, leading to the CNV in the proband. Mouse models of these CNVs differ in the size of the deletion or duplication, affecting either 24 (Portmann, Yang et al. 2014), 26 (Arbogast, Ouagazzal et al. 2016), or 30 (Horev, Ellegood et al. 2011) genes. While all three sets of 16p11.2 CNV animal models have reasonable construct validity, it will likely be more important to evaluate the face and predictive validity of these models before making overall statements about utility as a model of human disease.

5.5: Other strategies to model FX or known genetic causes of disease.

Studies of mouse models, in particular the *Fmr1* KO mouse and 16p11.2 CNV mouse models, are the mainstream in the FX and ID field. Although zebrafish models

of both disorders as well as a drosophila model of FX have been established and characterized, the vast majority of our knowledge and understanding of these disorders, and in particular, potential treatments for these disorders, stems from mouse models. Recent advances in technology, in particular the optimization of CRISPR, an efficient gene editing technology, has paved the way for the development of higher order transgenic animal models, including rat and marmoset models of disease. These animal models would enable the evaluation of more complex cognition and behavior and may prove to show superior predicative validity as animal models of disease. Similarly, manipulation of induced pluripotent stem cells (iPSCs) from individuals with FX or 16p11.2 CNVs may offer significant advantages and predictive validity over animal models. Time will tell if these new experimental strategies will demonstrate more predictive validity than animal models and have the capacity to better inform therapeutic interventions for the treatment of FX, 16p11.2 CNVs and similar disorders.

5.6: Concluding remarks.

An overarching theme reflected in this thesis supports the theory that troubled translation at the synapse may be a core feature of the pathophysiology of a wide variety of disorders that cause ID in humans. In the case of FX, a monogenic disorder, it is known that synaptic dysfunction is a direct result of the loss of FMRP. However, in polygenic disorders such as 16p11.2 CNVs in which ~29 genes are affected, the mechanistic cause of synaptic dysfunction may not be as clear. Evidence presented here supports the possibility that identification of pathological phenotypes (for example, elevated Arc or cortical hyperexcitability), may be good predictors of overall synaptic dysfunction. More importantly, evaluating the efficacy of various targeted treatments in monogenic causes of these phenotypes may provide sufficient evidence to apply these same interventions to polygenic mutations marked by similar phenotypes.

Although the exact mechanism that couples $mGlu_5$ to the translational machinery at the synapse has not yet been fully deciphered, evidence collected here suggests that the adaptor protein β-arrestin2 is a key component that mediates the ERK1/2 signaling pathway. Similarly, GKS3α, more traditionally known for its role in WNT signaling, is

coupled to protein synthesis at some point downstream of ERK1/2 signaling. Finally, 16p11.2 CNVs share core features and phenotypes with FX based on evidence from animal models and human carriers of these mutations. Therefore, it is possible that potential treatments proven to be efficacious and safe in patients with FX may represent promising treatments for 16p11.2 CNVs as well.

References:

Abou Farha, K., R. Bruggeman and C. Balje-Volkers (2014). "Metabotropic glutamate receptor 5 negative modulation in phase I clinical trial: potential impact of circadian rhythm on the neuropsychiatric adverse reactions-do hallucinations matter?" ISRN Psychiatry **2014**: 652750.

Adusei, D. C., L. K. Pacey, D. Chen and D. R. Hampson (2010). "Early developmental alterations in GABAergic protein expression in fragile X knockout mice." Neuropharmacology **59**(3): 167-171.

Aguilar-Valles, A., E. Matta-Camacho, A. Khoutorsky, C. Gkogkas, K. Nader, J. C. Lacaille and N. Sonenberg (2015). "Inhibition of Group I Metabotropic Glutamate Receptors Reverses Autistic-Like Phenotypes Caused by Deficiency of the Translation Repressor eIF4E Binding Protein 2." J Neurosci **35**(31): 11125-11132.

Ahn, S., J. Kim, M. R. Hara, X. R. Ren and R. J. Lefkowitz (2009). "{beta}-Arrestin-2 Mediates Anti-apoptotic Signaling through Regulation of BAD Phosphorylation." J Biol Chem **284**(13): 8855-8865.

Arbogast, T., A. M. Ouagazzal, C. Chevalier, M. Kopanitsa, N. Afinowi, E. Migliavacca, B. S. Cowling, M. C. Birling, M. F. Champy, A. Reymond and Y. Herault (2016). "Reciprocal Effects on Neurocognitive and Metabolic Phenotypes in Mouse Models of 16p11.2 Deletion and Duplication Syndromes." PLoS Genet **12**(2): e1005709.

Aschrafi, A., B. A. Cunningham, G. M. Edelman and P. W. Vanderklish (2005). "The fragile X mental retardation protein and group I metabotropic glutamate receptors regulate levels of mRNA granules in brain." Proc Natl Acad Sci U S A **102**(6): 2180-2185.

Ashley, C. T., Jr., K. D. Wilkinson, D. Reines and S. T. Warren (1993). "FMR1 protein: conserved RNP family domains and selective RNA binding." Science **262**(5133): 563-566.

Auerbach, B. D., E. K. Osterweil and M. F. Bear (2011). "Mutations causing syndromic autism define an axis of synaptic pathophysiology." Nature **480**(7375): 63-68.

Bachner, D., P. Steinbach, D. Wohrle, W. Just, W. Vogel, H. Hameister, A. Manca and A. Poustka (1993). "Enhanced Fmr-1 expression in testis." Nat Genet **4**(2): 115-116.

Bailey, A., A. Le Couteur, I. Gottesman, P. Bolton, E. Simonoff, E. Yuzda and M. Rutter (1995). "Autism as a strongly genetic disorder: evidence from a British twin study." Psychol Med **25**(1): 63-77.

Bailey, D. B., Jr., M. Raspa, M. Olmsted and D. B. Holiday (2008). "Co-occurring conditions associated with FMR1 gene variations: findings from a national parent survey." Am J Med Genet A **146A**(16): 2060-2069.

Bakker, C., C. Verheij, R. Willemsen, R. van der Helm, F. Oerlemans, M. Vermey, A. Bygrave, A. Hoogeveen, B. Oostra, E. Reyniers, K. De Boule, R. D'Hooge, P. Cras, D. van Velzen, G. Nagels, J. Martin and P. De Deyn (1994). "Fmr1 knockout mice: a model to study fragile X mental retardation. The Dutch-Belgian Fragile X Consortium." Cell **78**(1): 23-33.

Banko, J. L., L. Hou, F. Poulin, N. Sonenberg and E. Klann (2006). "Regulation of eukaryotic initiation factor 4E by converging signaling pathways during metabotropic glutamate receptor-dependent long-term depression." J Neurosci **26**(8): 2167-2173.

Barnes, S. A., L. S. Wijetunge, A. D. Jackson, D. Katsanevaki, E. K. Osterweil, N. H. Komiyama, S. G. Grant, M. F. Bear, U. V. Nagerl, P. C. Kind and D. J. Wyllie (2015). "Convergence of Hippocampal Pathophysiology in Syngap+/- and Fmr1-/y Mice." J Neurosci **35**(45): 15073-15081.

Bassuk, A. G., E. Geraghty, S. Wu, S. A. Mullen, S. F. Berkovic, I. E. Scheffer and H. C. Mefford (2013). "Deletions of 16p11.2 and 19p13.2 in a family with intellectual disability and generalized epilepsy." Am J Med Genet A **161A**(7): 1722-1725.

Bear, M. F., K. M. Huber and S. T. Warren (2004). "The mGluR theory of fragile X mental retardation." Trends Neurosci **27**(7): 370-377.

Beaulieu, J. M., T. D. Sotnikova, W. D. Yao, L. Kockeritz, J. R. Woodgett, R. R. Gainetdinov and M. G. Caron (2004). "Lithium antagonizes dopamine-dependent behaviors mediated by an AKT/glycogen synthase kinase 3 signaling cascade." Proc Natl Acad Sci U S A **101**(14): 5099-5104.

Berry-Kravis, E., V. Des Portes, R. Hagerman, S. Jacquemont, P. Charles, J. Visootsak, M. Brinkman, K. Rerat, B. Koumaras, L. Zhu, G. M. Barth, T. Jaecklin, G. Apostol and F. von Raison (2016). "Mavoglurant in fragile X syndrome: Results of two randomized, double-blind, placebo-controlled trials." Sci Transl Med **8**(321): 321ra325.

Berry-Kravis, E., D. Hessl, L. Abbeduto, A. L. Reiss, A. Beckel-Mitchener and T. K. Urv (2013). "Outcome measures for clinical trials in fragile X syndrome." J Dev Behav Pediatr **34**(7): 508-522.

Berry-Kravis, E., R. Levin, H. Shah, S. Mathur, J. C. Darnell and B. Ouyang (2015). "Cholesterol levels in fragile X syndrome." Am J Med Genet A **167a**(2): 379-384.

Berry-Kravis, E., A. Sumis, C. Hervey, M. Nelson, S. W. Porges, N. Weng, I. J. Weiler and W. T. Greenough (2008). "Open-label treatment trial of lithium to target the underlying defect in fragile X syndrome." J Dev Behav Pediatr **29**(4): 293-302.

Berry-Kravis, E. M., D. Hessl, B. Rathmell, P. Zarevics, M. Cherubini, K. Walton-Bowen, Y. Mu, D. V. Nguyen, J. Gonzalez-Heydrich, P. P. Wang, R. L. Carpenter, M. F. Bear and R. J. Hagerman (2012). "Effects of STX209 (arbaclofen) on neurobehavioral function in children and adults with fragile X syndrome: a randomized, controlled, phase 2 trial." Sci Transl Med **4**(152): 152ra127.

Bersudsky, Y., A. Shaldubina, N. Kozlovsky, J. R. Woodgett, G. Agam and R. H. Belmaker (2008). "Glycogen synthase kinase-3beta heterozygote knockout mice as a model of findings in postmortem schizophrenia brain or as a model of behaviors mimicking lithium action: negative results." Behav Pharmacol **19**(3): 217-224.

Bhakar, A. L., G. Dolen and M. F. Bear (2012). "The pathophysiology of fragile X (and what it teaches us about synapses)." Annu Rev Neurosci **35**: 417-443.

Bhattacharya, A., H. Kaphzan, A. C. Alvarez-Dieppa, J. P. Murphy, P. Pierre and E. Klann (2012). "Genetic removal of p70 S6 kinase 1 corrects molecular, synaptic, and behavioral phenotypes in fragile X syndrome mice." Neuron **76**(2): 325-337.

Bhattacharya, A., M. Mamcarz, C. Mullins, A. Choudhury, R. G. Boyle, D. G. Smith, D. W. Walker and E. Klann (2016). "Targeting Translation Control with p70 S6 Kinase 1 Inhibitors to Reverse Phenotypes in Fragile X Syndrome Mice." Neuropsychopharmacology **41**(8): 1991-2000.

Bijlsma, E. K., A. C. Gijsbers, J. H. Schuurs-Hoeijmakers, A. van Haeringen, D. E. Fransen van de Putte, B. M. Anderlid, J. Lundin, P. Lapunzina, L. A. Perez Jurado, B. Delle Chiaie, B. Loeys, B. Menten, A. Oostra, H. Verhelst, D. J. Amor, D. L. Bruno, A. J. van Essen, R. Hordijk, B. Sikkema-Raddatz, K. T. Verbruggen, M. C. Jongmans, R. Pfundt, H. M. Reeser, M. H. Breuning and C. A. Ruivenkamp (2009). "Extending the phenotype of recurrent rearrangements of 16p11.2: deletions in mentally retarded patients without autism and in normal individuals." Eur J Med Genet **52**(2-3): 77-87.

Blanchard, D. C., C. H. Summers and R. J. Blanchard (2013). "The role of behavior in translational models for psychopathology: functionality and dysfunctional behaviors." Neurosci Biobehav Rev **37**(8): 1567-1577.

Blizinsky, K. D., B. Diaz-Castro, M. P. Forrest, B. Schurmann, A. P. Bach, M. D. Martin-de-Saavedra, L. Wang, J. G. Csernansky, J. Duan and P. Penzes (2016). "Reversal of dendritic phenotypes in 16p11.2 microduplication mouse model neurons by pharmacological targeting of a network hub." Proc Natl Acad Sci U S A **113**(30): 8520-8525.

Boulton, T. G., G. D. Yancopoulos, J. S. Gregory, C. Slaughter, C. Moomaw, J. Hsu and M. H. Cobb (1990). "An insulin-stimulated protein kinase similar to yeast kinases involved in cell cycle control." Science **249**(4964): 64-67.

Bozdagi, O., T. Sakurai, D. Papapetrou, X. Wang, D. L. Dickstein, N. Takahashi, Y. Kajiwara, M. Yang, A. M. Katz, M. L. Scattoni, M. J. Harris, R. Saxena, J. L. Silverman, J. N. Crawley, Q. Zhou, P. R. Hof and J. D. Buxbaum (2010). "Haploinsufficiency of the autism-associated Shank3 gene leads to deficits in synaptic function, social interaction, and social communication." Mol Autism **1**(1): 15.

Braat, S., C. D'Hulst, I. Heulens, S. De Rubeis, E. Mientjes, D. L. Nelson, R. Willemsen, C. Bagni, D. Van Dam, P. P. De Deyn and R. F. Kooy (2015). "The GABAA receptor is an FMRP target with therapeutic potential in fragile X syndrome." Cell Cycle **14**(18): 2985-2995.

Brennan, F. X., D. S. Albeck and R. Paylor (2006). "Fmr1 knockout mice are impaired in a leverpress escape/avoidance task." Genes Brain Behav **5**(6): 467-471.

Budimirovic, D. B. and W. E. Kaufmann (2011). "What can we learn about autism from studying fragile X syndrome?" Dev Neurosci **33**(5): 379-394.

Buescher, A. V., Z. Cidav, M. Knapp and D. S. Mandell (2014). "Costs of autism spectrum disorders in the United Kingdom and the United States." JAMA Pediatr **168**(8): 721-728.

Busquets-Garcia, A., M. Gomis-Gonzalez, T. Guegan, C. Agustin-Pavon, A. Pastor, S. Mato, A. Perez-Samartin, C. Matute, R. de la Torre, M. Dierssen, R. Maldonado and A. Ozaita (2013). "Targeting the endocannabinoid system in the treatment of fragile X syndrome." Nat Med **19**(5): 603-607.

Caku, A., D. Pellerin, P. Bouvier, E. Riou and F. Corbin (2014). "Effect of lovastatin on behavior in children and adults with fragile X syndrome: an open-label study." Am J Med Genet A **164a**(11): 2834-2842.

Carlsson, M. and A. Carlsson (1989). "The NMDA antagonist MK-801 causes marked locomotor stimulation in monoamine-depleted mice." J Neural Transm **75**(3): 221-226.

Castro-Gago, M., L. Perez-Gay, C. Gomez-Lado, D. Dacruz and F. Barros-Angueira (2013). "[16p11.2 microdeletion associated to early onset benign childhood seizures]." Rev Neurol **56**(2): 125-127.

Ceman, S., W. T. O'Donnell, M. Reed, S. Patton, J. Pohl and S. T. Warren (2003). "Phosphorylation influences the translation state of FMRP-associated polyribosomes." Hum Mol Genet **12**(24): 3295-3305.

Centonze, D., S. Rossi, V. Mercaldo, I. Napoli, M. T. Ciotti, V. De Chiara, A. Musella, C. Prosperetti, P. Calabresi, G. Bernardi and C. Bagni (2008). "Abnormal striatal GABA transmission in the mouse model for the fragile X syndrome." Biol Psychiatry **63**(10): 963-973.

Chen, H. H., P. F. Liao and M. H. Chan (2011). "mGluR5 positive modulators both potentiate activation and restore inhibition in NMDA receptors by PKC dependent pathway." J Biomed Sci **18**: 19.

Chen, L., S. W. Yun, J. Seto, W. Liu and M. Toth (2003). "The fragile X mental retardation protein binds and regulates a novel class of mRNAs containing U rich target sequences." Neuroscience **120**(4): 1005-1017.

Chen, T., J. S. Lu, Q. Song, M. G. Liu, K. Koga, G. Descalzi, Y. Q. Li and M. Zhuo (2014). "Pharmacological rescue of cortical synaptic and network potentiation in a mouse model for fragile X syndrome." Neuropsychopharmacology **39**(8): 1955-1967.

Chen, X., W. Sun, Y. Pan, Q. Yang, K. Cao, J. Zhang, Y. Zhang, M. Chen, F. Chen, Y. Huang, L. Dai and S. Chen (2013). "Lithium ameliorates open-field and elevated plus maze behaviors, and brain phospho-glycogen synthase kinase 3-beta expression in fragile X syndrome model mice." Neurosciences (Riyadh) **18**(4): 356-362.

Chiu, C. T. and D. M. Chuang (2011). "Neuroprotective action of lithium in disorders of the central nervous system." Zhong Nan Da Xue Xue Bao Yi Xue Ban **36**(6): 461-476.

Choi, C. H., B. P. Schoenfeld, A. J. Bell, P. Hinchey, M. Kollaros, M. J. Gertner, N. H. Woo, M. R. Tranfaglia, M. F. Bear, R. S. Zukin, T. V. McDonald, T. A. Jongens and S.

M. McBride (2011). "Pharmacological reversal of synaptic plasticity deficits in the mouse model of fragile X syndrome by group II mGluR antagonist or lithium treatment." Brain Res **1380**: 106-119.

Christensen, D. L., J. Baio, K. V. Braun, D. Bilder, J. Charles, J. N. Constantino, J. Daniels, M. S. Durkin, R. T. Fitzgerald, M. Kurzius-Spencer, L. C. Lee, S. Pettygrove, C. Robinson, E. Schulz, C. Wells, M. S. Wingate, W. Zahorodny and M. Yeargin-Allsopp (2016). "Prevalence and Characteristics of Autism Spectrum Disorder Among Children Aged 8 Years - Autism and Developmental Disabilities Monitoring Network, 11 Sites, United States, 2012." MMWR Surveill Summ **65**(3): 1-23.

Christian, S. L., C. W. Brune, J. Sudi, R. A. Kumar, S. Liu, S. Karamohamed, J. A. Badner, S. Matsui, J. Conroy, D. McQuaid, J. Gergel, E. Hatchwell, T. C. Gilliam, E. S. Gershon, N. J. Nowak, W. B. Dobyns and E. H. Cook, Jr. (2008). "Novel submicroscopic chromosomal abnormalities detected in autism spectrum disorder." Biol Psychiatry **63**(12): 1111-1117.

Chuang, S. C., W. Zhao, R. Bauchwitz, Q. Yan, R. Bianchi and R. K. Wong (2005). "Prolonged epileptiform discharges induced by altered group I metabotropic glutamate receptor-mediated synaptic responses in hippocampal slices of a fragile X mouse model." J Neurosci **25**(35): 8048-8055.

Ciuladaite, Z., J. Kasnauskiene, L. Cimbalistiene, E. Preiksaitiene, P. C. Patsalis and V. Kucinskas (2011). "Mental retardation and autism associated with recurrent 16p11.2 microdeletion: incomplete penetrance and variable expressivity." J Appl Genet **52**(4): 443-449.

Cleva, R. M. and M. F. Olive (2011). "Positive allosteric modulators of type 5 metabotropic glutamate receptors (mGluR5) and their therapeutic potential for the treatment of CNS disorders." Molecules **16**(3): 2097-2106.

Coffee, B., M. Ikeda, D. B. Budimirovic, L. N. Hjelm, W. E. Kaufmann and S. T. Warren (2008). "Mosaic FMR1 deletion causes fragile X syndrome and can lead to molecular misdiagnosis: a case report and review of the literature." Am J Med Genet A **146A**(10): 1358-1367.

Collett, V. J. and G. L. Collingridge (2004). "Interactions between NMDA receptors and mGlu5 receptors expressed in HEK293 cells." Br J Pharmacol **142**(6): 991-1001.

Comery, T. A., J. B. Harris, P. J. Willems, B. A. Oostra, S. A. Irwin, I. J. Weiler and W. T. Greenough (1997). "Abnormal dendritic spines in fragile X knockout mice: maturation and pruning deficits." Proc Natl Acad Sci U S A **94**(10): 5401-5404.

Conn, P. J., A. Christopoulos and C. W. Lindsley (2009). "Allosteric modulators of GPCRs: a novel approach for the treatment of CNS disorders." Nat Rev Drug Discov **8**(1): 41-54.

Cooper, G. M., B. P. Coe, S. Girirajan, J. A. Rosenfeld, T. H. Vu, C. Baker, C. Williams, H. Stalker, R. Hamid, V. Hannig, H. Abdel-Hamid, P. Bader, E. McCracken, D. Niyazov, K. Leppig, H. Thiese, M. Hummel, N. Alexander, J. Gorski, J. Kussmann, V. Shashi, K. Johnson, C. Rehder, B. C. Ballif, L. G. Shaffer and E. E. Eichler (2011). "A copy number variation morbidity map of developmental delay." Nat Genet **43**(9): 838-846.

Cosford, N. D., L. Tehrani, J. Roppe, E. Schweiger, N. D. Smith, J. Anderson, L. Bristow, J. Brodkin, X. Jiang, I. McDonald, S. Rao, M. Washburn and M. A. Varney (2003). "3-[(2-Methyl-1,3-thiazol-4-yl)ethynyl]-pyridine: a potent and highly selective metabotropic glutamate subtype 5 receptor antagonist with anxiolytic activity." J Med Chem **46**(2): 204-206.

Crepel, A., J. Steyaert, W. De la Marche, V. De Wolf, J. P. Fryns, I. Noens, K. Devriendt and H. Peeters (2011). "Narrowing the critical deletion region for autism spectrum disorders on 16p11.2." Am J Med Genet B Neuropsychiatr Genet **156**(2): 243-245.

Curia, G., T. Papouin, P. Seguela and M. Avoli (2009). "Downregulation of tonic GABAergic inhibition in a mouse model of fragile X syndrome." Cereb Cortex **19**(7): 1515-1520.

D'Antoni, S., M. Spatuzza, C. M. Bonaccorso, S. A. Musumeci, L. Ciranna, F. Nicoletti, K. M. Huber and M. V. Catania (2014). "Dysregulation of group-I metabotropic glutamate (mGlu) receptor mediated signalling in disorders associated with Intellectual Disability and Autism." Neurosci Biobehav Rev **46 Pt 2**: 228-241.

D'Hulst, C., N. De Geest, S. P. Reeve, D. Van Dam, P. P. De Deyn, B. A. Hassan and R. F. Kooy (2006). "Decreased expression of the GABAA receptor in fragile X syndrome." Brain Res **1121**(1): 238-245.

D'Hulst, C., I. Heulens, J. R. Brouwer, R. Willemsen, N. De Geest, S. P. Reeve, P. P. De Deyn, B. A. Hassan and R. F. Kooy (2009). "Expression of the GABAergic system in animal models for fragile X syndrome and fragile X associated tremor/ataxia syndrome (FXTAS)." Brain Res **1253**: 176-183.

Dajani, R., E. Fraser, S. M. Roe, N. Young, V. Good, T. C. Dale and L. H. Pearl (2001). "Crystal structure of glycogen synthase kinase 3 beta: structural basis for phosphate-primed substrate specificity and autoinhibition." Cell **105**(6): 721-732.

Darnell, J. C., S. J. Van Driesche, C. Zhang, K. Y. Hung, A. Mele, C. E. Fraser, E. F. Stone, C. Chen, J. J. Fak, S. W. Chi, D. D. Licatalosi, J. D. Richter and R. B. Darnell (2011). "FMRP stalls ribosomal translocation on mRNAs linked to synaptic function and autism." Cell **146**(2): 247-261.

De Boulle, K., A. J. Verkerk, E. Reyniers, L. Vits, J. Hendrickx, B. Van Roy, F. Van den Bos, E. de Graaff, B. A. Oostra and P. J. Willems (1993). "A point mutation in the FMR-1 gene associated with fragile X mental retardation." Nat Genet **3**(1): 31-35.

de Vrij, F. M., J. Levenga, H. C. van der Linde, S. K. Koekkoek, C. I. De Zeeuw, D. L. Nelson, B. A. Oostra and R. Willemsen (2008). "Rescue of behavioral phenotype and neuronal protrusion morphology in Fmr1 KO mice." Neurobiol Dis **31**(1): 127-132.

den Broeder, M. J., H. van der Linde, J. R. Brouwer, B. A. Oostra, R. Willemsen and R. F. Ketting (2009). "Generation and characterization of FMR1 knockout zebrafish." PLoS One **4**(11): e7910.

Deng, P. Y. and V. A. Klyachko (2016). "Genetic upregulation of BK channel activity normalizes multiple synaptic and circuit defects in a mouse model of fragile X syndrome." J Physiol **594**(1): 83-97.

Devys, D., Y. Lutz, N. Rouyer, J. P. Bellocq and J. L. Mandel (1993). "The FMR-1 protein is cytoplasmic, most abundant in neurons and appears normal in carriers of a fragile X premutation." Nat Genet **4**(4): 335-340.

DeWire, S. M., S. Ahn, R. J. Lefkowitz and S. K. Shenoy (2007). "Beta-arrestins and cell signaling." Annu Rev Physiol **69**: 483-510.

DeWire, S. M., J. Kim, E. J. Whalen, S. Ahn, M. Chen and R. J. Lefkowitz (2008). "Beta-arrestin-mediated signaling regulates protein synthesis." J Biol Chem **283**(16): 10611-10620.

Doble, B. W., S. Patel, G. A. Wood, L. K. Kockeritz and J. R. Woodgett (2007). "Functional redundancy of GSK-3alpha and GSK-3beta in Wnt/beta-catenin signaling shown by using an allelic series of embryonic stem cell lines." Dev Cell **12**(6): 957-971.

Dolen, G., E. Osterweil, B. S. Rao, G. B. Smith, B. D. Auerbach, S. Chattarji and M. F. Bear (2007). "Correction of fragile X syndrome in mice." Neuron **56**(6): 955-962.

Dudek, S. M. and M. F. Bear (1989). "A biochemical correlate of the critical period for synaptic modification in the visual cortex." Science **246**(4930): 673-675.

Dziembowska, M., D. I. Pretto, A. Janusz, L. Kaczmarek, M. J. Leigh, N. Gabriel, B. Durbin-Johnson, R. J. Hagerman and F. Tassone (2013). "High MMP-9 activity levels in fragile X syndrome are lowered by minocycline." Am J Med Genet A **161a**(8): 1897-1903.

Eberhart, D. E., H. E. Malter, Y. Feng and S. T. Warren (1996). "The fragile X mental retardation protein is a ribonucleoprotein containing both nuclear localization and nuclear export signals." Hum Mol Genet **5**(8): 1083-1091.

Ebrahimi-Fakhari, D. and M. Sahin (2015). "Autism and the synapse: emerging mechanisms and mechanism-based therapies." Curr Opin Neurol **28**(2): 91-102.

Ehninger, D., S. Han, C. Shilyansky, Y. Zhou, W. Li, D. J. Kwiatkowski, V. Ramesh and A. J. Silva (2008). "Reversal of learning deficits in a Tsc2+/- mouse model of tuberous sclerosis." Nat Med **14**(8): 843-848.

El Idrissi, A., X. H. Ding, J. Scalia, E. Trenkner, W. T. Brown and C. Dobkin (2005). "Decreased GABA(A) receptor expression in the seizure-prone fragile X mouse." Neurosci Lett **377**(3): 141-146.

Embi, N., D. B. Rylatt and P. Cohen (1980). "Glycogen synthase kinase-3 from rabbit skeletal muscle. Separation from cyclic-AMP-dependent protein kinase and phosphorylase kinase." Eur J Biochem **107**(2): 519-527.

Emes, R. D., L. Goodstadt, E. E. Winter and C. P. Ponting (2003). "Comparison of the genomes of human and mouse lays the foundation of genome zoology." Hum Mol Genet **12**(7): 701-709.

Feng, Y., D. Absher, D. E. Eberhart, V. Brown, H. E. Malter and S. T. Warren (1997). "FMRP associates with polyribosomes as an mRNP, and the I304N mutation of severe fragile X syndrome abolishes this association." Mol Cell **1**(1): 109-118.

Feng, Y., C. A. Gutekunst, D. E. Eberhart, H. Yi, S. T. Warren and S. M. Hersch (1997). "Fragile X mental retardation protein: nucleocytoplasmic shuttling and association with somatodendritic ribosomes." J Neurosci **17**(5): 1539-1547.

Ferrer, I., M. Barrachina and B. Puig (2002). "Glycogen synthase kinase-3 is associated with neuronal and glial hyperphosphorylated tau deposits in Alzheimer's disease, Pick's disease, progressive supranuclear palsy and corticobasal degeneration." Acta Neuropathol **104**(6): 583-591.

Fitzjohn, S. M., M. J. Palmer, J. E. May, A. Neeson, S. A. Morris and G. L. Collingridge (2001). "A characterisation of long-term depression induced by metabotropic glutamate receptor activation in the rat hippocampus in vitro." J Physiol **537**(Pt 2): 421-430.

Franklin, A. V., M. K. King, V. Palomo, A. Martinez, L. L. McMahon and R. S. Jope (2014). "Glycogen synthase kinase-3 inhibitors reverse deficits in long-term potentiation and cognition in fragile X mice." Biol Psychiatry **75**(3): 198-206.

Fu, Y. H., D. P. Kuhl, A. Pizzuti, M. Pieretti, J. S. Sutcliffe, S. Richards, A. J. Verkerk, J. J. Holden, R. G. Fenwick, Jr., S. T. Warren and et al. (1991). "Variation of the CGG repeat at the fragile X site results in genetic instability: resolution of the Sherman paradox." Cell **67**(6): 1047-1058.

Gallagher, S. M., C. A. Daly, M. F. Bear and K. M. Huber (2004). "Extracellular signal-regulated protein kinase activation is required for metabotropic glutamate receptor-dependent long-term depression in hippocampal area CA1." J Neurosci **24**(20): 4859-4864.

Garber, K. B., J. Visootsak and S. T. Warren (2008). "Fragile X syndrome." Eur J Hum Genet **16**(6): 666-672.

Gasparini, F., K. Lingenhohl, N. Stoehr, P. J. Flor, M. Heinrich, I. Vranesic, M. Biollaz, H. Allgeier, R. Heckendorn, S. Urwyler, M. A. Varney, E. C. Johnson, S. D. Hess, S. P. Rao, A. I. Sacaan, E. M. Santori, G. Velicelebi and R. Kuhn (1999). "2-Methyl-6-(phenylethynyl)-pyridine (MPEP), a potent, selective and systemically active mGlu5 receptor antagonist." Neuropharmacology **38**(10): 1493-1503.

Gholizadeh, S., S. K. Halder and D. R. Hampson (2015). "Expression of fragile X mental retardation protein in neurons and glia of the developing and adult mouse brain." Brain Res **1596**: 22-30.

Gibson, J. R., A. F. Bartley, S. A. Hays and K. M. Huber (2008). "Imbalance of neocortical excitation and inhibition and altered UP states reflect network hyperexcitability in the mouse model of fragile X syndrome." J Neurophysiol **100**(5): 2615-2626.

Gieros, K., A. Sobczuk and E. Salinska (2012). "Differential involvement of mGluR1 and mGluR5 in memory reconsolidation and retrieval in a passive avoidance task in 1-day old chicks." Neurobiol Learn Mem **97**(1): 165-172.

Gkogkas, C. G., A. Khoutorsky, R. Cao, S. M. Jafarnejad, M. Prager-Khoutorsky, N. Giannakas, A. Kaminari, A. Fragkouli, K. Nader, T. J. Price, B. W. Konicek, J. R. Graff,

A. K. Tzinia, J. C. Lacaille and N. Sonenberg (2014). "Pharmacogenetic inhibition of eIF4E-dependent Mmp9 mRNA translation reverses fragile X syndrome-like phenotypes." Cell Rep **9**(5): 1742-1755.

Godfraind, J. M., E. Reyniers, K. De Boulle, R. D'Hooge, P. P. De Deyn, C. E. Bakker, B. A. Oostra, R. F. Kooy and P. J. Willems (1996). "Long-term potentiation in the hippocampus of fragile X knockout mice." Am J Med Genet **64**(2): 246-251.

Gogliotti, R. G., R. K. Senter, J. M. Rook, A. Ghoshal, R. Zamorano, C. Malosh, S. R. Stauffer, T. M. Bridges, J. M. Bartolome, J. S. Daniels, C. K. Jones, C. W. Lindsley, P. J. Conn and C. M. Niswender (2016). "mGlu5 positive allosteric modulation normalizes synaptic plasticity defects and motor phenotypes in a mouse model of Rett syndrome." Hum Mol Genet.

Gokoolparsadh, A., G. J. Sutton, A. Charamko, N. F. Green, C. J. Pardy and I. Voineagu (2016). "Searching for convergent pathways in autism spectrum disorders: insights from human brain transcriptome studies." Cell Mol Life Sci.

Golzio, C., J. Willer, M. E. Talkowski, E. C. Oh, Y. Taniguchi, S. Jacquemont, A. Reymond, M. Sun, A. Sawa, J. F. Gusella, A. Kamiya, J. S. Beckmann and N. Katsanis (2012). "KCTD13 is a major driver of mirrored neuroanatomical phenotypes of the 16p11.2 copy number variant." Nature **485**(7398): 363-367.

Gould, R. W., R. J. Amato, M. Bubser, M. E. Joffe, M. T. Nedelcovych, A. D. Thompson, H. H. Nickols, J. P. Yuh, X. Zhan, A. S. Felts, A. L. Rodriguez, R. D. Morrison, F. W. Byers, J. M. Rook, J. S. Daniels, C. M. Niswender, P. J. Conn, K. A. Emmitte, C. W. Lindsley and C. K. Jones (2016). "Partial mGlu5 Negative Allosteric Modulators Attenuate Cocaine-Mediated Behaviors and Lack Psychotomimetic-Like Effects." Neuropsychopharmacology **41**(4): 1166-1178.

Grimes, C. A. and R. S. Jope (2001). "The multifaceted roles of glycogen synthase kinase 3beta in cellular signaling." Prog Neurobiol **65**(4): 391-426.

Gross, C., C. W. Chang, S. M. Kelly, A. Bhattacharya, S. M. McBride, S. W. Danielson, M. Q. Jiang, C. B. Chan, K. Ye, J. R. Gibson, E. Klann, T. A. Jongens, K. H. Moberg, K. M. Huber and G. J. Bassell (2015). "Increased expression of the PI3K enhancer PIKE mediates deficits in synaptic plasticity and behavior in fragile X syndrome." Cell Rep **11**(5): 727-736.

Gross, C., A. Hoffmann, G. J. Bassell and E. M. Berry-Kravis (2015). "Therapeutic Strategies in Fragile X Syndrome: From Bench to Bedside and Back." Neurotherapeutics **12**(3): 584-608.

Gross, C., M. Nakamoto, X. Yao, C. B. Chan, S. Y. Yim, K. Ye, S. T. Warren and G. J. Bassell (2010). "Excess phosphoinositide 3-kinase subunit synthesis and activity as a novel therapeutic target in fragile X syndrome." J Neurosci **30**(32): 10624-10638.

Gross, C., N. Raj, G. Molinaro, A. G. Allen, A. J. Whyte, J. R. Gibson, K. M. Huber, S. L. Gourley and G. J. Bassell (2015). "Selective role of the catalytic PI3K subunit p110beta in impaired higher order cognition in fragile X syndrome." Cell Rep **11**(5): 681-688.

Guo, W., G. Molinaro, K. A. Collins, S. A. Hays, R. Paylor, P. F. Worley, K. K. Szumlinski and K. M. Huber (2016). "Selective Disruption of Metabotropic Glutamate Receptor 5-Homer Interactions Mimics Phenotypes of Fragile X Syndrome in Mice." J Neurosci **36**(7): 2131-2147.

Guo, W., A. C. Murthy, L. Zhang, E. B. Johnson, E. G. Schaller, A. M. Allan and X. Zhao (2012). "Inhibition of GSK3beta improves hippocampus-dependent learning and rescues neurogenesis in a mouse model of fragile X syndrome." Hum Mol Genet **21**(3): 681-691.

Gupta, K., F. Gulen, L. Sun, R. Aguilera, A. Chakrabarti, J. Kiselar, M. K. Agarwal and D. N. Wald (2012). "GSK3 is a regulator of RAR-mediated differentiation." Leukemia **26**(6): 1277-1285.

Hagerman, R. J., E. Berry-Kravis, W. E. Kaufmann, M. Y. Ono, N. Tartaglia, A. Lachiewicz, R. Kronk, C. Delahunty, D. Hessl, J. Visootsak, J. Picker, L. Gane and M. Tranfaglia (2009). "Advances in the treatment of fragile X syndrome." Pediatrics **123**(1): 378-390.

Hamilton, S. M., J. R. Green, S. Veeraragavan, L. Yuva, A. McCoy, Y. Wu, J. Warren, L. Little, D. Ji, X. Cui, E. Weinstein and R. Paylor (2014). "Fmr1 and Nlgn3 knockout rats: novel tools for investigating autism spectrum disorders." Behav Neurosci **128**(2): 103-109.

Hanson, E., R. H. Nasir, A. Fong, A. Lian, R. Hundley, Y. Shen, B. L. Wu, I. A. Holm and D. T. Miller (2010). "Cognitive and behavioral characterization of 16p11.2 deletion syndrome." J Dev Behav Pediatr **31**(8): 649-657.

Hathaway, H. A., S. Pshenichkin, E. Grajkowska, T. Gelb, A. C. Emery, B. B. Wolfe and J. T. Wroblewski (2015). "Pharmacological characterization of mGlu1 receptors in cerebellar granule cells reveals biased agonism." Neuropharmacology **93**: 199-208.

Hays, S. A., K. M. Huber and J. R. Gibson (2011). "Altered neocortical rhythmic activity states in Fmr1 KO mice are due to enhanced mGluR5 signaling and involve changes in excitatory circuitry." J Neurosci **31**(40): 14223-14234.

He, Q., T. Nomura, J. Xu and A. Contractor (2014). "The developmental switch in GABA polarity is delayed in fragile X mice." J Neurosci **34**(2): 446-450.

Henderson, C., L. Wijetunge, M. N. Kinoshita, M. Shumway, R. S. Hammond, F. R. Postma, C. Brynczka, R. Rush, A. Thomas, R. Paylor, S. T. Warren, P. W. Vanderklish, P. C. Kind, R. L. Carpenter, M. F. Bear and A. M. Healy (2012). "Reversal of disease-related pathologies in the fragile X mouse model by selective activation of GABAB receptors with arbaclofen." Sci Transl Med **4**(152): 152ra128.

Heulens, I., C. D'Hulst, D. Van Dam, P. P. De Deyn and R. F. Kooy (2012). "Pharmacological treatment of fragile X syndrome with GABAergic drugs in a knockout mouse model." Behav Brain Res **229**(1): 244-249.

Hinds, H. L., C. T. Ashley, J. S. Sutcliffe, D. L. Nelson, S. T. Warren, D. E. Housman and M. Schalling (1993). "Tissue specific expression of FMR-1 provides evidence for a functional role in fragile X syndrome." Nat Genet **3**(1): 36-43.

Hinton, V. J., W. T. Brown, K. Wisniewski and R. D. Rudelli (1991). "Analysis of neocortex in three males with the fragile X syndrome." Am J Med Genet **41**(3): 289-294.

Ho, O. H., J. Y. Delgado and T. J. O'Dell (2004). "Phosphorylation of proteins involved in activity-dependent forms of synaptic plasticity is altered in hippocampal slices maintained in vitro." J Neurochem **91**(6): 1344-1357.

Hoeffer, C. A. and E. Klann (2010). "mTOR signaling: at the crossroads of plasticity, memory and disease." Trends Neurosci **33**(2): 67-75.

Hoeflich, K. P., J. Luo, E. A. Rubie, M. S. Tsao, O. Jin and J. R. Woodgett (2000). "Requirement for glycogen synthase kinase-3beta in cell survival and NF-kappaB activation." Nature **406**(6791): 86-90.

Homayoun, H., M. R. Stefani, B. W. Adams, G. D. Tamagan and B. Moghaddam (2004). "Functional Interaction Between NMDA and mGlu5 Receptors: Effects on Working Memory, Instrumental Learning, Motor Behaviors, and Dopamine Release." Neuropsychopharmacology **29**(7): 1259-1269.

Horev, G., J. Ellegood, J. P. Lerch, Y. E. Son, L. Muthuswamy, H. Vogel, A. M. Krieger, A. Buja, R. M. Henkelman, M. Wigler and A. A. Mills (2011). "Dosage-dependent phenotypes in models of 16p11.2 lesions found in autism." Proc Natl Acad Sci U S A **108**(41): 17076-17081.

Hou, L., M. D. Antion, D. Hu, C. M. Spencer, R. Paylor and E. Klann (2006). "Dynamic translational and proteasomal regulation of fragile X mental retardation protein controls mGluR-dependent long-term depression." Neuron **51**(4): 441-454.

Hou, L. and E. Klann (2004). "Activation of the phosphoinositide 3-kinase-Akt-mammalian target of rapamycin signaling pathway is required for metabotropic glutamate receptor-dependent long-term depression." J Neurosci **24**(28): 6352-6361.

Houamed, K. M., J. L. Kuijper, T. L. Gilbert, B. A. Haldeman, P. J. O'Hara, E. R. Mulvihill, W. Almers and F. S. Hagen (1991). "Cloning, expression, and gene structure of a G protein-coupled glutamate receptor from rat brain." Science **252**(5010): 1318-1321.

Hu, H., Y. Qin, G. Bochorishvili, Y. Zhu, L. van Aelst and J. J. Zhu (2008). "Ras signaling mechanisms underlying impaired GluR1-dependent plasticity associated with fragile X syndrome." J Neurosci **28**(31): 7847-7862.

Huber, K. M., S. M. Gallagher, S. T. Warren and M. F. Bear (2002). "Altered synaptic plasticity in a mouse model of fragile X mental retardation." Proc Natl Acad Sci U S A **99**(11): 7746-7750.

Huber, K. M., M. S. Kayser and M. F. Bear (2000). "Role for rapid dendritic protein synthesis in hippocampal mGluR-dependent long-term depression." Science **288**(5469): 1254-1257.

Huber, K. M., J. C. Roder and M. F. Bear (2001). "Chemical induction of mGluR5- and protein synthesis--dependent long-term depression in hippocampal area CA1." J Neurophysiol **86**(1): 321-325.

Hultman, C. M., S. Sandin, S. Z. Levine, P. Lichtenstein and A. Reichenberg (2011). "Advancing paternal age and risk of autism: new evidence from a population-based study and a meta-analysis of epidemiological studies." Mol Psychiatry **16**(12): 1203-1212.

Iacoangeli, A., T. S. Rozhdestvensky, N. Dolzhanskaya, B. Tournier, J. Schutt, J. Brosius, R. B. Denman, E. W. Khandjian, S. Kindler and H. Tiedge (2008). "On BC1 RNA and the fragile X mental retardation protein." Proc Natl Acad Sci U S A **105**(2): 734-739.

Iacoangeli, A., T. S. Rozhdestvensky, N. Dolzhanskaya, B. Tournier, J. Schutt, J. Brosius, R. B. Denman, E. W. Khandjian, S. Kindler and H. Tiedge (2008). "Reply to

Bagni: On BC1 RNA and the fragile X mental retardation protein." Proc Natl Acad Sci U S A **105**(22): E29.

Iacovelli, L., M. Felicioni, R. Nistico, F. Nicoletti and A. De Blasi (2014). "Selective regulation of recombinantly expressed mGlu7 metabotropic glutamate receptors by G protein-coupled receptor kinases and arrestins." Neuropharmacology **77**: 303-312.

Insel, P. A., C. M. Tang, I. Hahntow and M. C. Michel (2007). "Impact of GPCRs in clinical medicine: monogenic diseases, genetic variants and drug targets." Biochim Biophys Acta **1768**(4): 994-1005.

Irwin, S. A., R. Galvez and W. T. Greenough (2000). "Dendritic spine structural anomalies in fragile-X mental retardation syndrome." Cereb Cortex **10**(10): 1038-1044.

Irwin, S. A., B. Patel, M. Idupulapati, J. B. Harris, R. A. Crisostomo, B. P. Larsen, F. Kooy, P. J. Willems, P. Cras, P. B. Kozlowski, R. A. Swain, I. J. Weiler and W. T. Greenough (2001). "Abnormal dendritic spine characteristics in the temporal and visual cortices of patients with fragile-X syndrome: a quantitative examination." Am J Med Genet **98**(2): 161-167.

Jakkamsetti, V., N. P. Tsai, C. Gross, G. Molinaro, K. A. Collins, F. Nicoletti, K. H. Wang, P. Osten, G. J. Bassell, J. R. Gibson and K. M. Huber (2013). "Experience-induced Arc/Arg3.1 primes CA1 pyramidal neurons for metabotropic glutamate receptor-dependent long-term synaptic depression." Neuron **80**(1): 72-79.

Job, C. and J. Eberwine (2001). "Identification of sites for exponential translation in living dendrites." Proc Natl Acad Sci U S A **98**(23): 13037-13042.

Kaidanovich-Beilin, O., T. V. Lipina, K. Takao, M. van Eede, S. Hattori, C. Laliberte, M. Khan, K. Okamoto, J. W. Chambers, P. J. Fletcher, K. MacAulay, B. W. Doble, M. Henkelman, T. Miyakawa, J. Roder and J. R. Woodgett (2009). "Abnormalities in brain structure and behavior in GSK-3alpha mutant mice." Mol Brain **2**: 35.

Kaidanovich-Beilin, O. and J. R. Woodgett (2011). "GSK-3: Functional Insights from Cell Biology and Animal Models." Front Mol Neurosci **4**: 40.

Kang, H. and E. M. Schuman (1996). "A requirement for local protein synthesis in neurotrophin-induced hippocampal synaptic plasticity." Science **273**(5280): 1402-1406.

Kanner, L. and L. Eisenberg (1957). "Early infantile autism, 1943-1955." Psychiatr Res Rep Am Psychiatr Assoc(7): 55-65.

Khandjian, E. W., M. E. Huot, S. Tremblay, L. Davidovic, R. Mazroui and B. Bardoni (2004). "Biochemical evidence for the association of fragile X mental retardation protein with brain polyribosomal ribonucleoparticles." Proc Natl Acad Sci U S A **101**(36): 13357-13362.

Kim, S. H., J. A. Markham, I. J. Weiler and W. T. Greenough (2008). "Aberrant early-phase ERK inactivation impedes neuronal function in fragile X syndrome." Proc Natl Acad Sci U S A **105**(11): 4429-4434.

Kimura, T., S. Yamashita, S. Nakao, J. M. Park, M. Murayama, T. Mizoroki, Y. Yoshiike, N. Sahara and A. Takashima (2008). "GSK-3beta is required for memory reconsolidation in adult brain." PLoS One **3**(10): e3540.

King, M. K. and R. S. Jope (2013). "Lithium treatment alleviates impaired cognition in a mouse model of fragile X syndrome." Genes Brain Behav **12**(7): 723-731.

Kirov, S. A., K. E. Sorra and K. M. Harris (1999). "Slices have more synapses than perfusion-fixed hippocampus from both young and mature rats." J Neurosci **19**(8): 2876-2886.

Koekkoek, S. K., K. Yamaguchi, B. A. Milojkovic, B. R. Dortland, T. J. Ruigrok, R. Maex, W. De Graaf, A. E. Smit, F. VanderWerf, C. E. Bakker, R. Willemsen, T. Ikeda, S. Kakizawa, K. Onodera, D. L. Nelson, E. Mientjes, M. Joosten, E. De Schutter, B. A. Oostra, M. Ito and C. I. De Zeeuw (2005). "Deletion of FMR1 in Purkinje cells enhances parallel fiber LTD, enlarges spines, and attenuates cerebellar eyelid conditioning in Fragile X syndrome." Neuron **47**(3): 339-352.

Kolli, S., C. I. Zito, M. H. Mossink, E. A. Wiemer and A. M. Bennett (2004). "The major vault protein is a novel substrate for the tyrosine phosphatase SHP-2 and scaffold protein in epidermal growth factor signaling." J Biol Chem **279**(28): 29374-29385.

Kumar, R. A., S. KaraMohamed, J. Sudi, D. F. Conrad, C. Brune, J. A. Badner, T. C. Gilliam, N. J. Nowak, E. H. Cook, Jr., W. B. Dobyns and S. L. Christian (2008). "Recurrent 16p11.2 microdeletions in autism." Hum Mol Genet **17**(4): 628-638.

Kuribara, H., T. Asami, I. Ida and S. Tadokoro (1992). "Characteristics of the ambulation-increasing effect of the noncompetitive NMDA antagonist MK-801 in mice: assessment by the coadministration with central-acting drugs." Jpn J Pharmacol **58**(1): 11-18.

Lai, J. K., M. Sobala-Drozdowski, L. Zhou, L. C. Doering, P. A. Faure and J. A. Foster (2014). "Temporal and spectral differences in the ultrasonic vocalizations of fragile X knock out mice during postnatal development." Behav Brain Res **259**: 119-130.

Lavedan, C., E. Grabczyk, K. Usdin and R. L. Nussbaum (1998). "Long uninterrupted CGG repeats within the first exon of the human FMR1 gene are not intrinsically unstable in transgenic mice." Genomics **50**(2): 229-240.

Lavelle, T. A., M. C. Weinstein, J. P. Newhouse, K. Munir, K. A. Kuhlthau and L. A. Prosser (2014). "Economic burden of childhood autism spectrum disorders." Pediatrics **133**(3): e520-529.

Lee, F. H., O. Kaidanovich-Beilin, J. C. Roder, J. R. Woodgett and A. H. Wong (2011). "Genetic inactivation of GSK3alpha rescues spine deficits in Disc1-L100P mutant mice." Schizophr Res **129**(1): 74-79.

Leger, M., A. Quiedeville, V. Bouet, B. Haelewyn, M. Boulouard, P. Schumann-Bard and T. Freret (2013). "Object recognition test in mice." Nat Protoc **8**(12): 2531-2537.

Leigh, M. J., D. V. Nguyen, Y. Mu, T. I. Winarni, A. Schneider, T. Chechi, J. Polussa, P. Doucet, F. Tassone, S. M. Rivera, D. Hessl and R. J. Hagerman (2013). "A randomized double-blind, placebo-controlled trial of minocycline in children and adolescents with fragile x syndrome." J Dev Behav Pediatr **34**(3): 147-155.

Levenga, J., S. Hayashi, F. M. de Vrij, S. K. Koekkoek, H. C. van der Linde, I. Nieuwenhuizen, C. Song, R. A. Buijsen, A. S. Pop, B. Gomezmancilla, D. L. Nelson, R. Willemsen, F. Gasparini and B. A. Oostra (2011). "AFQ056, a new mGluR5 antagonist for treatment of fragile X syndrome." Neurobiol Dis **42**(3): 311-317.

Levy, D., M. Ronemus, B. Yamrom, Y. H. Lee, A. Leotta, J. Kendall, S. Marks, B. Lakshmi, D. Pai, K. Ye, A. Buja, A. Krieger, S. Yoon, J. Troge, L. Rodgers, I. Iossifov and M. Wigler (2011). "Rare de novo and transmitted copy-number variation in autistic spectrum disorders." Neuron **70**(5): 886-897.

Li, Z., Y. Zhang, L. Ku, K. D. Wilkinson, S. T. Warren and Y. Feng (2001). "The fragile X mental retardation protein inhibits translation via interacting with mRNA." Nucleic Acids Res **29**(11): 2276-2283.

Lindemann, L., G. Jaeschke, A. Michalon, E. Vieira, M. Honer, W. Spooren, R. Porter, T. Hartung, S. Kolczewski, B. Buttelmann, C. Flament, C. Diener, C. Fischer, S. Gatti, E. P. Prinssen, N. Parrott, G. Hoffmann and J. G. Wettstein (2011). "CTEP: a novel,

potent, long-acting, and orally bioavailable metabotropic glutamate receptor 5 inhibitor." J Pharmacol Exp Ther **339**(2): 474-486.

Lipina, T. V., O. Kaidanovich-Beilin, S. Patel, M. Wang, S. J. Clapcote, F. Liu, J. R. Woodgett and J. C. Roder (2011). "Genetic and pharmacological evidence for schizophrenia-related Disc1 interaction with GSK-3." Synapse **65**(3): 234-248.

Liu, F., X. Gong, G. Zhang, K. Marquis, P. Reinhart and T. H. Andree (2005). "The inhibition of glycogen synthase kinase 3beta by a metabotropic glutamate receptor 5 mediated pathway confers neuroprotection to Abeta peptides." J Neurochem **95**(5): 1363-1372.

Liu, X., L. Ma, H. H. Li, B. Huang, Y. X. Li, Y. Z. Tao and L. Ma (2015). "beta-Arrestin-biased signaling mediates memory reconsolidation." Proc Natl Acad Sci U S A **112**(14): 4483-4488.

Liu, Z. and C. B. Smith (2014). "Lithium: a promising treatment for fragile X syndrome." ACS Chem Neurosci **5**(6): 477-483.

Liu, Z. H., D. M. Chuang and C. B. Smith (2011). "Lithium ameliorates phenotypic deficits in a mouse model of fragile X syndrome." Int J Neuropsychopharmacol **14**(5): 618-630.

Liu, Z. H., T. Huang and C. B. Smith (2012). "Lithium reverses increased rates of cerebral protein synthesis in a mouse model of fragile X syndrome." Neurobiol Dis **45**(3): 1145-1152.

Liu, Z. H. and C. B. Smith (2009). "Dissociation of social and nonsocial anxiety in a mouse model of fragile X syndrome." Neurosci Lett **454**(1): 62-66.

Lo Monte, F., T. Kramer, J. Gu, M. Brodrecht, J. Pilakowski, A. Fuertes, J. M. Dominguez, B. Plotkin, H. Eldar-Finkelman and B. Schmidt (2013). "Structure-based optimization of oxadiazole-based GSK-3 inhibitors." Eur J Med Chem **61**: 26-40.

Lu, Y. M., Z. Jia, C. Janus, J. T. Henderson, R. Gerlai, J. M. Wojtowicz and J. C. Roder (1997). "Mice lacking metabotropic glutamate receptor 5 show impaired learning and reduced CA1 long-term potentiation (LTP) but normal CA3 LTP." J Neurosci **17**(13): 5196-5205.

MacAulay, K., B. W. Doble, S. Patel, T. Hansotia, E. M. Sinclair, D. J. Drucker, A. Nagy and J. R. Woodgett (2007). "Glycogen synthase kinase 3alpha-specific regulation of murine hepatic glycogen metabolism." Cell Metab **6**(4): 329-337.

Malhotra, D. and J. Sebat (2012). "CNVs: harbingers of a rare variant revolution in psychiatric genetics." Cell **148**(6): 1223-1241.

Martin, B. S., J. G. Corbin and M. M. Huntsman (2014). "Deficient tonic GABAergic conductance and synaptic balance in the fragile X syndrome amygdala." J Neurophysiol **112**(4): 890-902.

Martin, B. S., G. Martinez-Botella, C. M. Loya, F. G. Salituro, A. J. Robichaud, M. M. Huntsman, M. A. Ackley, J. J. Doherty and J. G. Corbin (2016). "Rescue of deficient amygdala tonic gamma-aminobutyric acidergic currents in the Fmr(-/y) mouse model of fragile X syndrome by a novel gamma-aminobutyric acid type A receptor-positive allosteric modulator." J Neurosci Res **94**(6): 568-578.

Masu, M., Y. Tanabe, K. Tsuchida, R. Shigemoto and S. Nakanishi (1991). "Sequence and expression of a metabotropic glutamate receptor." Nature **349**(6312): 760-765.

Mauceri, D., H. E. Freitag, A. M. Oliveira, C. P. Bengtson and H. Bading (2011). "Nuclear calcium-VEGFD signaling controls maintenance of dendrite arborization necessary for memory formation." Neuron **71**(1): 117-130.

McBride, S. M., C. H. Choi, Y. Wang, D. Liebelt, E. Braunstein, D. Ferreiro, A. Sehgal, K. K. Siwicki, T. C. Dockendorff, H. T. Nguyen, T. V. McDonald and T. A. Jongens (2005). "Pharmacological rescue of synaptic plasticity, courtship behavior, and mushroom body defects in a Drosophila model of fragile X syndrome." Neuron **45**(5): 753-764.

McCarthy, S. E., V. Makarov, G. Kirov, A. M. Addington, J. McClellan, S. Yoon, D. O. Perkins, D. E. Dickel, M. Kusenda, O. Krastoshevsky, V. Krause, R. A. Kumar, D. Grozeva, D. Malhotra, T. Walsh, E. H. Zackai, P. Kaplan, J. Ganesh, I. D. Krantz, N. B. Spinner, P. Roccanova, A. Bhandari, K. Pavon, B. Lakshmi, A. Leotta, J. Kendall, Y. H. Lee, V. Vacic, S. Gary, L. M. Iakoucheva, T. J. Crow, S. L. Christian, J. A. Lieberman, T. S. Stroup, T. Lehtimaki, K. Puura, C. Haldeman-Englert, J. Pearl, M. Goodell, V. L. Willour, P. Derosse, J. Steele, L. Kassem, J. Wolff, N. Chitkara, F. J. McMahon, A. K. Malhotra, J. B. Potash, T. G. Schulze, M. M. Nothen, S. Cichon, M. Rietschel, E. Leibenluft, V. Kustanovich, C. M. Lajonchere, J. S. Sutcliffe, D. Skuse, M. Gill, L. Gallagher, N. R. Mendell, N. Craddock, M. J. Owen, M. C. O'Donovan, T. H. Shaikh, E. Susser, L. E. Delisi, P. F. Sullivan, C. K. Deutsch, J. Rapoport, D. L. Levy, M. C. King and J. Sebat (2009). "Microduplications of 16p11.2 are associated with schizophrenia." Nat Genet **41**(11): 1223-1227.

McCubrey, J. A., L. S. Steelman, F. E. Bertrand, N. M. Davis, M. Sokolosky, S. L. Abrams, G. Montalto, A. B. D'Assoro, M. Libra, F. Nicoletti, R. Maestro, J. Basecke, D. Rakus, A. Gizak, Z. N. Demidenko, L. Cocco, A. M. Martelli and M. Cervello (2014).

"GSK-3 as potential target for therapeutic intervention in cancer." Oncotarget **5**(10): 2881-2911.

McKinney, W. T., Jr. and W. E. Bunney, Jr. (1969). "Animal model of depression. I. Review of evidence: implications for research." Arch Gen Psychiatry **21**(2): 240-248.

Meredith, R. M., R. de Jong and H. D. Mansvelder (2011). "Functional rescue of excitatory synaptic transmission in the developing hippocampus in Fmr1-KO mouse." Neurobiol Dis **41**(1): 104-110.

Merlin, L. R., P. J. Bergold and R. K. Wong (1998). "Requirement of protein synthesis for group I mGluR-mediated induction of epileptiform discharges." J Neurophysiol **80**(2): 989-993.

Michalon, A., M. Sidorov, T. M. Ballard, L. Ozmen, W. Spooren, J. G. Wettstein, G. Jaeschke, M. F. Bear and L. Lindemann (2012). "Chronic pharmacological mGlu5 inhibition corrects fragile X in adult mice." Neuron **74**(1): 49-56.

Min, W. W., C. J. Yuskaitis, Q. Yan, C. Sikorski, S. Chen, R. S. Jope and R. P. Bauchwitz (2009). "Elevated glycogen synthase kinase-3 activity in Fragile X mice: key metabolic regulator with evidence for treatment potential." Neuropharmacology **56**(2): 463-472.

Mines, M. A., C. J. Yuskaitis, M. K. King, E. Beurel and R. S. Jope (2010). "GSK3 influences social preference and anxiety-related behaviors during social interaction in a mouse model of fragile X syndrome and autism." PLoS One **5**(3): e9706.

Mineur, Y. S., L. X. Huynh and W. E. Crusio (2006). "Social behavior deficits in the Fmr1 mutant mouse." Behav Brain Res **168**(1): 172-175.

Miyashiro, K. Y., A. Beckel-Mitchener, T. P. Purk, K. G. Becker, T. Barret, L. Liu, S. Carbonetto, I. J. Weiler, W. T. Greenough and J. Eberwine (2003). "RNA cargoes associating with FMRP reveal deficits in cellular functioning in Fmr1 null mice." Neuron **37**(3): 417-431.

Mockett, B. G., D. Guevremont, M. Wutte, S. R. Hulme, J. M. Williams and W. C. Abraham (2011). "Calcium/calmodulin-dependent protein kinase II mediates group I metabotropic glutamate receptor-dependent protein synthesis and long-term depression in rat hippocampus." J Neurosci **31**(20): 7380-7391.

Muddashetty, R. S., S. Kelic, C. Gross, M. Xu and G. J. Bassell (2007). "Dysregulated metabotropic glutamate receptor-dependent translation of AMPA receptor and

postsynaptic density-95 mRNAs at synapses in a mouse model of fragile X syndrome." J Neurosci **27**(20): 5338-5348.

Murakami, A., M. Matsuda, A. Nakasima and M. Hirata (2006). "Characterization of the human PRIP-1 gene structure and transcriptional regulation." Gene **382**: 129-139.

Musumeci, S. A., P. Bosco, G. Calabrese, C. Bakker, G. B. De Sarro, M. Elia, R. Ferri and B. A. Oostra (2000). "Audiogenic seizures susceptibility in transgenic mice with fragile X syndrome." Epilepsia **41**(1): 19-23.

Musumeci, S. A., R. Ferri, C. Scuderi, P. Bosco and M. Elia (2001). "Seizures and epileptiform EEG abnormalities in FRAXE syndrome." Clin Neurophysiol **112**(10): 1954-1955.

Musumeci, S. A., R. J. Hagerman, R. Ferri, P. Bosco, B. Dalla Bernardina, C. A. Tassinari, G. B. De Sarro and M. Elia (1999). "Epilepsy and EEG findings in males with fragile X syndrome." Epilepsia **40**(8): 1092-1099.

Na, Y., S. Park, C. Lee, D. K. Kim, J. M. Park, S. Sockanathan, R. L. Huganir and P. F. Worley (2016). "Real-Time Imaging Reveals Properties of Glutamate-Induced Arc/Arg 3.1 Translation in Neuronal Dendrites." Neuron.

Nakamoto, M., V. Nalavadi, M. P. Epstein, U. Narayanan, G. J. Bassell and S. T. Warren (2007). "Fragile X mental retardation protein deficiency leads to excessive mGluR5-dependent internalization of AMPA receptors." Proc Natl Acad Sci U S A **104**(39): 15537-15542.

Napoli, I., V. Mercaldo, P. P. Boyl, B. Eleuteri, F. Zalfa, S. De Rubeis, D. Di Marino, E. Mohr, M. Massimi, M. Falconi, W. Witke, M. Costa-Mattioli, N. Sonenberg, T. Achsel and C. Bagni (2008). "The fragile X syndrome protein represses activity-dependent translation through CYFIP1, a new 4E-BP." Cell **134**(6): 1042-1054.

Nicoletti, F., C. Valerio, C. Pellegrino, F. Drago, U. Scapagnini and P. L. Canonico (1988). "Spatial learning potentiates the stimulation of phosphoinositide hydrolysis by excitatory amino acids in rat hippocampal slices." J Neurochem **51**(3): 725-729.

Niere, F., J. R. Wilkerson and K. M. Huber (2012). "Evidence for a fragile X mental retardation protein-mediated translational switch in metabotropic glutamate receptor-triggered Arc translation and long-term depression." J Neurosci **32**(17): 5924-5936.

Nosyreva, E. D. and K. M. Huber (2006). "Metabotropic receptor-dependent long-term depression persists in the absence of protein synthesis in the mouse model of fragile X syndrome." J Neurophysiol **95**(5): 3291-3295.

O'Brien, W. T., A. D. Harper, F. Jove, J. R. Woodgett, S. Maretto, S. Piccolo and P. S. Klein (2004). "Glycogen synthase kinase-3beta haploinsufficiency mimics the behavioral and molecular effects of lithium." J Neurosci **24**(30): 6791-6798.

O'Leary, O. and Y. Nolan (2015). "Glycogen synthase kinase-3 as a therapeutic target for cognitive dysfunction in neuropsychiatric disorders." CNS Drugs **29**(1): 1-15.

O'Roak, B. J., L. Vives, S. Girirajan, E. Karakoc, N. Krumm, B. P. Coe, R. Levy, A. Ko, C. Lee, J. D. Smith, E. H. Turner, I. B. Stanaway, B. Vernot, M. Malig, C. Baker, B. Reilly, J. M. Akey, E. Borenstein, M. J. Rieder, D. A. Nickerson, R. Bernier, J. Shendure and E. E. Eichler (2012). "Sporadic autism exomes reveal a highly interconnected protein network of de novo mutations." Nature **485**(7397): 246-250.

Okubo, Y., S. Kakizawa, K. Hirose and M. Iino (2004). "Cross talk between metabotropic and ionotropic glutamate receptor-mediated signaling in parallel fiber-induced inositol 1,4,5-trisphosphate production in cerebellar Purkinje cells." J Neurosci **24**(43): 9513-9520.

Olmos-Serrano, J. L., S. M. Paluszkiewicz, B. S. Martin, W. E. Kaufmann, J. G. Corbin and M. M. Huntsman (2010). "Defective GABAergic neurotransmission and pharmacological rescue of neuronal hyperexcitability in the amygdala in a mouse model of fragile X syndrome." J Neurosci **30**(29): 9929-9938.

Osterweil, E. K., S. C. Chuang, A. A. Chubykin, M. Sidorov, R. Bianchi, R. K. Wong and M. F. Bear (2013). "Lovastatin corrects excess protein synthesis and prevents epileptogenesis in a mouse model of fragile X syndrome." Neuron **77**(2): 243-250.

Osterweil, E. K., D. D. Krueger, K. Reinhold and M. F. Bear (2010). "Hypersensitivity to mGluR5 and ERK1/2 leads to excessive protein synthesis in the hippocampus of a mouse model of fragile X syndrome." J Neurosci **30**(46): 15616-15627.

Pacey, L. K., S. P. Heximer and D. R. Hampson (2009). "Increased GABA(B) receptor-mediated signaling reduces the susceptibility of fragile X knockout mice to audiogenic seizures." Mol Pharmacol **76**(1): 18-24.

Pacey, L. K., S. Tharmalingam and D. R. Hampson (2011). "Subchronic administration and combination metabotropic glutamate and GABAB receptor drug therapy in fragile X syndrome." J Pharmacol Exp Ther **338**(3): 897-905.

Paradee, W., H. E. Melikian, D. L. Rasmussen, A. Kenneson, P. J. Conn and S. T. Warren (1999). "Fragile X mouse: strain effects of knockout phenotype and evidence suggesting deficient amygdala function." Neuroscience **94**(1): 185-192.

Paspalas, C. D., C. C. Perley, D. V. Venkitaramani, S. M. Goebel-Goody, Y. Zhang, P. Kurup, J. H. Mattis and P. J. Lombroso (2008). "Major Vault Protein is Expressed along the Nucleus-Neurite Axis and Associates with mRNAs in Cortical Neurons." Cereb Cortex.

Pecknold, J. C., D. J. McClure, L. Appeltauer, L. Wrzesinski and T. Allan (1982). "Treatment of anxiety using fenobam (a nonbenzodiazepine) in a double-blind standard (diazepam) placebo-controlled study." J Clin Psychopharmacol **2**(2): 129-133.

Pellerin, D., A. Caku, M. Fradet, P. Bouvier, J. Dube and F. Corbin (2016). "Lovastatin corrects ERK pathway hyperactivation in fragile X syndrome: potential of platelet's signaling cascades as new outcome measures in clinical trials." Biomarkers **21**(6): 497-508.

Perez-Costas, E., J. C. Gandy, M. Melendez-Ferro, R. C. Roberts and G. N. Bijur (2010). "Light and electron microscopy study of glycogen synthase kinase-3beta in the mouse brain." PLoS One **5**(1): e8911.

Pieretti, M., F. P. Zhang, Y. H. Fu, S. T. Warren, B. A. Oostra, C. T. Caskey and D. L. Nelson (1991). "Absence of expression of the FMR-1 gene in fragile X syndrome." Cell **66**(4): 817-822.

Pietraszek, M., A. Gravius, D. Schafer, T. Weil, D. Trifanova and W. Danysz (2005). "mGluR5, but not mGluR1, antagonist modifies MK-801-induced locomotor activity and deficit of prepulse inhibition." Neuropharmacology **49**(1): 73-85.

Pignatelli, M., S. Piccinin, G. Molinaro, L. Di Menna, B. Riozzi, M. Cannella, M. Motolese, G. Vetere, M. V. Catania, G. Battaglia, F. Nicoletti, R. Nistico and V. Bruno (2014). "Changes in mGlu5 receptor-dependent synaptic plasticity and coupling to homer proteins in the hippocampus of Ube3A hemizygous mice modeling angelman syndrome." J Neurosci **34**(13): 4558-4566.

Pinto, D., K. Darvishi, X. Shi, D. Rajan, D. Rigler, T. Fitzgerald, A. C. Lionel, B. Thiruvahindrapuram, J. R. Macdonald, R. Mills, A. Prasad, K. Noonan, S. Gribble, E. Prigmore, P. K. Donahoe, R. S. Smith, J. H. Park, M. E. Hurles, N. P. Carter, C. Lee, S. W. Scherer and L. Feuk (2011). "Comprehensive assessment of array-based platforms and calling algorithms for detection of copy number variants." Nat Biotechnol **29**(6): 512-520.

Pop, A. S., B. Gomez-Mancilla, G. Neri, R. Willemsen and F. Gasparini (2014). "Fragile X syndrome: a preclinical review on metabotropic glutamate receptor 5 (mGluR5) antagonists and drug development." Psychopharmacology (Berl) **231**(6): 1217-1226.

Porter, R. H., G. Jaeschke, W. Spooren, T. M. Ballard, B. Buttelmann, S. Kolczewski, J. U. Peters, E. Prinssen, J. Wichmann, E. Vieira, A. Muhlemann, S. Gatti, V. Mutel and P. Malherbe (2005). "Fenobam: a clinically validated nonbenzodiazepine anxiolytic is a potent, selective, and noncompetitive mGlu5 receptor antagonist with inverse agonist activity." J Pharmacol Exp Ther **315**(2): 711-721.

Portmann, T., M. Yang, R. Mao, G. Panagiotakos, J. Ellegood, G. Dolen, P. L. Bader, B. A. Grueter, C. Goold, E. Fisher, K. Clifford, P. Rengarajan, D. Kalikhman, D. Loureiro, N. L. Saw, Z. Zhengqui, M. A. Miller, J. P. Lerch, R. M. Henkelman, M. Shamloo, R. C. Malenka, J. N. Crawley and R. E. Dolmetsch (2014). "Behavioral abnormalities and circuit defects in the basal ganglia of a mouse model of 16p11.2 deletion syndrome." Cell Rep **7**(4): 1077-1092.

Portmann, T., M. Yang, R. Mao, G. Panagiotakos, J. Ellegood, G. Dolen, P. L. Bader, B. A. Grueter, C. Goold, E. Fisher, K. Clifford, P. Rengarajan, D. Kalikhman, D. Loureiro, N. L. Saw, Z. Zhengqui, M. A. Miller, J. P. Lerch, R. M. Henkelman, M. Shamloo, R. C. Malenka, J. N. Crawley and R. E. Dolmetsch (2014). "Behavioral Abnormalities and Circuit Defects in the Basal Ganglia of a Mouse Model of 16p11.2 Deletion Syndrome." Cell Rep.

Price, T. J., M. H. Rashid, M. Millecamps, R. Sanoja, J. M. Entrena and F. Cervero (2007). "Decreased nociceptive sensitization in mice lacking the fragile X mental retardation protein: role of mGluR1/5 and mTOR." J Neurosci **27**(51): 13958-13967.

Pucilowska, J., P. A. Puzerey, J. C. Karlo, R. F. Galan and G. E. Landreth (2012). "Disrupted ERK signaling during cortical development leads to abnormal progenitor proliferation, neuronal and network excitability and behavior, modeling human neuro-cardio-facial-cutaneous and related syndromes." J Neurosci **32**(25): 8663-8677.

Pucilowska, J., J. Vithayathil, E. J. Tavares, C. Kelly, J. C. Karlo and G. E. Landreth (2015). "The 16p11.2 deletion mouse model of autism exhibits altered cortical progenitor proliferation and brain cytoarchitecture linked to the ERK MAPK pathway." J Neurosci **35**(7): 3190-3200.

Qin, M., T. Huang, M. Kader, L. Krych, Z. Xia, T. Burlin, Z. Zeidler, T. Zhao and C. B. Smith (2015). "R-Baclofen Reverses a Social Behavior Deficit and Elevated Protein Synthesis in a Mouse Model of Fragile X Syndrome." Int J Neuropsychopharmacol **18**(9).

Qin, M., J. Kang, T. V. Burlin, C. Jiang and C. B. Smith (2005). "Postadolescent changes in regional cerebral protein synthesis: an in vivo study in the FMR1 null mouse." J Neurosci **25**(20): 5087-5095.

Qin, M., J. Kang and C. B. Smith (2002). "Increased rates of cerebral glucose metabolism in a mouse model of fragile X mental retardation." Proc Natl Acad Sci U S A **99**(24): 15758-15763.

Qin, M., K. C. Schmidt, A. J. Zametkin, S. Bishu, L. M. Horowitz, T. V. Burlin, Z. Xia, T. Huang, Z. M. Quezado and C. B. Smith (2013). "Altered cerebral protein synthesis in fragile X syndrome: studies in human subjects and knockout mice." J Cereb Blood Flow Metab **33**(4): 499-507.

Raymond, C. R., V. L. Thompson, W. P. Tate and W. C. Abraham (2000). "Metabotropic glutamate receptors trigger homosynaptic protein synthesis to prolong long-term potentiation." J Neurosci **20**(3): 969-976.

Richter, J. D., G. J. Bassell and E. Klann (2015). "Dysregulation and restoration of translational homeostasis in fragile X syndrome." Nat Rev Neurosci **16**(10): 595-605.

Ronesi, J. A., K. A. Collins, S. A. Hays, N. P. Tsai, W. Guo, S. G. Birnbaum, J. H. Hu, P. F. Worley, J. R. Gibson and K. M. Huber (2012). "Disrupted Homer scaffolds mediate abnormal mGluR5 function in a mouse model of fragile X syndrome." Nat Neurosci **15**(3): 431-440, s431.

Rush, A. M., J. Wu, M. J. Rowan and R. Anwyl (2002). "Group I metabotropic glutamate receptor (mGluR)-dependent long-term depression mediated via p38 mitogen-activated protein kinase is inhibited by previous high-frequency stimulation and activation of mGluRs and protein kinase C in the rat dentate gyrus in vitro." J Neurosci **22**(14): 6121-6128.

Sajikumar, S., S. Navakkode and J. U. Frey (2005). "Protein synthesis-dependent long-term functional plasticity: methods and techniques." Curr Opin Neurobiol **15**(5): 607-613.

Santoro, M. R., S. M. Bray and S. T. Warren (2012). "Molecular mechanisms of fragile X syndrome: a twenty-year perspective." Annu Rev Pathol **7**: 219-245.

Scharf, S. H., G. Jaeschke, J. G. Wettstein and L. Lindemann (2015). "Metabotropic glutamate receptor 5 as drug target for Fragile X syndrome." Curr Opin Pharmacol **20**: 124-134.

Schnabel, R., I. C. Kilpatrick and G. L. Collingridge (1999). "An investigation into signal transduction mechanisms involved in DHPG-induced LTD in the CA1 region of the hippocampus." Neuropharmacology **38**(10): 1585-1596.

Schoepp, D. D. and P. J. Conn (1993). "Metabotropic glutamate receptors in brain function and pathology." Trends Pharmacol Sci **14**(1): 13-20.

Selby, L., C. Zhang and Q. Q. Sun (2007). "Major defects in neocortical GABAergic inhibitory circuits in mice lacking the fragile X mental retardation protein." Neurosci Lett **412**(3): 227-232.

Sethna, F., C. Moon and H. Wang (2014). "From FMRP function to potential therapies for fragile X syndrome." Neurochem Res **39**(6): 1016-1031.

Sharma, A., C. A. Hoeffer, Y. Takayasu, T. Miyawaki, S. M. McBride, E. Klann and R. S. Zukin (2010). "Dysregulation of mTOR signaling in fragile X syndrome." J Neurosci **30**(2): 694-702.

Sheffler, D. J., K. J. Gregory, J. M. Rook and P. J. Conn (2011). "Allosteric modulation of metabotropic glutamate receptors." Adv Pharmacol **62**: 37-77.

Sherry, J. M., S. L. Milsome and S. F. Crowe (2010). "The roles of RNA synthesis and protein translation during reconsolidation of passive-avoidance learning in the day-old chick." Pharmacol Biochem Behav **94**(3): 438-446.

Shimojima, K., T. Inoue, Y. Fujii, K. Ohno and T. Yamamoto (2009). "A familial 593-kb microdeletion of 16p11.2 associated with mental retardation and hemivertebrae." Eur J Med Genet **52**(6): 433-435.

Sidhu, H., L. E. Dansie, P. W. Hickmott, D. W. Ethell and I. M. Ethell (2014). "Genetic removal of matrix metalloproteinase 9 rescues the symptoms of fragile X syndrome in a mouse model." J Neurosci **34**(30): 9867-9879.

Sidorov, M. S., D. D. Krueger, M. Taylor, E. Gisin, E. K. Osterweil and M. F. Bear (2014). "Extinction of an instrumental response: a cognitive behavioral assay in Fmr1 knockout mice." Genes Brain Behav **13**(5): 451-458.

Siegel, M., C. A. Beresford, M. Bunker, M. Verdi, D. Vishnevetsky, C. Karlsson, O. Teer, A. Stedman and K. A. Smith (2014). "Preliminary investigation of lithium for mood disorder symptoms in children and adolescents with autism spectrum disorder." J Child Adolesc Psychopharmacol **24**(7): 399-402.

Simonyi, A., T. R. Schachtman and G. R. Christoffersen (2005). "The role of metabotropic glutamate receptor 5 in learning and memory processes." Drug News Perspect **18**(6): 353-361.

Snyder, E. M., B. D. Philpot, K. M. Huber, X. Dong, J. R. Fallon and M. F. Bear (2001). "Internalization of ionotropic glutamate receptors in response to mGluR activation." Nat Neurosci **4**(11): 1079-1085.

Song, F. J., P. Barton, V. Sleightholme, G. L. Yao and A. Fry-Smith (2003). "Screening for fragile X syndrome: a literature review and modelling study." Health Technol Assess **7**(16): 1-106.

Spencer, C. M., O. Alekseyenko, S. M. Hamilton, A. M. Thomas, E. Serysheva, L. A. Yuva-Paylor and R. Paylor (2011). "Modifying behavioral phenotypes in Fmr1KO mice: genetic background differences reveal autistic-like responses." Autism Res **4**(1): 40-56.

Spencer, C. M., O. Alekseyenko, E. Serysheva, L. A. Yuva-Paylor and R. Paylor (2005). "Altered anxiety-related and social behaviors in the Fmr1 knockout mouse model of fragile X syndrome." Genes Brain Behav **4**(7): 420-430.

Srivastava, A., B. Gupta, C. Gupta and A. K. Shukla (2015). "Emerging Functional Divergence of beta-Arrestin Isoforms in GPCR Function." Trends Endocrinol Metab **26**(11): 628-642.

Stefani, G., C. E. Fraser, J. C. Darnell and R. B. Darnell (2004). "Fragile X mental retardation protein is associated with translating polyribosomes in neuronal cells." J Neurosci **24**(33): 7272-7276.

Steffenburg, S., C. Gillberg, L. Hellgren, L. Andersson, I. C. Gillberg, G. Jakobsson and M. Bohman (1989). "A twin study of autism in Denmark, Finland, Iceland, Norway and Sweden." J Child Psychol Psychiatry **30**(3): 405-416.

Stiedl, O., M. Palve, J. Radulovic, K. Birkenfeld and J. Spiess (1999). "Differential impairment of auditory and contextual fear conditioning by protein synthesis inhibition in C57BL/6N mice." Behav Neurosci **113**(3): 496-506.

Stoop, R., F. Conquet and E. Pralong (2003). "Determination of group I metabotropic glutamate receptor subtypes involved in the frequency of epileptiform activity in vitro using mGluR1 and mGluR5 mutant mice." Neuropharmacology **44**(2): 157-162.

Su, T., H. X. Fan, T. Jiang, W. W. Sun, W. Y. Den, M. M. Gao, S. Q. Chen, Q. H. Zhao and Y. H. Yi (2011). "Early continuous inhibition of group 1 mGlu signaling partially

rescues dendritic spine abnormalities in the Fmr1 knockout mouse model for fragile X syndrome." Psychopharmacology (Berl) **215**(2): 291-300.

Sutton, M. A., A. M. Taylor, H. T. Ito, A. Pham and E. M. Schuman (2007). "Postsynaptic decoding of neural activity: eEF2 as a biochemical sensor coupling miniature synaptic transmission to local protein synthesis." Neuron **55**(4): 648-661.

Suvrathan, A., C. A. Hoeffer, H. Wong, E. Klann and S. Chattarji (2010). "Characterization and reversal of synaptic defects in the amygdala in a mouse model of fragile X syndrome." Proc Natl Acad Sci U S A **107**(25): 11591-11596.

Tamanini, F., N. Meijer, C. Verheij, P. J. Willems, H. Galjaard, B. A. Oostra and A. T. Hoogeveen (1996). "FMRP is associated to the ribosomes via RNA." Hum Mol Genet **5**(6): 809-813.

Thomas, A. M., N. Bui, D. Graham, J. R. Perkins, L. A. Yuva-Paylor and R. Paylor (2011). "Genetic reduction of group 1 metabotropic glutamate receptors alters select behaviors in a mouse model for fragile X syndrome." Behav Brain Res **223**(2): 310-321.

Thomas, A. M., N. Bui, J. R. Perkins, L. A. Yuva-Paylor and R. Paylor (2012). "Group I metabotropic glutamate receptor antagonists alter select behaviors in a mouse model for fragile X syndrome." Psychopharmacology (Berl) **219**(1): 47-58.

Tian, D., L. J. Stoppel, A. J. Heynen, L. Lindemann, G. Jaeschke, A. A. Mills and M. F. Bear (2015). "Contribution of mGluR5 to pathophysiology in a mouse model of human chromosome 16p11.2 microdeletion." Nat Neurosci **18**(2): 182-184.

Till, S. M., A. Asiminas, A. D. Jackson, D. Katsanevaki, S. A. Barnes, E. K. Osterweil, M. F. Bear, S. Chattarji, E. R. Wood, D. J. Wyllie and P. C. Kind (2015). "Conserved hippocampal cellular pathophysiology but distinct behavioural deficits in a new rat model of FXS." Hum Mol Genet **24**(21): 5977-5984.

Todd, P. K., K. J. Mack and J. S. Malter (2003). "The fragile X mental retardation protein is required for type-I metabotropic glutamate receptor-dependent translation of PSD-95." Proc Natl Acad Sci U S A **100**(24): 14374-14378.

Tsiouris, J. A. and W. T. Brown (2004). "Neuropsychiatric symptoms of fragile X syndrome: pathophysiology and pharmacotherapy." CNS Drugs **18**(11): 687-703.

Turner, G., T. Webb, S. Wake and H. Robinson (1996). "Prevalence of fragile X syndrome." Am J Med Genet **64**(1): 196-197.

Vanderklish, P. W. and G. M. Edelman (2002). "Dendritic spines elongate after stimulation of group 1 metabotropic glutamate receptors in cultured hippocampal neurons." Proc Natl Acad Sci U S A **99**(3): 1639-1644.

Veeraragavan, S., N. Bui, J. R. Perkins, L. A. Yuva-Paylor, R. L. Carpenter and R. Paylor (2011). "Modulation of behavioral phenotypes by a muscarinic M1 antagonist in a mouse model of fragile X syndrome." Psychopharmacology (Berl) **217**(1): 143-151.

Veeraragavan, S., N. Bui, J. R. Perkins, L. A. Yuva-Paylor and R. Paylor (2011). "The modulation of fragile X behaviors by the muscarinic M4 antagonist, tropicamide." Behav Neurosci **125**(5): 783-790.

Veeraragavan, S., D. Graham, N. Bui, L. A. Yuva-Paylor, J. Wess and R. Paylor (2012). "Genetic reduction of muscarinic M4 receptor modulates analgesic response and acoustic startle response in a mouse model of fragile X syndrome (FXS)." Behav Brain Res **228**(1): 1-8.

Verkerk, A. J., M. Pieretti, J. S. Sutcliffe, Y. H. Fu, D. P. Kuhl, A. Pizzuti, O. Reiner, S. Richards, M. F. Victoria, F. P. Zhang and et al. (1991). "Identification of a gene (FMR-1) containing a CGG repeat coincident with a breakpoint cluster region exhibiting length variation in fragile X syndrome." Cell **65**(5): 905-914.

Vinueza Veloz, M. F., R. A. Buijsen, R. Willemsen, A. Cupido, L. W. Bosman, S. K. Koekkoek, J. W. Potters, B. A. Oostra and C. I. De Zeeuw (2012). "The effect of an mGluR5 inhibitor on procedural memory and avoidance discrimination impairments in Fmr1 KO mice." Genes Brain Behav **11**(3): 325-331.

Volk, L. J., B. E. Pfeiffer, J. R. Gibson and K. M. Huber (2007). "Multiple Gq-coupled receptors converge on a common protein synthesis-dependent long-term depression that is affected in fragile X syndrome mental retardation." J Neurosci **27**(43): 11624-11634.

Volkmar, F. R. and B. Reichow (2013). "Autism in DSM-5: progress and challenges." Mol Autism **4**(1): 13.

Wahlstrom-Helgren, S. and V. A. Klyachko (2015). "GABAB receptor-mediated feed-forward circuit dysfunction in the mouse model of fragile X syndrome." J Physiol **593**(22): 5009-5024.

Wan, L., T. C. Dockendorff, T. A. Jongens and G. Dreyfuss (2000). "Characterization of dFMR1, a Drosophila melanogaster homolog of the fragile X mental retardation protein." Mol Cell Biol **20**(22): 8536-8547.

Wang, H., A. Iacoangeli, D. Lin, K. Williams, R. B. Denman, C. U. Hellen and H. Tiedge (2005). "Dendritic BC1 RNA in translational control mechanisms." J Cell Biol **171**(5): 811-821.

Wang, L. W., E. Berry-Kravis and R. J. Hagerman (2010). "Fragile X: leading the way for targeted treatments in autism." Neurotherapeutics **7**(3): 264-274.

Waung, M. W., B. E. Pfeiffer, E. D. Nosyreva, J. A. Ronesi and K. M. Huber (2008). "Rapid translation of Arc/Arg3.1 selectively mediates mGluR-dependent LTD through persistent increases in AMPAR endocytosis rate." Neuron **59**(1): 84-97.

Weber, A., A. Kohler, A. Hahn, B. Neubauer and U. Muller (2013). "Benign infantile convulsions (IC) and subsequent paroxysmal kinesigenic dyskinesia (PKD) in a patient with 16p11.2 microdeletion syndrome." Neurogenetics **14**(3-4): 251-253.

Weiler, I. J. and W. T. Greenough (1993). "Metabotropic glutamate receptors trigger postsynaptic protein synthesis." Proc Natl Acad Sci U S A **90**(15): 7168-7171.

Weiler, I. J. and W. T. Greenough (1999). "Synaptic synthesis of the Fragile X protein: possible involvement in synapse maturation and elimination." Am J Med Genet **83**(4): 248-252.

Weiler, I. J., S. A. Irwin, A. Y. Klintsova, C. M. Spencer, A. D. Brazelton, K. Miyashiro, T. A. Comery, B. Patel, J. Eberwine and W. T. Greenough (1997). "Fragile X mental retardation protein is translated near synapses in response to neurotransmitter activation." Proc Natl Acad Sci U S A **94**(10): 5395-5400.

Weiss, L. A., Y. Shen, J. M. Korn, D. E. Arking, D. T. Miller, R. Fossdal, E. Saemundsen, H. Stefansson, M. A. Ferreira, T. Green, O. S. Platt, D. M. Ruderfer, C. A. Walsh, D. Altshuler, A. Chakravarti, R. E. Tanzi, K. Stefansson, S. L. Santangelo, J. F. Gusella, P. Sklar, B. L. Wu and M. J. Daly (2008). "Association between microdeletion and microduplication at 16p11.2 and autism." N Engl J Med **358**(7): 667-675.

Wenger, T. L., C. Kao, D. M. McDonald-McGinn, E. H. Zackai, A. Bailey, R. T. Schultz, B. E. Morrow, B. S. Emanuel and H. Hakonarson (2016). "The Role of mGluR Copy Number Variation in Genetic and Environmental Forms of Syndromic Autism Spectrum Disorder." Sci Rep **6**: 19372.

Westmark, C. J., P. R. Westmark, K. J. O'Riordan, B. C. Ray, C. M. Hervey, M. S. Salamat, S. H. Abozeid, K. M. Stein, L. A. Stodola, M. Tranfaglia, C. Burger, E. M. Berry-Kravis and J. S. Malter (2011). "Reversal of fragile X phenotypes by manipulation of AbetaPP/Abeta levels in Fmr1KO mice." PLoS One **6**(10): e26549.

Whalen, E. J., S. Rajagopal and R. J. Lefkowitz (2011). "Therapeutic potential of beta-arrestin- and G protein-biased agonists." Trends Mol Med **17**(3): 126-139.

Whittingham, T. S., W. D. Lust, D. A. Christakis and J. V. Passonneau (1984). "Metabolic stability of hippocampal slice preparations during prolonged incubation." J Neurochem **43**(3): 689-696.

Wilkerson, J. R., N. P. Tsai, M. A. Maksimova, H. Wu, N. P. Cabalo, K. W. Loerwald, J. B. Dictenberg, J. R. Gibson and K. M. Huber (2014). "A role for dendritic mGluR5-mediated local translation of Arc/Arg3.1 in MEF2-dependent synapse elimination." Cell Rep **7**(5): 1589-1600.

Willner, P. (1984). "The validity of animal models of depression." Psychopharmacology (Berl) **83**(1): 1-16.

Wisniewski, K. E., S. M. Segan, C. M. Miezejeski, E. A. Sersen and R. D. Rudelli (1991). "The Fra(X) syndrome: neurological, electrophysiological, and neuropathological abnormalities." Am J Med Genet **38**(2-3): 476-480.

Woodgett, J. R. (1990). "Molecular cloning and expression of glycogen synthase kinase-3/factor A." Embo j **9**(8): 2431-2438.

Yan, Q. J., M. Rammal, M. Tranfaglia and R. P. Bauchwitz (2005). "Suppression of two major Fragile X Syndrome mouse model phenotypes by the mGluR5 antagonist MPEP." Neuropharmacology **49**(7): 1053-1066.

Yang, M., E. J. Mahrt, F. Lewis, G. Foley, T. Portmann, R. E. Dolmetsch, C. V. Portfors and J. N. Crawley (2015). "16p11.2 Deletion Syndrome Mice Display Sensory and Ultrasonic Vocalization Deficits During Social Interactions." Autism Res.

Yao, H. B., P. C. Shaw, C. C. Wong and D. C. Wan (2002). "Expression of glycogen synthase kinase-3 isoforms in mouse tissues and their transcription in the brain." J Chem Neuroanat **23**(4): 291-297.

Yuskaitis, C. J., M. A. Mines, M. K. King, J. D. Sweatt, C. A. Miller and R. S. Jope (2010). "Lithium ameliorates altered glycogen synthase kinase-3 and behavior in a mouse model of fragile X syndrome." Biochem Pharmacol **79**(4): 632-646.

Zalfa, F., M. Giorgi, B. Primerano, A. Moro, A. Di Penta, S. Reis, B. Oostra and C. Bagni (2003). "The fragile X syndrome protein FMRP associates with BC1 RNA and regulates the translation of specific mRNAs at synapses." Cell **112**(3): 317-327.

Zang, J. B., E. D. Nosyreva, C. M. Spencer, L. J. Volk, K. Musunuru, R. Zhong, E. F. Stone, L. A. Yuva-Paylor, K. M. Huber, R. Paylor, J. C. Darnell and R. B. Darnell (2009). "A mouse model of the human Fragile X syndrome I304N mutation." PLoS Genet **5**(12): e1000758.

Zantomio, D., G. Chana, L. Laskaris, R. Testa, I. Everall, C. Pantelis and E. Skafidas (2015). "Convergent evidence for mGluR5 in synaptic and neuroinflammatory pathways implicated in ASD." Neurosci Biobehav Rev **52**: 172-177.

Zhang, L. and B. E. Alger (2010). "Enhanced endocannabinoid signaling elevates neuronal excitability in fragile X syndrome." J Neurosci **30**(16): 5724-5729.

Zhang, Y. E., P. Landback, M. D. Vibranovski and M. Long (2011). "Accelerated recruitment of new brain development genes into the human genome." PLoS Biol **9**(10): e1001179.

Zhao, M. G., H. Toyoda, S. W. Ko, H. K. Ding, L. J. Wu and M. Zhuo (2005). "Deficits in trace fear memory and long-term potentiation in a mouse model for fragile X syndrome." J Neurosci **25**(32): 7385-7392.

Zhao, S., J. Shetty, L. Hou, A. Delcher, B. Zhu, K. Osoegawa, P. de Jong, W. C. Nierman, R. L. Strausberg and C. M. Fraser (2004). "Human, mouse, and rat genome large-scale rearrangements: stability versus speciation." Genome Res **14**(10a): 1851-1860.

Zhao, W., J. Wang, S. Song, F. Li and F. Yuan (2015). "Reduction of alpha1GABAA receptor mediated by tyrosine kinase C (PKC) phosphorylation in a mouse model of fragile X syndrome." Int J Clin Exp Med **8**(8): 13219-13226.

Zho, W. M., J. L. You, C. C. Huang and K. S. Hsu (2002). "The group I metabotropic glutamate receptor agonist (S)-3,5-dihydroxyphenylglycine induces a novel form of depotentiation in the CA1 region of the hippocampus." J Neurosci **22**(20): 8838-8849.

Zufferey, F., E. H. Sherr, N. D. Beckmann, E. Hanson, A. M. Maillard, L. Hippolyte, A. Mace, C. Ferrari, Z. Kutalik, J. Andrieux, E. Aylward, M. Barker, R. Bernier, S. Bouquillon, P. Conus, B. Delobel, W. A. Faucett, R. P. Goin-Kochel, E. Grant, L. Harewood, J. V. Hunter, S. Lebon, D. H. Ledbetter, C. L. Martin, K. Mannik, D. Martinet, P. Mukherjee, M. B. Ramocki, S. J. Spence, K. J. Steinman, J. Tjernagel, J. E. Spiro, A. Reymond, J. S. Beckmann, W. K. Chung and S. Jacquemont (2012). "A 600 kb deletion syndrome at 16p11.2 leads to energy imbalance and neuropsychiatric disorders." J Med Genet **49**(10): 660-668.